

Irrigation with desalinated and raw produced waters: Effects on soil properties, and germination and growth of five forages

Akram R. Ben Ali^{a,*}, Manoj K. Shukla^a, Mark Marsalis^b, Nyle Khan^c

^a Plant and Environmental Sciences Department, New Mexico State University, P.O. Box 30003, MSC-3Q, Las Cruces, NM 88003-8003, USA

^b Los Lunas Agricultural Science Center, USA

^c HPOC, LLC, USA

ARTICLE INFO

Handling Editor - Dr. B.E. Clothier

Keywords:

Produced water
Evapotranspiration
Russian wildrye
Alfalfa
Tall fescue

ABSTRACT

Produced water is generated during oil and gas production in copious amounts daily in the United States. With increasing water shortfalls in arid and semi-arid regions, it could be a valuable source of water for irrigation purposes after treatment. The present study examined the effects of irrigation with produced waters on five perennials cool season forage, species western wheatgrass (*Pascopyrum smithii*), alfalfa (*Medicago sativa*), meadow bromegrass (*Bromus biebersteinii*), Russian wildrye (*Psathyrostachys juncea*), and tall fescue (*Schedonorus arundinaceus*). The forages were grown in a greenhouse, in loamy soil, and irrigated with desalinated reverse osmosis RO (231 mg/l), diluted RAW (1400 mg/l), RAW produced (8610 mg/l), and tap (427 mg/l) water. All forages were harvested three times at an interval of ≈ 90 days after 30 days germination period. Tall fescue germinated (100 %) and grew well under all four treatments. The higher biomass was with alfalfa, tall fescue, wheatgrass, bromegrass, and Russian wildrye, respectively. Evapotranspiration (ET) of the five species decreased with increasing soil and irrigation water salinity. Na, Cl, and B ions concentrations were 10.7, 13.6, and 42.3 mg/l, respectively in wheatgrass; 24.7, 17, and 14.5 mg/l, respectively in alfalfa; 27.7, 25.6, and 92.5 mg/l, respectively in bromegrass; 18, 14.6, and 59.6 mg/l, respectively in Russian wildrye; and 33, 35, and 207.5 mg/l, respectively in tall fescue, in plant tissues obtained after the second harvest. In soil, Na and B ions concentrations were 1173, 2.1 mg/l, respectively in wheatgrass pots; 1047, 1.7 mg/l, respectively in alfalfa pots; 874.6, 1.4 mg/l, respectively in bromegrass pots; 782, 1.6 mg/l, respectively in Russian wildrye pots; and 1974, 3.17 mg/l, respectively in tall fescue pots. Plant biomass decreased with increasing salinity; however, plants continued to grow even after the third harvest. Utilizing desalinated and diluted produced waters as a valuable source of water for irrigation after treatment could alleviate water demand in arid oil producing regions of the world.

1. Introduction

The search for alternative water sources for agricultural purposes due to continued drought and reduction in fresh water supplies has become mandatory in arid areas to save water for human consumption. Oil and gas industries generate large volumes (around 630 – 840 billion gallons/year) of water during extraction processes, and the largest by-product called “produced water” (Clark and Veil, 2009; Veil, 2011). This valuable source of water has been investigated as a useful source of irrigation in drylands in the US (Pica et al., 2017; Eichelh et al., 2020).

In the US, west of the 98th meridian, the federal National Pollutant Discharge Elimination System (NPDES) exemption allows the use of produced water for agricultural irrigation if oil and grease are less than

35 mg/L (McLaughlin et al., 2020). Reusing saline waters including produced water to irrigate croplands can contribute to food security (Flores et al., 2015). However, salt content of produced water could be extremely high; therefore, long-term irrigation would cause decline in soil fertility and crop productivity and increase groundwater contamination (Eichelh et al., 2020). High salinity, organic matter load, and toxic organic compounds are some of the main pollutant constituents in produced water that have to be accounted for prior to the reuse as an irrigation source (Pica et al., 2017). Treatment of the produced water to remove organics, microbial contaminants and heavy metals, prior to use will also be required.

Ben Ali et al. (2021); (2020) illustrated that irrigation with RO concentrate (5600 mg/l) negatively impacted soil properties and plant

* Correspondence to: Plant and Environmental Science Department, New Mexico State University, Las Cruces, NM, USA.

E-mail addresses: bena1971@nmsu.edu (A.R. Ben Ali), shuklamk@nmsu.edu (M.K. Shukla), marsalis@nmsu.edu (M. Marsalis), n.khan@hpocllc.com (N. Khan).

<https://doi.org/10.1016/j.agwat.2022.107966>

Received 1 August 2022; Received in revised form 22 September 2022; Accepted 24 September 2022

Available online 4 October 2022

0378-3774/Published by Elsevier B.V. This is an open access article under the CC BY-NC-ND license (<http://creativecommons.org/licenses/by-nc-nd/4.0/>).

growth. Reduction in pecan (*Carya illinoensis*) chlorophyll, height, and growth was the results of irrigation with 5600 mg/l saline water (Ben Ali et al., 2020). Previous studies reported small decreases in halophytic species biomass irrigated with saline water (5600 – 7000 mg/l) (Flores et al., 2016; Ozturk et al., 2018). Decreases in tomato growth and yield were reported due to irrigation with 2800 mg/l saline water (Yang et al., 2020; Farooq et al., 2021). Accumulation of Na and Cl caused reductions in plant height, chlorophyll content and leaf area of *Dichroa febrifuga*, *H. macrophylla*, and *D. febrifuga* irrigated due to the irrigation with saline water of concentrations ranging from 3500 to 7000 mg/l (Sun et al., 2022).

Changes in soil properties have to be monitored on a regular basis when produced water is utilized for irrigation. Burkhardt et al. (2015) reported increasing accumulation of Na and other salts in the soil with increasing concentration of produced water. Other studies conducted in arid areas have reported that produced water quality was responsible for increases in soil salinity and sodicity that negatively affected the soil structure and soil hydraulic properties (Biggs et al., 2012; Burkhardt et al., 2015), consequently, decreasing crop productivity (Yang et al., 2020; Echchelhel et al., 2020).

Pica et al. (2017) reported decreases in Rapeseed (*Brassica napus* L.) and switchgrass (*Panicum virgatum* L.) growth when irrigated with produced water (up to 21,000 mg/l salinity). Plant growth and consequently biomass production can be inhibited when soil salinity increase due to irrigation with produced water (Munns, 2005). Burkhardt et al. (2015) reported a decline in wormwood and switchgrass growth with increases in produced water concentration due to high Na content (\approx 1156 mg/l). A dilution to less than 1000 mg/l of row-produced water was utilized to irrigate greenhouse tomatoes (Martel-Valles et al., 2014). The feasibility of utilizing produced water in crop irrigation is related to its ion and organics. To that end, desalination of produced water to acceptable levels of various plants could be a viable solution.

HPOC, LLC is one of the oil and gas companies that produces substantial amounts of produced water during oil explorations. The company provided produced water (source water) of a salinity of about 8600 mg/l. In the state of New Mexico, produced water salinity is highly variable and can range from 8000 mg/l to 250,000 mg/l. In the present study, we created a salinity gradient of irrigation waters from 230 mg/l to 8600 mg/l to irrigate five forages species. The objectives of this study were to: (i) investigate the effects of produced water on seed germination and plants growth parameters, and (ii) monitor the changes in the soil properties due to irrigation with produced water.

2. Materials and methods

2.1. Experimental design and treatments

Two harvests (from 22 May 2021–15 December 2021) were conducted in the Fabian Garcia Science Center greenhouse in Las Cruces, NM, USA (32.2805° N and 106.770° W; elevation 1186 m). An extended third harvest continued from December 15, 2021, to February 27, 2022, to confirm the viability of the experiment. For each experimental harvest, the experimental unit was a pot (15 cm deep and 15 cm in diameter) packed with air-dried and sieved through a 2 mm sieve loamy soil (52.56 % sand, 22.72 % silt, 24.72 % clay) with a bulk density of 1.43 g/cm³. Three produced water treatments with total dissolved solids (TDS) of 231 mg/l RO water (desalinated using reverse osmosis, RO), 1400 mg/l diluted RAW (RAW produced water diluted with city water), 8610 mg/l RAW produced water (source water), and 427 mg/l tap (or city) water (Table 1) were arranged in a completely randomized design with four replicates. The RAW produced water or source water was provided by HPOC and was first run through a carbon filter then desalinated using RO at the Brackish Groundwater National Desalination Research Facility (BGNDRF), Alamogordo, New Mexico. All treatment waters are shown in Table 1, which also provides pH, sodium adsorption ratio (SAR), total dissolved solids (TDS), and concentrations of some ions.

Table 1
Ion concentrations (mg/l), SAR, and pH in four treatment waters.

Treatment waters	TDS mg/l	Mg mg/l	Ca mg/l	Na mg/l	SAR	Cl mg/l	pH
RO	231	0.48	13.16	67.49	4.83	36.2	8.2
Tap	427	8.25	40.77	58.22	1.93	56.0	7.4
Diluted RAW	1400	8.91	54.56	360.94	10.81	141.0	8.3
RAW	8610	9.61	172.84	3425.80	65.81	856.0	8.3

Note: RO is the raw water desalinated using reverse osmosis (231 mg/l). Tap water = 427 mg/l. Diluted RAW produced water = 1400 mg/l. RAW produced water = 8610 mg/l. TDS = total dissolved solids. SAR = Sodium adsorption ratio

2.2. Plant selection

Western wheatgrass (*Pascopyrum smithii*), alfalfa (*Medicago sativa*), meadow bromegrass (*Bromus biebersteinii*), Russian wildrye (*Psathyrostachys junceus*), and tall fescue (*Schedonorus arundinaceus*) seeds were selected for the study because they are broadly adapted to grow in the colder climates of northern New Mexico. In a completely randomized design, these five forage species were arranged in four replicates and irrigated with four water treatments in 80 pots (5 * 4 * 4 = 80) in each harvest. Randomization was achieved by generating random numbers using Microsoft Excel (2013). Prior to sowing, seeds were subjected to water –test to check for seed viability. Twenty-five seeds per pot of each species were planted in the top 2 cm of the soil. The pots with the seedlings were irrigated with the four treatments from the beginning of the experiment. Depending on soil moisture content, plants were irrigated five to six times every month. Germination percentage was calculated 30 days after seeding. Plants were harvested on September 22, 2021, for the first harvest, December 15, 2021, for the second harvest, and February 27, 2021, for the extended third harvest.

2.3. Evapotranspiration

Evapotranspiration (ET) was determined using a water balance equation; (Shukla, 2014).

$$ET = IR + R - \Delta S - RO - DP \quad (1)$$

where IR is the depth of irrigation (cm), R is rainfall (cm; R = 0), ΔS is the change in soil water storage between irrigations (cm; assumed= 0), RO is runoff (cm; RO= 0), and DP is the deep percolation (cm; leachate collected from the bottom of pots). Irrigations were made at a management allowed depletion of about 50 %.

2.4. Plant measurements

Each month, plant heights (from the base of the stem to the tip of the shoot), chlorophyll content, and leaf temperature were measured during the two harvests of the experiment using a tape measure, SPAD meter, and IR thermometer, respectively. The exact number of plants were allowed to grow for three months with no thinning during each harvest. At the end of each harvest, shoots were harvested and fresh weights were recorded. The shoots were dried in the oven at 65 °C for 48 h, and dry weights were recorded for biomass calculation. Dried shoots were ground and packed in small storage bags and sent to Ag Source Laboratory, Lincoln, Nebraska for chemical analysis along with irrigation water and leachate samples.

2.5. Soil bulk density and chemical analysis

Core samples were collected from each of the pots under irrigation salinity treatments at the end of the experiment. Soil bulk density was determined using cores (Blake and Hartge, 1986). Loose soil samples were collected from the pots, air-dried, mixed and sieved through a 2

mm sieve, prior to shipping them to the Ag Source Laboratories, Lincoln, Nebraska for chemical analysis.

Sodium adsorption ratio (SAR) was calculated based on (Robbins, 1983) using the following equation:

$$SAR = \frac{(Na^{+1})}{\sqrt{\frac{(Ca^{+2})+(Mg^{+2})}{2}}}$$

where [Na] is sodium ion concentration (meq/l), [Ca] is calcium ion concentration (meq/l), and [Mg] is magnesium ion concentration (meq/l).

2.6. Statistical analysis

The experimental design was a completely randomized design with four replications. All statistical analyses were performed using SAS software, v 9.4. Differences due to treatments on plant germination and growth were determined using one-way analysis of variance (ANOVA) and means were separated using the least significant difference (LSD). An alpha level of 0.05 was used to determine statistical significance.

3. Results

3.1. Greenhouse meteorology

Greenhouse temperatures ranged from 15.1 to 46.9 °C prior to first harvest, 13.4–33.5 °C before the second harvest, and 13.7–28.4 °C prior to the third harvest (Fig. 1). Relative humidity in the greenhouse ranged from 10 % to 88 %, 12 – 80 %, and 16.4–50.2 % for the three harvests, respectively (Fig. 1). Daily light integral (DLI) is important for

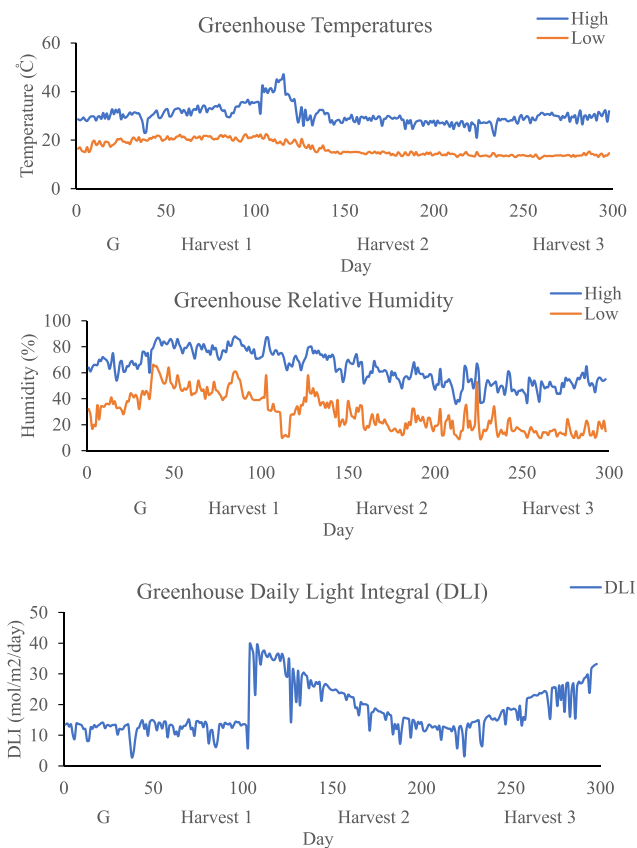


Fig. 1. Greenhouse data from May 22, 2021, to December 15, 2021, for temperature (°C), relative humidity (%), and daily light integral (mol/m²/day). G = Germination.

Table 2 Mean and standard error of seed germination (%) and two harvests of dry biomass (g) of five forages under irrigation with produced water.

Plant ID	Treatment TDS mg/l	Seed germination (%)		Dry biomass 1 (g)		Dry biomass 2 (g)		Cumulative biomass (g)
		Mean ± SE	Mean ± SE	Mean ± SE	Mean ± SE	Mean ± SE	Mean ± SE	
Wheatgrass	231	49 ± 3.70 a	0.79 ± 0.20 a	1.01 ± 0.08 b	1.80 ± 0.28 a			
	427	17 ± 5.00 b	0.79 ± 0.04 a	1.28 ± 0.07 a	2.07 ± 0.11 a			
	1400	23 ± 6.10 b	0.77 ± 0.08 a	1.34 ± 0.04 a	2.11 ± 0.09 a			
Alfalfa	8610	NA	NA	NA	NA			
	231	98 ± 2.00 a	3.76 ± 0.04 ab	4.59 ± 0.43 b	8.36 ± 0.98 b			
	427	88 ± 6.90 a	5.11 ± 0.57 a	8.73 ± 0.24 a	13.84 ± 0.44 a			
Bromegrass	1400	50 ± 17.10 b	2.18 ± 0.56 b	4.82 ± 0.44 b	7.00 ± 0.58 b			
	8610	NA	NA	NA	NA			
	231	86 ± 0.14 a	0.49 ± 0.12 b	0.87 ± 0.02 b	1.36 ± 0.10 a			
Russian wildrye	427	100 ± 0.00 a	0.91 ± 0.09 a	1.19 ± 0.10 a	2.10 ± 0.18 a			
	1400	100 ± 0.00 a	0.99 ± 0.47 a	0.94 ± 0.07 b	1.94 ± 0.47 a			
	8610	100 ± 0.00 a	NA	NA	NA			
Tall fescue	231	7 ± 1.90 b	0.60 ± 0.05 a	0.69 ± 0.09 a	1.29 ± 0.13 a			
	427	18 ± 3.80 a	0.62 ± 0.12 a	1.10 ± 0.30 a	1.72 ± 0.24 a			
	1400	9 ± 4.10 ab	0.52 ± 0.08 a	0.92 ± 0.03 a	1.45 ± 0.05 a			
Tall fescue	8610	NA	NA	NA	NA			
	231	100 ± 0.00 a	0.59 ± 0.09 ab	1.17 ± 0.16 a	1.76 ± 0.19 b			
	427	100 ± 0.00 a	1.25 ± 0.38 a	1.81 ± 0.08 a	3.07 ± 0.46 a			
Tall fescue	1400	100 ± 0.00 a	1.16 ± 0.27 a	1.86 ± 0.39 a	3.02 ± 0.57 a			
	8610	93 ± 7.00 a	0.30 ± 0.05 b	1.20 ± 0.30 a	1.50 ± 0.26 b			

Note: RO = 231 mg/l. Tap = 427 mg/l. Diluted RAW = 1400 mg/l. RAW = 8610 mg/l. TDS = total dissolved solids. Means within columns with same letter are not significant at α ≤ 0.05. NA= not available.

plant growth, development, yield and quality. DLI was 16.21, 19.82, and 18.63 mol/m²/day for the three harvests respectively (Fig. 1). At day 104 of the experiment period, greenhouse shade was removed which explained the increase in DLI at that time.

3.2. Seed germination

Table 2 shows the germination percentage of the five forage species. Only bromegrass and tall fescue germinated in RAW water (Table 2). Bromegrass had an 86 % germination in RO water but 100 % in RAW water; however, plants did not survive beyond the first month of

irrigation with RAW water (Table 2). A similar germination trend was observed for Alfalfa irrigated with RO and tap water; however, germination was 50 % in diluted RAW (Table 2). Russian wildrye had the lowest germination percentages in RO, tap, and diluted RAW followed by wheatgrass species (Table 2). Among the five forage species, tall fescue germinated well with all the irrigation treatments. Wheatgrass, alfalfa, and Russian wildrye germination significantly decreased with increases in salinity but none germinated in the soil irrigated with RAW water (Table 2).

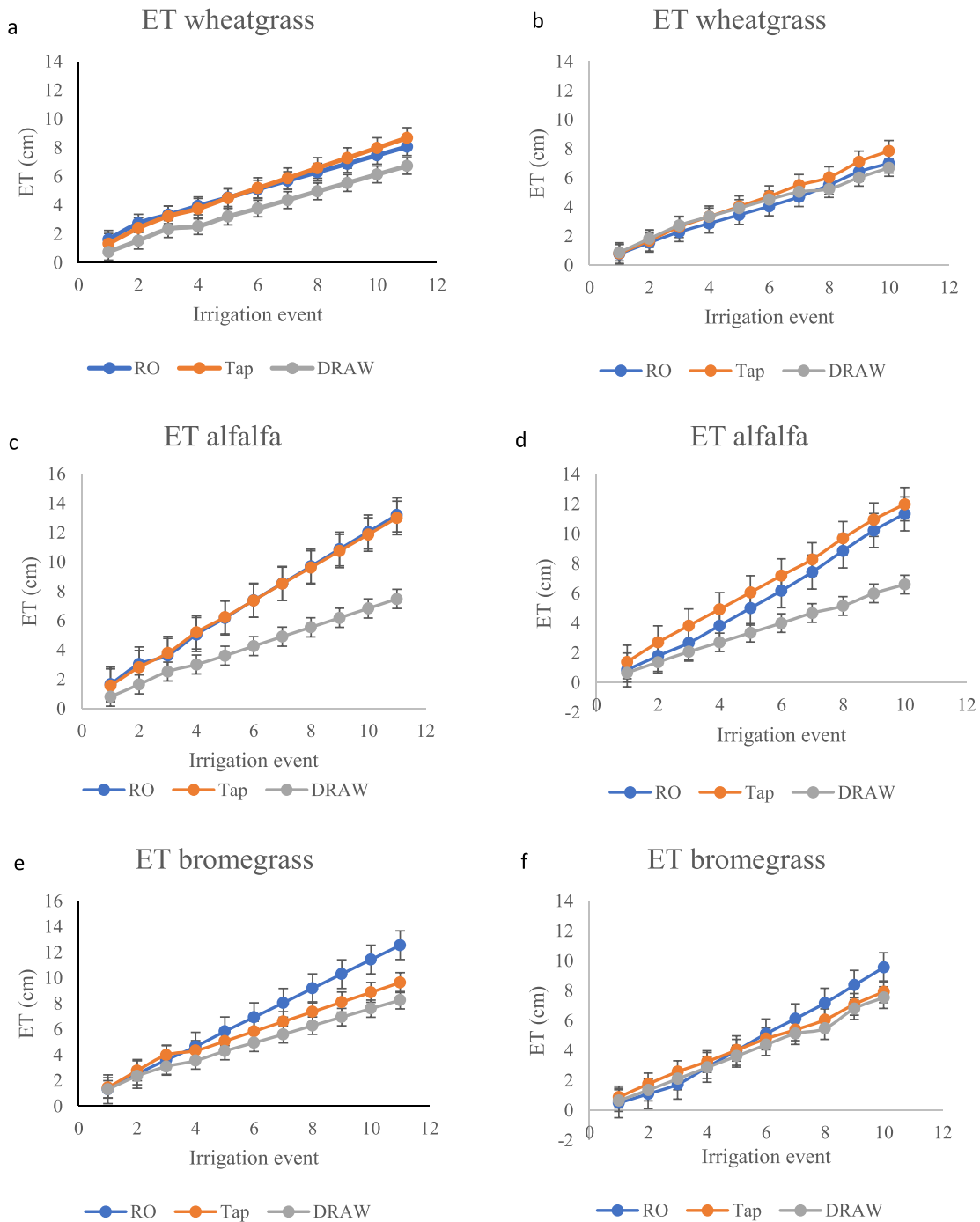


Fig. 2. Cumulative evapotranspiration ET (cm) of wheatgrass a, b, alfalfa c, d, bromegrass e, f, Russian wildrye g, h, and Tall fescue i, j irrigated with produced water during the two harvests. RO = 231 mg/l. Tap = 427 mg/l. Diluted RAW = 1400 mg/l. RAW = 8610 mg/l.

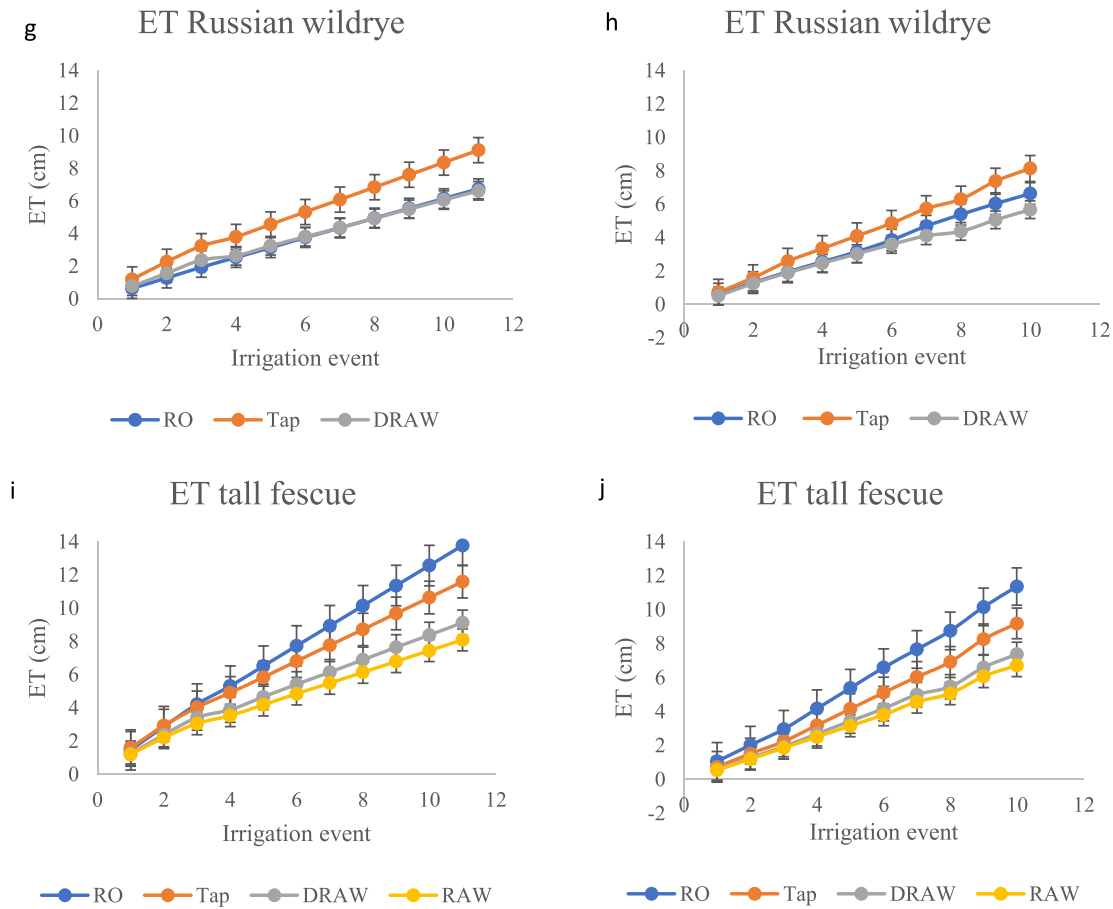


Fig. 2. (continued).

3.3. Plant dry biomass

Forage species dry biomass of the first harvest (biomass 1), and the second harvest (biomass 2) are presented in (Table 2). Wheatgrass dry biomass was similar in all the irrigation treatments in the first harvest (Table 2). In the second harvest, however, increase in dry biomass in all the three treatments was observed compared to the first harvest and the greater increase was in diluted RAW water followed by tap water (Table 2). Alfalfa dry biomass decreased in diluted RAW compared with tap water in the first harvest (Table 2). Increases in alfalfa dry biomass in all three treatments can be observed whereas alfalfa dry biomass in RO and diluted RAW water remained the lowest compared with tap water in the second harvest (Table 2). No differences were found in bromegrass dry biomass between the three treatments in the first harvest (Table 2). All three treatments showed increases in dry biomass in the second harvest while dry biomass was lower in RO and diluted RAW water, respectively, compared with tap water (Table 2). Russian wildrye dry biomass showed no differences in the first and the second harvests while the dry biomass increased in all treatments in the second harvest compared with first harvest (Table 2). In the first harvest, tall fescue dry biomass significantly decreased in RAW water compared with tap water; however, in the second harvest, all dry biomass increased with no significant differences observed (Table 2). Diluted RAW and RAW irrigation decreased wheatgrass, alfalfa, bromegrass, and tall fescue dry biomass. There were no statistically differences in cumulative biomass among the treatments for wheatgrass, bromegrass, and Russian wildrye (Table 2). However, the cumulative tall fescue biomass was lower in RO and RAW irrigated pots than other treatments. For alfalfa, the cumulative biomass was lower for RO and diluted RAW irrigated pots than other city or tap water (Table 2).

3.4. Evapotranspiration

Fig. 2a to j shows the cumulative ET for wheatgrass (western), alfalfa, bromegrass, Russian wildrye, and tall fescue. The results illustrated decreases in cumulative ET for all the five forages in diluted RAW and RAW (Fig. 2). As treatment salinity increased, wheatgrass, alfalfa, bromegrass, Russian wildrye, and tall fescue ET decreased for both harvests (Fig. 2). Pots irrigated with RAW water remained wetter than other treatments.

3.5. Plants heights and SPAD value

Table 3 shows the first measurement, in July, of the height and SPAD value of forage species during the first harvest. Wheatgrass (western) height and SPAD value were higher in diluted RAW irrigated water, than tap and RO treatments (Table 3). This trend was similar for the second measurement in August (Table 3). Alfalfa height was greater in RO treatment while SPAD value was slightly higher in diluted RAW with no significant differences than other treatments (Table 3). No differences were recorded in the second measurement in August for alfalfa heights and SPAD value (Table 3). For bromegrass, the lowest recorded height in July was in RAW irrigated water while the SPAD value was highest in RAW water (Table 3); however, bromegrass irrigated continuously with RAW irrigation died by August. In August, bromegrass SPAD was higher in tap water than diluted RAW and RO (Table 3).

Russian wildrye height was similar in RO, tap, and diluted RAW water while the SPAD value was higher in diluted RAW water than RO and tap water (Table 3). This trend shifted in August when height was greater in the diluted RAW irrigation with no differences observed in the SPAD value (Table 3). Greater tall fescue height was recorded in tap

Table 3
Mean and standard error of plant's heights (cm) and SPAD value irrigated with produced water (first harvest, July and August).

Plant ID	Treatment TDS mg/l	July		August	
		Height (cm)	SPAD	Height (cm)	SPAD
Wheatgrass	231	24.25 ± 2.09 b	4.67 ± 1.60 b	27.05 ± 3.04 b	4.58 ± 0.45 b
	427	31.65 ± 1.84 a	5.87 ± 1.00 b	34.25 ± 1.25 a	15.55 ± 2.93 ab
	1400	32.87 ± 1.98 a	12.42 ± 0.94 a	36.50 ± 1.94 a	25.20 ± 6.33 a
	8610	NA	NA	NA	NA
	231	24 ± 1.22 a	48.62 ± 1.92 a	30.00 ± 2.74 a	51.90 ± 2.30 a
	427	22.77 ± 0.75 ab	45.47 ± 2.54 a	30.25 ± 4.39 a	53.93 ± 2.73 a
Alfalfa	1400	19.37 ± 1.79 b	50.82 ± 2.33 a	28.00 ± 2.86 a	44.13 ± 6.35 a
	8610	NA	NA	NA	NA
	231	21.5 ± 1.51 a	2.85 ± 0.89 b	19.25 ± 2.25 a	8.13 ± 2.87 b
	427	23 ± 0.40 a	6.8 ± 1.14 a	23.63 ± 1.07 a	17.48 ± 2.99 a
	1400	20.75 ± 3.19 a	3.6 ± 0.58 b	23.75 ± 1.65 a	13.85 ± 2.71 ab
	8610	9.75 ± 0.87 b	7.67 ± 1.02 a	NA	NA
Russian wildrye	231	17.75 ± 1.56 a	9.35 ± 1.03 b	22.38 ± 1.55 b	15.83 ± 5.86 a
	427	23.85 ± 1.35 a	6.6 ± 1.10 b	28.50 ± 2.10 ab	17.00 ± 2.87 a
	1400	20.5 ± 3.95 a	32.85 ± 2.06 a	33.05 ± 2.54 a	23.55 ± 4.37 a
	8610	NA	NA	NA	NA
	231	20.3 ± 1.89 ab	8.27 ± 1.41c	22.50 ± 2.22 a	7.43 ± 2.04 b
	427	24.5 ± 1.37 a	16.75 ± 0.91 b	25.00 ± 2.52 a	14.13 ± 2.34 b
Tall fescue	1400	19.62 ± 1.86 ab	8.55 ± 0.73c	23.00 ± 1.22 a	12.53 ± 1.20 b
	8610	16.6 ± 1.80 b	24.82 ± 1.12 a	18.75 ± 2.69 a	22.90 ± 4.13 a

Note: RO = 231 mg/l. Tap = 427 mg/l. Diluted RAW = 1400 mg/l. RAW = 8610 mg/l. TDS = total dissolved solids. Means within columns with same the letter are not significant at $\alpha \leq 0.05$. NA= not available.

Table 4
Mean and standard error of plant heights (cm) and SPAD value irrigated with produced water (second harvest, October and November).

Plant ID	Treatment TDS mg/l	October		November	
		Height (cm)	SPAD	Height (cm)	SPAD
Wheatgrass	231	21.00 ± 1.73 b	23.68 ± 2.65 a	22.75 ± 2.10 b	10.48 ± 4.44 a
	427	27.25 ± 1.93 a	24.83 ± 3.35 a	29.25 ± 3.35 ab	19.83 ± 4.65 a
	1400	29.00 ± 0.91 a	28.95 ± 4.22 a	32.25 ± 2.75 a	21.40 ± 4.26 a
	8610	NA	NA	NA	NA
	231	18.75 ± 0.31 a	41.98 ± 3.80 a	20.75 ± 2.10 a	46.83 ± 4.04 a
	427	26.50 ± 4.35 a	49.78 ± 1.79 a	27.25 ± 3.99 a	34.00 ± 3.20 b
Brome grass	1400	17.00 ± 4.53 a	30.83 ± 1.58 b	26.25 ± 1.11 a	46.50 ± 3.21 a
	8610	NA	NA	NA	NA
	231	14.00 ± 0.82 a	11.23 ± 1.61 a	15.25 ± 2.72 a	16.68 ± 8.73 a
	427	17.00 ± 1.08 a	19.70 ± 2.82 a	16.75 ± 1.65 a	10.03 ± 4.49 a
	1400	16.25 ± 1.11 a	19.20 ± 4.01 a	18.25 ± 2.10 a	21.15 ± 3.08 a
	8610	NA	NA	NA	NA
Russian wildrye	231	16.50 ± 0.87 b	25.03 ± 2.91 ab	16.75 ± 1.49 a	8.38 ± 2.99 b
	427	21.75 ± 2.50 ab	21.50 ± 3.56 b	21.25 ± 0.85 a	15.55 ± 4.06 b
	1400	24.50 ± 2.72 a	33.45 ± 0.13 a	23.75 ± 3.75 a	27.80 ± 3.00 a
	8610	NA	NA	NA	NA
	231	13.25 ± 0.75 a	14.88 ± 2.46 a	11.5 ± 1.55 b	7.33 ± 3.60 b
	427	13.45 ± 0.63 a	15.83 ± 1.23 a	13 ± 1.41 b	9.73 ± 0.92 b
Tall fescue	1400	13.50 ± 1.32 a	11.58 ± 3.46 a	16 ± 1.08 ab	12.68 ± 4.27 ab
	8610	22.67 ± 2.75 a	29.00 ± 1.73 a	19 ± 3.03 a	22.15 ± 5.52 a

Note: RO = 231 mg/l. Tap = 427 mg/l. Diluted RAW = 1400 mg/l. RAW = 8610 mg/l. TDS = total dissolved solids. Means within columns with the same letter are not significant at $\alpha \leq 0.05$. NA= not available.

Table 5
Mean and standard error of Na, Mg, Ca, and Cl ion concentration (mg/l), SAR, and TDS (mg/l) of first sample leachate water, first harvest of five forages irrigated with produced water.

Plant ID	Treatment TDS mg/l	Na mg/l	Mg mg/l	Ca mg/l	SAR	Cl mg/l	EC mg/l
Wheatgrass (western)	231	275.70 ± 38.06 b	39.12 ± 13.89 b	229.24 ± 84.42 a	6.53 ± 0.31 b	693.33 ± 180.87 b	666 ± 0.51 b
	427	199.17 ± 6.44 b	47.99 ± 2.82 ab	210.48 ± 21.64 a	4.56 ± 0.07 b	589.33 ± 63.30 b	1624 ± 0.21 b
	1400	2341.47 ± 366.81 a	84.84 ± 22.70 a	391.6 ± 95.43 a	39.71 ± 1.30 a	1250 ± 170.59 a	6652 ± 1.23 a
Alfalfa	8610	NA	NA	NA	NA	NA	NA
	231	382.33 ± 72.86 b	57.41 ± 14.83 a	355.76 ± 97.75 a	7.05 ± 0.34 b	879.33 ± 189.83 b	2741 ± 0.88 b
	427	242.50 ± 23.10 b	80.03 ± 8.96 a	326.73 ± 34.03 a	4.39 ± 0.21 b	848 ± 91.08 b	2426 ± 0.30 b
Brome grass (Meadow)	1400	2893.83 ± 440.30 a	138.85 ± 43.16 a	533.32 ± 109.09 a	41.38 ± 3.09 a	1526.67 ± 229.35 a	8151 ± 1.90 a
	8610	NA	NA	NA	NA	NA	NA
	231	316.63 ± 40.07 b	35.13 ± 6.42 a	202.44 ± 36.35 b	7.68 ± 0.56 b	651 ± 99.12 b	1762 ± 0.35 b
Russian wildrye	427	211.88 ± 2.86 b	59.48 ± 3.66 a	228.18 ± 12.34 b	4.56 ± 0.14 b	627.67 ± 38.22 b	1754 ± 0.08 b
	1400	3371.97 ± 484.11 a	76.47 ± 19.46 a	499.1 ± 116.45 a	52.97 ± 1.00 a	1400 ± 183.79 a	8451 ± 1.82 a
	8610	NA	NA	NA	NA	NA	NA
Tall fescue	231	787.21 ± 367.18 b	59.42 ± 24.17 b	343.96 ± 142.73 a	13.7 ± 3.68c	1069.67 ± 374.75 b	2524 ± 0.86 b
	427	475.69 ± 248.23 b	104.3 ± 40.08 b	427.77 ± 166.78 a	6.92 ± 2.36c	1019.33 ± 314.85 b	1953 ± 0.29 b
	1400	2538.43 ± 176.79 b	51.11 ± 5.24 b	345.35 ± 24.54 a	47.95 ± 4.77 b	983 ± 30.47 b	6393 ± 0.14 b
Tall fescue	8610	21,617.7 ± 122.97 a	284.47 ± 73.73 a	336.87 ± 22.40 a	292.2 ± 37.97 a	1953.33 ± 214.29 a	10,232 ± 1.21 a
	231	161.09 ± 13.13c	14.63 ± 2.99 d	70.08 ± 10.44 d	6.57 ± 0.76c	216 ± 34.35 d	949 ± 0.17c
	427	227.21 ± 34.65c	56.01 ± 9.72c	31.23 ± 44.60c	4.9 ± 0.31c	570.33 ± 128.07c	1733 ± 0.41c
Tall fescue	1400	3106.57 ± 118.30 a	98.1 ± 7.02 b	541.43 ± 21.34 a	45.66 ± 2.81 b	1170 ± 11.56 b	7424 ± 0.88 b
	8610	21,778.3 ± 815.26 b	293.81 ± 14.70 a	345.25 ± 3.90 b	293.73 ± 15.97 a	2080 ± 46.24 a	17,290 ± 0.75 a

Note: RO = 231 mg/l. Tap = 427 mg/l. Diluted RAW = 1400 mg/l. RAW = 8610 mg/l. SAR = Sodium adsorption ratio; TDS = total dissolved solids. Means within columns with the same letter are not significant at $\alpha \leq 0.05$. NA = not available. EC = Electrical conductivity.

water while the lowest height was recorded in RAW water; whereas the SPAD value was greater in the RAW water in July (Table 3). A similar trend was observed in August (Table 3). Diluted RAW irrigation increased SPAD value of wheatgrass, and Russian wildrye while decreased the SPAD value of brome grass. Decreases in tall fescue heights as the irrigation water salinity increases.

In the second harvest, first and second measurements in October and November, wheatgrass height and SPAD value were greater numerically in diluted RAW than RO and tap water (Table 4). No differences were observed with regard to alfalfa height in October and November (Table 4) and the SPAD value was the lowest in diluted RAW irrigation and of with tap irrigation in October and November, respectively (Table 4). The observations illustrated no differences among the treatments with regard to brome grass height and SPAD value for both measurement time (Table 4). Russian wildrye was the tallest and SPAD value was the highest in diluted RAW water in October (Table 4). However, in November, no differences between the grass heights were observed; although, SPAD value remained higher in diluted RAW irrigation than RO and tap (Table 4). Tall fescue grass showed only numerical differences with regard to height and SPAD value with the RAW treatment in October (Table 4). In November, however, the height of 19 cm and SPAD value of 22.15 were recorded with RAW water (Table 4). Wheatgrass, Russian wildrye, and tall fescue height and SPAD value increased with increasing water salinity while alfalfa height and SPAD value decreased with increases in water salinity.

3.6. Leachate ions concentrate

Collected leachate water samples from all the five forage species showed increases in Na, Mg, Ca, and Cl ion concentration in produced water compared with the tap water for the two measurement times during the first harvest (Table 5). Large increases in Na ions followed by Cl from resulted leachate from the pots irrigated with RAW and diluted RAW water. Leachate water of the diluted RAW and RAW irrigation was considered sodic (SAR > 13) and saline (EC > 2800 mg/l) for the two times measurements for the first harvest (Table 5, S1). Similarly, in the second harvest, the ion concentrations were higher in the leachate water samples with increasing salt concentration of the irrigation treatment (Table 6, S2). Similar to the first harvest, leachate water in the second harvest was considered saline and sodic in RAW and diluted RAW irrigation (Table 6, S2). Increases in irrigation water salinity increased the leachate water Na, Mg, Ca, and Cl ions concentration and SAR.

3.7. Plants ion contents

The plant tissue samples, at the end of the first harvest, showed non-significant differences with regard to total N with increasing irrigation water salinity (Table 7). Alfalfa did not show a significant difference in phosphorus content with increasing treatment salinity (Table 7). Nonsignificant differences were observed in brome grass samples with regard to P, K, Ca, Mn, Fe, and S content with increasing irrigation water salinity (Tables 7, 8). Increasing irrigation water salinity did not significantly affect the content of P, Mg, Fe, and Al in Russian wildrye (Tables 7, 8). Increases in irrigation water salinity had no significant effect on the Mg, Ca, and Zn concentration in tall fescue (Table 7).

Increases in irrigation water salinity (diluted RAW) significantly decreased the concentration of P, K, Mg, Ca, Zn, Fe, and Al in wheatgrass tissue while Mn, S, and Na increased in wheatgrass tissue (Tables 7, 8). With the increases in water salinity (diluted RAW), K, and Ca in alfalfa decreased (Table 7) while Mg, Mn, S, and Na increased (Tables 7, 8). Increases in Mg, S, Zn, and Na content in brome grass can be observed with increases in water salinity (diluted RAW) whereas B decreased (Tables 7, 8). Russian wildrye showed significant increases in Mg, Mn, S, and Na ion concentrations with increases in irrigation water salinity (from RO to diluted RAW) (Tables 7, 8) while K, Ca, Zn, and B decreased (Tables 7, 8). Tall fescue's Fe, B, Al, S, and Na ion concentrations

increased with increases in water salinity (RAW) (Table 8); however, P, K, Mn, and B decreased (Tables 7, 8).

Tables 9 and 10 show the plants ion concentrations in the second harvest. The second harvest continued to show similar trends as the first harvest with regard to the ion concentration of forage species. Salts accumulation in plant tissues can be observed with increases in salt uptake when comparing the results of the two harvests; however, species survived both harvests and also grew back again after the second harvest with continued irrigation with the same treatments.

3.8. Soil bulk density, organic matter, pH, and electrical conductivity EC

Soil bulk density at the end of the experiment is presented in (Table 11). Within species, the results indicated a slight increase in soil bulk density with continued irrigation with diluted RAW; however, this increase was not statistically significant (Table 11). A significant increase in soil bulk density can be observed in RAW irrigated pots followed by diluted RAW within tall fescue illustrating that increases in irrigation water salinity increased soil bulk density (Table 11). Pots irrigated with RO and diluted RAW showed significant decline in soil OM % compared with the control for wheatgrass, alfalfa, bromegrass, and Russian wildrye species (Table 11). For tall fescue species, the decline in soil OM % continued in RO and diluted water; however, the lowest soil OM % was recorded in RAW water irrigated soil (Table 11). The soil pH trend was near neutral in RO water; however, alkalinity increased as water salinity increased (Table 11). Soil EC increased in diluted RAW for wheatgrass, alfalfa, bromegrass, and Russian wildrye pots. The highest EC recorded was in RAW water in tall fescue followed by diluted RAW (Table 11).

3.9. Soil ions concentrations

For wheatgrass, soil P, Fe, and B decreased with increases in salinity while K, S, Mg, Ca, Na significantly increased (Tables 12, 13). In alfalfa pots irrigated with diluted RAW, soil N, Fe, and B significantly decreased, while K, S, Na increased in pots irrigated with diluted RAW (Tables 12, 13). Reduction in soil K, Mg, Ca, and B ion concentrations resulted in diluted RAW whereas S, Na, increased in bromegrass pots irrigated with diluted RAW (Tables 12, 13). Russian wildrye pots showed increases in soil S and Na with increasing water salinity while K, Mg, and B decreased (Tables 12, 13). Increases were seen in soil P, S, Na, Mn and Fe ion concentrations in tall fescue pots irrigated with RAW water. However, Mg, Ca, and B decreased (Table 13). Soil SAR significantly increased in diluted RAW water pots of wheatgrass, alfalfa, and bromegrass and was considered saline soil but not sodic (Table 13). In tall fescue pots, soil in RAW water was considered saline and sodic (Table 13).

4. Discussion

4.1. Seed germination

Forage species germination results showed differences in their response to the four irrigation treatments. This could be due to their level of tolerance to various levels of saline water. Flores et al. (2015), with regard to germination rate, reported similarities between six halophytic species *X triticosecale*, *Atriplex canescens*, *Hordeum vulgare*, *Lepidium alyssoides*, *Distichlis stricta*, and *Panicum virgatum* irrigated with saline water up to 7000 mg/l. As results showed, russian wildrye germination percentage was the lowest among the species utilized in this study and that might be due to the seeds vitality since it was for all three treatments. As the level of salinity increased, alfalfa, wheatgrass, bromegrass, and Russian wildrye germination percentages decreased and never germinated under RAW water (8610 mg/l) and this emphasized that these species are more sensitive to increases in water salinity. Among the five species, tall fescue species germinated well with RAW

Table 6

Mean and standard error of Na, Mg, Ca, and Cl ion concentration (mg/l), SAR and TDS (mg/l) of first sample leachate water, second harvest of five forages irrigated with produced water.

Plant ID	Treatment TDS mg/l	Na mg/l	Mg mg/l	Ca mg/l	SAR	Cl mg/l	EC mg/l
Wheatgrass (western)	231	460.39 ± 60.36 b	13.65 ± 1.83 b	77.22 ± 10.55 b	17.84 ± 1.29 b	249.00 ± 35.54 b	1573 ± 0.40 b
	427	360.93 ± 59.31 b	34.27 ± 8.01 b	115.84 ± 25.80 b	10.70 ± 0.52 b	416.33 ± 104.29 b	1674 ± 0.19 b
	1400	3725.27 ± 621.55 a	134.17 ± 26.94 a	395.45 ± 41.31 a	57.72 ± 6.32 a	1586.67 ± 268.79 a	6892 ± 1.19 a
Alfalfa	231	313.42 ± 46.35c	8.48 ± 1.58 b	57.00 ± 12.05 b	14.60 ± 1.09 b	208.67 ± 36.49 b	2691 ± 0.85 b
	427	846.51 ± 177.99 b	92.52 ± 25.71 a	338.16 ± 133.16 a	15.24 ± 0.49 b	911.33 ± 222.96 a	2532 ± 0.26 b
	1400	1375.70 ± 60.71 a	43.26 ± 3.90 ab	184.77 ± 19.53 ab	33.52 ± 1.14 a	458.33 ± 25.16 ab	8310 ± 1.95 a
Bromegrass (Meadow)	8610	NA	NA	NA	NA	NA	NA
	231	365.40 ± 96.65 b	13.58 ± 3.81 b	78.23 ± 19.52 a	13.96 ± 1.93 b	251 ± 71.27 ab	1783 ± 0.36 b
	427	207.37 ± 27.23 b	25.47 ± 2.06 ab	76.71 ± 9.00 a	7.35 ± 0.60 b	221.67 ± 34.15 b	1793 ± 0.07 b
Russian wildrye	1400	1697.47 ± 306.40 a	31.95 ± 6.37 a	163.01 ± 39.54 a	45.07 ± 4.87 a	641.67 ± 180.84 a	8400 ± 1.65 a
	8610	NA	NA	NA	NA	NA	NA
	231	505.15 ± 178.93 b	13.82 ± 3.88 b	72.42 ± 16.09 b	19.38 ± 4.55 b	314 ± 127.71 b	2524 ± 0.75 b
Tall fescue	427	592.08 ± 60.15 b	52.88 ± 8.11 a	170.99 ± 31.02 ab	14.59 ± 1.99 b	687 ± 125.43 ab	2019 ± 0.24 b
	1400	2402.15 ± 408.01 a	43.50 ± 9.90 a	206.58 ± 48.65 a	56.14 ± 2.95 a	1050 ± 255.71 a	6481 ± 0.20 a
	8610	NA	NA	NA	NA	NA	NA
Tall fescue	231	256.69 ± 9.48c	14.91 ± 2.36 a	62.49 ± 6.71c	10.76 ± 0.30c	210.33 ± 14.33c	969 ± 0.14c
	427	281.63 ± 114.34c	29.45 ± 10.05 a	104.25 ± 35.09 BCE	8.43 ± 1.98c	366 ± 173.34 BCE	1760 ± 0.36c
	1400	2011.74 ± 430.18 b	52.50 ± 2.26 a	210.29 ± 68.39 b	46.42 ± 1.68 b	813.67 ± 231.08 b	7512 ± 0.55 b
8610	13.304 ± 443.29 a	61.13 ± 18.88 a	336.12 ± 2.10 a	247.69 ± 5.98 a	1846.67 ± 63.93 a	17,803 ± 0.80 a	

Note: RO = 231 mg/l. Tap = 427 mg/l. Diluted RAW = 1400 mg/l. RAW = 8610 mg/l. SAR = Sodium adsorption ratio, TDS = total dissolved solids. Means within columns with the same letter are not significant at $\alpha \leq 0.05$. NA = not available. EC = Electrical conductivity.

Table 7
Mean and standard error of total N, P, K, Mg, Ca, and Zn ion concentration (mg/l) in shoots of five forages irrigated with produced water (first harvest).

Plant ID	Treatment TDS mg/l	Total N mg/l	P mg/l	K mg/l	Mg mg/l	Ca mg/l	Zn mg/l
Wheatgrass (western)	231	11.18 ± 1.04 a	1.54 ± 0.01 ab	13.8 ± 0.70 a	1.97 ± 0.32 ab	4.7 ± 0.71 a	161 ± 13.33 a
	427	10.87 ± 0.29 a	1.92 ± 0.19 a	14.5 ± 0.30 a	2.57 ± 0.20 a	3.97 ± 0.20 ab	50.78 ± 16.53 b
	1400	10.55 ± 0.70 a	1.38 ± 0.08 b	10.6 ± 0.56 b	1.73 ± 0.12 b	2.63 ± 0.17 b	31.45 ± 4.40 b
	8610	NA	NA	NA	NA	NA	NA
Alfalfa	231	21.77 ± 0.79 a	1.04 ± 0.10 a	14.2 ± 0.18 a	2.77 ± 0.12 b	20.23 ± 1.36 a	70.35 ± 14.50 a
	427	21.03 ± 1.02 a	1.07 ± 0.12 a	13.4 ± 0.39 a	3.87 ± 0.46 a	22.37 ± 1.46 a	21.14 ± 4.23 b
	1400	20.4 ± 2.45 a	1.27 ± 0.07 a	7.87 ± 0.58 b	2.97 ± 0.20 ab	15.47 ± 0.67 b	27.37 ± 0.43 b
	8610	NA	NA	NA	NA	NA	NA
Bromegrass (Meadow)	231	11.6 ± 1.00 a	1.95 ± 0.20 a	18 ± 1.07 a	3.17 ± 0.18 b	14.17 ± 3.49 a	47.82 ± 7.66 a
	427	11.61 ± 0.88 a	1.72 ± 0.02 a	19.6 ± 0.83 a	4.4 ± 0.25 a	9.4 ± 0.65 a	21.36 ± 2.42 b
	1400	11.2 ± 0.25 a	1.49 ± 0.14 a	18.7 ± 0.48 a	3.47 ± 0.37 ab	7.2 ± 1.21 a	31.24 ± 4.52 ab
	8610	NA	NA	NA	NA	NA	NA
Russian wildrye	231	16.83 ± 1.73 a	1.94 ± 0.26 a	21.9 ± 0.80 a	3.2 ± 0.25 a	8.13 ± 0.03 a	77.91 ± 3.40 a
	427	29.1 ± 10.54 a	2.02 ± 0.12 a	19.3 ± 0.84 a	4.2 ± 0.32 a	6.3 ± 0.55 b	42.89 ± 12.18 b
	1400	17.2 ± 0.93 a	1.66 ± 0.14 a	15.9 ± 0.70 b	3.23 ± 0.45 a	4.97 ± 0.69 b	42.52 ± 2.16 b
	8610	NA	NA	NA	NA	NA	NA
Tall fescue	231	11.37 ± 0.93 a	2.42 ± 0.12 a	11.7 ± 0.72 ab	7.03 ± 0.47 a	8.6 ± 0.57 a	47.27 ± 7.80 a
	427	12.14 ± 3.21 a	2.41 ± 0.28 a	15.1 ± 1.21 a	7.17 ± 0.90 a	9.7 ± 1.55 a	41.12 ± 5.34 a
	1400	9.38 ± 0.15 a	1.55 ± 0.09 b	9.17 ± 0.77 b	4.53 ± 0.18 a	6.57 ± 0.27 a	29.16 ± 3.87 a
	8610	13.73 ± 0.95 a	1.17 ± 0.28 b	8.73 ± 2.22 b	5.17 ± 1.27 a	17.1 ± 12.13 a	68.7 ± 19.45 a

Note: RO = 231 mg/l. Tap = 427 mg/l. Diluted RAW = 1400 mg/l. RAW = 8610 mg/l. TDS = total dissolved solids. Means within columns with the same letter are not significant at $\alpha \leq 0.05$. NA = not available.

Table 8
Mean and standard error of Mn, Fe, B, Al, S, and Na ion concentration (mg/l) in shoots of five forages irrigated with produced water (first harvest).

Plant ID	Treatment TDS mg/l	Mn mg/l	Fe mg/l	B mg/l	Al mg/l	S mg/l	Na mg/l
Wheatgrass (western)	231	79.64 ± 2.68 b	367.85 ± 8.92 a	237.35 ± 2.71 a	214 ± 4.82 a	3.4 ± 0.38 b	7.38 ± 0.60 b
	427	75.61 ± 11.79 b	48.7 ± 8.49 b	14.99 ± 1.60 b	17.15 ± 3.15 b	2.57 ± 0.03 b	7.15 ± 1.14 b
	1400	113.9 ± 6.18 a	28.38 ± 0.97 b	19.18 ± 2.01 b	11.71 ± 0.48 b	5.73 ± 0.43 a	11.5 ± 0.81 a
	8610	NA	NA	NA	NA	NA	NA
Alfalfa	231	217.95 ± 5.80 a	103.45 ± 5.38 a	369.19 ± 5.51 b	45.67 ± 2.68 a	7.5 ± 1.35 b	11.7 ± 2.86 b
	427	65.31 ± 0.53 b	76.62 ± 2.02 b	80.86 ± 2.01 b	36.23 ± 5.06 a	5.97 ± 1.88 b	7.11 ± 2.18 b
	1400	142.6 ± 3.84 ab	87.33 ± 1.32 b	125.84 ± 3.98 a	31.49 ± 1.15 a	22.73 ± 2.02 a	42.7 ± 2.96 a
	8610	NA	NA	NA	NA	NA	NA
Bromegrass (Meadow)	231	186.5 ± 5.59 a	81.08 ± 1.74 a	737.82 ± 4.40 a	55.87 ± 2.02 a	8.7 ± 1.23 b	16.08 ± 1.48 b
	427	134.22 ± 5.91 a	61.76 ± 1.43 a	35.93 ± 1.60 b	45.15 ± 2.39 a	5.93 ± 0.62 b	13.43 ± 0.90 b
	1400	166.98 ± 9.93 a	60.12 ± 6.88 a	101.09 ± 9.76 b	44.08 ± 2.63 a	20.83 ± 2.80 a	44.96 ± 3.70 a
	8610	NA	NA	NA	NA	NA	NA
Russian wildrye	231	119.97 ± 5.58 a	129.78 ± 9.61 a	413.17 ± 5.97 a	94.26 ± 3.18 a	5.97 ± 0.41 b	16.16 ± 1.95 b
	427	64.35 ± 1.80 b	49.4 ± 1.69 a	22.45 ± 0.64 b	31.56 ± 1.58 a	3.43 ± 0.26c	8.20 ± 1.24 b
	1400	130.4 ± 10.21 a	66.35 ± 4.57 a	53.47 ± 2.79 b	44.04 ± 2.42 a	13.57 ± 0.60 a	33.62 ± 3.59 a
	8610	NA	NA	NA	NA	NA	NA
Tall fescue	231	336.14 ± 6.11 b	96.03 ± 4.78 b	306.95 ± 4.94 a	75.09 ± 2.82 ab	9.03 ± 2.07 b	24.27 ± 3.79 BCE
	427	326.84 ± 8.47 b	75.34 ± 1.29 b	35.89 ± 2.36c	60.1 ± 1.96 ab	5.33 ± 1.16 b	15.95 ± 3.66c
	1400	552.8 ± 7.11 a	80.68 ± 5.84 b	77.76 ± 4.57 BCE	48.48 ± 2.34 b	17.33 ± 0.50 b	35.61 ± 1.56 b
	8610	136.33 ± 5.36c	138.46 ± 8.37 a	159.95 ± 8.80 b	94 ± 3.76 a	45.2 ± 15.50 a	70.20 ± 8.12 a

Note: RO = 231 mg/l. Tap = 427 mg/l. Diluted RAW = 1400 mg/l. RAW = 8610 mg/l. TDS = total dissolved solids. Means within columns with the same letter are not significant at $\alpha \leq 0.05$. NA = not available.

Table 9
Mean and standard error of Total N, P, K, Mg, Ca, Zn, and Mn ion concentration (mg/l) in shoots of five forages irrigated with produced water (second harvest).

Plant ID	Treatment	TDS mg/l	Mean \pm SE						
			Total N mg/l	P mg/l	K mg/l	Mg mg/l	Ca mg/l	Zn mg/l	Mn mg/l
Wheatgrass (western)	231		7.30 \pm 0.20 b	1.17 \pm 0.09 b	9.5 \pm 0.30 b	1.83 \pm 0.13 a	5.03 \pm 0.34 a	24.32 \pm 3.27 a	83.01 \pm 5.74 b
	427		8.79 \pm 0.45 a	1.53 \pm 0.07 a	12 \pm 0.55 a	2.2 \pm 0.31 a	4.8 \pm 0.61 a	22.86 \pm 1.35 a	61.56 \pm 7.81 b
	1400		8.43 \pm 0.36 ab	1.23 \pm 0.07 b	9.27 \pm 0.38 b	2.03 \pm 0.19 a	3.77 \pm 0.32 a	18.3 \pm 2.21 a	131.55 \pm 7.32 a
Alfalfa	8610		NA	NA	NA	NA	NA	NA	NA
	231		31.27 \pm 6.33 a	0.95 \pm 0.05 b	10.2 \pm 1.35 a	2.63 \pm 0.24 b	19.47 \pm 0.64 b	19.1 \pm 3.85 ab	195.14 \pm 7.31 a
	427		29.53 \pm 2.11 a	0.88 \pm 0.07 b	10.7 \pm 1.51 a	5.03 \pm 0.44 a	30.07 \pm 1.32 a	18.28 \pm 2.45 b	80.89 \pm 1.91 b
Brome grass (Meadow)	1400		35.53 \pm 2.14 a	1.94 \pm 0.05 a	10.3 \pm 1.74 a	2.3 \pm 0.15 b	12.7 \pm 1.74c	30.04 \pm 3.33 a	64 \pm 1.65 b
	8610		NA	NA	NA	NA	NA	NA	NA
	231		11.7 \pm 0.46 b	2.93 \pm 0.09 a	20.97 \pm 0.38 a	3.27 \pm 0.12 b	12.3 \pm 0.21 a	19.3 \pm 0.90 a	96.1 \pm 6.41 a
Russian wildrye	427		12.5 \pm 0.73 ab	2.21 \pm 0.10 b	19.4 \pm 0.85 ab	4.87 \pm 0.20 a	13.4 \pm 0.93 a	16.24 \pm 1.87 a	78.53 \pm 4.05 a
	1400		14.43 \pm 1.30 a	1.74 \pm 0.31 a	16.37 \pm 1.2 a	3.33 \pm 0.29 b	13.37 \pm 2.15 a	16.69 \pm 4.32 a	90.38 \pm 9.96 a
	8610		NA	NA	NA	NA	NA	NA	NA
Tall fescue	231		11.99 \pm 1.22 a	2.04 \pm 0.34 a	16.97 \pm 0.37 a	3.7 \pm 0.17 b	8 \pm 0.21 a	16.02 \pm 2.46 a	66.23 \pm 1.17 b
	427		12.57 \pm 0.24 a	1.81 \pm 0.16 a	17.83 \pm 0.18 a	5.1 \pm 0.40 a	9.03 \pm 0.56 a	16.43 \pm 2.34 a	45.78 \pm 3.01 b
	1400		14.43 \pm 1.30 a	1.74 \pm 0.31 a	16.37 \pm 1.2 a	3.73 \pm 0.43 b	7.27 \pm 1.11 a	17.79 \pm 2.79 a	122.08 \pm 1.32 a
Tall fescue	8610		NA	NA	NA	NA	NA	NA	NA
	231		10.45 \pm 0.96 a	2.07 \pm 0.25 a	12.87 \pm 1.19 a	4.43 \pm 0.33 a	8.9 \pm 0.93 a	20.73 \pm 1.14 a	232.86 \pm 9.79 b
	427		10.39 \pm 0.43 a	1.74 \pm 0.08 a	12.9 \pm 0.44 a	4.3 \pm 0.40 a	9.07 \pm 0.56 a	19.05 \pm 1.54 a	228.77 \pm 9.29 b
Tall fescue	1400		15.67 \pm 4.27 a	1.96 \pm 0.03 a	12.33 \pm 1.67 a	3.4 \pm 0.36 a	6.93 \pm 0.72 a	21.74 \pm 1.76 a	616.45 \pm 7.41 a
	8610		15.13 \pm 1.25 a	1.96 \pm 0.27 a	14.8 \pm 1.90 a	1.47 \pm 0.20 b	4.1 \pm 0.32 b	13.45 \pm 1.00 b	225.01 \pm 5.80 b

Note: RO = 231 mg/l. Tap = 427 mg/l. Diluted RAW = 1400 mg/l. RAW = 8610 mg/l. TDS = total dissolved solids. Means within columns with the same letter are not significant at $\alpha \leq 0.05$. NA= not available.

Table 10

Mean and standard error of Fe, B, Al, S, Cl, and Na ion concentration (mg/l) in shoots of five forages irrigated with produced water (second harvest).

Plant ID	Treatment	TDS mg/l	Mean \pm SE						
			Fe mg/l	B mg/l	Al mg/l	S mg/l	Cl mg/l	Na mg/l	
Wheatgrass (western)	231		105.07 \pm 4.13 a	391.68 \pm 3.19 a	79.06 \pm 5.67 a	1.77 \pm 0.07 b	11.9 \pm 1.68 a	3.06 \pm 0.10 b	
	427		40.56 \pm 0.19 a	15.96 \pm 0.61 b	21.66 \pm 1.51 a	2.57 \pm 0.53 ab	16.23 \pm 0.91 a	4.84 \pm 1.92 ab	
	1400		43.05 \pm 2.72 a	42.31 \pm 1.97 b	24.74 \pm 2.68 a	4 \pm 0.76 a	13.6 \pm 0.34 a	10.7 \pm 2.35 a	
Alfalfa	8610		NA	NA	NA	NA	NA	NA	
	231		173.73 \pm 7.58 a	520.86 \pm 9.65 a	44.99 \pm 4.22 a	3.87 \pm 0.62 b	13.9 \pm 0.55 a	8.43 \pm 0.85 b	
	427		131.98 \pm 2.97 a	132.2 \pm 2.93 b	77.74 \pm 3.55 a	5.2 \pm 0.45 b	14.07 \pm 0.94 a	5.82 \pm 1.05 b	
Brome grass (Meadow)	1400		150.08 \pm 6.90 a	140.57 \pm 5.54 b	69.41 \pm 3.93 a	12.17 \pm 0.93 a	17.17 \pm 0.16 a	24.79 \pm 4.41 a	
	8610		NA	NA	NA	NA	NA	NA	
	231		148.65 \pm 4.80 a	791.16 \pm 9.71 a	102.14 \pm 1.52 a	4.97 \pm 0.24 b	9.03 \pm 0.18 a	7.72 \pm 0.65 b	
Russian wildrye	427		98.33 \pm 1.08 a	33.37 \pm 3.50 b	92.13 \pm 2.21 a	7.1 \pm 0.35 b	14.17 \pm 0.36 a	13.34 \pm 0.66 b	
	1400		92.64 \pm 1.55 a	92.53 \pm 4.20 b	48.86 \pm 0.09 a	14.57 \pm 2.47 a	25.63 \pm 0.71 a	27.78 \pm 5.43 a	
	8610		NA	NA	NA	NA	NA	NA	
Tall fescue	231		87.98 \pm 2.38 a	388.53 \pm 8.28 a	42.04 \pm 0.50 a	4.4 \pm 0.47 a	16.53 \pm 0.69 a	11.02 \pm 0.97 b	
	427		65.82 \pm 3.68 a	22.17 \pm 0.66 b	48.11 \pm 4.31 a	4.5 \pm 0.36 a	10.87 \pm 0.02 a	11.36 \pm 1.08 ab	
	1400		72.74 \pm 4.48 a	59.65 \pm 9.96 b	7.5 \pm 1.51 a	14.6 \pm 0.70 a	14.6 \pm 0.70 a	18.06 \pm 3.17 a	
Tall fescue	8610		NA	NA	NA	NA	NA	NA	
	231		70.18 \pm 1.76 a	686.45 \pm 6.20 a	39.8 \pm 0.10 ab	5.63 \pm 0.04 BCE	18.3 \pm 0.20 a	10.83 \pm 1.54 BCE	
	427		72.29 \pm 3.45 a	31.79 \pm 3.85 b	49.4 \pm 0.67 a	4.17 \pm 0.12c	16.1 \pm 1.75 a	8.22 \pm 1.19c	
Tall fescue	1400		74.8 \pm 6.66 a	93.72 \pm 4.61 b	38.5 \pm 0.25 ab	7.8 \pm 0.40 b	76.4 \pm 0.03 a	16.55 \pm 1.98 b	
	8610		75.05 \pm 9.23 a	207.58 \pm 4.52 b	30.52 \pm 0.19 b	12.6 \pm 0.91 a	35.57 \pm 0.95 a	33.62 \pm 4.00 a	

Note: RO = 231 mg/l. Tap = 427 mg/l. Diluted RAW = 1400 mg/l. RAW = 8610 mg/l. TDS = total dissolved solids. Means within columns with the same letter are not significant at $\alpha \leq 0.05$. NA= not available.

Table 11
Mean and standard error of soil bulk density (g/cm^3), Organic matter OM (%), pH, and EC (mg/l) irrigated with produced water.

Plant ID	Treatment TDS mg/l		Soil bulk density g/cm^3		OM %	pH	EC mg/l
	231	427	Mean	SE			
Wheatgrass (western)	231	427	1.30 ± 0.05 b	0.67 ± 0.03 b	0.67 ± 0.03 b	7.53 ± 0.15 b	401.3 ± 91.76 b
	1400		1.49 ± 0.03 a	0.93 ± 0.03 a	0.93 ± 0.03 a	8.3 ± 0.06 a	140 ± 25.26c
Alfalfa	231	427	1.51 ± 0.06 a	0.77 ± 0.07 b	0.77 ± 0.07 b	8.4 ± 0.00 a	877.3 ± 67.86 a
	1400		1.51 ± 0.03 a	0.67 ± 0.03 b	0.67 ± 0.03 b	7.63 ± 0.20 b	165.6 ± 30.36 b
Bromegrass (Meadow)	231	427	1.53 ± 0.05 a	1.07 ± 0.03 a	1.07 ± 0.03 a	8.27 ± 0.03 a	135.3 ± 16.84 b
	1400		1.52 ± 0.10 a	0.77 ± 0.03 b	0.77 ± 0.03 b	8.4 ± 0.00 a	938 ± 112.20 a
Russian wildrye	231	427	1.54 ± 0.06 a	0.60 ± 0.00 b	0.60 ± 0.00 b	7.63 ± 0.12 b	233.3 ± 100.77 b
	1400		1.56 ± 0.03 a	0.90 ± 0.06 a	0.90 ± 0.06 a	8.1 ± 0.06 a	177.3 ± 18.24 b
Tall fescue	231	427	1.60 ± 0.01 a	0.53 ± 0.03 b	0.53 ± 0.03 b	8.27 ± 0.03 a	1064 ± 37.08 a
	1400		1.58 ± 0.03 a	0.60 ± 0.00 b	0.60 ± 0.00 b	7.67 ± 0.09 b	133 ± 4.04 b
Tall fescue	231	427	1.54 ± 0.03 a	0.90 ± 0.06 a	0.90 ± 0.06 a	8.17 ± 0.03 a	172.6 ± 14.20 b
	1400		1.60 ± 0.04 a	0.60 ± 0.00 b	0.60 ± 0.00 b	8.23 ± 0.09 a	966 ± 71.58 a
Tall fescue	231	427	1.56 ± 0.01 ab	0.80 ± 0.00 ab	0.80 ± 0.00 ab	8.23 ± 0.03 a	165.6 ± 24.72c
	1400		1.50 ± 0.03 b	0.90 ± 0.10 a	0.90 ± 0.10 a	8.13 ± 0.09 a	205.3 ± 26.94c
Tall fescue	231	427	1.60 ± 0.01 ab	0.63 ± 0.03 BCE	0.63 ± 0.03 BCE	8.17 ± 0.03 a	1008 ± 50.53 b
	8610		1.61 ± 0.04 a	0.50 ± 0.00c	0.50 ± 0.00c	8.13 ± 0.03 a	1726.6 ± 61.80 a

Note: RO = 231 mg/l . Tap = 427 mg/l . Diluted RAW = 1400 mg/l . RAW = 8610 mg/l . TDS = total dissolved solids. EC = Electrical conductivity. Means within columns with the same letter are not significant at $\alpha \leq 0.05$.

Table 12
Mean and standard error of N, P, K, S, Zn, and Mn ion concentrations in soil irrigated with produced water.

Plant ID	Treatment TDS mg/l		N mg/l	P mg/l	K mg/l	S mg/l	Zn mg/l	Mn mg/l
	231	427						
Wheatgrass	231	427	3.57 ± 0.13 b	4.67 ± 0.67 b	60.67 ± 0.67 b	41.33 ± 2.34 b	0.61 ± 0.11 a	0.87 ± 0.19 a
	1400		6.3 ± 0.75 a	8 ± 0.00 a	112 ± 11.55 a	34 ± 11.55 b	0.55 ± 0.06 a	0.43 ± 0.07 a
Wheatgrass	231	427	4.4 ± 0.81 ab	6.3 ± 0.88 ab	114.33 ± 6.18 a	494.67 ± 41.24 a	1.21 ± 0.34 a	0.93 ± 0.24 a
	1400		12.6 ± 3.14 a	5.33 ± 1.33 a	56 ± 7.01 b	25 ± 1.53 b	1.31 ± 0.58 a	2.13 ± 0.15 a
Alfalfa	231	427	6.67 ± 0.86 ab	4.67 ± 0.67 a	100.33 ± 6.34 a	21 ± 1.16 b	0.84 ± 0.07 a	3.33 ± 1.84 a
	1400		4.23 ± 0.37 b	4.33 ± 0.33 a	105.33 ± 7.81 a	288 ± 31.99 a	0.36 ± 0.03 a	1.93 ± 0.47 a
Bromegrass	231	427	3.6 ± 0.36 a	4.33 ± 1.33 a	66 ± 2.52 b	31.33 ± 1.45 b	0.85 ± 0.27 a	0.93 ± 0.07 a
	1400		5.63 ± 0.50 a	8.67 ± 2.19 a	111 ± 7.78 a	42.67 ± 4.92 b	0.80 ± 0.13 a	0.70 ± 0.10 a
Bromegrass	231	427	5.8 ± 0.95 a	8 ± 1.00 a	81.67 ± 0.33 b	323.33 ± 20.43 a	0.51 ± 0.06 a	1.40 ± 0.65 a
	1400		2.97 ± 0.12 a	5.33 ± 0.67 b	63.33 ± 4.92c	30 ± 3.79 b	0.40 ± 0.01 a	0.83 ± 0.23 a
Russian wildrye	231	427	5.67 ± 2.04 a	9.67 ± 0.88 a	127.67 ± 2.91 a	33.67 ± 3.85 b	0.62 ± 0.16 a	0.53 ± 0.09 a
	1400		5.53 ± 0.27 a	8.33 ± 0.33 a	90.33 ± 1.86 b	295.33 ± 76.08 a	0.52 ± 0.06 a	1.10 ± 0.15 a
Tall fescue	231	427	2.73 ± 0.22 a	5.33 ± 1.33 b	80.67 ± 51.00 a	51 ± 13.13c	0.84 ± 0.03 a	0.57 ± 0.12 b
	1400		5.07 ± 2.22 a	5.33 ± 0.33 b	96.33 ± 10.68 a	50.33 ± 26.99c	0.90 ± 0.41 a	0.60 ± 0.00 b
Tall fescue	231	427	4.8 ± 0.93 a	7 ± 0.58 b	81.33 ± 2.97 a	211.67 ± 73.87 b	0.73 ± 0.19 a	0.97 ± 0.17 b
	8610		4.73 ± 0.12 a	10.3 ± 0.67 a	99.67 ± 7.06 a	982.67 ± 20.19 a	0.60 ± 0.05 a	1.93 ± 0.23 a

Note: RO = 231 mg/l . Tap = 427 mg/l . Diluted RAW = 1400 mg/l . RAW = 8610 mg/l . TDS = total dissolved solids. Means within columns with the same letter are not significant at $\alpha \leq 0.05$.

Table 13
Mean and standard error of Mg, Ca, Na, Fe, and B ion concentrations and SAR in soil irrigated with produced water.

Plant ID	Treatment TDS mg/l	Mg mg/l	Ca mg/l	Na mg/l	SAR	Fe mg/l	B mg/l
Wheatgrass	231	105.67 ± 0.88 b	849.67 ± 25.74 b	267.33 ± 25.16 b	3.25 ± 0.34 b	11.2 ± 1.71 a	3.87 ± 0.24 a
Wheatgrass	427	277.67 ± 38.83 a	2393.6 ± 291.88 a	187.33 ± 37.40 b	1.38 ± 0.30c	5.1 ± 0.36 b	0.90 ± 0.06c
Wheatgrass	1400	254.67 ± 33.93 a	2191 ± 245.19 a	1173 ± 18.93 a	9.01 ± 0.61 a	5 ± 0.20 b	2.10 ± 0.15 b
Alfalfa	231	119.67 ± 5.21c	1008 ± 170.03 b	220.33 ± 30.05 b	2.52 ± 0.46 b	21.13 ± 2.27 a	2.43 ± 0.29 a
Alfalfa	427	360 ± 19.70 a	2692 ± 194.99 a	186.33 ± 13.26 b	1.26 ± 0.07c	11.8 ± 1.85 b	0.73 ± 0.07c
Alfalfa	1400	259.67 ± 36.60 b	1909 ± 310.77 a	1047 ± 74.01 a	8.51 ± 0.42 a	9.73 ± 2.14 b	1.70 ± 0.17 b
Bromegrass	231	108.67 ± 3.76 b	963 ± 97.97 b	209.33 ± 12.16 b	2.41 ± 0.06 b	10.47 ± 0.62 a	3.07 ± 0.13 a
Bromegrass	427	312 ± 30.04 a	2417.6 ± 223.78 a	250.67 ± 25.79 b	1.79 ± 0.10 b	8.60 ± 1.40 a	0.77 ± 0.09c
Bromegrass	1400	130 ± 7.10 b	1050.67 ± 72.50 b	874.67 ± 54.61 a	9.61 ± 0.82 a	8.30 ± 2.18 a	1.37 ± 0.09 b
Russian wildrye	231	101.33 ± 5.90 b	785 ± 13.44c	203 ± 18.79 b	2.56 ± 0.23 a	9.97 ± 1.97 a	3.03 ± 0.20 a
Russian wildrye	427	301.67 ± 20.54 a	2359.3 ± 183.15 a	243 ± 28.97 ab	1.79 ± 0.26 a	6.33 ± 1.09 a	0.80 ± 0.10c
Russian wildrye	1400	145.67 ± 8.96 b	1397.3 ± 189.28 b	782 ± 272.71 a	7.89 ± 3.19 a	6.07 ± 1.59 a	1.60 ± 0.26 b
Tall fescue	231	219 ± 13.07 ab	1766 ± 65.01 ab	265.33 ± 45.75c	2.22 ± 0.34c	7.13 ± 0.32 ab	4.67 ± 0.57 a
Tall fescue	427	283.67 ± 49.93 a	2248 ± 423.53 a	234 ± 62.37c	1.72 ± 0.34c	6.43 ± 0.73 b	0.80 ± 0.10c
Tall fescue	1400	150.67 ± 8.66 BCE	1162.3 ± 46.16 BCE	666.6 ± 166.89 b	6.84 ± 1.62 b	8.17 ± 1.20 ab	1.33 ± 0.23c
Tall fescue	8610	39 ± 4.36c	920.67 ± 27.32c	197.4 ± 7.65 a	24.5 ± 0.27 a	10.37 ± 1.44 a	3.17 ± 0.15 b

Note: RO = 231 mg/l. Tap = 427 mg/l. Diluted RAW = 1400 mg/l. RAW = 8610 mg/l. TDS = total dissolved solids. SAR = Sodium adsorption ratio. Means within columns with the same letter are not significant at $\alpha \leq 0.05$.

water which shows suitability of this species for irrigation with RAW water.

4.2. Plant dry biomass

Within species, alfalfa biomass decreased with diluted RAW; however, compared with other species, alfalfa produced higher dry biomass in RO, tap and diluted RAW water. This could be due to the rapid growth of alfalfa aboveground biomass compared with the other grass species. This agrees with a previous study comparing the growth of alfalfa and triticale irrigated with various levels of saline water up to 5600 mg/l where alfalfa growth decreased with increasing irrigation water salinity (Kankarla et al., 2019). Barley (*Hordeum vulgare*) grew well with high biomass as the irrigation treatment salinity increased (Katerji et al., 2009). In contrast, with increasing water salinity, Khan and Glenn (1996) reported reduction in barley biomass. Tall fescue grew well in RAW up to 8610 mg/l; therefore, it can be considered a halophyte. Kankarla et al. (2019) and Ozturk et al. (2018) reported no reduction in triticale biomass irrigated with 5600 and 7000 mg/l saline water, respectively, which agrees with our finding for tall fescue species.

4.3. Evapotranspiration

Continuous irrigation with saline water caused decreases in cumulative ET for all five species and resulted in decreased plant growth and biomass. Yang et al. (2020) reported related results when ET of tomato decreased with increasing irrigation water salinity ranged between 1400 and 4200 mg/l. On accord with this study, decreases in pecan ET with increasing irrigation water salinity up to 5600 mg/l have been reported (Ben Ali et al., 2021). However, no changes in plant biomass and ET were reported when irrigation up to 7000 mg/l was applied to halophytic species (Ozturk et al., 2018).

4.4. Plant height and SPAD value

The results indicated no significant changes in the forage species with continued irrigation with diluted RAW and tall fescue with RAW water irrigation. On the contrary, Pessaraki (2011) reported decreases in salt-grass species *Distichlis spicata* L. shoot length with increasing water salinity. SPAD value was higher in tap and diluted RAW water irrigated plants than with RO treatment. A decrease in chlorophyll content was reported on pecan leaves irrigated with water up to 5600 mg/l (Ben Ali et al., 2020). Tomato chlorophyll content decreased with increases in salinity (Taffou et al., 2010; Zhang et al., 2016). Li et al. (2018) reported decreases in chlorophyll content of *Eremochloa ophiuroids* irrigated with NaCl dominant saline water.

4.5. Plant ion contents

Three major tools to distinguish ions toxicity are plant analysis, soil testing, and field observations (McCauley et al., 2009). The irrigation water showed increases in Na, Ca, Mg, and Cl with increasing salinity of water. These ions respond in one of paths: leach out of the soil, accumulate in the soil, or accumulate in plants tissue by root water uptake. As the results indicated, Na, Ca, Mg, and Cl ions presented in the plants' tissues increased as the treatment salinity increased. Wheatgrass, alfalfa, brome grass, Russian wildrye, and tall fescue gained and accumulate Na and Cl and which may have led to the decreases in the biomass by increasing water salinity. These results are consistent with a previous study that applied saline water on alfalfa and triticale (Kankarla et al., 2019). Pica et al. (2017) reported that produced water with a Na concentration of 1156 mg/l inhibited sweet wormwood and switchgrass growth.

Tall fescue thrived and grew back after the two harvests despite the Na content in RAW water being 59 times greater than in the control,

demonstrating that tall fescue is more tolerant to high Na levels than other species. A previous study reported that the tolerance of tissue to accumulated Na or Cl, osmotic stress tolerance, and Na or Cl exclusion are the three adaptation types of plant to salinity stress (Munns and Tester, 2008), and plants differ in their response to Na and Cl accumulation (Tavakkoli et al., 2010). Ca performs a significant role in mitigating salt toxicity, which is associated with the selective effect of K/Na by controlling the flow of Na through non-selective ion channels (Rahnesan et al., 2018). The results showed decreases in Ca in RAW irrigated species meaning that tall fescue might have the potential of utilizing Na for growth while higher Ca might assist wheatgrass, alfalfa, bromegrass, and Russian wildrye to reduce the toxic effects of Na on their growth. This role might be the reason for the grasses' survival since the increases in Na were higher with increases in the treatment's salinity; however, these plants might have a mechanism that controls the increases in Na and Cl by sequestering these ions in the vacuoles to manage low concentrations in the cytoplasm therefore resulting in good metabolism (Kankarla et al., 2019).

Nitrogen is responsible for Nucleic acid, chlorophyll, and protein production (McCauley et al., 2009). Magnesium has a key role on enzyme activation and is related to chlorophyll content (Ben Ali et al., 2020). In our study, Mg declined as the irrigation water increased, which might explain the increases in chlorophyll content by increasing water salinity. A previous study mentioned that increased Mg decreased chlorophyll content of pecan trees irrigated with saline water up to 5600 mg/l (Ben Ali et al., 2020). Phosphorus reduction causes interruption in cell signaling and protein synthesis (Epstein and Bloom, 2005). Our results showed decreases in P concentration in the forage tissues with increasing water salinity. These results agreed with a previous study (Hussain et al., 2014).

Potassium's role is to activate enzymes contributed with ATP production and to regulate photosynthetic presses (Epstein and Bloom, 2005). The increases in Na might eliminate plant K uptake and interrupt photosynthesis regulation (Hussain et al., 2014). In this study, K decreased in wheatgrass, bromegrass, and tall fescue tissues with increased Na concentration. The sulfur ion is important for chlorophyll and protein synthesis (McCauley et al., 2009). Our results showed increases in S ions when water salinity increased. Zinc is used primarily for internode elongation and chlorophyll therefore any deficiency can affect the plants growth (McCauley et al., 2009). The forage species presented reduction in Zn as the irrigation water salinity increased; however, growth was not affected.

Iron is a principal element for plant respiration (McCauley et al., 2009). Fe decreased with increased water salinity; however, the plant's growth was not clearly affected. Manganese is important in chloroplasts where photosynthesis takes place (McCauley et al., 2009). In this study, Mn declined with increased water salinity with all the forage species. Boron has a role on cell wall formation and reproductive tissue (McCauley et al., 2009). Boron can be toxic to plants; however, plants are varied in acceptable concentrations that they can manage (McCauley et al., 2009). Even with the increases in B concentration in the forages irrigated with RO and RAW, plant species did not show any signs of B toxicity such as chlorosis and necrosis, meaning that the plants could have managed the increase in B concentration. One exception was with bromegrass showing signs of B toxicity due to the increases in B concentration with RO irrigation treatment.

4.6. Soil bulk density, organic matter, pH, and EC

As the water salinity increased with continuous irrigation, soil bulk density increased. This was due to salt precipitation in the soil pores with attendant decreases in the pores size. In contrast, Al-Nabulsi (2001) reported decreases in soil bulk density when irrigated with 7700 mg/l sodic drainage water while Ben Ali et al. (2021) reported no differences with continuous irrigation with saline water up to 5600 mg/l. Our results indicated significant reduction in soil OM % as the salinity

increased. In agreement with our findings, Zhang et al. (2019) also reported a reduction in OM % and increases in alkalinity with increasing salinity. Results indicated that as the irrigation water salinity increased, soil EC significantly increased. This increase, however, was not as large as expected and this was due to the leaching fraction, which ranged between 40 % and 50 % of the irrigation water amount which prevented salt build up in the soil. According to Ayres and Wescot, (1985) leachate of 50 % could control salt build up in the soil reflecting in reduced salt accumulation in plants. In consent with this study, previous greenhouse studies reported greater increases in soil EC than ours along with continued irrigation with brackish water (EC 2870 – 7000 mg/l) to irrigate halophytic species (Flores et al., 2016; Ozturk et al., 2018).

4.7. Leachate and soil ion concentrations

Leaching, accumulation, and root uptake are the three major pathways for water and soil ion transport. Irrigation with produced water could increase salinity and sodicity, which can be observed on leachate water results collected from the pots. As the water salinity concentration increased, the leachate became more saline and sodic. The increase in treatment salinity led to leaching of Mg, Ca, Na, and Cl in the collected leachate samples. Comparable results were reported with alfalfa species irrigated with various levels of saline water (Kankarla et al., 2019). Compared to the control irrigated soil, soil Na concentration was five times higher in diluted RAW water in wheatgrass and alfalfa pots while it was around three times in bromegrass and Russian wildrye pots. Due to the increases in Na ion concentration as the water salinity increased, soil SAR increased and reached 24.46, which is highly sodic. From the observed data, tall fescue had the ability to utilize Na ions to build up its biomass in RAW water and that might explain the decline in Na ions in RAW water irrigated soil compared to other species. Bromegrass and alfalfa could not maintain an adequate Ca/Na ratio and that resulted in the decline in biomass in diluted RAW water compared to the control. Potassium has been reported to increase the soil microporosity resulting in increases in soil moisture capacity (Zaker and Emami, 2019). This was observed in the greenhouse in tall fescue pots irrigated with RAW water and those pots remained wet for longer durations than other pots. In consent with our results, soil irrigated with reverse osmosis concentrate remained wet for longer than control treatment (Ben Ali et al., 2021). To control salt build up in plant tissues, plants might reduce the root water uptake as a mechanism to survive the unpreparable conditions (Munns and Tester, 2008).

Toxicity is usually related to boron, sodium and chloride concentrations (Ayres and Wescot, 1985). Toxic and excessive levels of boron has been reported in arid and semi-arid regions (Padbhushan and Kumar, 2017). Based on soil saturated extract, 5–10 mg/l soil boron concentration represent semi-tolerant and tolerant plants respectively while the toxicity threshold begins at 2 mg/l soil boron concentration for sensitive plants (Gough et al., 1980). Our boron results exceeded the threshold of 2 mg/l, as reported previously, in RO, diluted RAW, and RAW for all species; however, toxicity signs were observed in bromegrass species. A previous study reported reduction in boron toxicity in wheat, numerous vegetables, and rootstock with increasing in salinity (Henry Ezechi et al., 2012). This could be what happened with those plants with increases in salinity, thus surviving two harvests. Munns and Tester (2008) reported that in soil, 40 mM (\approx 2800 mg/l) of NaCl concentration is toxic for most of the plants species. Soil sodium concentration, in this study was about 1974 mg/l in RAW water in tall fescue pots, which is the highest concentration among all the species. Toxicity level differs among plants species and depends on the plant's sensitivity for salts type and concentration; thus, some plants are sensitive to Na while others are more sensitive for Cl (Ayres and Wescot, 1985). Some water, plant, and soil ion concentrations thresholds are included in (Table S3). To confirm our results, continuous irrigation with the same treatments, after the second harvest, resulted in those species growing well again for two more full harvests. This provides the evidence of the

feasibility to utilize desalinated and diluted produced waters for irrigating forage plants.

5. Conclusion

The present study investigated the effects of irrigating western wheatgrass, alfalfa, meadow bromegrass, Russian wildrye, and tall fescue with RO desalinated produced water, Tap water, diluted RAW produced water, and RAW produced water as a valuable source of water in arid areas. Desalination of produced water reduced the salt buildup in soil and plants. ET decreased with increasing water salinity but wheatgrass, alfalfa, bromegrass, and Russian wildrye grew well during two harvests of the experiment and grew back again with continued RO, tap, and diluted RAW irrigation after the second harvest; however, tall fescue survived even the RAW irrigation. Alfalfa biomass decreased in diluted RAW water while tall fescue was a tolerant species and can be irrigated with higher salinity water. Increasing soil salinity is a major issue when considering irrigation with produced water; however, a good leaching ratio, especially in areas where water tables are deep, can reduce Na, Cl, and other ions from building up in the rootzone and in plant tissue. Boron toxicity symptoms were noticed only in the meadow bromegrass. There was no sign of toxicity regarding Na and Cl in all the surviving plants in this study with continued irrigation with saline water. The research results promote the feasibility of using desalinated and diluted produced water to irrigate forage grasses; however, an effective monitoring system is required especially when RAW or diluted RAW is used for irrigation.

Declaration of Competing Interest

The authors declare that they have no known competing financial interests or personal relationships that could have appeared to influence the work reported in this paper.

Data Availability

Data will be made available on request.

Acknowledgment

The authors are thankful to NMSU Agricultural Experiment Station, NIFA, HPOC, LLC, and Brackish Groundwater National Desalination Research Facility in Alamogordo, New Mexico.

Appendix A. Supporting information

Supplementary data associated with this article can be found in the online version at [doi:10.1016/j.agwat.2022.107966](https://doi.org/10.1016/j.agwat.2022.107966).

References

- Al-Nabulsi, Y.A., 2001. Saline drainage water, irrigation frequency and crop species effects on some physical properties of soils. *J. Agron. Crop Sci.* 186 (1), 15–20.
- Ayers, R., Westcot, D., 1985. *Water quality for agriculture*. In: *Irrigation and Drainage, Paper, 29*. Food and Agriculture Organization of the United Nations, Rome, p. 174.
- Ben Ali, A.R., Yang, H., Shukla, M., 2021. Brackish groundwater and reverse osmosis concentrate influence soil physical and thermal properties and pecan evapotranspiration. *Soil Sci. Soc. Am. J.* 85 (5), 1519–1533. <https://doi.org/10.1002/saj2.20281>.
- Ben Ali, A.R., Shukla, M.K., Schutte, B.J., Gard, C.C., 2020. Irrigation with RO concentrate and brackish groundwater impacts pecan tree growth and physiology. *Agric. Water Manag.* 240, 106328 <https://doi.org/10.1016/j.agwat.2020.106328>.
- Biggs, A.J., Biggs, A.J.W., Witheyman, S.L., Williams, K.M., Cupples, N., De Voil, C.A., Power, R.E. and Stone, B.J., 2012. Assessing the salinity impacts of coal seam gas water on landscapes and surface streams. Department of Natural Resources.
- Blake, G.R., Hartge, K.H., 1986. Particle density. *Methods Soil Anal.: Part 1 Phys. Mineral. Methods* 5, 377–382. <https://doi.org/10.2136/sssabookser5.1.2ed.c13>.
- Burkhardt, A., Gawde, A., Cantrell, C.L., Baxter, H.L., Joyce, B.L., Stewart Jr, C.N., Zheljzakov, V.D., 2015. Effects of produced water on soil characteristics, plant biomass, and secondary metabolites. *J. Environ. Qual.* 44 (6), 1938–1947. <https://doi.org/10.2134/jeq2015.06.0299>.
- Clark, C.E. and Veil, J.A., 2009. Produced water volumes and management practices in the United States (No. ANL/EVS/R-09-1). Argonne National Lab.(ANL), Argonne, IL (United States).
- Echchel, A., Hess, T., Sakrabani, R., 2020. Agro-environmental sustainability and financial cost of reusing gas field-produced water for agricultural irrigation. *Agric. Water Manag.* 227, 105860 <https://doi.org/10.1016/j.agwat.2019.105860>.
- Epstein, E., Bloom, A.J., 2005. *Mineral nutrition of plants: Principles and perspective*. 2nd ed. Sinauer Associates, Sunderland.
- Farooq, H., Bashir, M.A., Khalofah, A., Khan, K.A., Ramzan, M., Hussain, A., Wu, L., Simunek, L., Aziz, I., Samdani, M.S., Alghanem, S.M., 2021. Interactive effects of saline water irrigation and nitrogen fertilization on tomato growth and yield. *Fresenius Environ. Bull.* 30 (04), 3557–3564.
- Flores, A.M., Schutte, B.J., Shukla, M.K., Picchioni, G.A., Ulerly, A.L., 2015. Time-integrated measurements of seed germination for salt tolerant plant species. *Seed Sci. Technol.* 43 (3), 541–547. <https://doi.org/10.15258/sst.2015.43.3.09>.
- Flores, A.M., Shukla, M.K., Daniel, D., Ulerly, A.L., Schutte, B.J., Picchioni, G.A., Fernald, S., 2016. Evapotranspiration changes with irrigation using saline groundwater and RO concentrate. *J. Arid Environ.* 131, 35–45.
- Gough, L.P., Pearson, R.C., Shacklette, H.T. and Case, A.A., 1980. *Element Concentrations Toxic to Plants, Animals, and Man: An Appraisal of the Toxicity Hazard to Plants, Animals, and Man from Natural and Manmade Element Concentrations of Environmental Concern* (No. 1463–1467). US Government Printing Office.
- Henry Ezechi, E., Isa, M.H., Mohamed Kutty, S.R., 2012. Boron in Produced Water: Challenges and Improvements: A Comprehensive Review. *J. Appl. Sci.* 12, 402–415. <https://doi.org/10.3923/jas.2012.402.415>.
- Hussain, R.A., Ahmad, R., Waraich, E.A., Nawaz, F., 2014. Nutrient uptake, water relations, and yield performance of different wheat cultivars (*Triticum aestivum* L.) under salinity stress. *J. Plant Nutr.* 35, 961–974.
- Kankarla, V., Shukla, M.K., VanLeeuwen, D., Schutte, B.J., Picchioni, G.A., 2019. Growth, evapotranspiration, and ion uptake characteristics of alfalfa and triticale irrigated with brackish groundwater and desalination concentrate. *Agronomy* 9 (12), 789. <https://doi.org/10.3390/agronomy9120789>.
- Katerji, N., Mastroianni, M., Van Hoorn, J.W., Lahmer, F.Z., Hamdy, A., Oweis, T., 2009. Durum wheat and barley productivity in saline-drought environments. *Eur. J. Agron.* 31 (1), 1–9. <https://doi.org/10.1016/j.eja.2009.01.003>.
- Khan, M.J., Glenn, E.P., 1996. Yield and evapotranspiration of two barley varieties as affected by sodium chloride salinity and leaching fraction in lysimeter tanks. *Commun. Soil Sci. Plant Anal.* 27 (1–2), 157–177. <https://doi.org/10.1080/00103629609369550>.
- Li, J., Wan, Y., Wang, B., Waqas, M.A., Cai, W., Guo, C., Zhou, S., Su, R., Qin, X., Gao, Q., Wilkes, A., 2018. Combination of modified nitrogen fertilizers and water saving irrigation can reduce greenhouse gas emissions and increase rice yield. *Geoderma* 315, 1–10. <https://doi.org/10.1016/j.geoderma.2017.11.033>.
- Martel-Valles, F., Benavides-Mendoza, A., Mendoza-Villarreal, R., Zermeño-González, A., Juárez-Maldonado, A., 2014. Agronomic use of produced water in tomato plants (*Lycopersicon esculentum* L.) under greenhouse conditions. *Rev. Int. De. Contam. Ambient.* 30 (4), 365–377. (http://www.scielo.org.mx/scielo.php?script=sci_abstract&pid=S0188-49992014000400005&lng=es&nrm=iso&tlang=en).
- McCauley, A., Jones, C., Jacobsen, J., 2009. Plant nutrient functions and deficiency and toxicity symptoms. *Nutr. Manag. Modul.* 9, 1–16.
- McLaughlin, M.C., Blotvogel, J., Watson, R.A., Schell, B., Blewett, T.A., Folkerts, E.J., Goss, G.G., Truong, L., Tanguay, R.L., Argueso, J.L., Borch, T., 2020. Mutagenicity assessment downstream of oil and gas produced water discharges intended for agricultural beneficial reuse. *Sci. Total Environ.* 715, 136944 <https://doi.org/10.1016/j.scitotenv.2020.136944>.
- Munns, R., 2005. Genes and salt tolerance: bringing them together. *N. Phytol.* 167 (3), 645–663. <https://doi.org/10.1111/j.1469-8137.2005.01487.x>.
- Munns, R., Tester, M., 2008. Mechanisms of salinity tolerance. *Annu. Rev. Plant Biol.* 59, 651–681. <https://doi.org/10.1146/annurev.arplant.59.032607.092911>.
- Ozturk, O.F., Shukla, M.K., Stringam, B., Picchioni, G.A., Gard, C., 2018. Irrigation with brackish water changes evapotranspiration, growth and ion uptake of halophytes. *Agric. Water Manag.* 195, 142–153. <https://doi.org/10.1016/j.agwat.2017.10.012>.
- Padbhushan, R., Kumar, D., 2017. Fractions of soil boron: a review. *J. Agric. Sci.* 155 (7), 1023–1032.
- Pessaraki, M., 2011. Saltgrass, a high salt and drought tolerant species for sustainable agriculture in desert regions. *Int. J. Water Resour. Arid Environ.* 1 (1), 55–64.
- Pica, N.E., Carlson, K., Steiner, J.J., Waskom, R., 2017. Produced water reuse for irrigation of non-food biofuel crops: Effects on switchgrass and rapeseed germination, physiology and biomass yield. *Ind. Crops Prod.* 100, 65–76. <https://doi.org/10.1016/j.indcrop.2017.02.011>.
- Rahneshan, Z., Nasibi, F., Moghadam, A.A., 2018. Effects of salinity stress on some growth, physiological, biochemical parameters and nutrients in two pistachio (*Pistacia vera* L.) rootstocks. *J. Plant Interact.* 13 (1), 73–82.
- Robbins, C.W., 1983. Sodium adsorption ratio-exchangeable sodium percentage relationships in a high potassium saline-sodic soil. *Irrig. Sci.* 5 (3), 173–179.
- Shukla, M.K., 2014. *Soil Physics: An Introduction*. CRC Press, Boca Raton, FL, p. 58.
- Sun, Y., Niu, G., Dou, H., Perez, C., Alexander, L., 2022. Growth, gas exchange, and mineral nutrients of hydrangea hybrids irrigated with saline water. *HortScience* 57 (2), 319–325. <https://doi.org/10.21273/HORTSCI6196-21>.
- Taffou, V.D., Nouck, A.H., Dibong, S.D., Amougou, A., 2010. Effects of salinity stress on seedlings growth, mineral nutrients and total chlorophyll of some tomato (*Lycopersicon esculentum* L.) cultivars. *Afr. J. Biotechnol.* 9 (33) <https://doi.org/10.4314/ajb.v9i33>.

- Tavakkoli, E., Rengasamy, P., McDonald, G.K., 2010. High concentrations of Na⁺ and Cl⁻ ions in soil solution have simultaneous detrimental effects on growth of faba bean under salinity stress. *J. Exp. Bot.* 61 (15), 4449–4459. <https://doi.org/10.1093/jxb/erq251>.
- Veil, J.A., 2011. Produced water management options and technologies. In: Lee, K., Neff, J. (Eds.), *Produced Water: Environmental Risks and Advances in Mitigation Technologies* (. Springer, pp. 537–571. https://doi.org/10.1007/978-1-4614-0046-2_29.
- Yang, H., Du, T., Mao, X., Shukla, M.K., 2020. Modeling tomato evapotranspiration and yield responses to salinity using different macroscopic reduction functions. *Vadose Zone J.* 19 (1), e20074 <https://doi.org/10.1002/vzj2.20074>.
- Zaker, M., Emami, H., 2019. Effect of potassium to bivalent cations ratio in irrigation water on some physical and hydraulic properties of sandy loam soil. *Soil & Environment*, 38, 1.
- Zhang, P., Senge, M., Dai, Y., 2016. Effects of salinity stress on growth, yield, fruit quality and water use efficiency of tomato under hydroponics system. *Rev. Agric. Sci.* 4, 46–55. <https://doi.org/10.7831/ras.4.46>.
- Zhang, W.W., Chong, W.A.N.G., Rui, X.U.E., Wang, L.J., 2019. Effects of salinity on the soil microbial community and soil fertility. *J. Integr. Agric.* 18 (6), 1360–1368.

Review

Interplay of the Factors Affecting Water Flux and Salt Rejection in Membrane Distillation: A State-of-the-Art Critical Review

Lin Chen , Pei Xu  and Huiyao Wang *

Department of Civil Engineering, New Mexico State University, Las Cruces, NM 88003, USA;
chenlin@nmsu.edu (L.C.); pxu@nmsu.edu (P.X.)

* Correspondence: huiyao@nmsu.edu

Received: 16 August 2020; Accepted: 10 October 2020; Published: 13 October 2020



Abstract: High water flux and elevated rejection of salts and contaminants are two primary goals for membrane distillation (MD). It is imperative to study the factors affecting water flux and solute transport in MD, the fundamental mechanisms, and practical applications to improve system performance. In this review, we analyzed in-depth the effects of membrane characteristics (e.g., membrane pore size and distribution, porosity, tortuosity, membrane thickness, hydrophobicity, and liquid entry pressure), feed solution composition (e.g., salts, non-volatile and volatile organics, surfactants such as non-ionic and ionic types, trace organic compounds, natural organic matter, and viscosity), and operating conditions (e.g., temperature, flow velocity, and membrane degradation during long-term operation). Intrinsic interactions between the feed solution and the membrane due to hydrophobic interaction and/or electro-interaction (electro-repulsion and adsorption on membrane surface) were also discussed. The interplay among the factors was developed to qualitatively predict water flux and salt rejection considering feed solution, membrane properties, and operating conditions. This review provides a structured understanding of the intrinsic mechanisms of the factors affecting mass transport, heat transfer, and salt rejection in MD and the intra-relationship between these factors from a systematic perspective.

Keywords: membrane distillation; desalination; water flux; salt rejection; solute transport; superhydrophobic membranes

1. Introduction

Freshwater scarcity is a grand challenge that threatens water security and economic development. Desalination and water reuse provides a viable solution to improving water security and alleviating water stress by expanding alternative water supplies, such as seawater, brackish water, wastewater, and other impaired water sources [1–3]. Current desalination technologies are energy intensive. For example, reverse osmosis (RO) is the most extensively implemented membrane technology for desalination. Although the specific energy consumption (SEC) of RO has been reduced significantly from 5–10 kWh/m³ to 3–4 kWh/m³ [4–6], energy consumption generally amounts to 50%–60% of the total water costs [7,8]. Worldwide fossil fuels such as crude oil, coal, and gas are non-renewable and have been diminishing rapidly. In addition, environmental issues associated with brine disposal pose a challenge to conventional desalination technologies. Developing transformational technologies using alternative energy sources is vital to reduce treatment costs, improve energy efficiency, enhance water supply resilience, and increase access to affordable, safe, and clean water.

Membrane distillation (MD) is a non-isothermal integrated process by combining thermal evaporation and membrane separation, which was first patented by Bodell in 1963 [9]. MD is driven by

the transmembrane temperature difference between the hot/warm feed side and the cold permeate side with a barrier of hydrophobic microporous membranes. Water vapor can pass through the hydrophobic pores inside the membranes and condense at the cold permeate side. MD can take advantage of solar energy, geothermal energy, and waste heat of industries to sustain the driving force. MD process covers a myriad of applications such as desalination [10–27], wastewater treatment [28–31], heavy metal removal [32], separation of organic solutes [33,34], treatment of water contaminated by arsenic [35] and boron [36], brine treatment or crystallization [37–40], and concentration of juice [41].

Studies on MD have advanced rapidly with a substantial increase in publications since 2010 (Figure 1). Recently, research on MD has focused on novel hydrophobic membranes with anti-wetting and anti-fouling properties for various MD applications [42–52], Janus membranes with significantly reduced specific energy consumption for MD [53,54], and hybrid MD systems [55–57]. In addition, since Lawson and Lloyd [58] published the extensively cited comprehensive review paper in 1997, numerous review papers covering various aspects of MD have been published. Recent reviews on MD have mainly focused on theoretical modeling [59–62], membrane fouling [63–65], energy efficiency analysis [66–72], MD performance criteria [73], design and fabrication of membranes for MD application [74–76], wettability of membranes [77–79], the influence of membrane properties on MD performance [80], hybrid MD systems [66,67], some specific fields of MD such as direct contact membrane distillation (DCMD) [81], vacuum membrane distillation (VMD) [82], air gap membrane distillation (AGMD) [83], ceramic membranes applied for MD [84], and perspective on sustainable and renewable desalination using MD [68,85]. These review papers have covered broad research areas including energy efficiency analysis, membrane development, effects of membrane properties and MD module configurations on MD performance, fouling and scaling control in MD, modeling heat transfer, and mass transfer in MD.

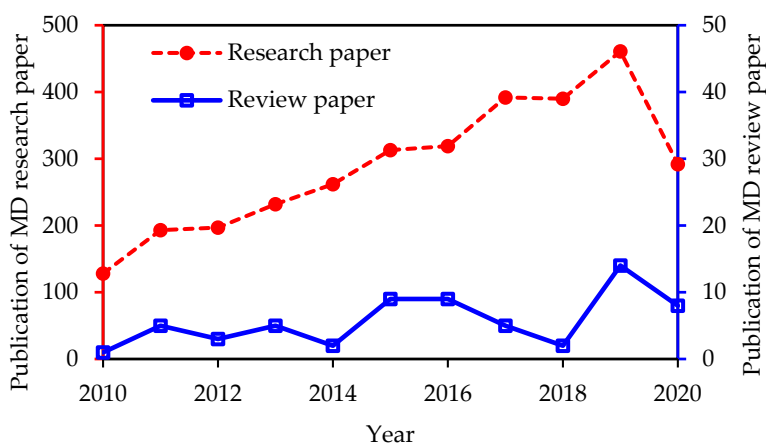


Figure 1. Number of publications on MD research papers and review papers from 2010 to August 2020 (obtained from Google Scholar).

However, there is a lack of systematic overview of factors affecting the water flux, salt rejection, and interactive correlations of both in terms of membrane properties, feedwater chemistry, long-term operation, and their physicochemical interactions for MD applications, especially in desalination. For example, a research paper by Schofield et al. [86] studied the factors affecting flux using sensitivity analysis. They concluded that vapor pressure reduction was the dominant factor for the flux decline of sodium chloride solution, while the viscosity for sucrose solution was the primary factor reducing the flux. Nevertheless, they did not analyze the effect of other factors such as membrane properties, the chemistry of the feed solution, and module parameters on water flux.

Based on Raoult's law, water vapor pressure decreases due to increasing salt concentration, thereby causing permeate flux reduction. However, Ozbey-Unal et al. [36] reported that water flux increased 1.1 to 1.3 folds when the salinity of the geothermal feedwater increased from 1.5 wt.% to 3.0 wt.% using polypropylene (PP) and polytetrafluoroethylene (PTFE) membranes in MD systems. Meanwhile,

permeate flux was not affected by salinity increase from 1.5 wt.% to 3.0 wt.% of the feed stream using polyvinylidene fluoride (PVDF) membrane. Although it is easy to understand that physical sieving and anti-wettability due to hydrophobicity of the membranes can together be considered to be the primary mechanism of salt rejection (SR) and water flux permeation, SR and permeation of water flux are complicated and have not been thoroughly explored and understood. In addition, aquatic chemistry of the feed solution, viscosity, and membrane properties such as thermal conductivity, thickness, pore size, pore size distribution (PSD), and porosity may significantly affect SR and water flux.

This review proposes a holistic system approach to understand and identify the factors affecting SR and permeate flux (solute transport) in MD for desalination and wastewater treatment. This review focuses on analysis and deliberations of membranes (e.g., wettability, pore size and PSD, porosity, thickness, tortuosity, thermal conductivity), feedwater chemistry (e.g., inorganic salts, colloidal particles, natural organic matters, volatile solutes), operating conditions (e.g., temperature, flow rate, operating mode, degasification, long-term operation) and their interactions on MD performance in terms of their impacts on flux and SR. Because energy analysis, membrane fabrication, MD configuration design, modeling, and membrane fouling have been discussed in other review papers, these are not the focus of this review. Based on the critical review and system analysis, a decision diagram was proposed to illustrate the effects of the primary factors involving membrane properties, feed solution compositions, operating conditions on SR, flux, and their intrinsic correlations. To the best of our knowledge, this review paper is the first that has proposed a decision framework to determine the factors and their interplay on MD performance.

2. Fundamentals of MD

2.1. Typical MD Configurations

Figure 2 illustrates the schematic diagram of four typical MD configurations, including direct contact membrane distillation (DCMD), air gap membrane distillation (AGMD), vacuum membrane distillation (VMD), and sweeping gas membrane distillation (SGMD) [87,88]. The feed stream is in direct contact with the hydrophobic membrane in all these MD configurations. The membrane contacts directly with the cold permeate stream in DCMD, which is the most used design for research because of its simplicity. In AGMD, there is a stagnant air gap between the membrane and the cooling plate over which the vapor condenses. In VMD, a vacuum pump is applied to provide a driving force to induce the vapor to penetrate the membrane pores and condense outside the VMD chamber. In SGMD, an inert gas is used to sweep the vapor at the permeate side and condense at the outside of the MD module [89].

2.2. Membranes in MD

In an MD process, the membrane is of vital importance to system performance. Because the fundamental requirement for the selected membrane is the hydrophobicity, which can be determined by the water contact angle (CA) of the membrane surface. MD cannot work if the membrane is hydrophilic, which means the CA of the membrane is less than 90° [90,91]. To maintain the hydrophobicity, the hydrostatic pressure induced by a flowing fluid should be below the liquid entry pressure (LEP) of the membrane to avoid pore wetting [92,93]. LEP can be calculated by the Laplace equation [58,94]:

$$LEP = \frac{-2B\gamma_l \cos \theta}{r_{max}} = \Delta P_{entry} > \Delta P_{interface} = P_f - P_p \quad (1)$$

where B is a geometry coefficient for pore structure, being unity for cylindrical pores, γ_l is the liquid surface tension (for water and common inorganic solution mixture, γ_l is equal to 72 mN/m at 25 °C), θ is the CA, r_{max} is the maximum allowable pore size of the membrane, P_f and P_p are the hydraulic pressure at feed and permeate sides. However, this equation does not consider the effects of operating temperature and feed solution composition on liquid surface tension.

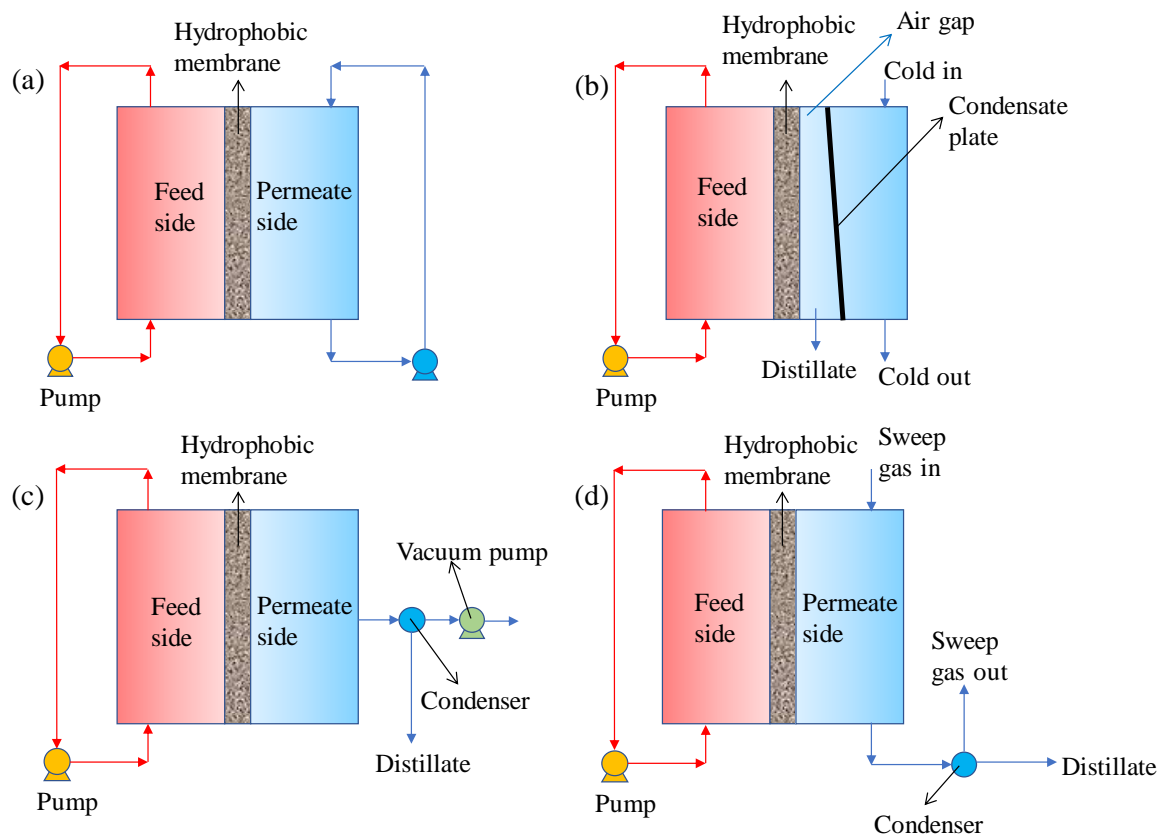


Figure 2. Schematic diagram of four typical MD configurations: (a) DCMD, (b) AGMD, (c) VMD, and (d) SGMD.

In addition, surface energy and surface roughness (or morphology) govern the characteristics of wettability of a solid surface [95,96] (i.e., the membrane surface in MD). Surface energy is the intrinsic property of a material including a membrane material. The maximum CA on a flat surface obtained was 119° using low surface energy material only (the recorded lowest surface energy value was 6.7 mJ/m^2 of a surface with regularly arrayed hexagonal-packed CF_3 groups) [97]. Other properties of the membrane such as thickness, pore size, PSD, porosity, thermal conductivity, mechanical strength, and chemical-resistance are generally considered to be factors affecting the performance of MD systems [73,87].

Anti-wetting or non-wetting surface of a membrane is what researchers expect in MD systems. The mechanism of wetting is very complex. Gostoli et al. [98] suggested that a high liquid surface tension facilitates a convex meniscus, which prevents the liquid from penetrating the membrane pores and forming a non-wetted liquid/vapor/membrane interface—a three-phase interface which maintains a stable hydrophobicity [96,99]. They considered the pressure difference arose from surface tension as the capillary pressure. The wetting will happen if the capillary pressure becomes greater than the partial vapor pressure across the membrane pores [79]. The capillary pressure mentioned here actually is the previously introduced term of *LEP*. To maintain a long-term stable hydrophobicity, a higher *LEP* is needed for a specific membrane. Therefore, smaller maximum pore size and higher surface tension result in a higher *LEP* based on Equation (1). Nevertheless, the maximum pore size should not be so small that the vapor molecules cannot pass through the membrane pores. There should be a “critical” value of the allowable maximum pore size. Because of the importance of pore size of the hydrophobic membrane and mean free path of water molecules on mass transfer mechanisms (Knudsen and molecular diffusion), these two factors are discussed in detail later.

2.3. Heat Transfer

Heat transfer and mass transfer occur simultaneously in MD systems. Figure 3 shows the schematic diagram of heat transfer and mass transfer in a DCMD.

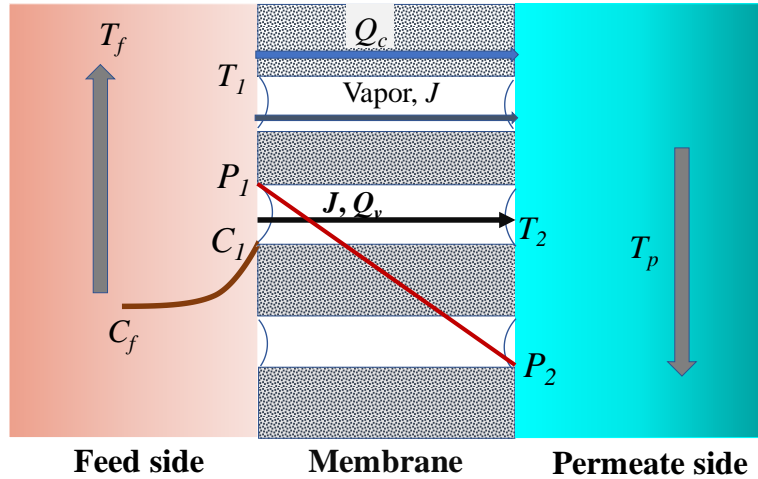


Figure 3. Schematic diagram of heat transfer and mass transfer in DCMD.

Generally, heat transfer can be divided into three steps [62]: (i) heat transfer from the bulk hot side to the hot liquid/membrane boundary layer (Q_f); (ii) heat transfer through the membrane ($Q_m = Q_v + Q_c$); (iii) heat transfer through the cold side liquid/membrane boundary layer (Q_p). At steady state, $Q_f = Q_m = Q_p = Q$, thus, the heat transferred from the hot side to the cold side can be described as follows [62]:

$$h_f(T_f - T_1) = \frac{k_m}{\delta}(T_1 - T_2) + J\Delta H_{v,w} = h_p(T_2 - T_p) = H(T_f - T_p) \quad (2)$$

The total heat flux Q is written as:

$$Q = \left[\frac{1}{h_f} + \frac{1}{\frac{k_m}{\delta} + \frac{J\Delta H_{v,w}}{\Delta T_m}} + \frac{1}{h_p} \right]^{-1} \Delta T = H(\Delta T) \quad (3)$$

where H is the overall heat transfer coefficient, h_f and h_p are the heat transfer coefficients at the bulk feed side and the bulk permeate side, T_f and T_p are the absolute temperature of the bulk solution at the feed side and permeate side respectively, T_1 and T_2 are the interfacial temperature of the membrane surface at feed and permeate side, respectively, ΔT ($\Delta T = T_f - T_p$) is the global temperature difference between feed and permeate side, ΔT_m ($\Delta T_m = T_1 - T_2$) is the transmembrane temperature difference, k_m is the overall thermal conductivity of the membrane, δ is the thickness of the membrane, $\Delta H_{v,w}$ is the latent heat of vaporization of water and can be estimated by equation [58]: $\Delta H_{v,w} = 1.7535T + 2024.3$, where T is the absolute temperature in K. In addition, h_f and h_p are expressed using Equations (4) and (5) based on Nusselt number (Nu).

$$h_f = \frac{Nu_f k_f}{d_h} \quad (4)$$

$$h_p = \frac{Nu_p k_p}{d_h} \quad (5)$$

where the substitutes f and p refer to feed stream and permeate side, respectively, k is the fluid thermal conductivity, d_h is the hydraulic diameter. Nu number can be calculated using Equation (6):

$$Nu = 1.86 \left(RePr \frac{d_h}{L} \right)^{0.33} \quad (6)$$

where L is the length of channels on both sides. Reynolds number (Re) and Prandtl number (Pr) can be evaluated using Equations (7) and (8):

$$Re = \frac{d_h u \rho}{\mu} \quad (7)$$

$$Pr = \frac{c_p \mu}{k} \quad (8)$$

where u , μ , ρ , k and c_p are the average velocity, viscosity, density, thermal conductivity, and the specific heat of the fluids, respectively. Additionally, the heat transferred for vaporization of liquid (Q_v), heat flux of Q_c due to sensible heat loss through the membrane, and thermal efficiency of MD system (η) are written as [62]:

$$Q_c = -k_m \frac{dT}{dl} = \frac{k_m}{\delta} (T_1 - T_2) \quad (9)$$

$$Q_v = J \times \Delta H_{v,w} \quad (10)$$

$$\eta = \frac{Q_v}{Q_m} \times 100\% = \frac{Q_v}{Q_v + Q_c} \times 100\% \quad (11)$$

where l is the distance from the membrane surface (facing the hot feed side), δ the membrane thickness, T_1 and T_2 refer to the temperatures at the membrane surface of the feed and permeate side, respectively, k_m is the overall thermal conductivity of the membranes and can be calculated using a parallel model (Iso-strain equation) [100–106]:

$$k_m = \varepsilon k_g + (1 - \varepsilon) k_s \quad (12)$$

where k_s is the thermal conductivity of membrane material, and k_g is the thermal conductivity of the gas (air and water vapor mixture) within the pores.

Moreover, a temperature polarization phenomenon (TPP), which means the temperature at the membrane surface differs from the measurable bulk liquid temperatures, exists in the MD process [58,107]. The temperature polarization coefficient (TPC) characterizes the variation of TPP. Equation (13) shows the definition of TPC.

$$TPC = \frac{\Delta T_m}{\Delta T} = \frac{T_1 - T_2}{T_f - T_p} \quad (13)$$

If $TPC < 0.2$, the DCMD is limited by heat transfer, and if $TPC > 0.6$, the DCMD is controlled by mass transfer with a low membrane permeability [62]. Normally, TPC value varies from 0.2 to 0.9 [108]. Equation (8) can be rewritten as Equation (14) based on Equations (2)–(5) and (9).

$$TPC = \frac{1}{1 + \frac{k_m}{\delta} \left(\frac{1}{h_f} + \frac{1}{h_p} \right)} \quad (14)$$

where k_m , δ , h_f and h_p stand as the same previously.

2.4. Mass Transfer

Mass transfer models are established under the assumptions of steady state and negligible effect on equilibrium at the pore entrance by the curvature of the liquid-vapor interface. The permeate flux (J) is related to the transmembrane pressure difference, the membrane materials, and the composition of hot/warm feed solutions. Flux (J) can be expressed as [58,107]:

$$J = B_w \times \Delta P_m = B_w (P_1 - P_2) \quad (15)$$

where B_w is the mass transfer coefficient, P_1 and P_2 are the partial water vapor pressure at liquid-vapor interfaces at each side. In addition, correlated partial vapor pressure P_i (the subscript i stands for 1 or 2) can be written as:

$$P_i = p_w^0(T) \times (1 - x) \times (1 - 0.5x - 10x^2) \quad (16)$$

where, $p_w^0(T)$ is the vapor pressure of pure water, and x is the mole fraction of non-volatile solute (i.e., NaCl). Antoine equation can be used to calculate the vapor pressure of pure water [58]:

$$p_w^0(T) = \exp\left(23.238 - \frac{3841}{T - 45}\right) \quad (17)$$

Mass transport (water vapor transfer in desalination) mechanism is governed by four basic models—Knudsen diffusion, molecular diffusion, Poiseuille flow and surface diffusion, and a combination of them. Knudsen number (K_n) is used to determine which model dominates the mass transfer [109]. K_n is calculated using Equation (18):

$$K = \frac{\lambda}{d_p} = \frac{\lambda}{2r} \quad (18)$$

where d_p is the membrane pore size, r is the average pore radius, λ is the mean free path of water molecules in water vapor phase that can be written as [58]:

$$\lambda = \frac{k_B T}{\sqrt{2}\pi P_m (2.641 \times 10^{-10})^2} \quad (19)$$

where k_B is the Boltzmann constant, P_m is the mean pressure within the membrane pores, T is the absolute temperature, and 2.641×10^{-10} is the collision diameter of water molecules ($2.641 \times 10^{-10} \text{ m} = 2.641 \text{ \AA}$).

If $K_n > 1$, the flow type is Knudsen, and if $K_n < 0.01$, the flow then belongs to molecular diffusion, and it is a combination of Knudsen and molecular diffusion (K-M diffusion) when $0.01 < K_n < 1$ [109]. Typically, the flow types in MD systems except VMD are the same as the K-M diffusion [110]. For the K-M diffusion, mass transfer coefficient B_w can be calculated as follows:

$$B_w = \frac{1}{\left(\frac{1}{B_w^M} + \frac{1}{B_w^K}\right)} \quad (20)$$

where, B_w^M and B_w^K are mass transfer coefficients for molecular diffusion and Knudsen diffusion, respectively. These two parameters can be determined using Equations (21) and (22):

$$B_w^M = \frac{\varepsilon}{\tau\delta} \frac{PD}{P_a} \frac{M}{RT} \quad (21)$$

$$B_w^K = \frac{2}{3} \frac{\varepsilon\bar{r}}{\tau\delta} \left(\frac{8M}{\pi RT}\right)^{\frac{1}{2}} \quad (22)$$

where ε , τ , and δ are the membrane porosity, pore tortuosity of the membrane, and membrane thickness, respectively, D is the water molecule diffusion coefficient, M refers to the molecule weight of water vapor, R is the gas constant, \bar{r} is the mean pore radius, P and P_a are the total pressure and the air pressure inside the membrane pores, respectively.

Generally, the combined K-M diffusion is much closer to actual situations. It was reported that the combined model predictive results were close to the experimental data with a Knudsen number below 0.7, whereas the simulated data of Knudsen diffusion model alone were almost twice greater than the experimental results [109].

Moreover, the solutes concentration in the bulk solution differs from that at the liquid/membrane interface due to mass transfer. This is called the concentration polarization phenomenon. Concentration polarization coefficient, which is used to characterize the concentration polarization phenomenon, can be defined as [111,112]:

$$\text{Concentration polarization coefficient} = \frac{C_1}{C_f} \quad (23)$$

where C_1 and C_f are the non-volatile solutes concentration at liquid/membrane interface and bulk feed solution, respectively.

3. Effect of Membrane Properties, Feed Solution, and Operating Conditions

3.1. Membrane Properties

3.1.1. LEP and Anti-Wettability

The *LEP* defines the critical pressure value of hydrostatic pressure at the feed side. This pressure represents the minimum membrane-wetting pressure value. The *LEP* value of a commercial or a lab-made membrane is explicit once the membrane is produced. Based on Equation (1) (the Laplace equation), pore geometry structure, pore size, *CA*, and surface tension all determine the value of *LEP*. Therefore, the materials and fabrication process conditions are useful for selecting and controlling the desired membrane properties for MD applications. Low surface energy materials and small pore size are good options for manufacturing MD membranes. Because surface tension, pore size, and pore geometry are all fixed once the materials and manufacturing process conditions are determined, it is essential to select lower surface energy materials prior to production, thereby generating a higher *CA* (hydrophobic of more than 90° , or superhydrophobic of ultra-higher than 150°) and a higher value of $\cos\theta$ as well [113]. In addition, smaller maximum pore size and higher *CA* can together ensure a higher minimum *LEP* for fluctuating operating pressures. Therefore, lower surface energy materials and smaller maximum pore size can result in a higher minimum *LEP*, which is beneficial for flexible and adaptive operation. It is worth noting that conventionally *LEP* is measured with the other side of the membrane exposed to atmospheric pressure, which is not valid for the measurement of *LEP* in VMD. The vacuum level should be considered when calculating the pressure difference. Moreover, flow pressure drops occur when a flat membrane is applied in a cell, and pressure fluctuations occur near the *LEP* value [114].

According to the Laplace equation (Equation (1)) that provides the relationship between the membrane pore size and the operating conditions, the operating pressure should be less than the minimum *LEP* to ensure non-wetting. The *LEP* of hydrophobic membranes varies depending on the mean membrane pore sizes. Typically, a smaller mean pore size renders a higher *LEP*. The reported *LEP* of 0.75–5 bar over the mean pore size range of 0.034–0.516 μm is summarized in Figure 4. High SR and stable permeate flux can be obtained only if the operating pressure is below *LEP*. Even under this premise, it is still difficult and almost impossible to explicitly demonstrate how the *LEP* variations alone influence the SR and the permeate flux fluctuation. Because the mass transfer and heat transfer are complicated and can be affected by a myriad of factors that will be systematically discussed in this review. Intrinsically, the effect of *LEP* on heat and mass transfer can be qualitatively estimated based on the correlation of operating pressure induced by feed flow rate or feed velocity, which will significantly affect the flow regime (laminar or turbulent or transitional flow) and thereby influence the heat and mass transfer. The essential relationship among them will be elucidated later in detail.

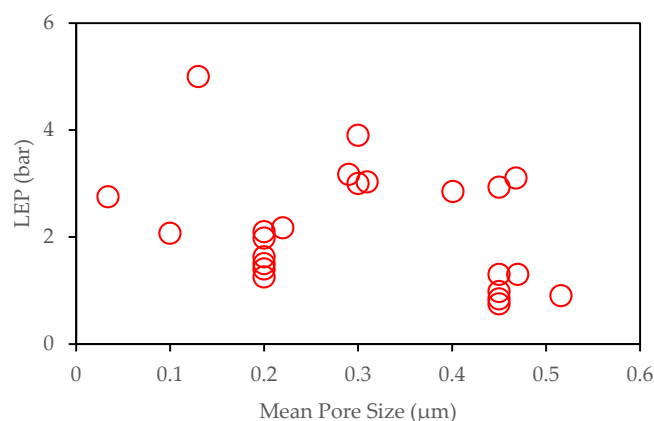


Figure 4. Summary of *LEP* over mean pore sizes (data obtained from references [43,45,48,52,115–123]).

The composition of the feed solution can influence the surface tension of the liquid on a hydrophobic membrane surface. Franken et al. [94] recommended that liquid surface tension would not be significantly affected when the feed solution was in the absence of organic matters. However, the surface tension of the mixture solution reduces when organics present in the liquid. If the organic concentration exceeds a “critical” value, then the liquid surface tension decreases rapidly, which causes an instant decrease of *LEP*. Simultaneously, the complete wetting occurs, indicating the liquid mixture fully penetrates the pores, and therefore the MD system is broken down immediately.

Recently, superhydrophobic membranes used with enhanced anti-wettability in MD were studied [15,124–132]. Superhydrophobic membranes have a higher CA of more than 150°, which renders stronger wetting resistance [79,132,133]. Li et al. [131] reported that superhydrophobic, self-cleaning nanofiber membranes were fabricated using polysulfone-poly-dimethylsiloxane (PS-PDMS) via electrospun methods. The membranes achieved a competitive and stable water flux of 21.5 kg/m²/h as well as a lower electrical conductivity of distillate ranging from 4.2 to 4.5 μS/cm with a 30 g/L NaCl solution as feed and a bulk temperature difference of 50 °C. Moreover, no wetting of the pores was observed over 12 h operation in their DCMD experiments. Another example of a superhydrophobic membrane was reported by Razmjou et al. [124]. They fabricated a superhydrophobic PVDF membrane via TiO₂ nanoparticles coating by a low temperature hydrothermal process and subsequent grafting using a low surface energy material H, 1H, 2H, 2H-perfluorododecyltrichlorosilane. They then found that the *LEP* and CA of the modified membrane increased from 120 kPa and 125° before modification to 190 kPa and 166°, respectively. The fabricated superhydrophobic membrane demonstrated a stronger anti-wetting property confirmed by two different experiments: a sharp flux reduction just after 2 h operation was observed before modification when 15 wt.% ethanol was added into the feed, whereas after modification, the drastic reduction time for flux was more than 6 h. On the other hand, the permeate conductivity before modification increased to more than 500 μS/cm merely after 4 h operation in DCMD using 3.5 wt.% NaCl as the feed. In contrast, the permeate conductivity of the superhydrophobic coated membrane remained stable and less than 50 μS/cm throughout the entire experiments. This phenomenon was also confirmed by other researchers [134,135]. Additionally, they observed that the superhydrophobic membrane performed a higher recovery ability (94%) of flux than the unmodified membrane (~54%) after cleaning membrane fouling using a 0.2 wt.% NaOH solution when compared to the flux of the pristine membrane.

An example of hydrophobic PP hollow fiber membranes for desalination in pilot-scale DCMD studies was reported in Ref. [136]. PP hollow fiber membrane with 330 μm ID, 150 μm wall thickness, and maximum pore size of 0.60 μm used in this study [136] was deposited a thin layer of plasma polymerized silicone-fluoropolymer coating on the fiber outside surface. Water CA measurements showed that the advancing contact angles of the fresh fiber samples were between 138.34° and 142.18° with receding contact angles of 22.01°–22.17°. The pilot plant operated in crossflow DCMD with the coated PP hollow fiber membranes achieved the highest water vapor flux of 55 LMH over 3 months of operation with feed and distillate temperatures of 64–93 °C and 20–54 °C, respectively. Moreover, the plant achieved a minimal flux reduction using seawater as feed with a salinity up to 19.5%, mainly due to the application of the coated PP hollow fiber membranes.

In general, polymeric membranes are the most extensively used in MD, and ceramic membranes are growingly applied in MD application. The hydrophobic property of the membranes is of the first importance as it is the key property for successful operation for all types of MD modules. Due to the hydrophobic nature of frequently studied polymeric materials, some popular polymers were used extensively to manufacture hydrophobic porous membranes such as PTFE, PVDF, polystyrene nylon-6, and PP. Ceramic membranes must be modified to be hydrophobic prior to MD application because of their hydrophilic nature. Table 1 summarizes the membranes and their performances in MD studies.

Table 1. Summary of extensively studied hydrophobic membranes in MD.

Membranes	Hydrophobic Modification Methods	Pore Size (μm)	CA ($^\circ$)	LEP (kPa)	MD Types	SR (%)	Ref.
PTFE-PVDF hollow fibers	/	0.116–0.308	103 ± 4	/	DCMD	~99.8	[137]
PVDF nanofibers	/	1–1.3	137.4–141.1	60	DCMD	99.8	[138]
Polystyrene nanofibers	/	0.19	114	130	DCMD	99.99	[139]
Alumina hollow fibers	hydrophobic modification using 1H, 1H, 2H, 2H-Perfluorodecyltriethoxysilane after ZnO deposition on alumina substrates	0.179	138.1	/	DCMD	>99.9	[140]
Dual-layer PVDF-co-hexafluoropropylene-nylon-6 nonwoven nanofibers	/	0.18	126.3	185	AGMD	>99	[141]
Fluorographite modified PVDF hollow fibers	/	0.476 ± 0.134	121	≥ 130	DCMD	99.99	[118]
Hierarchical PVDF micro/nano-composite flat sheet membranes	SiO ₂ nanoparticles coating followed by fluoroalkylsilane grafting	0.20 ± 0.01	161.5 ± 1.0	/	DCMD	>99.99	[142]
Asymmetric flat sheet ultrafiltration mixed cellulose ester membranes	Vapor deposition treatment using hepta-decafluoro-1,1,2,2-tetrahydrodecyltrichlorosilane	0.05 0.025	120.9–123.4 116.3–126.5	~2410 >2760	DCMD DCMD	>99.9	[48]
Hydrophobic tubular asymmetric Al ₂ O ₃ membrane	Dip-coating using Hexadecyltrimethoxysilane dissolved in ethanol	0.15	>150	/	VMD	~99.9	[143]

3.1.2. Pore Size and Pore Size Distribution

Pore size is another important membrane property that significantly affects MD performance. Typically, an increase of the average pore size r indicates the increase of the allowable maximum pore size r_{max} . Therefore, pore size directly determines the Knudsen number that influences the mass transfer mechanism based on the definition of Knudsen number (Equation (8)). Suppose the membrane pore size is smaller than the mean free path of vapor molecules (λ), it would be suitable for maintaining a relative higher LEP based on the Laplace equation (Equation (1)). The Knudsen number K_n will be greater than the unit, indicating that the molecular pore walls collisions dominate the mass transport process, and the Knudsen diffusion (K diffusion) is the primary mechanism for mass transfer of vapor. On the other hand, K_n will be less than 0.01 if the membrane has greater pore sizes. In this case, the dominant mass transfer mechanism will be an ordinary molecular diffusion. Typically, membrane pore size ranges from 0.2 to 1 μm [144]. However, this range can be extended to some larger pore sizes due to the fabrication process for the membranes. For example, the pore size range of 0.2 to 20 μm was reported [137,145,146] using a stretching technique for preparing PP and PTFE membranes and using phase inversion to fabricate PVDF membranes. Alkudhiri and Hidal [25] studied the effects of high concentration of four salts and three different pore size PTFE membranes on the permeate flux and SR using an AGMD. Their study indicated that the flux increased significantly by 39.6% and 56.9% for a maximum NaCl feed concentration of 180,000 mg/L when the pore sizes increased from 0.2 μm to 0.45 μm and from 0.2 μm to 1 μm , respectively. A similar lower flux enhancement for the other three different feed saline solutions was also observed. The Knudsen-ordinary molecular diffusion (K-M diffusion) in the increased membrane pore size was considered the cause of the enhanced mass transfer of permeate flux [87]. Additionally, they revealed that the SR decreased because of LEP reduction induced by increased membrane pore sizes, which was already confirmed by other studies [147,148]. Gryta et al. [149] revealed that the occurrence of scaling and deposition of salts prefers more in larger pores that are more easily wetted.

PSD exists because a uniform pore size is almost impossible in specific membranes. Generally, MD membranes have a PSD ranging from 0.2 μm to 1 μm [87,108]. Phattaranawik et al. [150] indicated that the effects of PSD on water flux in DCMD could be ignored. Their results indicated that water flux fluctuation was only 4% using commercial PVDF membranes—GVHP (PSD is wider) and HVHP (PSD is narrower) membranes provided by Millipore. Moreover, they observed that water flux discrepancies using HVHP and GVHP membranes were 2.9% and 7.1% for laminar flow and 1.4% and 8.1% for turbulent flow. The discrepancy of the narrower PSD membrane was better than that of the larger PSD membrane. Typically, a narrower PSD is preferable in MD. However, they did not mention the effect of PSD on SR.

3.1.3. Porosity, Thickness, and Tortuosity

Porosity is an important parameter of membrane characteristics because it can directly determine the ratio of pores within a membrane [151–153]. For polymeric membranes, porosity (ϵ) can be calculated by Equation (24) [144].

$$\epsilon = 1 - \frac{m}{\rho_p \times A \times \delta} \quad (24)$$

where m and A are the mass and surface area of the membrane, ρ_p is the density of the membrane materials, and δ is the membrane thickness.

Higher porosity means more passages or space for water vapor to pass through. On the other hand, higher porosity reduces heat loss due to sensible heat conduction through the membrane material, thereby enhancing thermal efficiency. Theoretically, based on Equations (5) and (10)–(12), the increase of porosity (ϵ) enhances the mass transfer coefficient B_w^M and B_w^K , and then increases permeate flux J . In addition, porosity also affects the thermal conductivity of a membrane. Equations (3) and (4) reveal that the formulas for calculation of heat flux through the membrane conduction (Q_c) and the thermal conductivity of the membranes. Typical values of k_g and k_s of conventional commercial

polymeric membrane materials are 0.027 W/m/K and 0.1 to 0.5 W/m/K, respectively [76]. Therefore, Q_c and k_m will decline with the increasing porosity, which affects both mass transfer and heat transfer. Generally, a higher porosity without sacrificing mechanical strength is beneficial for MD applications. Nevertheless, it is difficult to predict how it influence the SR in desalination. Again, it is meaningless to discuss the decisive effect merely focusing on an individual parameter since the MD involves a complex process and its performance is governed by different synergistic effects and a combination of various related factors. Other factors other than porosity, such as mean pore size, membrane thickness, and thermal conductivity can affect flux and permeability, and SR. For instance, the membrane with high porosity of up to 90% showed less permeate flux than the case of lower porosity [92]. The study reported that this outcome resulted from a much higher thermal conductivity and a small pore size of about 20 nm of the membrane.

Membrane thickness (δ) is a parameter of significant importance. Typical membrane thickness ranges from 20 to 200 μm for polymeric membranes [62,93,154] and from ~ 500 to 2000 μm for inorganic membranes such as ceramic membranes [92]. Membrane thickness significantly affects mass transfer and heat transfer, along with thermal efficiency. According to Equations (7) and (12)–(14), an increase of membrane thickness reduces the mass transfer coefficients because a thicker membrane renders longer passage for water vapor to pass through. On the other hand, the increase of membrane thickness reduces the heat transfer coefficient of thermal conduction via membrane material because the heat transfer coefficient of conduction is inversely proportional to the membrane thickness based on Equations (2)–(4). Also, the increase of membrane thickness decreases the effective heat amount for feed stream vaporization. It thereby results in decreased thermal efficiency of the MD system, as indicated by Equation (5). Therefore, a higher mass transfer, namely a higher permeate flux, results in a smaller thermal efficiency, which is the typical drawback in AGMD.

An optimum or a critical membrane thickness based on the trade-off for higher mass transfer and lower heat conduction loss exists. L. Martínez et al. [155] studied the effects of membrane thickness reduction on DCMD performance. They investigated the flux as a function of membrane thickness via a resistances-in-series model using the TF200 (PTFE layer supported on PP base) and Durapore GVHP (unsupported homogeneous PVDF). They concluded that: (i) for a pure feedwater, the flux increase for unsupported membrane was mainly caused by a membrane resistance decay induced by membrane thickness reduction; and the water flux increased in a greater proportions than in unsupported membranes since the top layer (the active hydrophobic layer) thickness declined; (ii) using a NaCl and sucrose aqueous solution as feed, the water flux decreased with membrane thickness reduction for both types of membranes when the membrane thickness was below a specific thickness value, which was considered as a “critical” membrane thickness. Critical membrane thickness of ~ 10 μm was suggested for the two types of polymeric membranes. However, they did not study the effect of membrane thickness reduction on SR.

Additionally, there are different opinions on the range of optimum membranes thickness. For example, Eykens et al. [156] observed a very similar result using a commercial PVDF, PP membranes, and a lab-scale made e-PVDF membrane. They suggested broader optimum membrane thickness ranges of 2–30 μm for 3 wt.% NaCl feed solution, 7–112 μm for 13 wt.% NaCl feed solution, and 16–793 μm for 24 wt.% NaCl feed solution. Their results revealed that a higher hydrophobic layer thickness was more suitable for MD application when fed with a high salinity solution. They observed an SR greater than 99.98% using the commercial PVDF and PP membranes and SR above 98% using the lab-made membrane in their studies. However, Laganà et al. [41] reported a different optimum thickness range of 30–60 μm of polypropylene hollow fibers for producing highly concentrated apple juice using a hollow fiber DCMD module.

Tortuosity is another important membrane characteristic that, along with porosity and thickness, can greatly control transmembrane water vapor mass transport [157]. Permeate flux is conversely proportional to tortuosity based on Equations (7) and (12)–(14). A small tortuosity is beneficial to minimize mass transfer resistance due to the shorter pore pathway for water vapor [81,158]. Tortuosity is a geometrical parameter for the characterization of pores, which is equal to a ratio of the actual

length of the membrane pores divided by the membrane thickness [108]. A tortuosity value of unity indicates the pores are straight, or the actual length of the pores is identical with the overall membrane thickness. Tortuosity can be calculated using Equation (25) [80,159].

$$\tau = \frac{1}{\varepsilon} \quad (25)$$

Iversen et al. [160] calculated the tortuosity value of commercial PTFE membranes using a porosity of 0.78 provided by the manufacturer; the calculated value of tortuosity was 1.3 based on Equation (25) and this value of 1.3 was close to the provided value range of 1.1 to 1.2. With regard to the assumption of tortuosity values, Calabrò [161] assumed a tortuosity of 1.2 for the prediction of water flux that was approximate to 99.6% of the experimental outcome. However, the effect of tortuosity on SR in desalination using MD was not reported. A possible phenomenon that membrane thickness can decrease while tortuosity may increase due to the compaction of the membrane exists may not be noticed for its negative effect on the low-pressure membrane related applications (i.e., application in MD). However, this effect needs to be further studied. Lawson et al. [162] reported that thickness reduction caused by membrane compaction did not necessarily lead to flux increase in theory. Flux increases are affected by the product of tortuosity and thickness, namely $\tau\delta$, which is defined as the actual length of the path for vapor or gas. On the other hand, tortuosity increases under compaction, and the overall transmembrane pass length increases if the increased degree of tortuosity exceeds the degree of thickness decay. Therefore, it is recognized that predicting the degree of influence on the permeate flux and/or SR should consider the combined contributions of all related membrane characteristics rather than the individual property alone. Because these characteristic membrane parameters not only affect each other but also can be, to some extent, influenced by operating conditions.

In summary, membrane properties are essential to MD performance because they affect mass transfer and heat transfer. They also influence each other, which gives rise to the complexity of determining the effects of their characteristics. For example, porosity depends on membrane thickness (Equation (24)). Furthermore, a combination of these four properties affects the mass transfer coefficient (B_w), as shown in Equation (26) [58]:

$$B_w \propto \frac{\varepsilon r^\omega}{\tau\delta} \quad (26)$$

where ω is a diffusion coefficient, $\omega = 1$ and 2 for Knudsen diffusion and viscous flow. It is worth noting that $\tau\delta$, in Equation (26), stands for mass transport path length, which should be as small as possible. Predicting flux or discussing the effects of these four membrane parameters should always be based on their synergistic interaction of each other according to Equation (26).

3.1.4. Membrane Thermal Conductivity

Membrane thermal conductivity differs from the thermal conductivity of the membrane materials. Because a membrane is composed of membrane materials and a mixture of air, water vapor, and other volatile compositions inside the pores, porosity influences the membrane thermal conductivity (k_m), thereby affecting the heat loss via membrane materials. Based on Equations (3)–(6), the heat flux through the membrane material conduction (Q_c) is positively proportional to the overall membrane thermal conductivity (k_m), and is inversely proportional to the membrane thickness (δ). In this case, the water flux increases with lower membrane thermal conductivity when other conditions are the same. In other words, a higher thermal conductivity can lead to flux reduction and thermal efficiency decline. For instance, Alobaidani et al. [163] reported an increase of thermal conductivity from 0.1 to 0.5 W/m/K resulted in a 26% flux reduction and a 50% decrease in thermal efficiency. Moreover, the thermal conductivity of the membrane materials (k_s) is more important because k_s is typically one magnitude higher than that of the mixture of gas (air/vapor) [102,158,164]. For example, the typical reported thermal conductivities of PVDF, PP, and PTFE polymer materials are approximately 0.18 W/m/K (296 K) and 0.21 W/m/K (348 K), 0.11–0.16 W/m/K (296 K) and 0.2 W/m/K (348 K), and ~0.26 W/m/K (296 K) and 0.29 W/m/K (348 K) [165–167]. In contrast, the reported thermal conductivities of water vapor

were 0.02 W/m/K and 0.022 W/m/K for 298 K and 348 K, respectively [168]. However, the reported thermal conductivities of inorganic membranes such as ceramic membranes used in MD are greater than 1 W/m/K [14,169,170]. The membrane thermal conductivity is related to the membrane porosity because a higher porosity indicates a lower membrane thermal conductivity, which is beneficial for obtaining high flux. Deka et al. [52] reported a high flux of 33.1 ± 1.7 LMH along with a high CA of $\sim 170^\circ$ in DCMD using electrospun nanofiber membranes (silica aerogel/PDMS/PVDF membranes) due to the extremely low thermal conductivity of the silica aerogel of 0.009–0.012 W/m/K and high porosity of $85.8 \pm 0.28\%$.

3.2. Effect of Feed Solution Composition on Flux and SR

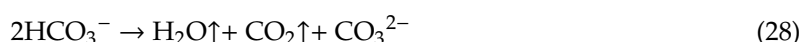
3.2.1. Effects of Inorganic Salts

Typically, feed solution applied in MD for desalination is an aqueous solution containing salts and other organic and inorganic constituents. A higher concentration of salts results in vapor pressure reduction, as indicated by the Raoult's law [171–174]. Li et al. [175] reported a significant decrease of water flux was observed when the concentration of NaCl, KCl, and MgCl₂ exceeded 2 M. And the water flux reduced by 44.4%, 59.6% and 86.8% for KCl, NaCl, and MgCl₂ when their concentration increased from 2 to 4 M. Guan et al. [176] stated that this was caused by the discrepancy of the water activity and viscosity of the solution due to increase of the salt concentrations. Besides, the sharp reduction of water flux for MgCl₂ was mainly caused by the dramatic decline of water activity with MgCl₂ concentration greater than 2 M. Both Li et al. [175] and Guan et al. [176] suggested the order of the water activity of aqueous mixture with the three salts was KCl > NaCl > MgCl₂ at concentrations higher than 2 M. Guan et al. and Li et al. [175,176] stated that water activity of aqueous solution was related to the non-volatile solutes in the solution. David et al. [177] and Tansel et al. [178] confirmed that Mg²⁺ ion has the smallest ionic radius and entropy of hydration compared to Na⁺ and K⁺, whereas the hydration free energy and hydrated radius are the greatest among them. In addition, the smaller crystal radius of Mg²⁺ ions enables a more compacted hydration shell and thereby associates with more highly structured water molecules along with the interaction of charged ions. Therefore, the water activity of the MgCl₂ solution was the lowest among the three salty aqueous solutions.

Another example was reported by Alkudhiri and Hidal [25]. They investigated the effects of various high salinity solutions on flux and SR by AGMD using four inorganic salts of NaCl, MgCl₂, Na₂CO₃, and Na₂SO₄. Their research showed that water flux decreased because of water activity reduction and a higher boiling point due to increased salts concentration [173]. Water activity reduced significantly with increasing salts concentration due to mole fraction reduction of water molecules in the solution. Furthermore, more salts deposited and accumulated on the membrane surface at the feed side and induced the concentration polarization. The combination of water activity reduction, concentration polarization and temperature polarization resulted in a significant reduction of the driving force – transmembrane vapor pressure decline. In addition, deposition and accumulation of salts may induce partially wetting of the membrane, which could in turn conversely influence permeate flux and SR [58,101,179]. On the other hand, this research and other studies [147,148] all confirmed that SR decreased with increasing salt concentrations for the membrane pore size of 1000 nm, and all of them stated that the SR reduction was mainly due to LEP reduction caused by the high pore size. Another important observation in their experiments indicated that the Na₂CO₃ concentration greater than 42,000 mg/L was a critical value for a sharp decrease of SR, decreasing from above 95% at a concentration of $\sim 10,000$ mg/L to $\sim 85\%$ at concentration of $\sim 42,000$ mg/L, with the membrane pore size of 0.45 μm , which was in the optimum pore size range. They concluded that this was mainly caused by significant membrane wetting. However, this was not observed on other three salts. Further studies on the intrinsic mechanisms should be conducted.

The effect of inorganic salts on the performance of MD involves membrane scaling such as CaSO₄ and CaCO₃ due to precipitation on the membrane surface. The scaling layer reduces both permeate flux and SR. Yu et al. [180] investigated the effects of NaHCO₃, Na₂SO₄, CaCl₂, and Na₂SiO₃·9H₂O on the

concentrated cooling tower blowdown water (CTBW) using synthetic CTBW in DCMD. They reported: (i) the flux and SR declined due to the formation of scaling; (ii) a flux as high as 30 LMH at $\Delta T = 40\text{ }^\circ\text{C}$ was relatively constant when TDS was below 2.6 wt.%; (iii) CaCO_3 was the main scalant for silica-free CTBW which was confirmed by pH reduction due to dissociation of bicarbonate groups as shown in the following reactions (Equations (27)–(29)); (iv) scaling of silica-free CTBW was alkaline and hardness scale indicated by the Langelier Saturation Index (LSI) higher than unity ($\text{LSI} > 1$), presenting CaCO_3 scale formation potential. LSI can be calculated using Equation (30) [64,65]:



$$\text{LSI} = \text{pH} - \text{pH}_s \quad (30)$$

pH is the actual pH value of the feed solution, and pH_s refers to the pH value of a saturated solution of calcite or CaCO_3 . LSI higher than zero indicates a greater potential of precipitation while below zero shows less potential of scaling.

Viscosity was reported as an important factor affecting the boundary layer and TPP, which can be evaluated through Equations (2) to (8). The viscosity and density of the feed solution increase with increasing salts concentration, and Re and Pr number will be dramatically affected. Heat transfer coefficients h_f and h_p will change directly because of the changed Nu number that is proportional to $(RePr)^{0.33}$. Therefore, viscosity definitely influences heat transfer in MD. Guan et al. [176] studied the effects of a high concentration of four salts NaCl, KCl, MgSO_4 , and MgCl_2 on the permeate flux in a DCMD. Their results showed that the increased viscosity of MgSO_4 and MgCl_2 feed solutions at higher salts concentrations had a remarkably negative impact on water flux. This can be explained by a more significant effect of multivalent ions on increased viscosity adjacent to the membrane surface (at the boundary layer) [178]. Alkhubhiri and Hidal [25] also stated that viscosity caused by higher salt concentration might deteriorate the TPP and reduce TPC value, and thereby resulting in a decrease in water flux. Also, the effects of viscosity due to the presence of sucrose was reported. Schofield et al. [86] demonstrated that viscosity of the feed solution with a concentration of sucrose up to 30 wt.% led to a 33% reduction of Nu number and deteriorated the TPP. The increase of viscosity eventually caused an 11% flux reduction and was considered the second most important factor for flux decline. Martínez et al. [155] stated that a high sucrose concentration of up to 40 wt.% resulted in a sharp decrease in heat transfer coefficients due to the exponential increase of solution viscosity.

3.2.2. Effects of Colloidal Particles

Colloids such as surfactants and oil can adsorb onto the surface of the hydrophobic membranes with complex mechanisms. Typically, electrostatic interactions and hydrophobic-hydrophobic interactions are used to explain these phenomena. The mechanisms are mainly based on the DLVO theory (established by Derjaguin, Landau, Verwey, and Overbeek) [181–183] and the extended DLVO (x -DLVO) theory. The DLVO mechanism states that the electrical double layer interaction and van der Waals force determine the affinity between colloidal particles and a surface of a medium. The x -DLVO theory combines the Lewis acid-base interaction and the short-range van der Waals interaction, such as hydration force, to explain the membrane wetting. The surface charge plays a vital role in the analysis of attachment and detachment of particles to a membrane surface, which can also explain the fouling formation and its alleviation due to colloidal interaction. It is suggested that the polar interaction at the surface were affected by the electrostatic interaction rather than by the electrical double layer interaction based on the x -DLVO theory [184]. Fouling due to hydrophobic or oleophilic interaction in MD can be mitigated using an underwater oleophobic surface, which means oil-resistant when submerged in water. Wang et al. [123] reported that a water flux as high as 24.3 LMH and remained stable over more than 12 h operation because of the anti-fouling effect attributable to the electrostatic

interaction (here refers to the polar-polar interaction) which was induced by the interaction between the negatively charged crude oil emulsion feed solution and the negatively charged PVDF membrane surface modified using polydopamine and silica nanoparticles. In contrast, the water flux of the non-modified PVDF membrane declined drastically and was almost equal to zero within merely two hours of operation, although the initial flux was as high as 31.0 LMH. In addition, the SR rates for these two membranes in DCMD experiments were both above 99.9% with a feed salinity of 1000 mg/L.

Surfactants are amphiphilic compounds composed of the hydrophobic non-polar tail and hydrophilic polar head [185]. The hydrophobic membrane becomes less hydrophobic in the presence of surfactants because of the lower hydrophilic-lipophilic balance (HLB) value and surface tension of the surfactant solution, which can lead to pore wetting. Typical surfactants include two types: non-ionic surfactants such as Span 20 and Tween 20, and the other is ionic surfactants such as sodium dodecyl sulfate (SDS). Their solution behavior, such as adsorption on the membrane surface, differs from each other. Chew et al. [186] studied the effects of surfactants of Span 20, Tween 20, and SDS on the performance of a DCMD using a hydrophobic PVDF membrane. Their experiments were conducted using a synthetic produced water composed of these three surfactants and petroleum and vacuum pump oil. Their research showed that wetting occurred earlier when non-ionic surfactants were present, and the severity of pore wetting followed the order of Tween 20 > Span 20 > SDS. The ultimate conductivities in each permeate were 8.51, 3.56, and 0.15 mS/cm for Tween 20, Span 20, and SDS solution, respectively, when all other parameters were constant. This observation resulted from a discrepancy in wetting and adsorption behavior on the membrane surface. It was reported that the HLB values and electrostatic interaction of the surfactants considerably influence the adsorption behavior [187,188]. For non-ionic surfactants, pore wetting and adsorption are mainly governed by hydrophobic interaction. Tween 20 has a higher HLB value of 16.7, which indicates a lower hydrophobic interaction effect [189]. Thus, Tween 20 has a higher potential to draw more water molecules towards membrane pores than Span 20 because a larger HLB value indicates higher hydrophilicity [188]. In addition, non-ionic surfactants unimers formed, not micelles but a monolayer, due to lipophilic adsorption onto the membrane surface. Therefore, earlier wetting occurred, and water flux sharply decreased. Both hydrophobic interaction and electrostatic interaction play an important role in the adsorption behavior of ionic surfactants such as SDS, which has the highest HLB of 40, indicating SDS is the most hydrophilic among the three surfactants. On the other hand, the repulsion between SDS and negatively charged PVDF membrane occurred, demonstrating that very few unimers of SDS adsorbed stably onto the membrane surface.

Boo et al. [190] also investigated the effects of surfactants in the presence of salts (1.0 M NaCl) on the water flux and SR using PVDF membranes. They observed a slight increase in water flux and SR reduction occurred when 0.05 mM SDS was added into the feed solution. Moreover, the flux increased sharply while SR declined dramatically when 0.1 mM SDS was added. These results demonstrated that the pore wetting occurred when SDS with a concentration higher than 0.05 mM was added in the feed solution. Intrinsically, the presence of SDS reduced the surface tension of the liquid, especially in the presence of salts such as NaCl. For surfactants, the diffusion of surfactants at the liquid-vapor interface is governed by the hydrophobic non-polar tail. In this case, the electrostatic interactions between surfactants and the membrane surface can be inhibited, and the hydrophilic polar head is screened by the adjacent counterions, and thereby resulting in a denser surfactant layer at the interface, which in turn dramatically reduces the liquid surface tension and caused pore wetting [191]. In general, micelles formed when surfactant concentration exceeds its critical micelle concentration. Micelles can grow from spherical aggregate to elongated ones with increasing surfactant concentrations [188]. The formation of micelles and the possible growth of micelles accelerate the onset of pore wetting and thereby lead to flux decline [186].

3.2.3. Effects of Natural Organic Matter

The presence of natural organic matter (NOM) such as proteins [192] and humic acids leads to flux reduction and decreasing non-volatile solutes rejection due to membrane fouling [193,194].

Gryta et al. [195] investigated the flux variation and fouling phenomenon in DCMD using a solution composed of sodium chloride (~50 g/L) and organic matters such as proteins from animal intestines processing as the feed solution and polypropylene (PP) capillary membranes. They reported rapid flux reduction due to the precipitation of organic matter (proteins) on the membrane surface, which was confirmed using Fourier Transform Infrared with diffuse reflectance spectroscopy. The maximum permeate flux declined two-folds during their experiments. However, the electrical conductivity of the permeate was stable at 3–5 $\mu\text{S}/\text{cm}$, although the flux reduced significantly after the formation of fouling layer.

Khayet [196] studied the rejection performance of humic acids in DCMD using PVDF and PTFE membranes together. The initial concentration of humic acid was 30 mg/L in the experiments. The permeate flux decreased for both membranes, whereas a higher rejection rate greater than 96% was observed for both membranes. Fouling due to the deposition of humic acids caused the flux reduction, and this phenomenon can be worse for hydrophobic membrane than for hydrophilic one [197]. They also investigated the effects of solution pH on the fouling and deposition behavior of humic acids. Results showed that humic substances were more soluble under high pH and fouling became worse under low pH ($\text{pH} < 4$). In other words, low pH condition makes humic substances more insoluble or difficult to dissolve. Electrostatic interaction between humic acid macromolecules and charged membrane surface was also affected by pH. At low pH, e.g., pH 4.0, the electrostatic repulsion between humic acids and membrane surface can be reduced and facilitated the fouling of the hydrophobic membrane surface because of the increased humic acid adsorption. Schäfer et al. [198] stated that membrane surface charge was reduced with the decreasing pH, and this can, in turn, accelerate the NOM adsorption, which was also reported by other researchers [199].

3.2.4. Effects of Volatile Solutes

Hydrophobicity of the hydrophobic membranes in MD is easy to get reduced and even damaged in the presence of high concentration of organics such as ethanol. However, the MD system still works if the feed is a mixture of water and low concentration organics. The penetration pressure of the mixture was observed when fed with water-ethanol in the low concentration range. Intrinsically, the liquid-vapor equilibrium of the liquid mixture and mole fraction of the components determine the results. If the mole fraction of ethanol is less than the equilibrium mole fraction of ethanol of the liquid-vapor mixture (namely $x_e < x_e^*$, the symbol * stands for equilibrium), ethanol is the dominant component in the vapor phase. Besides, they suggested a separation factor α (the selectivity), which is expressed in Equation (31):

$$\alpha = \frac{x_2}{1 - x_2} \frac{1 - x_1}{x_1} \quad (31)$$

where x_1 and x_2 refer to the ethanol mole fraction at the feed solution and the permeate, respectively. The selectivity greater than unity indicates the preferred transportation of ethanol vapor through the membrane pores due to its higher volatility.

Gostoli and Sarti [200] reported that the water vapor pressure decreased linearly with the increasing ethanol concentration and disappeared at the ethanol concentration of 75 wt.% when they investigated the separation performance of the mixture using PTFE membrane (TF200, pore size 0.2 μm , thickness 60 μm , and porosity 60%) in AGMD. The ethanol selectivity was between 2.0 and 2.5 when the transmembrane temperature difference ranged from 30–50 $^\circ\text{C}$. Moreover, the ethanol separation factor depended on the feed composition and can be as low as close to unity when the ethanol concentration was 23.8 wt.%. Using the Maxwell-Stefan model [201], which is an ideal model for predicting solute diffusion of multi-components in feed solutions, the predicted binary diffusivity of ethanol-water was $\sim 0.196 \text{ cm}^2/\text{s}$, consistent with the experimental data.

Another study on the separation of volatile organic compounds was reported by Banat [202]. The ethanol selectivity (ethanol concentration in feed was from 0.83 to 10.2 wt.%) was 3.1–3.4, and 3.05–3.48, at the feed temperatures of 60 and 70 $^\circ\text{C}$, respectively. The relative constant selectivity

and the increase of flux with the increasing temperature revealed that the flux increase was mainly due to the mass transfer of ethanol. Meanwhile, the acetone selectivity was observed higher than ethanol at the same conditions, and a lower cooling temperature was preferred to obtain a higher acetone selectivity. The direct wetting concentration of ethanol for the hydrophobic membrane was 34 wt.% ethanol in the ethanol-water mixture while it was 23 wt.% for the acetone-water mixture.

Kujawski et al. [203] investigated the selectivity of micro- and macro-porous ceramic membranes (TiO_2) grafted using fluoroalkylsilane on the separation of water-organic solvents mixture using VMD. They found that the selectivity of organic solvents was dependent on the pore size of the modified TiO_2 ceramic membranes. The microporous (2–4 nm) titania ceramic membrane had less selectivity of ethyl-acetate (the separation factor was 1.3–30) compared with the higher selectivity of ethyl-acetate (the separation factor was 32–60) using the macroporous membrane (~200 nm).

Wijekoon et al. [204] studied the rejection performance of 29 trace organic compounds (TrOCs) using hydrophobic PTFE membranes in DCMD. They reported that mass transfer of the 29 TrOCs from the feed side to the permeate side mainly depended on their volatility measured by pK_H value as defined in Equation (32):

$$\text{pK}_H = -\log_{10}K_H \quad (32)$$

where K_H is the Henry's law constant ($\text{atm}\cdot\text{m}^3/\text{mol}$). The pK_H greater than 9 ($\text{pK}_H > 9$) indicates low volatility (or can be classified as non-volatile) while a pK_H value less than 9 ($\text{pK}_H < 9$) indicates high volatility. Therefore, some TrOCs with pK_H values > 9 are not readily transferred to distillate and hence reached a higher rejection. The authors further stated that 4-tert-octylphenol, 4-tert-butylphenol, and benzophenone with $\text{pK}_H < 9$ exhibited rejection of 54%, 73% and 66%, the lowest among all the 29 TrOCs except oxybenzone. Oxybenzone had a pK_H values ranging from 8.39–9.23 when the pH of feed solution decreased from 9 to 8. The research suggested that the hydrophobic adsorption could explain this exception because the pK_H of oxybenzone and other TrOCs was less than 9. This phenomenon was also reported by Zuo and Wang [205].

The general mechanisms of feed solution compositions affecting permeate flux and SR in MD are summarized in Figure 5.

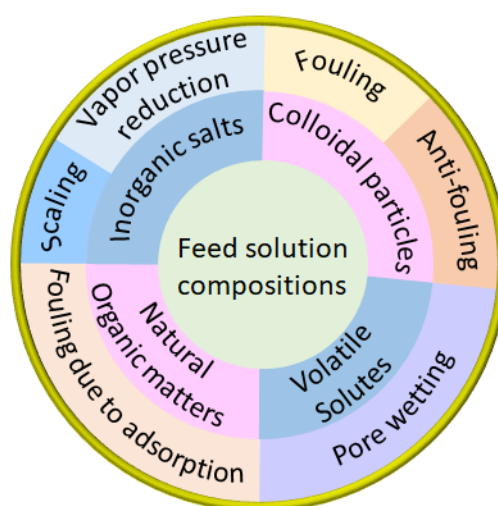


Figure 5. General mechanisms of feed solution compositions affecting permeate flux and salt rejection in MD.

3.3. Effects of Operating Conditions

3.3.1. Temperature

Temperature is an important operating parameter. As mentioned in Section 2, temperature difference at both sides determines the vapor pressure difference (or partial vapor pressure difference

or gradient), which is the driving force for mass transfer through the membrane pores [58,86,206,207]. Typically, the temperature at the cold side is fixed and the feed temperature is adjustable to study how temperature affects the flux in DCMD, AGMD, and SGMD. However, the vacuum pressure level determines the driving force for mass transfer in VMD. Theoretically, an increase of feed temperature not only enhances driving force to obtain more flux but also improves thermal efficiency due to improved TPC value when the permeate temperatures in DCMD, AGMD, and SGMD (or vacuum pressure level in VMD) were kept constant. In other words, feed temperature can influence not only mass transfer coefficients for transition flow regime but also the heat transfer coefficients, and these can be denoted directly based on Equations (2), (3), (9)–(11), and (13)–(17).

Researches [10,62,104–106,112,206,208–210] showed that increasing feed temperature could increase the interfacial temperature adjacent to the membrane surface at the feed side and alleviate temperature polarization. Many studies [19,119,132,211–213] demonstrated that water flux increased exponentially with the increase of feed temperatures according to the Antoine equation. In addition, the profile of temperature from liquid/membrane interface (T_1) to membrane/liquid interface (T_2) shows that it declines exponentially across the membrane [214]. The majority of heat flux through the membrane is the diffusive heat flux conducted via the membrane materials, defined as heat loss due to thermal conduction of membrane materials. Kim [214] reported that the linear approximation of transmembrane temperature decrease could be valid. It was suggested that a higher feed temperature with a fixed cooling temperature generates more water flux than a lower permeate cooling temperature with a fixed feed temperature. In other words, increased feed temperature can produce more water vapor molecules at the liquid/vapor interface when the temperature at the cold side is fixed.

Other research using higher feed inlet temperature showed the feed inlet temperature of 180 °C achieved much higher DCMD performance than the conventional maximal value of 80 °C [119]. The modeling results showed that the permeate flux increased by 9.4 folds, the thermal efficiency increased by 2.1 folds, and the SEC reduced by 2.9 folds.

On the other hand, increased feed solution temperature has an adverse impact on pore wetting. Nayar et al. [215] reported that increasing temperature resulted in surface tension reduction, making membrane pores wetting easier due to lowered *LEP* in higher temperature cases.

3.3.2. Flow Rate

The flow rate or flow velocity is of vital importance for MD. An increase in flow rate or velocity can increase the *Re* number. Therefore, a high flow rate or velocity is beneficial to obtain a turbulent flow regime, which renders the better mixing of the feed solution and reduces the thermal boundary layer along with the temperature polarization. Thus, increasing flow rate or flow velocity can enhance the TPC value and the vapor pressure difference and hence facilitate both mass transfer and heat transfer. Manawi et al. [209] reported that the flux increased from 18.1 LMH at both sides flow rates of 0.5 L/min to 29.1 LMH at both sides flow rate of 1.5 L/min with all other conditions the same. However, the flow rate cannot be increased infinitely because of the increasing pressure drop due to the increased flow rate or velocity. Pressure drop occurs due to the resistance of the fluid channel and cell walls in the modules. A certain flow rate is necessary to pump fluid into the MD cell and flow through the channel. Nevertheless, an excessive increase in flow rate or flow velocity will result in a great pressure drop. Typically, the pressure drop is positively proportional to the square of flow velocity. Their relationship is expressed in Equation (33) [216]:

$$\Delta P = f \frac{L}{d} \frac{u^2}{2} \rho \quad (33)$$

where ΔP is the pressure drop, L the length of channels, f the friction factor, d the hydraulic diameter of the flow channel, ρ the liquid density, and u the flow velocity.

The effects of flow rates on scaling in DCMD were reported in Ref. [136,217,218]. The researchers investigated the effects of feed flow rates (e.g., 84, 688, and 1438 mL/min) on flux and scaling behaviors

in cross-flow DCMD using silicone-fluoropolymer coated PP hollow fiber membranes. The water vapor flux increased with increasing feed flow rates due to an increase in Reynolds number (Re), which increased the heat transfer coefficient in the boundary layer. However, they observed that permeate flux dropped to ~ 5.5 mL/min at the end of both the cases of feed flow rates of 688 mL/min and 1438 mL/min, and the authors attributed this to the reduction of the brine inlet flow rate because the filter holder was clogged by gypsum precipitations.

Moreover, the effects of flow pressure drop can be significant if the hot brine flows through the bore of the hollow fibers, which differs from the case of hot brine flowing over the hollow fibers [136,217,218]. Singh and Sirkar reported [219] that a higher flow rate of hot brine through the bore of the porous PP hollow fibers resulted in a significant pressure drop. Considerable salt leakage (salt concentration in the permeate of >50 mg/L) was observed at the highest brine flow rate of 150 mL/min due to the negative effect of flow pressure drop.

Cath et al. [10] revealed that there was a maximum allowable flow rate or flow velocity, and the mixing of the liquid in the channel, to some extent, was limited. They also emphasized the importance of pressure drop in the design of an MD system.

To achieve a turbulent flow regime while maintaining a flow rate below the maximum allowable flow rate, researchers have used spacers to enhance Re number to improve the flow regime, reduce the TPP, and increase the TPC value [220–222]. Phattaranawik et al. [222] reported that TPC values ranged from 0.9 to 0.97, which was close to unity for spacers-filled channels, whereas the TPC ranged merely from 0.57 to 0.76 without spacers. Manawi et al. [223] confirmed the same effect that the highest TPC value in their experiments increased from 0.66 at a feed flow rate of 1.5 L/min to 0.82 at a feed flow rate of 3.0 L/min, and that TPC values were 0.66 with spacers and 0.47 without spacers. Their results showed that increased feed flow rate and use of spacers in channels could reduce TPP and enhance TPC values. Nevertheless, flow rate or flow velocity should not be increased excessively because too high flow velocity leads to higher hydraulic pressure, which may be greater than LEP and result in pore wetting.

3.3.3. Operating Mode

The operating mode here refers to co-current, counter-current flow mode, and other modes. The co-current refers to the flow directions at both sides are the same, while the counter-current flow means both sides have an opposite flow direction. Figure 1. shows the counter-current flow mode. Manawi et al. [209] reported that the counter-current flow gave rise to a higher distillate flux when other conditions kept constant. They observed a permeate flux of 37 LMH using counter-current flow while the flux was 34.8 LMH using co-current flow with all other parameters the same (flow rates of both sides were 1.5 L/min, temperatures at feed and cold side were 70 and 30 °C, respectively). This enhancement of flux is due to a higher driving force induced by greater tangential force of counter-current flow. They concluded that the counter-current flow could increase temperature difference, thereby improving mass transfer. The enhancement of flux should be mainly attributed to increased TPC rather than temperature difference. Manawi et al. [223] also found that the counter-current flow generated a higher TPC value (0.66) than the co-current flow mode (0.59). Their observation reflected the counter-current flow caused a less TPP and a higher temperature difference.

Crossflow is another operation mode in which the membrane surfaces are continuously scoured and therefore enhancing resistance to water vapor flux decline in the presence of salt precipitations. For example, He et al. [217,218] and Song et al. [136] conducted a series of studies to investigate scaling behavior on lab-scale as well as pilot-scale DCMD performances for desalination using silicone-fluoropolymer coated PP hollow fiber membranes in crossflow DCMD mode. The authors demonstrated that no significant flux and no salt rejection reduction was observed at increasing temperatures or high concentrations, indicating no effect of $CaCO_3$ scaling on permeate flux. The authors [136,217,218] also concluded that the crossflow pattern and hydrophobic porous coating were beneficial for scaling resistance.

In addition to the conventional operating modes, another method for enhancing flux in MD was reported by Cath et al. [10]. They operated their MD by changing the positions of the solution pump and investigated the effects of different negative pressure (vacuum) values on flux. In the conventional DCMD configuration, the pump was installed between the MD cells and solution tanks, and the direction of fluid was from the tanks via pumps to MD cells. However, in their design and experiments, Cath et al. put pumps after the MD cells to suck the fluid from MD channels into outer fluid tanks. Results showed that flux increased by 15% while the fluid pressure at the permeate side reduced from positive 108 kPa to slightly negative 94 kPa. Moreover, the flux increased by 84% when the pressure dropped from 108 to 55 kPa compared to the flux of the conventional MD system. Water flux increased because of enhanced mass transport, which resulted from the alleviation of temperature polarization and partial mitigation of mass transfer resistance due to the stagnant air trapped inside the pores. Therefore, elimination of the gas or air from the solution and pores is beneficial for the higher performance of MD as discussed in Section 3.3.4.

3.3.4. Degasification

Non-condensable gas such as air [224] can dissolve in feed solution and then can be entrapped inside the membrane pores, which in turn increases the additional molecule diffusion resistance for mass transport [87,206,225]. Degasification of the feed stream and/or permeate stream reduces the diffusion resistance for mass transfer because of the reduced stagnant air layer. Schneider and van Gassel [226] introduced degassed fluid into MD to reduce the partial air pressure. They reported the flux increased greater than two folds when the permeate side operated under vacuum. In addition, Schofield et al. [227] investigated the effect of degassing on flux using pure water, and they reported that permeate flux increased by 50% due to the deaeration of the feed stream. They also found that deaeration of feeds increased heat transfer coefficients by seven-fold and reduced the heat loss via conduction to less than 10%. However, they stated that MD performance was more dependent on membrane modules rather than membranes themselves.

3.3.5. Long-Term Operation

The long-term operation generates potential risks of fouling and scaling on the membrane surface, leading to wetting or partial wetting of membrane pores, reducing flux, and increasing distillate conductivity. An example of long-term operation using PP hollow fiber membranes in a small pilot plant for desalination of seawater in three single-pair cross-flow DCMD was reported by Song et al. [136]. They investigated the desalination performance using actual trucked-in seawater (TDS 28,050 mg/L) as feed for 3 months in this study [136]. No salt leakage was observed for 5 days with the concentrated salty brine of ~19% prior to salts precipitation. The hydrophobic, silicone-fluoropolymer thin coating layer polymerized via plasma generated a high advancing CA of 142.18° for fresh coated PP hollow fiber membranes and contributed to the excellent performance of MD. Besides, cross-flow also played an important role in mitigating scaling.

Flat sheet membranes were employed in long-term MD. McGaughey et al. [228] reported a significant decrease in hydrophobicity and surface roughness of the membrane during desalting a 35 g/L NaCl solution with flat sheet expanded polytetrafluoroethylene (PTFE) for 100 days. CA of the membrane decreased by 56% for the used membrane compared with the pristine one (decreased from $140 \pm 4.0^\circ$ to $61 \pm 9.1^\circ$) along with a decrease of *LEP* from 450 to 0 kPa, and corresponding surface roughness at the feed side decreased from 31.0 ± 5.40 nm to 3.0 ± 0.88 nm showing a reduction percentage of 92%. However, they observed a stable SR of 99.8% and permeate conductivity of less than 8 $\mu\text{S}/\text{cm}$ throughout the 100-days experiments, although the distillate flux decreased from 30 to ~25 LMH. The low distillate conductivity and high SR demonstrated that most of the membrane was dry (not wetted), which was confirmed by the fact that the node area between fibers was composed of merely membrane materials via higher magnification energy-dispersive X-ray spectroscopy. The authors [228] concluded that the internal pore wall and permeate-side hydrophobicity played an important role

in anti-wetting during long-term operation. Other studies also observed the reduction of distillate electrical conductivity [135,229,230]. For instance, Guillen-Burrieza et al. [229] studied the long-term operation (intermittent from the year 2010 to 2013) effect on the desalination performance of salty marine solution (3.5 wt.% NaCl solution) using AGMD system in a solar MD pilot plant. They reported a significant increase in the minimum electrical conductivity of the permeate from 20 $\mu\text{S}/\text{cm}$ in 2010 to 10 mS/cm in 2013. However, they stated that this decline of electrical conductivity was due to pore wetting because of severe and extensive damage of the membrane rather than the conventionally reported scaling and operating wetting. In other words, the long-term operation may exert a complex effect on flux and distillate quality, which can be influenced by membranes, operating spans, feed solution compositions, and other conditions.

4. Interplay of Affecting Factors

The interlaced relevance effects of each factor on the MD mass transfer are summarized in Figure 6, including membrane properties, feed solution chemistry, and operating conditions. The interplay between various factors that affect flux and SR in MD is illustrated based on the feed solution grouped into inorganic salts and organics, and then sub-grouped organics into non-volatile and volatile organics. Non-volatiles are further divided into non-ionic and ionic types attributed to their dominant governing mechanisms of either hydrophobic interaction or electro-interaction (typically the electro-repulsion due to the same charges between the chemicals and membrane surface). Adverse variation of even one factor can result in unfavorable effects on others because of the “bottleneck principle”. The negative effect of only one factor without the optimal value or slight change may reduce flux and/or SR although all other parameters are optimal.

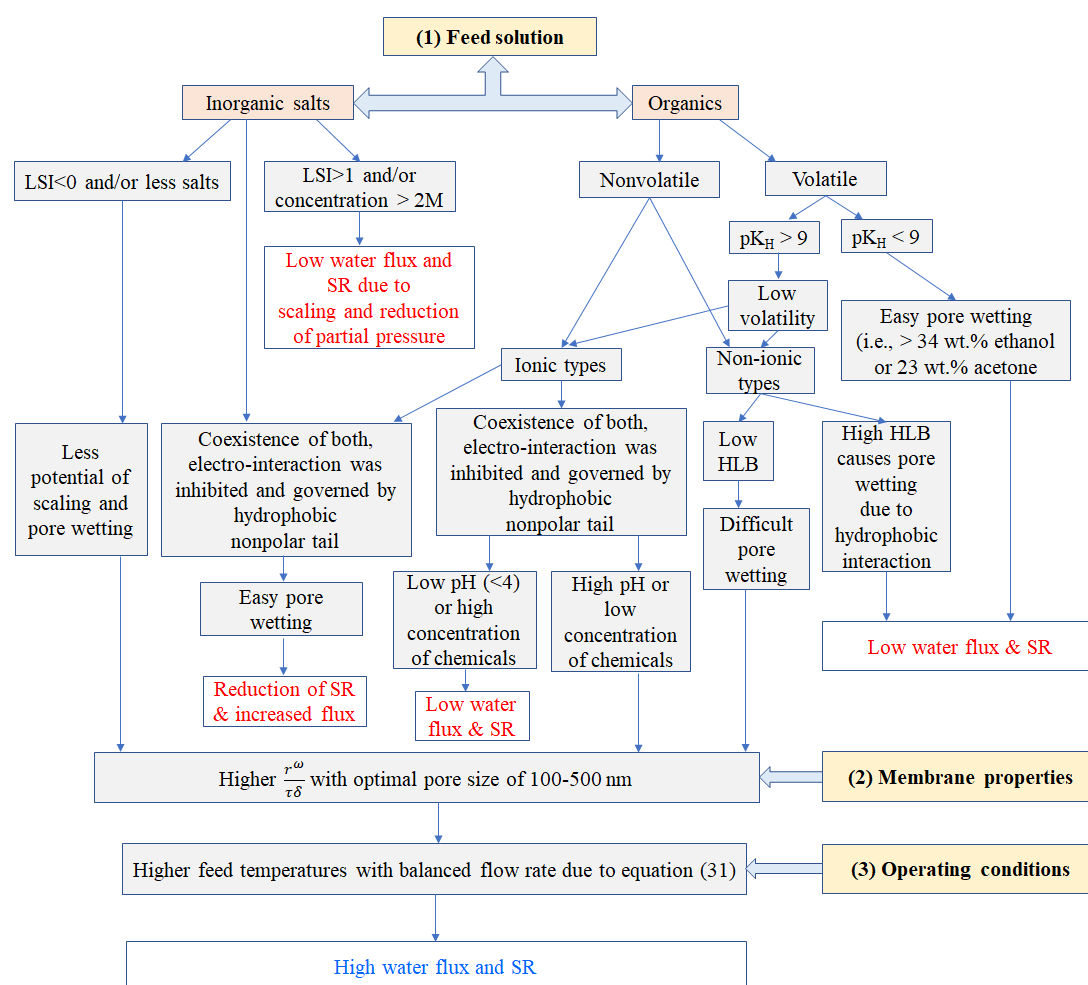


Figure 6. A diagram showing the interplay of factors affecting water flux and salt rejection in MD.

5. Conclusions

Estimating mass transfer and SR in MD is complicated and needs a systematic approach because many factors need to be considered, including membrane properties, feed solution, and operating conditions. A comprehensive understanding of interactions of these factors and their effects on heat transfer, mass transfer, and SR can provide a complete and valuable foundation for modeling mass and heat transfer, selecting membranes, optimizing operation, enhancing flux, and reducing membrane scaling and fouling. Although there were studies that examined some aspects of factors that may affect water vapor transport via analysis of operating conditions or membranes properties and the physico-chemical attributes of feed solutions, a systematic discussion and analysis of the importance of each factor is still of vital importance for the evaluation of MD performance in terms of predicting mass flux and SR. The interplay of the factors affecting the MD mass transfer showed the adverse variation of even one of the factors could cause negative effect because of the “bottleneck principle”, although all other parameters are optimal.

It is noteworthy that this review aims to qualitatively determine the interaction of each factor and the effect of all the factors on mass transfer and rejection of salts in the application of MD. Further research, such as mathematical and empirical modeling on the significance of parameters on the performance of MD system, should be conducted and validated by experimental results.

Author Contributions: L.C., P.X. and H.W. wrote the original draft and edited the manuscript. H.W. and P.X. acquired funding and managed the research project. All authors have read and agreed to the published version of the manuscript.

Funding: This research was funded by the United States Bureau of Reclamation Desalination and Water Purification Research and Development Program (Agreement No. R19AC00109) and ExxonMobil Upstream Research Company for financial support.

Acknowledgments: The authors thank Deepak Musale, Carlos Galdeano, and Ganesh L. Ghurye with ExxonMobil for technical discussions. Lin Chen thanks New Mexico Water Resource Research Institute (WRRRI) Student Research Grant for financial, conference communication, and administrative assistance in funding and managing the project.

Conflicts of Interest: The authors declare no conflict of interest. The funders had no role in the design of the study; in the collection, analyses, or interpretation of data; in the writing of the manuscript, or in the decision to publish the results.

Nomenclature

A	Surface area of membrane (m^2)
$AGMD$	Air gap membrane distillation
B	Geometry coefficient for pore structure
B_w^K	Mass transfer coefficients for Knudsen diffusion (m/s)
B_w^M	Mass transfer coefficients for molecular diffusion (m/s)
B_w	Mass transfer coefficient (m/s)
C_1	non-volatile solutes Concentration at liquid/membrane interface (mg/L)
C_f	Concentration of non-volatile solutes at bulk feed side (mg/L)
c_p	Specific heat of fluid (J/kg/K)
CA	Contact angle ($^\circ$)
$CTBW$	Cooling tower blowdown water
D	Water molecule diffusion coefficient (m^2/s)
d	Hydraulic diameter of the flow channel (m)
d_h	Hydraulic diameter (m)
d_p	Membrane pore size (nm)
$DCMD$	Direct contact membrane distillation
$DLVO$	Derjaguin, Landau, Verwey, and Overbeek
f	Friction factor (dimensionless)
H	Overall heat transfer coefficient ($W/m^2/K$)
h_f	Heat transfer coefficients at the bulk feed side

h_p	Heat transfer coefficients at the bulk permeate side
HLB	Hydrophilic-lipophilic balance value (dimensionless)
$\Delta H_{v,w}$	Latent heat of vaporization of water (KJ/kg)
J	Water flux (kg/m ² /h)
k	Fluid thermal conductivity (W/m/K)
k_B	Boltzmann constant
k_g	Thermal conductivity of gas inside pores (W/m/K)
K_H	Henry's law constant (atm·m ³ /mol)
k_m	Overall thermal conductivity of the membrane (W/m/K)
K_n	Knudsen number (dimensionless)
k_s	Thermal conductivity of membrane material (W/m/K)
L	Length of channels (m)
l	Distance from the membrane surface (m)
LEP	Liquid entry pressure (kPa)
LMH	Liters per meter square per hour (L/m ² /h)
LSI	Langelier Saturation Index (dimensionless)
m	Mass of membrane (kg)
MD	Membrane distillation
NOM	Natural organic matter
P	Total pressure (Pa)
ΔP	Pressure drop (Pa)
P_1	Partial pressure of vapor at liquid-vapor interface at feed side (Pa)
P_2	Partial pressure of vapor at liquid-vapor interface at permeate side (Pa)
P_a	Air pressure inside the membrane pores (Pa)
P_f	Pressure at feed side (Pa)
P_i	Partial pressure of liquid-vapor interface (Pa)
P_m	Mean pressure within pores (Pa)
P_p	Pressure at permeate side (Pa)
$PDMS$	Poly-dimethylsiloxane
PP	Polypropylene
PSD	Pore size distribution
$PS-PDMS$	Polysulfone-poly-dimethylsiloxane
$PTFE$	Polytetrafluoroethylene
$PVDF$	Polyvinylidene fluoride
Q	Heat flux (W)
R	Gas constant (J/mol/K)
r_{max}	Maximum pore size (nm)
RO	Reverse osmosis
SDS	Sodium dodecyl sulfate
SEC	Specific energy consumption
$SGMD$	Sweeping gas membrane distillation
SR	Salt rejection
T_1	Absolute temperature of membrane surface at feed side (K)
T_2	Absolute temperature of membrane surface at permeate side (K)
T_p	Absolute temperature of the bulk permeate side (K)
T_f	Absolute temperature of the bulk feed side (K)
TPC	Temperature polarization coefficient
TPP	Temperature polarization phenomenon
$TrOCs$	Trace organic compounds
VMD	Vacuum membrane distillation
u	Average velocity (m/s)
α	Selectivity of volatile chemical (dimensionless)
μ	Viscosity of fluid (Pa·s)
ρ	Density of fluid (kg/m ³)
ε	Porosity of membrane (dimensionless)

ρ_p	Density of membrane material (kg/m ³)
τ	Tortuosity of membrane (dimensionless)
ω	A diffusion coefficient for pore radius (dimensionless)
θ	Water contact angle (°)
λ	Mean free path of water molecules (m)
δ	Membrane thickness (μm)

References

- Xu, X.; He, Q.; Ma, G.; Wang, H.; Nirmalakhandan, N.; Xu, P. Selective separation of mono- and di-valent cations in electrodialysis during brackish water desalination: Bench and pilot-scale studies. *Desalination* **2018**, *428*, 146–160. [[CrossRef](#)]
- Scanlon, B.R.; Reedy, R.C.; Xu, P.; Engle, M.; Nicot, J.; Yoxtheimer, D.; Yang, Q.; Ikonnikova, S. Can we beneficially reuse produced water from oil and gas extraction in the U.S.? *Sci. Total Environ.* **2020**, *717*, 137085. [[CrossRef](#)] [[PubMed](#)]
- Hancock, N.T.; Xu, P.; Roby, M.J.; Gomez, J.D.; Cath, T.Y. Towards direct potable reuse with forward osmosis: Technical assessment of long-term process performance at the pilot scale. *J. Membr. Sci.* **2013**, *445*, 34–46. [[CrossRef](#)]
- Amy, G.; Ghaffour, N.; Li, Z.; Francis, L.; Linares, R.V.; Missimer, T.; Lattemann, S. Membrane-based seawater desalination: Present and future prospects. *Desalination* **2017**, *401*, 16–21. [[CrossRef](#)]
- Rao, P.; Aghajanzadeh, A.; Sheaffer, P.; Morrow, W.R.; Brueske, S.; Dollinger, C.; Price, K.; Sarker, P.; Ward, N.; Cresko, J. *Volume 1: Survey of Available Information in Support of the Energy-Water Bandwidth Study of Desalination Systems*; Report Prepared by Lawrence Berkeley National Laboratory (LBNL) and Energetics Incorporated for the U.S. Department of Energy's Advanced Manufacturing Office (AMO): Washington, DC, USA, 2016.
- USDOE. *Bandwidth Study on Energy Use and Potential Energy Savings Opportunities in U.S. Seawater Desalination Systems*; Report Published by Advanced Manufacturing Office (AMO) of the U.S. Department of Energy (USDOE) under Contract No. DE-AC02-05CH11231: Washington, DC, USA, 2017.
- Kaminski, W.; Marszalek, J.; Tomczak, E. Water desalination by pervaporation—Comparison of energy consumption. *Desalination* **2018**, *433*, 89–93. [[CrossRef](#)]
- Zarzo, D.; Prats, D. Desalination and energy consumption. What can we expect in the near future? *Desalination* **2018**, *427*, 1–9. [[CrossRef](#)]
- Bodell, B.R. Silicone Rubber Vapor Diffusion in Saline Water Distillation. Patent Serial No. 285,032, 3 June 1963.
- Cath, T.Y.; Adams, V.D.; Childress, A.E. Experimental study of desalination using direct contact membrane distillation: A new approach to flux enhancement. *J. Membr. Sci.* **2004**, *228*, 5–16. [[CrossRef](#)]
- Larbot, A.; Gazagnes, L.; Krajewski, S.; Bukowska, M.; Kujawski, W. Water desalination using ceramic membrane distillation. *Desalination* **2004**, *168*, 367–372. [[CrossRef](#)]
- Li, B.; Sirkar, K.K. Novel membrane and device for vacuum membrane distillation-based desalination process. *J. Membr. Sci.* **2005**, *257*, 60–75. [[CrossRef](#)]
- Xu, Y.; Zhu, B.-K.; Xu, Y.-Y. Pilot test of vacuum membrane distillation for seawater desalination on a ship. *Desalination* **2006**, *189*, 165–169. [[CrossRef](#)]
- Cerneaux, S.; Struzyńska, I.; Kujawski, W.; Persin, M.; Larbot, A. Comparison of various membrane distillation methods for desalination using hydrophobic ceramic membranes. *J. Membr. Sci.* **2009**, *337*, 55–60. [[CrossRef](#)]
- Ma, Z.; Hong, Y.; Ma, L.; Su, M. Superhydrophobic Membranes with Ordered Arrays of Nanospiked Microchannels for Water Desalination. *Langmuir* **2009**, *25*, 5446–5450. [[CrossRef](#)] [[PubMed](#)]
- Safavi, M.; Mohammadi, T. High-salinity water desalination using VMD. *Chem. Eng. J.* **2009**, *149*, 191–195. [[CrossRef](#)]
- Cipollina, A.; Di Sparti, M.; Tamburini, A.; Micale, G. Development of a Membrane Distillation module for solar energy seawater desalination. *Chem. Eng. Res. Des.* **2012**, *90*, 2101–2121. [[CrossRef](#)]
- Fang, H.; Gao, J.; Wang, H.; Chen, C. Hydrophobic porous alumina hollow fiber for water desalination via membrane distillation process. *J. Membr. Sci.* **2012**, *403*, 41–46. [[CrossRef](#)]
- Singh, D.; Sirkar, K.K. Desalination of brine and produced water by direct contact membrane distillation at high temperatures and pressures. *J. Membr. Sci.* **2012**, *389*, 380–388. [[CrossRef](#)]

20. Geng, H.; Wu, H.; Li, P.; He, Q. Study on a new air-gap membrane distillation module for desalination. *Desalination* **2014**, *334*, 29–38. [[CrossRef](#)]
21. Wang, Y.; Xu, Z.; Lior, N.; Zeng, H. An experimental study of solar thermal vacuum membrane distillation desalination. *Desalin. Water Treat.* **2014**, *53*, 887–897. [[CrossRef](#)]
22. Khalifa, A.E.; Lawal, D.U. Performance and Optimization of Air Gap Membrane Distillation System for Water Desalination. *Arab. J. Sci. Eng.* **2015**, *40*, 3627–3639. [[CrossRef](#)]
23. Ren, C.; Fang, H.; Gu, J.; Winnubst, L.; Chen, C. Preparation and characterization of hydrophobic alumina planar membranes for water desalination. *J. Eur. Ceram. Soc.* **2015**, *35*, 723–730. [[CrossRef](#)]
24. Woo, Y.C.; Tijing, L.D.; Shim, W.-G.; Choi, J.-S.; Kim, S.-H.; He, T.; Drioli, E.; Shon, H.K. Water desalination using graphene-enhanced electrospun nanofiber membrane via air gap membrane distillation. *J. Membr. Sci.* **2016**, *520*, 99–110. [[CrossRef](#)]
25. Alkhubdhiri, A.; Hilal, N. Air gap membrane distillation: A detailed study of high saline solution. *Desalination* **2017**, *403*, 179–186. [[CrossRef](#)]
26. Hubadillah, S.K.; Othman, M.H.D.; Matsuura, T.; Rahman, M.A.; Jaafar, J.; Ismail, A.; Amin, S.Z.M. Green silica-based ceramic hollow fiber membrane for seawater desalination via direct contact membrane distillation. *Sep. Purif. Technol.* **2018**, *205*, 22–31. [[CrossRef](#)]
27. Nthunya, L.N.; Gutierrez, L.; Lapeire, L.; Verbeken, K.; Zaouri, N.; Nxumalo, E.N.; Mamba, B.B.; Verliefe, A.R.; Mhlanga, S.D. Fouling-resistant PVDF nanofibre membranes for the desalination of brackish water in membrane distillation. *Sep. Purif. Technol.* **2019**, *228*, 115793. [[CrossRef](#)]
28. Macedonio, F.; Ali, A.; Poerio, T.; El-Sayed, E.; Drioli, E.; Abdel-Jawad, M. Direct contact membrane distillation for treatment of oilfield produced water. *Sep. Purif. Technol.* **2014**, *126*, 69–81. [[CrossRef](#)]
29. Lokare, O.R.; Tavakkoli, S.; Wadekar, S.; Khanna, V.; Vidic, R.D. Fouling in direct contact membrane distillation of produced water from unconventional gas extraction. *J. Membr. Sci.* **2017**, *524*, 493–501. [[CrossRef](#)]
30. Li, F.; Huang, J.; Xia, Q.; Lou, M.; Yang, B.; Tian, Q.; Liu, Y. Direct contact membrane distillation for the treatment of industrial dyeing wastewater and characteristic pollutants. *Sep. Purif. Technol.* **2018**, *195*, 83–91. [[CrossRef](#)]
31. Xu, J.; Srivatsa Bettahalli, N.M.; Chisca, S.; Khalid, M.K.; Ghaffour, N.; Vilagines, R.; Nunes, S.P. Polyoxadiazole hollow fibers for produced water treatment by direct contact membrane distillation. *Desalination* **2018**, *432*, 32–39. [[CrossRef](#)]
32. Attia, H.; Osman, M.S.; Johnson, D.J.; Wright, C.; Hilal, N. Modelling of air gap membrane distillation and its application in heavy metals removal. *Desalination* **2017**, *424*, 27–36. [[CrossRef](#)]
33. Fujii, Y.; Kigoshi, S.; Iwatani, H.; Aoyama, M. Selectivity and characteristics of direct contact membrane distillation type experiment. I. Permeability and selectivity through dried hydrophobic fine porous membranes. *J. Membr. Sci.* **1992**, *72*, 53–72. [[CrossRef](#)]
34. Fujii, Y.; Kigoshi, S.; Iwatani, H.; Aoyama, M.; Fusaoka, Y. Selectivity and characteristics of direct contact membrane distillation type experiment. II. Membrane treatment and selectivity increase. *J. Membr. Sci.* **1992**, *72*, 73–89. [[CrossRef](#)]
35. Criscuoli, A.; Bafaro, P.; Drioli, E. Vacuum membrane distillation for purifying waters containing arsenic. *Desalination* **2013**, *323*, 17–21. [[CrossRef](#)]
36. Ozbey-Unal, B.; Koseoglu-Imer, D.Y.; Keskinler, B.; Koyuncu, I. Boron removal from geothermal water by air gap membrane distillation. *Desalination* **2018**, *433*, 141–150. [[CrossRef](#)]
37. Bush, J.A.; Vanneste, J.; Cath, T.Y. Comparison of membrane distillation and high-temperature nanofiltration processes for treatment of silica-saturated water. *J. Membr. Sci.* **2019**, *570–571*, 258–269. [[CrossRef](#)]
38. Choi, Y.; Naidu, G.; Lee, S.; Vigneswaran, S. Recovery of sodium sulfate from seawater brine using fractional submerged membrane distillation crystallizer. *Chemosphere* **2020**, *238*, 124641. [[CrossRef](#)] [[PubMed](#)]
39. Li, Q.; Omar, A.; Cha-Umpong, W.; Liu, Q.; Li, X.; Wen, J.; Wang, Y.; Razmjou, A.; Guan, J.; Izadgoshasb, I. The potential of hollow fiber vacuum multi-effect membrane distillation for brine treatment. *Appl. Energy* **2020**, *276*, 115437. [[CrossRef](#)]
40. AlRehaili, O.; Perreault, F.; Sinha, S.; Westerhoff, P. Increasing net water recovery of reverse osmosis with membrane distillation using natural thermal differentials between brine and co-located water sources: Impacts at large reclamation facilities. *Water Res.* **2020**, *184*, 116134. [[CrossRef](#)] [[PubMed](#)]
41. Laganà, F.; Barbieri, G.; Drioli, E. Direct contact membrane distillation: Modelling and concentration experiments. *J. Membr. Sci.* **2000**, *166*, 1–11. [[CrossRef](#)]

42. Pagliero, M.; Bottino, A.; Comite, A.; Costa, C. Novel hydrophobic PVDF membranes prepared by nonsolvent induced phase separation for membrane distillation. *J. Membr. Sci.* **2020**, *596*. [[CrossRef](#)]
43. Grasso, G.; Galiano, F.; Yoo, M.J.; Mancuso, R.; Park, H.B.; Gabriele, B.; Figoli, A.; Drioli, E. Development of graphene-PVDF composite membranes for membrane distillation. *J. Membr. Sci.* **2020**, *604*. [[CrossRef](#)]
44. Rana, D.; Rana, D.; Matsuura, T.; Yang, F.; Cong, Y.; Lan, C.Q. Triple-Layered Nanofibrous Metal–Organic Framework-Based Membranes for Desalination by Direct Contact Membrane Distillation. *ACS Sustain. Chem. Eng.* **2020**, *8*, 6601–6610. [[CrossRef](#)]
45. Ahmed, F.E.; Lalia, B.S.; Hashaikh, R.; Hilal, N. Enhanced performance of direct contact membrane distillation via selected electrothermal heating of membrane surface. *J. Membr. Sci.* **2020**, *610*, 118224. [[CrossRef](#)]
46. Xu, K.; Cai, Y.; Hassankiadeh, N.T.; Cheng, Y.; Li, X.; Wang, X.; Wang, Z.; Drioli, E.; Cui, Z. ECTFE membrane fabrication via TIPS method using ATBC diluent for vacuum membrane distillation. *Desalination* **2019**, *456*, 13–22. [[CrossRef](#)]
47. Wang, W.; Du, X.; Vahabi, H.; Zhao, S.; Yin, Y.; Kota, A.K.; Tong, T. Trade-off in membrane distillation with monolithic omniphobic membranes. *Nat. Commun.* **2019**, *10*, 3220. [[CrossRef](#)]
48. Shaulsky, E.; Karanikola, V.; Straub, A.P.; Deshmukh, A.; Zucker, I.; Elimelech, M. Asymmetric membranes for membrane distillation and thermo-osmotic energy conversion. *Desalination* **2019**, *452*, 141–148. [[CrossRef](#)]
49. Khayet, M.; García-Payo, C.; Matsuura, T. Superhydrophobic nanofibers electrospun by surface segregating fluorinated amphiphilic additive for membrane distillation. *J. Membr. Sci.* **2019**, *588*, 117215. [[CrossRef](#)]
50. Khayet, M.; Essalhi, M.; Qtaishat, M.R.; Matsuura, T. Robust surface modified polyetherimide hollow fiber membrane for long-term desalination by membrane distillation. *Desalination* **2019**, *466*, 107–117. [[CrossRef](#)]
51. Gustafson, R.D.; McGaughey, A.L.; Ding, W.; McVety, S.C.; Childress, A.E. Morphological changes and creep recovery behavior of expanded polytetrafluoroethylene (ePTFE) membranes used for membrane distillation. *J. Membr. Sci.* **2019**, *584*, 236–245. [[CrossRef](#)]
52. Deka, B.J.; Lee, E.-J.; Guo, J.; Kharraz, J.; An, A.K. Electrospun Nanofiber Membranes Incorporating PDMS-Aerogel Superhydrophobic Coating with Enhanced Flux and Improved Antiwettability in Membrane Distillation. *Environ. Sci. Technol.* **2019**, *53*, 4948–4958. [[CrossRef](#)] [[PubMed](#)]
53. Li, M.; Lu, K.J.; Wang, L.; Zhang, X.; Chung, T.-S. Janus membranes with asymmetric wettability via a layer-by-layer coating strategy for robust membrane distillation. *J. Membr. Sci.* **2020**, *603*, 118031. [[CrossRef](#)]
54. Chew, N.G.P.; Zhang, Y.; Goh, K.; Ho, J.S.; Xu, R.; Wang, R. Hierarchically Structured Janus Membrane Surfaces for Enhanced Membrane Distillation Performance. *ACS Appl. Mater. Interfaces* **2019**, *11*, 25524–25534. [[CrossRef](#)] [[PubMed](#)]
55. Nguyen, N.C.; Duong, H.C.; Nguyen, H.T.; Chen, S.-S.; Le, H.Q.; Ngo, H.H.; Guo, W.; Duong, C.C.; Le, N.C.; Bui, X.T. Forward osmosis–membrane distillation hybrid system for desalination using mixed trivalent draw solution. *J. Membr. Sci.* **2020**, *603*, 118029. [[CrossRef](#)]
56. Wang, W.; Shi, Y.; Zhang, C.; Hong, S.; Shi, L.; Chang, J.; Li, R.; Jin, Y.; Ong, C.S.; Zhuo, S.; et al. Simultaneous production of fresh water and electricity via multistage solar photovoltaic membrane distillation. *Nat. Commun.* **2019**, *10*, 3012. [[CrossRef](#)] [[PubMed](#)]
57. Tufa, R.A.; Noviello, Y.; Di Profio, G.; Macedonio, F.; Ali, A.; Drioli, E.; Fontananova, E.; Bouzek, K.; Curcio, E. Integrated membrane distillation–reverse electrodialysis system for energy-efficient seawater desalination. *Appl. Energy* **2019**, *253*, 113551. [[CrossRef](#)]
58. Lawson, K.W.; Lloyd, D.R. Membrane distillation. *J. Membr. Sci.* **1997**, *124*, 1–25. [[CrossRef](#)]
59. Olatunji, S.O.; Camacho, L.M. Heat and Mass Transport in Modeling Membrane Distillation Configurations: A Review. *Front. Energy Res.* **2018**, *6*, 130. [[CrossRef](#)]
60. Hitsov, I.; Maere, T.; De Sitter, K.; Dotremont, C.; Nopens, I. Modelling approaches in membrane distillation: A critical review. *Sep. Purif. Technol.* **2015**, *142*, 48–64. [[CrossRef](#)]
61. He, Q.; Li, P.; Geng, H.; Zhang, C.; Wang, J.; Chang, H. Modeling and optimization of air gap membrane distillation system for desalination. *Desalination* **2014**, *354*, 68–75. [[CrossRef](#)]
62. Khayet, M. Membranes and theoretical modeling of membrane distillation: A review. *Adv. Colloid Interface Sci.* **2011**, *164*, 56–88. [[CrossRef](#)]
63. Choudhury, M.R.; Anwar, N.; Jassby, D.; Rahaman, S. Fouling and wetting in the membrane distillation driven wastewater reclamation process—A review. *Adv. Colloid Interface Sci.* **2019**, *269*, 370–399. [[CrossRef](#)]
64. Warsinger, D.M.; Swaminathan, J.; Guillen-Burrieza, E.; Ararat, H.A.; Lienhard, V.J.H. Scaling and fouling in membrane distillation for desalination applications: A review. *Desalination* **2015**, *356*, 294–313. [[CrossRef](#)]

65. Tijjng, L.D.; Woo, Y.C.; Choi, J.-S.; Lee, S.; Kim, S.-H.; Shon, H.K. Fouling and its control in membrane distillation—A review. *J. Membr. Sci.* **2015**, *475*, 215–244. [[CrossRef](#)]
66. Naidu, G.; Tijjng, L.; Johir, M.; Shon, H.K.; Vigneswaran, S. Hybrid membrane distillation: Resource, nutrient and energy recovery. *J. Membr. Sci.* **2020**, *599*, 117832. [[CrossRef](#)]
67. Ghaffour, N.; Soukane, S.; Lee, J.-G.; Kim, Y.; Alpatova, A. Membrane distillation hybrids for water production and energy efficiency enhancement: A critical review. *Appl. Energy* **2019**, *254*, 113698. [[CrossRef](#)]
68. Gopi, G.; Arthanareeswaran, G.; Ismail, A.F. Perspective of renewable desalination by using membrane distillation. *Chem. Eng. Res. Des.* **2019**, *144*, 520–537. [[CrossRef](#)]
69. Ullah, R.; Khraisheh, M.; Esteves, R.J.; McLeskey, J.T.; AlGhouthi, M.; Gad-El-Hak, M.; Tafreshi, H.V. Energy efficiency of direct contact membrane distillation. *Desalination* **2018**, *433*, 56–67. [[CrossRef](#)]
70. Deshmukh, A.; Boo, C.; Karanikola, V.; Lin, S.; Straub, A.P.; Tong, T.; Warsinger, D.M.; Elimelech, M. Membrane distillation at the water-energy nexus: Limits, opportunities, and challenges. *Energy Environ. Sci.* **2018**, *11*, 1177–1196. [[CrossRef](#)]
71. Zhang, Y.; Peng, Y.; Ji, S.; Li, Z.; Chen, P. Review of thermal efficiency and heat recycling in membrane distillation processes. *Desalination* **2015**, *367*, 223–239. [[CrossRef](#)]
72. Khayet, M. Solar desalination by membrane distillation: Dispersion in energy consumption analysis and water production costs (a review). *Desalination* **2013**, *308*, 89–101. [[CrossRef](#)]
73. Luo, A.; Lior, N. Critical review of membrane distillation performance criteria. *Desalination Water Treat.* **2016**, *57*, 20093–20140. [[CrossRef](#)]
74. Yalcinkaya, F. A review on advanced nanofiber technology for membrane distillation. *J. Eng. Fibers Fabr.* **2019**, *14*, 1558925018824901. [[CrossRef](#)]
75. Shaulsky, E.; Nejati, S.; Boo, C.; Perreault, F.; Osuji, C.O.; Elimelech, M. Post-fabrication modification of electrospun nanofiber mats with polymer coating for membrane distillation applications. *J. Membr. Sci.* **2017**, *530*, 158–165. [[CrossRef](#)]
76. Eykens, L.; De Sitter, K.; Dotremont, C.; Pinoy, L.; Van Der Bruggen, B. How to Optimize the Membrane Properties for Membrane Distillation: A Review. *Ind. Eng. Chem. Res.* **2016**, *55*, 9333–9343. [[CrossRef](#)]
77. Yao, M.; Tijjng, L.D.; Naidu, G.; Kim, S.-H.; Matsuyama, H.; Fane, A.G.; Shon, H.K. A review of membrane wettability for the treatment of saline water deploying membrane distillation. *Desalination* **2020**, *479*, 114312. [[CrossRef](#)]
78. Ray, S.S.S.; Lee, H.K.; Kwon, Y.-N. Review on Blueprint of Designing Anti-Wetting Polymeric Membrane Surfaces for Enhanced Membrane Distillation Performance. *Polymers* **2019**, *12*, 23. [[CrossRef](#)]
79. Rezaei, M.; Warsinger, D.M.; Lienhard, J.H.; Duke, M.C.; Matsuura, T.; Samhaber, W.M. Wetting phenomena in membrane distillation: Mechanisms, reversal, and prevention. *Water Res.* **2018**, *139*, 329–352. [[CrossRef](#)]
80. Li, L.; Sirkar, K.K. Influence of microporous membrane properties on the desalination performance in direct contact membrane distillation. *J. Membr. Sci.* **2016**, *513*, 280–293. [[CrossRef](#)]
81. Ashoor, B.B.; Mansour, S.; Giwa, A.; Dufour, V.; Hasan, S.W. Principles and applications of direct contact membrane distillation (DCMD): A comprehensive review. *Desalination* **2016**, *398*, 222–246. [[CrossRef](#)]
82. Abu-Zeid, M.A.E.-R.; Zhang, Y.; Dong, H.; Zhang, L.; Chen, H.-L.; Hou, L.-A. A comprehensive review of vacuum membrane distillation technique. *Desalination* **2015**, *356*, 1–14. [[CrossRef](#)]
83. Shahu, V.; Thombre, S.B. Air gap membrane distillation: A review. *J. Renew. Sustain. Energy* **2019**, *11*, 045901. [[CrossRef](#)]
84. Ramlow, H.; Ferreira, R.K.M.; Marangoni, C.; Machado, R.A.F. Ceramic membranes applied to membrane distillation: A comprehensive review. *Int. J. Appl. Ceram. Technol.* **2019**, *16*, 2161–2172. [[CrossRef](#)]
85. González, D.; Amigo, J.; Suárez, F. Membrane distillation: Perspectives for sustainable and improved desalination. *Renew. Sustain. Energy Rev.* **2017**, *80*, 238–259. [[CrossRef](#)]
86. Schofield, R.W.; Fane, A.G.; Fell, C.J.D.; Macoun, R. Factors affecting flux in membrane distillation. *Desalination* **1990**, *77*, 279–294. [[CrossRef](#)]
87. El-Bourawi, M.; Ding, Z.; Ma, R.; Khayet, M. A framework for better understanding membrane distillation separation process. *J. Membr. Sci.* **2006**, *285*, 4–29. [[CrossRef](#)]
88. Alkhudhiri, A.; Darwish, N.; Hilal, N. Membrane distillation: A comprehensive review. *Desalination* **2012**, *287*, 2–18. [[CrossRef](#)]
89. Criscuoli, A. Membrane Distillation: Principles, Applications and Perspectives. *J. Membr. Sci. Technol.* **2017**, *7*, e123. [[CrossRef](#)]

90. Bhushan, B.; Jung, Y.C. Wetting, adhesion and friction of superhydrophobic and hydrophilic leaves and fabricated micro/nanopatterned surfaces. *J. Phys. Condens. Matter* **2008**, *20*, 225010. [[CrossRef](#)]
91. Yoshimitsu, Z.; Nakajima, A.; Watanabe, T.; Hashimoto, K. Effects of Surface Structure on the Hydrophobicity and Sliding Behavior of Water Droplets. *Langmuir* **2002**, *18*, 5818–5822. [[CrossRef](#)]
92. Camacho, L.M.; Dumée, L.F.; Zhang, J.; Li, J.-D.; Duke, M.C.; Gomez, J.; Gray, S.R. Advances in Membrane Distillation for Water Desalination and Purification Applications. *Water* **2013**, *5*, 94–196. [[CrossRef](#)]
93. Drioli, E.; Ali, A.; Macedonio, F. Membrane distillation: Recent developments and perspectives. *Desalination* **2015**, *356*, 56–84. [[CrossRef](#)]
94. Franken, A.; Nolten, J.; Mulder, M.; Bargeman, D.; Smolders, C. Wetting criteria for the applicability of membrane distillation. *J. Membr. Sci.* **1987**, *33*, 315–328. [[CrossRef](#)]
95. Miwa, M.; Nakajima, A.; Fujishima, A.; Hashimoto, K.; Watanabe, T. Effects of the Surface Roughness on Sliding Angles of Water Droplets on Superhydrophobic Surfaces. *Langmuir* **2000**, *16*, 5754–5760. [[CrossRef](#)]
96. Nakajima, A.; Hashimoto, K.; Watanabe, T. Recent studies on super-hydrophobic films. In *Molecular Materials and Functional Polymers*; Springer: Vienna, Austria, 2001; pp. 31–41.
97. Nishino, T.; Meguro, M.; Nakamae, K.; Matsushita, A.M.; Ueda, Y. The Lowest Surface Free Energy Based on $-CF_3$ Alignment. *Langmuir* **1999**, *15*, 4321–4323. [[CrossRef](#)]
98. Gostoli, C.; Sarti, G.C.; Matulli, S. Low Temperature Distillation through Hydrophobic Membranes. *Sep. Sci. Technol.* **1987**, *22*, 855–872. [[CrossRef](#)]
99. Marmur, A. Wetting on Hydrophobic Rough Surfaces: To Be Heterogeneous or Not to Be? *Langmuir* **2003**, *19*, 8343–8348. [[CrossRef](#)]
100. Gryta, M.; Tomaszewska, M. Heat transport in the membrane distillation process. *J. Membr. Sci.* **1998**, *144*, 211–222. [[CrossRef](#)]
101. Lawson, K.W.; Lloyd, D.R. Membrane distillation. II. Direct contact MD. *J. Membr. Sci.* **1996**, *120*, 123–133. [[CrossRef](#)]
102. Tomaszewska, M. Preparation and properties of flat-sheet membranes from poly (vinylidene fluoride) for membrane distillation. *Desalination* **1996**, *104*, 1–11. [[CrossRef](#)]
103. Khayet, M.; Velazquez, A.; Mengual, J.I. Modelling mass transport through a porous partition: Effect of pore size distribution. *J. Non-Equilibrium Thermodyn.* **2004**, *29*, 279–299. [[CrossRef](#)]
104. Qtaishat, M.; Matsuura, T.; Kruczek, B.; Khayet, M. Heat and mass transfer analysis in direct contact membrane distillation. *Desalination* **2008**, *219*, 272–292. [[CrossRef](#)]
105. Khayet, M.; Imdakm, A.; Matsuura, T. Monte Carlo simulation and experimental heat and mass transfer in direct contact membrane distillation. *Int. J. Heat Mass Transf.* **2010**, *53*, 1249–1259. [[CrossRef](#)]
106. Zhang, J.; Gray, S.R.; Li, J.-D. Modelling heat and mass transfers in DCMD using compressible membranes. *J. Membr. Sci.* **2012**, *387*, 7–16. [[CrossRef](#)]
107. Schofield, R.; Fane, A.; Fell, C. Heat and mass transfer in membrane distillation. *J. Membr. Sci.* **1987**, *33*, 299–313. [[CrossRef](#)]
108. Burgoyne, A.; Vahdati, M.M. Direct Contact Membrane Distillation. *Sep. Sci. Technol.* **2000**, *35*, 1257–1284. [[CrossRef](#)]
109. Khayet, M.; Godino, M.P.; Mengual, J.I. Modelling Transport Mechanism through a Porous Partition. *J. Non-Equilibrium Thermodyn.* **2001**, *26*, 1–14. [[CrossRef](#)]
110. Ding, Z.; Ma, R.; Fane, A.G. A new model for mass transfer in direct contact membrane distillation. *Desalination* **2003**, *151*, 217–227. [[CrossRef](#)]
111. Martínez, L.; Rodríguez-Maroto, J.M. Characterization of membrane distillation modules and analysis of mass flux enhancement by channel spacers. *J. Membr. Sci.* **2006**, *274*, 123–137. [[CrossRef](#)]
112. Martínez, L.; Rodríguez-Maroto, J.M. On transport resistances in direct contact membrane distillation. *J. Membr. Sci.* **2007**, *295*, 28–39. [[CrossRef](#)]
113. Lu, J.; Yu, Y.; Zhou, J.; Song, L.; Hu, X.; Larbot, A. FAS grafted superhydrophobic ceramic membrane. *Appl. Surf. Sci.* **2009**, *255*, 9092–9099. [[CrossRef](#)]
114. Li, L.; Sirkar, K.K. Studies in vacuum membrane distillation with flat membranes. *J. Membr. Sci.* **2017**, *523*, 225–234. [[CrossRef](#)]
115. Laqbaqbi, M.; García-Payo, M.C.; Khayet, M.; El Kharraz, J.; Chaouch, M. Application of direct contact membrane distillation for textile wastewater treatment and fouling study. *Sep. Purif. Technol.* **2019**, *209*, 815–825. [[CrossRef](#)]

116. Kebria, M.R.S.; Rahimpour, A.; Bakeri, G.; Abedini, R. Experimental and theoretical investigation of thin ZIF-8/chitosan coated layer on air gap membrane distillation performance of PVDF membrane. *Desalination* **2019**, *450*, 21–32. [[CrossRef](#)]
117. Ali, A.; Criscuoli, A.; Macedonio, F.; Drioli, E. A comparative analysis of flat sheet and capillary membranes for membrane distillation applications. *Desalination* **2019**, *456*, 1–12. [[CrossRef](#)]
118. Zhao, D.; Zuo, J.; Lu, K.-J.; Chung, T.-S. Fluorographite modified PVDF membranes for seawater desalination via direct contact membrane distillation. *Desalination* **2017**, *413*, 119–126. [[CrossRef](#)]
119. Luo, A.; Lior, N. Study of advancement to higher temperature membrane distillation. *Desalination* **2017**, *419*, 88–100. [[CrossRef](#)]
120. Fan, Y.; Chen, S.; Zhao, H.; Liu, Y. Distillation membrane constructed by TiO₂ nanofiber followed by fluorination for excellent water desalination performance. *Desalination* **2017**, *405*, 51–58. [[CrossRef](#)]
121. Eykens, L.; Hitsov, I.; De Sitter, K.; Dotremont, C.; Pinoy, L.; Van der Bruggen, B. Direct contact and air gap membrane distillation: Differences and similarities between lab and pilot scale. *Desalination* **2017**, *422*, 91–100. [[CrossRef](#)]
122. Xu, J.; Singh, Y.B.; Amy, G.L.; Ghaffour, N. Effect of operating parameters and membrane characteristics on air gap membrane distillation performance for the treatment of highly saline water. *J. Membr. Sci.* **2016**, *512*, 73–82. [[CrossRef](#)]
123. Wang, Z.; Jin, J.; Hou, D.; Lin, S. Tailoring surface charge and wetting property for robust oil-fouling mitigation in membrane distillation. *J. Membr. Sci.* **2016**, *516*, 113–122. [[CrossRef](#)]
124. Razmjou, A.; Arifin, E.; Dong, G.; Mansouri, J.; Chen, V. Superhydrophobic modification of TiO₂ nanocomposite PVDF membranes for applications in membrane distillation. *J. Membr. Sci.* **2012**, *415–416*, 850–863. [[CrossRef](#)]
125. Dong, Z.-Q.; Ma, X.-h.; Xu, Z.-L.; You, W.-T.; Li, F.-b. Superhydrophobic PVDF-PTFE electrospun nanofibrous membranes for desalination by vacuum membrane distillation. *Desalination* **2014**, *347*, 175–183. [[CrossRef](#)]
126. Meng, S.; Ye, Y.; Mansouri, J.; Chen, V. Fouling and crystallisation behaviour of superhydrophobic nano-composite PVDF membranes in direct contact membrane distillation. *J. Membr. Sci.* **2014**, *463*, 102–112. [[CrossRef](#)]
127. Fan, X.; Liu, Y.; Quan, X.; Zhao, H.; Chen, S.; Yi, G.; Du, L. High desalination permeability, wetting and fouling resistance on superhydrophobic carbon nanotube hollow fiber membrane under self-powered electrochemical assistance. *J. Membr. Sci.* **2016**, *514*, 501–509. [[CrossRef](#)]
128. Tijging, L.D.; Woo, Y.C.; Shim, W.-G.; He, T.; Choi, J.-S.; Kim, S.-H.; Shon, H.K. Superhydrophobic nanofiber membrane containing carbon nanotubes for high-performance direct contact membrane distillation. *J. Membr. Sci.* **2016**, *502*, 158–170. [[CrossRef](#)]
129. An, A.K.; Guo, J.; Lee, E.-J.; Jeong, S.; Zhao, Y.; Wang, Z.; Leiknes, T. PDMS/PVDF hybrid electrospun membrane with superhydrophobic property and drop impact dynamics for dyeing wastewater treatment using membrane distillation. *J. Membr. Sci.* **2017**, *525*, 57–67. [[CrossRef](#)]
130. Attia, H.; Alexander, S.; Wright, C.J.; Hilal, N. Superhydrophobic electrospun membrane for heavy metals removal by air gap membrane distillation (AGMD). *Desalination* **2017**, *420*, 318–329. [[CrossRef](#)]
131. Li, X.; García-Payo, M.C.; Khayet, M.; Wang, M.; Wang, X. Superhydrophobic polysulfone/polydimethylsiloxane electrospun nanofibrous membranes for water desalination by direct contact membrane distillation. *J. Membr. Sci.* **2017**, *542*, 308–319. [[CrossRef](#)]
132. Yang, Y.; Liu, Q.; Wang, H.; Ding, F.; Jin, G.; Li, C.; Meng, H. Superhydrophobic modification of ceramic membranes for vacuum membrane distillation. *Chin. J. Chem. Eng.* **2017**, *25*, 1395–1401. [[CrossRef](#)]
133. Bhushan, B.; Jung, Y.C.; Koch, K. Micro-, nano- and hierarchical structures for superhydrophobicity, self-cleaning and low adhesion. *Philos. Trans. R. Soc. A Math. Phys. Eng. Sci.* **2009**, *367*, 1631–1672. [[CrossRef](#)]
134. Banat, F.A.; Simandl, J. Theoretical and experimental study in membrane distillation. *Desalination* **1994**, *95*, 39–52. [[CrossRef](#)]
135. Gryta, M. Long-term performance of membrane distillation process. *J. Membr. Sci.* **2005**, *265*, 153–159. [[CrossRef](#)]
136. Song, L.; Ma, Z.; Liao, X.; Kosaraju, P.B.; Irish, J.R.; Sirkar, K.K. Pilot plant studies of novel membranes and devices for direct contact membrane distillation-based desalination. *J. Membr. Sci.* **2008**, *323*, 257–270. [[CrossRef](#)]

137. Teoh, M.M.; Chung, T.-S. Membrane distillation with hydrophobic macrovoid-free PVDF–PTFE hollow fiber membranes. *Sep. Purif. Technol.* **2009**, *66*, 229–236. [[CrossRef](#)]
138. Essalhi, M.; Khayet, M. Self-sustained webs of polyvinylidene fluoride electrospun nanofibers at different electrospinning times: 1. Desalination by direct contact membrane distillation. *J. Membr. Sci.* **2013**, *433*, 167–179. [[CrossRef](#)]
139. Ke, H.; Feldman, E.; Guzman, P.; Cole, J.; Wei, Q.; Chu, B.; Alkudhiri, A.; Alrasheed, R.; Hsiao, B.S. Electrospun polystyrene nanofibrous membranes for direct contact membrane distillation. *J. Membr. Sci.* **2016**, *515*, 86–97. [[CrossRef](#)]
140. Chen, L.-H.; Chen, Y.-R.; Huang, A.; Chen, C.-H.; Su, D.-Y.; Hsu, C.-C.; Tsai, F.-Y.; Tung, K.-L. Nanostructure depositions on alumina hollow fiber membranes for enhanced wetting resistance during membrane distillation. *J. Membr. Sci.* **2018**, *564*, 227–236. [[CrossRef](#)]
141. Woo, Y.C.; Tijjng, L.D.; Park, M.J.; Yao, M.; Choi, J.-S.; Lee, S.; Kim, S.-H.; An, K.-J.; Shon, H.K. Electrospun dual-layer nonwoven membrane for desalination by air gap membrane distillation. *Desalination* **2017**, *403*, 187–198. [[CrossRef](#)]
142. Zhang, W.; Li, Y.; Liu, J.; Li, B.; Wang, S. Fabrication of hierarchical poly (vinylidene fluoride) micro/nano-composite membrane with anti-fouling property for membrane distillation. *J. Membr. Sci.* **2017**, *535*, 258–267. [[CrossRef](#)]
143. Chen, X.; Gao, X.; Fu, K.; Qiu, M.; Xiong, F.; Ding, D.; Cui, Z.; Wang, Z.; Fan, Y.; Drioli, E. Tubular hydrophobic ceramic membrane with asymmetric structure for water desalination via vacuum membrane distillation process. *Desalination* **2018**, *443*, 212–220. [[CrossRef](#)]
144. Zhang, J.; Dow, N.; Duke, M.C.; Ostarcevic, E.; Li, J.-D.; Gray, S.R. Identification of material and physical features of membrane distillation membranes for high performance desalination. *J. Membr. Sci.* **2010**, *349*, 295–303. [[CrossRef](#)]
145. Huang, J.; Zhang, J.; Hao, X.; Guo, Y. Study of a new novel process for preparing and co-stretching PTFE membrane and its properties. *Eur. Polym. J.* **2004**, *40*, 667–671. [[CrossRef](#)]
146. Jiao, B.; Cassano, A.; Drioli, E. Recent advances on membrane processes for the concentration of fruit juices: A review. *J. Food Eng.* **2004**, *63*, 303–324. [[CrossRef](#)]
147. Calabro, V.; Pantano, G.; Kang, M.; Molinari, R.; Drioli, E. Experimental study on integrated membrane processes in the treatment of solutions simulating textile effluents. Energy and exergy analysis. *Desalination* **1990**, *78*, 257–277. [[CrossRef](#)]
148. He, K.; Hwang, H.J.; Moon, I.S. Air gap membrane distillation on the different types of membrane. *Korean J. Chem. Eng.* **2011**, *28*, 770–777. [[CrossRef](#)]
149. Gryta, M.; Tomaszewska, M.; Karakulski, K. Wastewater treatment by membrane distillation. *Desalination* **2006**, *198*, 67–73. [[CrossRef](#)]
150. Phattaranawik, J. Effect of pore size distribution and air flux on mass transport in direct contact membrane distillation. *J. Membr. Sci.* **2003**, *215*, 75–85. [[CrossRef](#)]
151. Abu Al-Rub, F.A.; Banat, F.; Beni-Melhim, K. Parametric Sensitivity Analysis of Direct Contact Membrane Distillation. *Sep. Sci. Technol.* **2002**, *37*, 3245–3271. [[CrossRef](#)]
152. Adnan, S.; Hoang, M.; Wang, H.; Xie, Z. Commercial PTFE membranes for membrane distillation application: Effect of microstructure and support material. *Desalination* **2012**, *284*, 297–308. [[CrossRef](#)]
153. Schneider, K.; Hölz, W.; Wollbeck, R. Membranes and modules for transmembrane distillation. *J. Membr. Sci.* **1988**, *39*, 25–42. [[CrossRef](#)]
154. Eykens, L.; De Sitter, K.; Dotremont, C.; Pinoy, L.; Van der Bruggen, B. Characterization and performance evaluation of commercially available hydrophobic membranes for direct contact membrane distillation. *Desalination* **2016**, *392*, 63–73. [[CrossRef](#)]
155. Martínez, L.; Rodríguez-Maroto, J.M. Membrane thickness reduction effects on direct contact membrane distillation performance. *J. Membr. Sci.* **2008**, *312*, 143–156. [[CrossRef](#)]
156. Eykens, L.; Hitsov, I.; De Sitter, K.; Dotremont, C.; Pinoy, L.; Nopens, I.; Van der Bruggen, B. Influence of membrane thickness and process conditions on direct contact membrane distillation at different salinities. *J. Membr. Sci.* **2016**, *498*, 353–364. [[CrossRef](#)]
157. Hendren, Z.D.; Brant, J.; Wiesner, M.R. Surface modification of nanostructured ceramic membranes for direct contact membrane distillation. *J. Membr. Sci.* **2009**, *331*, 1–10. [[CrossRef](#)]

158. Wang, P.; Chung, T.-S. Recent advances in membrane distillation processes: Membrane development, configuration design and application exploring. *J. Membr. Sci.* **2015**, *474*, 39–56. [[CrossRef](#)]
159. Elias-Kohav, T.; Moshe, S.; Avnir, D. Steady-state diffusion and reactions in catalytic fractal porous media. *Chem. Eng. Sci.* **1991**, *46*, 2787–2798. [[CrossRef](#)]
160. Iversen, S.B.; Bhatia, V.K.; Dam-Johansen, K.; Jonsson, G. Characterization of microporous membranes for use in membrane contactors. *J. Membr. Sci.* **1997**, *130*, 205–217. [[CrossRef](#)]
161. Calabrò, V.; Jiao, B.L.; Drioli, E. Theoretical and Experimental Study on Membrane Distillation in the Concentration of Orange Juice. *Ind. Eng. Chem. Res.* **1994**, *33*, 1803–1808. [[CrossRef](#)]
162. Lawson, K.W.; Hall, M.S.; Lloyd, D.R. Compaction of microporous membranes used in membrane distillation. I. Effect on gas permeability. *J. Membr. Sci.* **1995**, *101*, 99–108. [[CrossRef](#)]
163. Alobaidani, S.; Curcio, E.; Macedonio, F.; Diprofo, G.; Alhinai, H.; Drioli, E. Potential of membrane distillation in seawater desalination: Thermal efficiency, sensitivity study and cost estimation. *J. Membr. Sci.* **2008**, *323*, 85–98. [[CrossRef](#)]
164. Curcio, E.; Drioli, E. Membrane Distillation and Related Operations—A Review. *Sep. Purif. Rev.* **2005**, *34*, 35–86. [[CrossRef](#)]
165. Brandrup, J.; Immergut, E.H.; Grulke, E.A. *Polymer Handbook*; Wiley: New York, NY, USA, 1989.
166. Kreveleh, D.W.V. *Properties of Polymers*; Elsevier: Amsterdam, The Netherlands, 1990.
167. Harper, C.A. *Handbook of Plastics, Elastomers and Composites*; McGraw-Hill: New York, NY, USA, 1996.
168. Yaws, C.L. *Handbook of Transport Property Data: Viscosity, Thermal Conductivity, and Diffusion Coefficients of Liquids and Gases*; Gulf Publishing: Houston, TX, USA, 1995.
169. Gazagnes, L.; Cerneaux, S.; Persin, M.; Prouzet, E.; Larbot, A. Desalination of sodium chloride solutions and seawater with hydrophobic ceramic membranes. *Desalination* **2007**, *217*, 260–266. [[CrossRef](#)]
170. Wang, J.-W.; Li, L.; Zhang, J.-W.; Xu, X.; Chen, C.-S. β -Sialon ceramic hollow fiber membranes with high strength and low thermal conductivity for membrane distillation. *J. Eur. Ceram. Soc.* **2016**, *36*, 59–65. [[CrossRef](#)]
171. Martínez, L. Comparison of membrane distillation performance using different feeds. *Desalination* **2004**, *168*, 359–365. [[CrossRef](#)]
172. Yun, Y.; Ma, R.; Zhang, W.; Fane, A.G.; Li, J. Direct contact membrane distillation mechanism for high concentration NaCl solutions. *Desalination* **2006**, *188*, 251–262. [[CrossRef](#)]
173. Sharqawy, M.H.; Lienhard, J.H.; Zubair, S.M. Thermophysical properties of seawater: A review of existing correlations and data. *Desalin. Water Treat.* **2012**, *16*, 354–380. [[CrossRef](#)]
174. Alkhudhiri, A.; Darwish, N.; Hilal, N. Produced water treatment: Application of Air Gap Membrane Distillation. *Desalination* **2013**, *309*, 46–51. [[CrossRef](#)]
175. Li, J.; Guan, Y.; Cheng, F.; Liu, Y. Treatment of high salinity brines by direct contact membrane distillation: Effect of membrane characteristics and salinity. *Chemosphere* **2015**, *140*, 143–149. [[CrossRef](#)]
176. Guan, Y.; Li, J.; Cheng, F.; Zhao, J.; Wang, X. Influence of salt concentration on DCMD performance for treatment of highly concentrated NaCl, KCl, MgCl₂ and MgSO₄ solutions. *Desalination* **2015**, *355*, 110–117. [[CrossRef](#)]
177. David, F.; Vokhmin, V.; Ionova, G. Water characteristics depend on the ionic environment. Thermodynamics and modelisation of the aquo ions. *J. Mol. Liq.* **2001**, *90*, 45–62. [[CrossRef](#)]
178. Tansel, B. Significance of thermodynamic and physical characteristics on permeation of ions during membrane separation: Hydrated radius, hydration free energy and viscous effects. *Sep. Purif. Technol.* **2012**, *86*, 119–126. [[CrossRef](#)]
179. Alkhudhiri, A.; Darwish, N.; Hilal, N. Treatment of saline solutions using Air Gap Membrane Distillation: Experimental study. *Desalination* **2013**, *323*, 2–7. [[CrossRef](#)]
180. Yu, X.; Yang, H.; Lei, H.; Shapiro, A. Experimental evaluation on concentrating cooling tower blowdown water by direct contact membrane distillation. *Desalination* **2013**, *323*, 134–141. [[CrossRef](#)]
181. Brant, J.A.; Childress, A.E. Colloidal adhesion to hydrophilic membrane surfaces. *J. Membr. Sci.* **2004**, *241*, 235–248. [[CrossRef](#)]
182. Subramani, A.; Hoek, E.M.V. Direct observation of initial microbial deposition onto reverse osmosis and nanofiltration membranes. *J. Membr. Sci.* **2008**, *319*, 111–125. [[CrossRef](#)]
183. Elimelech, M.; Gregory, J.; Jia, X. *Particle Deposition and Aggregation Measurement, Modelling and Simulation*; Elsevier, Butterworth-Heinemann: Oxford, UK, 1998. [[CrossRef](#)]

184. Brant, J.A.; Childress, A.E. Assessing short-range membrane–colloid interactions using surface energetics. *J. Membr. Sci.* **2002**, *203*, 257–273. [[CrossRef](#)]
185. Domínguez, A.; Fernández, A.; González, N.; Iglesias, E.; Montenegro, L. Determination of critical micelle concentration of some surfactants by three techniques. *J. Chem. Educ.* **1997**, *74*, 1227–1231. [[CrossRef](#)]
186. Chew, N.G.P.; Zhao, S.; Loh, C.H.; Permogorov, N.; Wang, R. Surfactant effects on water recovery from produced water via direct-contact membrane distillation. *J. Membr. Sci.* **2017**, *528*, 126–134. [[CrossRef](#)]
187. Hansen, C.; Sorensen, C.; Velarde, M.; Gates, B.; Yin, Y.; Sun, Y. *Handbook of Surface and Colloid Chemistry*; Birdi, K., Ed.; CRC Press: Boca Raton, FL, USA, 2003.
188. Kronberg, B.; Holmberg, K.; Lindman, B. *Surface Chemistry of Surfactants and Polymers*; Wiley: Hoboken, NJ, USA, 2014.
189. Walstra, P. *Physical Chemistry of Foods*; CRC Press: Boca Raton, FL, USA, 2001.
190. Boo, C.; Lee, J.; Elimelech, M. Omniphobic Polyvinylidene Fluoride (PVDF) Membrane for Desalination of Shale Gas Produced Water by Membrane Distillation. *Environ. Sci. Technol.* **2016**, *50*, 12275–12282. [[CrossRef](#)]
191. Lu, J.R.; Marrocco, A.; Su, T.J.; Thomas, R.K.; Penfold, J. Adsorption of Dodecyl Sulfate Surfactants with Monovalent Metal Counterions at the Air-Water Interface Studied by Neutron Reflection and Surface Tension. *J. Colloid Interface Sci.* **1993**, *158*, 303–316. [[CrossRef](#)]
192. Schroën, C.G.P.H.; Stuart, C.; Padt, A.; Riet, K. Minimum breakthrough pressure as a measure for wettability changes caused by protein adsorption at hydrophobic membranes. *Bioseparation* **1994**, *4*, 151–163.
193. Cho, J.; Amy, G.; Pellegrino, J.; Yoon, Y. Characterization of clean and natural organic matter (NOM) fouled NF and UF membranes, and foulants characterization. *Desalination* **1998**, *118*, 101–108. [[CrossRef](#)]
194. Schäfer, A.I.; Fane, A.G.; Waite, T.D. Nanofiltration of natural organic matter: Removal, fouling and the influence of multivalent ions. *Desalination* **1998**, *118*, 109–122. [[CrossRef](#)]
195. Gryta, M.; Tomaszewska, M.; Grzechulska, J.; Morawski, A.W. Membrane distillation of NaCl solution containing natural organic matter. *J. Membr. Sci.* **2001**, *181*, 279–287. [[CrossRef](#)]
196. Khayet, M. Direct contact membrane distillation of humic acid solutions. *J. Membr. Sci.* **2004**, *240*, 123–128. [[CrossRef](#)]
197. Hong, S.; Elimelech, M. Chemical and physical aspects of natural organic matter (NOM) fouling of nanofiltration membranes. *J. Membr. Sci.* **1997**, *132*, 159–181. [[CrossRef](#)]
198. Schäfer, A.I.; Schwicker, U.; Fischer, M.M.; Fane, A.G.; Waite, T.D. Microfiltration of colloids and natural organic matter. *J. Membr. Sci.* **2000**, *171*, 151–172. [[CrossRef](#)]
199. Jucker, C.; Clark, M.M. Adsorption of aquatic humic substances on hydrophobic ultrafiltration membranes. *J. Membr. Sci.* **1994**, *97*, 37–52. [[CrossRef](#)]
200. Gostoli, C.; Sarti, G.C. Separation of liquid mixtures by membrane distillation. *J. Membr. Sci.* **1989**, *41*, 211–224. [[CrossRef](#)]
201. Taylor, R.; Webb, D.R. Film models for multicomponent mass transfer; computational methods: The exact solution of the maxwell-stefan equations. *Comput. Chem. Eng.* **1981**, *5*, 61–73. [[CrossRef](#)]
202. Banat, F.A. Membrane Distillation For Desalination And Removal Of Volatile Organic Compounds From Water. Ph.D. Thesis, Mcgill University, Montreal, QC, Canada, 1994.
203. Kujawski, W.; Kujawa, J.; Wierzbowska, E.; Cerneaux, S.; Bryjak, M.; Kujawski, J. Influence of hydrophobization conditions and ceramic membranes pore size on their properties in vacuum membrane distillation of water–organic solvent mixtures. *J. Membr. Sci.* **2016**, *499*, 442–451. [[CrossRef](#)]
204. Wijekoon, K.C.; Hai, F.I.; Kang, J.; Price, W.E.; Cath, T.Y.; Nghiem, L.D. Rejection and fate of trace organic compounds (TrOCs) during membrane distillation. *J. Membr. Sci.* **2014**, *453*, 636–642. [[CrossRef](#)]
205. Zuo, G.; Wang, R. Novel membrane surface modification to enhance anti-oil fouling property for membrane distillation application. *J. Membr. Sci.* **2013**, *447*, 26–35. [[CrossRef](#)]
206. Alklaibi, A.M.; Lior, N. Membrane-distillation desalination: Status and potential. *Desalination* **2005**, *171*, 111–131. [[CrossRef](#)]
207. Kimura, S.; Nakao, S.I.; Shimatani, S.I. Transport phenomena in membrane distillation. *J. Membr. Sci.* **1987**, *33*, 285–298. [[CrossRef](#)]
208. Srisurichan, S.; Jiratananon, R.; Fane, A. Mass transfer mechanisms and transport resistances in direct contact membrane distillation process. *J. Membr. Sci.* **2006**, *277*, 186–194. [[CrossRef](#)]

209. Manawi, Y.M.; Khraisheh, M.; Fard, A.K.; Benyahia, F.; Adham, S. Effect of operational parameters on distillate flux in direct contact membrane distillation (DCMD): Comparison between experimental and model predicted performance. *Desalination* **2014**, *336*, 110–120. [[CrossRef](#)]
210. Long, R.; Lai, X.; Liu, Z.; Liu, W. Direct contact membrane distillation system for waste heat recovery: Modelling and multi-objective optimization. *Energy* **2018**, *148*, 1060–1068. [[CrossRef](#)]
211. Zhang, J.; Gray, S.; Li, J.-D. Predicting the influence of operating conditions on DCMD flux and thermal efficiency for incompressible and compressible membrane systems. *Desalination* **2013**, *323*, 142–149. [[CrossRef](#)]
212. Geng, H.; Lin, L.; Li, P.; Zhang, C.; Chang, H. Study on the heat and mass transfer in AGMD module with latent heat recovery. *Desalination Water Treat.* **2015**, *57*, 1–9. [[CrossRef](#)]
213. Khalifa, A.; Ahmad, H.; Antar, M.; Laoui, T.; Khayet, M. Experimental and theoretical investigations on water desalination using direct contact membrane distillation. *Desalination* **2017**, *404*, 22–34. [[CrossRef](#)]
214. Kim, A.S. A two-interface transport model with pore-size distribution for predicting the performance of direct contact membrane distillation (DCMD). *J. Membr. Sci.* **2013**, *428*, 410–424. [[CrossRef](#)]
215. Nayar, K.G.; Panchanathan, D.; McKinley, G.H.; Lienhard, J.H. Surface Tension of Seawater. *J. Phys. Chem. Ref. Data* **2014**, *43*, 043103. [[CrossRef](#)]
216. Holman, J.P.J.P. *Heat Transfer*, 10th ed.; McGraw Hill Higher Education: Boston, PA, USA, 2010.
217. He, F.; Gilron, J.; Lee, H.; Song, L.; Sirkar, K.K. Potential for scaling by sparingly soluble salts in crossflow DCMD. *J. Membr. Sci.* **2008**, *311*, 68–80. [[CrossRef](#)]
218. He, F.; Sirkar, K.K.; Gilron, J. Studies on scaling of membranes in desalination by direct contact membrane distillation: CaCO₃ and mixed CaCO₃/CaSO₄ systems. *Chem. Eng. Sci.* **2009**, *64*, 1844–1859. [[CrossRef](#)]
219. Singh, D.; Sirkar, K.K. Desalination by air gap membrane distillation using a two hollow-fiber-set membrane module. *J. Membr. Sci.* **2012**, *421*, 172–179. [[CrossRef](#)]
220. Martínez-Diez, L.; Vázquez-González, M.I.; Florido-Díaz, F.J. Study of membrane distillation using channel spacers. *J. Membr. Sci.* **1998**, *144*, 45–56. [[CrossRef](#)]
221. Phattaranawik, J.; Jiraratananon, R.; Fane, A.G. Effects of net-type spacers on heat and mass transfer in direct contact membrane distillation and comparison with ultrafiltration studies. *J. Membr. Sci.* **2003**, *217*, 193–206. [[CrossRef](#)]
222. Phattaranawik, J.; Jiraratananon, R.; Fane, A.G.; Halim, C. Mass flux enhancement using spacer filled channels in direct contact membrane distillation. *J. Membr. Sci.* **2001**, *187*, 193–201. [[CrossRef](#)]
223. Manawi, Y.M.; Khraisheh, M.A.; Fard, A.K.; Benyahia, F.; Adham, S. A predictive model for the assessment of the temperature polarization effect in direct contact membrane distillation desalination of high salinity feed. *Desalination* **2014**, *341*, 38–49. [[CrossRef](#)]
224. Banat, F.A.; Abu Al-Rub, F.; Jumah, R.; Shannag, M. On the effect of inert gases in breaking the formic acid–water azeotrope by gas-gap membrane distillation. *Chem. Eng. J.* **1999**, *73*, 37–42. [[CrossRef](#)]
225. Andrijesdóttir, Ó.; Ong, C.L.; Nabavi, M.; Paredes, S.; Khalil, A.S.G.; Michel, B.; Poulikakos, D. An experimentally optimized model for heat and mass transfer in direct contact membrane distillation. *Int. J. Heat Mass Transf.* **2013**, *66*, 855–867. [[CrossRef](#)]
226. Schneider, K.; van Gassel, T.J. Membran distillation. *Chem. Ing. Tech.* **1984**, *56*, 514–521. [[CrossRef](#)]
227. Schofield, R.W.; Fane, A.G.; Fell, C.J.D. Gas and vapour transport through microporous membranes. II. Membrane distillation. *J. Membr. Sci.* **1990**, *53*, 173–185. [[CrossRef](#)]
228. McGaughey, A.L.; Gustafson, R.D.; Childress, A.E. Effect of long-term operation on membrane surface characteristics and performance in membrane distillation. *J. Membr. Sci.* **2017**, *543*, 143–150. [[CrossRef](#)]
229. Guillen-Burrieza, E.; Ruiz-Aguirre, A.; Zaragoza, G.; Arafat, H.A. Membrane fouling and cleaning in long term plant-scale membrane distillation operations. *J. Membr. Sci.* **2014**, *468*, 360–372. [[CrossRef](#)]
230. Duong, H.C.; Gray, S.; Duke, M.; Cath, T.Y.; Nghiem, L.D. Scaling control during membrane distillation of coal seam gas reverse osmosis brine. *J. Membr. Sci.* **2015**, *493*, 673–682. [[CrossRef](#)]



iDST: An Integrated Decision Support Tool for Treatment and Beneficial Use of Non-traditional Water Supplies – Part II. Marcellus and Barnett Shale Case Studies

Guanyu Ma¹, Mengistu Geza^{2,3,*}, Tzahi Y. Cath³, Jörg E. Drewes^{3,4}, Pei Xu^{1,*}

¹ Department of Civil Engineering, New Mexico State University, Las Cruces, New Mexico 88003, USA

² Department of Civil and Environmental Engineering, South Dakota School of Mines and Technology, Rapid City, South Dakota 57701, USA

³ Department of Civil and Environmental Engineering, Colorado School of Mines, Golden, Colorado 80401, USA

⁴ Chair of Urban Water Systems Engineering, Technical University of Munich, 85748 Garching, Germany

*Corresponding authors:

Pei Xu: e-mail: pxu@nmsu.edu | phone: 1-575-646-5870

Mengistu Geza: e-mail: stu.geza@sdsmt.edu | phone: 1-605-394-2284

Abstract

Development of unconventional gas resources is currently one of the most rapidly growing trends in the oil and natural gas industry. Exploration of shale gas requires significant quantities of water for hydraulic fracturing. Meanwhile, large volumes of produced water are generated during gas production. Treatment and beneficial use of hydraulic fracturing flowback and produced water provides opportunities for sustainable unconventional gas operations while minimizing impacts to environment, local water resources, and public health. Considering the broad variety of treatment technologies and the wide spectrum of flowback and produced water qualities, selecting appropriate treatment and management options involves a complex decision-making process that requires understanding of treatment technologies, water quality, reuse requirements, and consideration of multiple criteria, constraints, and objectives. This study presents an integrated decision-support tool (iDST) to assist in selection of treatment technologies and evaluation of the feasibility of potential water reuse options. The Marcellus Shale in Pennsylvania and the Barnett Shale in Texas were selected as case studies to demonstrate produced water treatment technologies and beneficial reuse options considering realistic site-specific conditions, assumptions, and future projections such as well numbers and locations, water demands, flowback and produced water quality and quantity, disposal availability, and costs. The iDST provides an interactive user interface to select suitable technologies for produced water treatment and reuse based on user preference, target water quality, and current disposal options.

Keywords: produced water; hydraulic fracturing; unconventional gas production; treatment technology; decision support tool

1 Introduction

The advances in directional drilling and hydraulic fracturing have allowed unconventional oil and gas (O&G) production from deep and less permeable shale formations. These breakthroughs have brought changes and challenges to water resources and environmental management, which are of particular concerns to producers, engineers, regulators, and the public. Hydraulic fracturing flowback and produced water represent the largest waste stream generated during O&G exploration and production. Annual flowback and produced water production in the United States was estimated to be 3.2 billion m³ (20.6 billion barrels) in 2012 [1]. More than 93% of produced water from onshore wells is injected underground for disposal and reservoir pressure maintenance [1]. However, there are increasing concerns that deep well injection may be responsible for increasing rates of seismic activity [2], potential comingling with freshwater aquifers, as well as negative impacts on the quality of adjacent surface waters and microbial communities in downstream sediments [3, 4].

The volume of unconventional O&G wastewater requiring disposal has continued to grow despite the recent slowing in drilling and production [5]. Meanwhile, substantial amounts of freshwater are used by the petroleum industry for well drilling and hydraulic fracturing [6]. If produced water is managed as a water resource instead of a waste product, the water generated could supplement regional water demand, while minimizing the volume of produced water for disposal, thus reducing O&G production costs and environmental implications.

Sustainable development of O&G production requires thorough understanding of produced water quality, selecting appropriate treatment technologies for beneficial uses, and establishing environmentally sound management strategies. Considering the broad range of treatment processes and the recent technological advances, it is essential to have a clear guidance and tools to assist in evaluation and selection of treatment technologies to meet site-specific reuse needs. Besides treatment capacity and removal efficiency of contaminants, other factors affecting the selection of treatment technologies, including technology industrial status (commercially available or under development), adaptability, feasibility, energy consumption, capital/operational and maintenance costs, footprint (space requirement), skilled labor requirement, infrastructure requirement, brine disposal, as well as user preferences should be considered in the selection process. Therefore, selecting treatment and management options involves a complex decision-making process that requires the consideration of multiple criteria,

constraints, and objectives. A decision-support tool (DST) that can assist in selection of treatment technologies and evaluation of the feasibility of potential water uses is in great need.

A number of DSTs have been developed based on multi-criteria decision analysis (MCDA) methods [7, 8]. Linear, nonlinear, and dynamic programming tools have been applied to optimize treatment selections from a large range of alternatives using boundary constraints [9-12]. However, very few of the tools have been applied to real produced water treatment and management because they are either too simple to provide detailed analysis and essential outputs, or too complicated for general users to understand and operate. A user-friendly DST should provide simple yet efficient interactions between a user and the DST, editable input choices, and easily understandable outputs.

An integrated DST (iDST) was previously developed for treatment and beneficial use of coalbed methane (CBM) produced water [13, 14]. It includes a comprehensive water quality database for several major CBM basins in the United States. This computerized produced water management tool assists users in assessing treatment options, costs, and environmental and institutional issues associated with treatment and beneficial use of CBM produced water. The iDST framework provides a quick analysis and screening of various produced water treatment and management options.

In this study, the iDST was upgraded with more functions and user choices, and further developed and enhanced beyond the CBM to shale gas and other unconventional water resources [15]. The primary objective of this publication is to demonstrate the application of the iDST for selecting the treatment technologies and evaluating the beneficial use feasibility of hydraulic fracturing flowback and produced water. The Marcellus Shale in Pennsylvania and the Barnett Shale in Texas were selected as case studies to determine produced water treatment technologies and beneficial use options considering realistic site-specific conditions, assumptions, and future projections such as well numbers and locations, water demands, flowback and produced water quality and quantity, availability of disposal sites, and costs. The iDST has built-in beneficial use options including hydraulic fracturing using gel and slickwater systems, potable reuse, crop irrigation, surface water discharge and user defined beneficial use water quality requirements for each of the beneficial use options. The tool also compares the costs of treatment and beneficial uses of produced water scenarios to the existing produced water disposal costs. As such, the tool can be used to perform a quick screening and break-even point for treatment relative to disposal

under site-specific conditions. A detailed description of the iDST methodology is in the Part I of the iDST series papers [15].

2 Logistics and modules of the iDST

The iDST consists of four basic modules: Water Quality Module (WQM), Treatment Selection Module (TSM), Beneficial Use Screening Module (BSM), and Beneficial Use Economic Module (BEM) (Fig. 1). The WQM is built upon a composite geochemical database previously developed for CBM produced water [13, 14]. It was created with 3,255 entries, covering major CBM basins in the Rocky Mountain region, including the Powder River Basin in Montana and Wyoming, the Raton Basin in Colorado and New Mexico, and the San Juan Basin in Colorado and New Mexico. The WQM contained comprehensive information on 58 parameters and constituents including field measurements (e.g. pH, temperature, conductivity, and dissolved oxygen), metals, non-metals, organics, and radionuclides [13]. In this study, the WQM was expanded with additional 2,791 entries for water quality data of flowback and produced water from the major O&G producing basins in the United States, including: the Barnett Shale Play in Texas, the Lansing-Kansas City Formation in Texas, the Marcellus Shale in Pennsylvania and West Virginia, the Morrow Shale in Anadarko Basin, Oklahoma, the Organic-rich Shale in Pennsylvania, New York, and Ohio, the Permian Basins in Texas and New Mexico, the Tuscarora play (tight gas) in Pennsylvania, and the Woodford Shale in Oklahoma.

The water quality data were collected from collaborative producers, the United States Geological Survey [5] National Produced Waters Geochemical Database v2.3 (Provisional), the Marcellus Shale Coalition Shale Gas Produced Water Database, the New Mexico Water and Infrastructure Data System, and the New Mexico Oil Conservation Division [16-19]. The iDST also allows users to enter their water quality data and fit into the WQM datasheet. The quality assurance and quality control for the WQM is described in the Supplementary Content file.

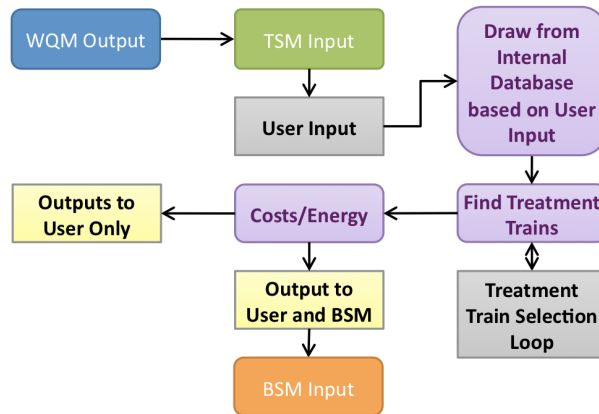


Fig. 1. A simplified schematic diagram of the iDST.

The TSM is designed to select proper treatment technologies based on feed water quality, user preferences, and desired product water quality. The TSM includes 62 processes as stand-alone pretreatment, desalination and post-treatment, as well as integrated and commercial treatment packages. Each technology is assigned removal efficiency for each contaminant corresponding to different total dissolved solids (TDS) bins: Bin 1: TDS <8,000 mg/L; Bin 2: 8,000–25,000 mg/L; Bin 3: 25,000–40,000 mg/L; Bin 4: 40,000–70,000 mg/L; and Bin 5: TDS >70,000 mg/L. The bin classification is based on the removal capacities of different water desalination technologies such as 25,000 mg/L for brackish water RO (BWRO), 40,000 mg/L for seawater RO (SWRO), 70,000 mg/L for thermal technologies. Desalination cost of feed water in the higher bins could be significantly higher than in the lower TDS bins. In addition to TDS bins, the selection of technologies considers the treatment limits of other contaminants such as organic matter, suspended solids, and toxicity of certain constituents.

The user inputs criteria such as water quality, water quantity, desired water recovery, and other site-specific operational objectives to assist in the selection of appropriate treatment processes. The user can also include or exclude certain treatment processes, such as including or excluding seawater RO in the selected treatment train. Using these inputs, along with a robust selection methodology, the tool generates potential treatment trains capable of treating flowback and produced water to a quality suitable for each pre-programmed or user defined beneficial use. The TSM preferentially selects the minimum number of processes, in a logical order, required to treat a given feed water stream for beneficial use requirements. The TSM generates a report detailing three suggested treatment trains with estimated product water quality and quantity,

energy requirements, brine quality and quantity, and a proposed brine management strategy for each beneficial use option.

In addition to onsite uses for hydraulic fracturing and drilling, produced water can be used for agricultural irrigation, in-stream flow augmentation, firefighting, dust control, cooling water for thermal power plants, and other user defined beneficial use options. The BSM stores eleven beneficial use options, each of them is assigned appropriate product water quality requirements that the selected treatment train needs to achieve. The user can also enter specific water quality parameters of interest. The BEM calculates costs based on the selected treatment technologies, desired product water flow rate, and economic inputs assigned by user, and outputs unit cost, and annual cost for capital cost, operation and maintenance (O&M) cost, and energy consumption. Capital and O&M costs presented in the BEM were developed based on specific design criteria defined through the TSM, general project criteria based on professional experience, and unit costs for power, chemicals, and labor. This cost estimate was developed to compare the treatment processes at screening-level.

3 Case study setup

To evaluate the beneficial use potential of flowback and produced water, case studies were conducted using the iDST for the Marcellus Shale and the Barnett Shale. The quantity of flowback and produced water generated during shale gas exploration and production was estimated based on historical data and production trends. Water treatment technologies were selected to meet the water quality requirements of beneficial uses. The beneficial reuse potentials were assessed and optimized by ranking user defined criteria such as technical viability, adoptability, energy and chemical demand, labor skill requirement, and screening-level estimated costs for treatment, reuse, and disposal.

3.1 Study field – the Marcellus Shale

The Marcellus Shale is the largest natural gas producing play in the United States, and is rapidly growing in recent years, especially in Pennsylvania. New wells drilled in Pennsylvania have been rapidly increasing since 2007 when breakthrough on hydraulic fracturing techniques occurred [20]. Flowback and produced water reuse increased remarkably from 15% to 20% in 2009 to approximately 90% in 2013, mainly for new well drilling [20]. Beneficial use of the

reclaimed water makes up to approximately 10% of the water needed for hydraulic fracturing job for a new well. Flowback and produced water requires proper treatment before reuse or disposal. In the Marcellus Shale, reuse for hydraulic fracturing needs oil/gas-water separation, filtration, and dilution. Dilution of the wastewater is aimed to decrease contaminant concentrations such as TDS, total suspended solids (TSS), total hardness, and chloride, to an acceptable level for hydraulic fracturing, and is the most common method for reuse of flowback and produced water. Disposal well injection is also used in the Marcellus Shale, with annual volume of approximately 2.5 million barrels (bbl, 0.4 million m³). The number of deep injection wells (salt water disposal wells, SWD) is limited in Pennsylvania. Only eight SWD wells were permitted to dispose shale gas flowback and produced water (Fig. 2). These SWD wells are Class II wells regulated by the United States Environmental Protection Agency (USEPA) Underground Injection Control program under the Safe Drinking Water Act.

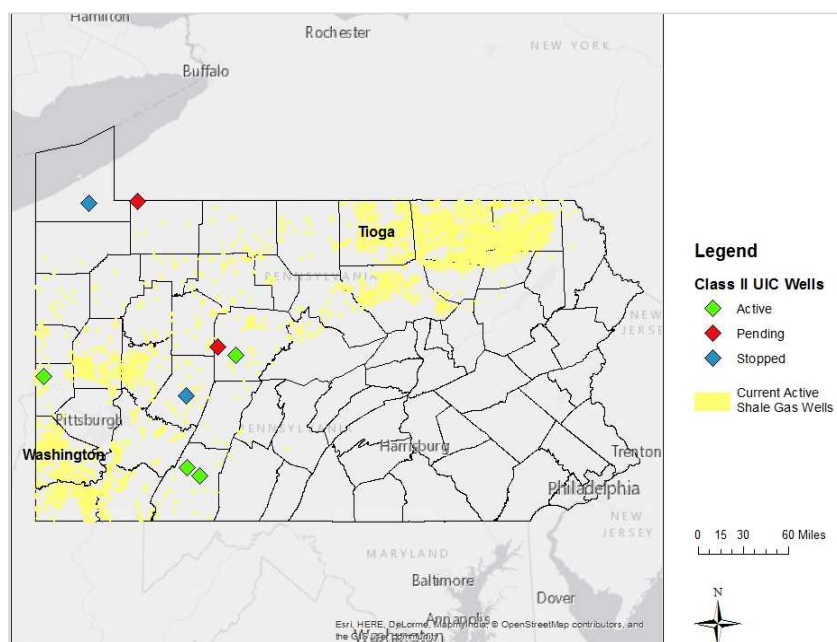


Fig. 2. Map of Marcellus shale gas wells and deep injection wells in Pennsylvania.

Tioga County and Washington County in Pennsylvania were selected for specific case study because of their locations and number of shale gas producing wells. Both counties have high density of shale gas wells and available water quality data. Tioga County is far from the disposal wells, while Washington County is close to the injection wells and the state of Ohio where more

disposal wells are available. Hauling cost was estimated to range from \$4/bbl to \$8/bbl (\$25/m³ to \$50/m³) in Pennsylvania, while injection cost was estimated to be \$0.50/bbl to \$2.50/bbl (\$3.1/m³ to \$15.7/m³) [21]. Pipeline cost was calculated assuming an average 10-mile distance from a wellhead to treatment facilities or impoundments.

3.2 Study field – the Barnett Shale

During its development, the Barnett Shale became a leading shale gas production field in the United States in 2008 when horizontal drilling techniques were first adopted and refined [22, 23]. Disposal well injection is the most common choice for Barnett Shale producers because of its economics and availability. As compared to the Marcellus Shale in Pennsylvania, lower hauling and injection costs were reported in the Barnett Shale because of the large number of injection wells and shorter distance to disposal sites. Hauling cost is estimated to be \$1.0/bbl/hr (\$6.3/m³/hr), while disposal cost is \$0.5-\$1.0/bbl (\$3.1–6.3/m³). Some producers are reusing a small amount of wastewater, and many have started considering beneficial use options. The Railroad Commission of Texas recognizes concerns over water use by the O&G industry and encourages recycling projects to reduce the amount of fresh water used in exploration and production [24].

4 Data collection and analysis

4.1 Projection of flowback and produced water quantity

4.1.1 Flowback water quantity in the Marcellus and Barnett shales

Marcellus flowback water quantity was calculated based on the portion of injected hydraulic fracturing liquid that returns to the surface and forms flowback water. The annual water demand and flowback water generation in the Marcellus Shale are summarized in Table S2 (Supplementary Content). An average of 6–7% of injected water could be recovered as flowback water [25, 26]. In this case study, an average of 6.5% was taken as flowback water recovery rate. The flowback water quantity was estimated based on the projected water demand corresponding to historic high and low gas production in the Marcellus Shale (Figure S1 in Supplementary Content). The calculated flowback water quantity for the year 2010 was 1.78 million m³ (470 million gallons), while the quantity reported by industry was 1.84 million m³ (485 million gallon) in 2010 [27]. This 3.1% difference is considered acceptable for flowback water projection,

indicating that the projection data would be reasonable to calculate future flowback water production used in this case study.

Flowback water quantity in the Barnett Shale was reported to be 500,000–600,000 gallons per well within 10 days after hydraulic fracturing [28]. In this case study, the average flowback flow rate was assumed to be 55,000 gallons per well per day for 10 days.

4.1.2 *Produced water quantity in the Marcellus and Barnett shales*

Because there is lack of produced water quantity data over well lifetime for the Marcellus and Barnett shales, the produced water quantity projection was based on a study of flowback and produced water volume in the Denver Basin, Wattenberg, Colorado [29]. A harmonic function provided good fit to the observed data, and is expressed as:

$$q_t = q_i / (1 + D_i t) \quad (1)$$

where q_t is produced water flow rate at time t ; q_i is the initial water production rate; and D_i is the initial decay rate [29].

After applying the water quantity data from the Marcellus Shale Coalition Database, average values of q_i and D_i were estimated, and the equation of produced water production as a function of well time for the Marcellus Shale is described as:

$$q_t = 15.5 / (1 + 2.718t) \quad (2)$$

Produced water quantity of a shale gas well for the first year was assumed to be 12.1 bbl/day based on industry reported values [29]. Compared with the Marcellus Shale, the Barnett Shale is a “high long-term produced water generating play” [29]. Barnett shale wells generate 5 times more produced water than Marcellus wells [28] (Fig. 3). Based on Equation 1, produced water flow rate for a Barnett shale well as a function of well time is estimated as:

$$q_t = 15.5 / (1 + 0.4t) \quad (3)$$

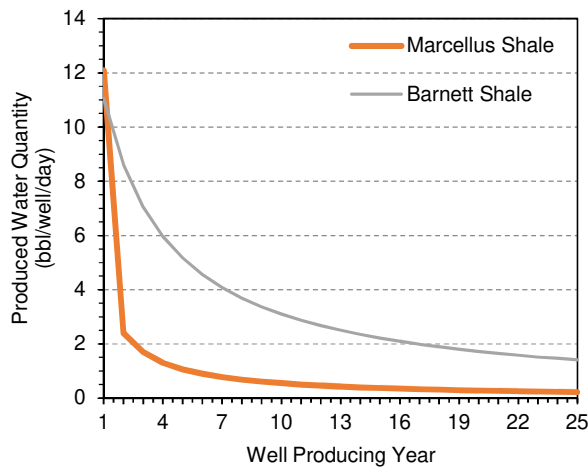


Fig. 3. Comparison of produced water quantity between the Barnett Shale and the Marcellus Shale.

4.2 Flowback and produced water quality database

In the case study, the quality of flowback and produced water was assumed to be stable over the lifetime of a well. Although flowback water quality changes significantly within the first few weeks after fracturing [30, 31], its overall quality was considered stable because of its smaller volume and mixing during storage in a pond before treatment or disposal.

The flowback and produced water quality data for the Marcellus Shale were retrieved from the USGS National Produced Waters Geochemical Database v2.3 (Provisional) and the Marcellus Shale Coalition Shale Gas Produced Water Quality Database [16]. Of the 161,915 produced water quality data sets in the USGS database, 2,723 sets are for shale gas produced water, distributed in Oklahoma, Pennsylvania, New York, Ohio, and Texas. A statistical analysis was conducted for the produced water quality data retrieved from the USGS database. The maximum, minimum, average, 25th, 50th, and 75th percentile values for each parameter and constituent were calculated by state and shale formation, and were included in the iDST for users to choose. Total number of TDS data points reported in this database was 979 after quality assurance and quality control (QA/QC), with the highest TDS concentration of 345,000 mg/L, and the lowest concentration of 390 mg/L. The TDS distribution in produced water by state and formation is illustrated in Figure S2 in Supplementary Content. The measured TDS concentration of shale gas produced water reported data averages 84,870 mg/L.

The Marcellus Shale Coalition Produced Water Database included the fracturing flowback

and produced water quality data of 19 wells in the Marcellus Shale. These data were collected and reported in (Figure S3 and S4 in the Supplementary Content) [18]. Water quality data at day 1, 5, 14, and 90 were collected following the hydraulic fracturing job. A total of 65 TDS values were reported in the database as flowback and produced water, and 19 values were reported as influent water stream (water used for hydraulic fracturing). The TDS of flowback water increased overtime and reached produced water TDS level in 14 to 90 days (Fig. 4).

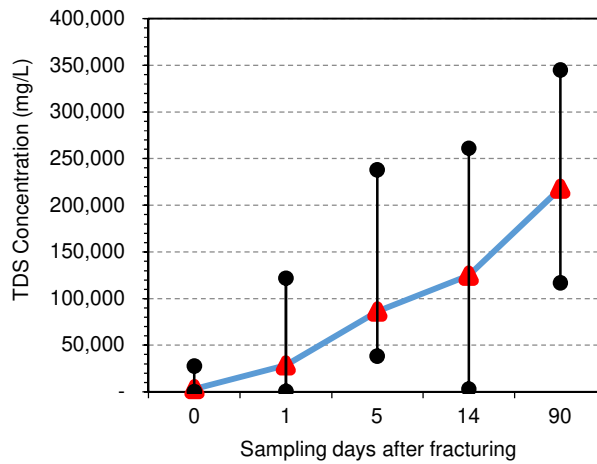


Fig. 4. TDS concentrations (minimum, average and maximum) of flowback water over time in the Marcellus Shale.

Compared to the Marcellus Shale, the flowback and produced water quality data for the Barnett Shale were very limited and not included in the USGS database [16]. The data were mainly retrieved from a study conducted by Hayes and Severin on the Barnett and Appalachian shale water management and reuse technologies [32]. This study reported the Barnett Shale flowback water quality data from five wells on days 1, 3, 5, 6, 7, 10, and 12. The average TDS concentration of flowback water was 37,800 mg/L. The produced water quality data for the Barnett Shale were obtained from multiple sources [28, 33]. The average TDS concentration of flowback water was 67,285 mg/L.

4.3 Beneficial use options

According to the United States Census of Agriculture data of Pennsylvania farms, both Tioga County and Washington County have more than 1000 farms, which makes agricultural irrigation

water use significant [34]. Thus, beneficial use for irrigation was included in this case study. Reuse options included hydraulic fracturing using gel and slickwater systems, and crop irrigation. Potable use of produced water was not considered in this study due to high salinity, economic consideration, potential liability concerns, and potential human health impacts.

The water quality requirements for beneficial uses in Pennsylvania are summarized in Table 1, where Class B is for edible crop irrigation and Class C for non-edible crop irrigation [35]. The TDS requirement for irrigation varies depending on the types of crops and soil. This study used 1,500 mg/L TDS as irrigation requirement. Surface discharge requires water quality no worse than the Class A requirement, with TDS less than 500 mg/L. Other contaminants that are required by the primary and secondary drinking water standards set by the USEPA are also required in the Class A water quality standard, which is regulated for potable water use, potable water aquifer recharge, and other residential uses [35]. These water quality requirements are only used for the case study purpose. For real applications, long-term impacts to plant health and soil conditions need to be monitored and further studied. Other components in produced water that rarely exist in domestic wastewater, such as naturally occurring radionuclides materials, petroleum hydrocarbons, and heavy metals, also need to be well evaluated for human and soil health.

Table 1. Water quality requirement for irrigation in Pennsylvania

Contaminants	Monthly average	Maximum
<i>Class A: potable water use, surface water discharge</i>		
Biochemical oxygen demand (BOD, mg/L)	2	5
Total organic carbon (TOC, mg/L)	10	
Turbidity (NTU)	2	5
Fecal coliform (/100 mL)	2.2	23
Total organic halogens (TOX, mg/L)	0.2	
Total nitrogen	10	
<i>Class B: edible crop irrigation</i>		
Biochemical oxygen demand (BOD, mg/L)	10	20
Turbidity (NTU)	10	15
Fecal coliform (/100 mL)	2.2	23
<i>Class C: non- edible crop irrigation</i>		
Biochemical oxygen demand (BOD, mg/L)	30	45
Total suspended solids (TSS, mg/L)	30	45
Fecal coliform (/100 mL)	200	800

Reusing flowback and produced water for hydraulic fracturing is becoming a common practice in the O&G industry. Hydraulic fracturing is conducted with one of two fluid systems: slickwater or crosslink gel methods. For slickwater fracturing, the fracturing liquid is pumped down the well-bore at very high flow rate, with the addition of friction reducer and proppant such as sand. For crosslink gel method gels are introduced into the fracturing liquid to increase its viscosity, thus increase the stability of proppant suspension. Compared to slickwater system, crosslink gel system can be used for fracturing of deeper formation, and it creates wider fractures; yet, it requires more experienced operators. The quality of the water is important for hydraulic fracturing because impurities can reduce the efficiency of the additives used in the process. However, there is lack of common standards to determine the quality requirement of the water for fracturing; it is highly dependent upon the formation, the fracturing methods, and chemicals added in the process. For example, a recent review showed the metal-crosslinked guar fluids prepared with produced water were successfully used in wells at bottomhole temperatures up to about 121°C with produced water TDS up to 300,000 mg/L and hardness up to 44,000 mg/L [36]. Compared to conventional gelled fracturing fluids, the performance of slickwater fluids is generally less sensitive to mix-water quality; however, high salinity mix-water will cause a loss in achievable friction reduction.

In this study, it was assumed that slickwater system requires water with TDS lower than 40,000 mg/L, while crosslink gel system does not have strict TDS requirement but have specific requirements on certain ions as listed in Table 2. These water quality requirements are examples for the case studies, and within the range of fracturing fluids mix-water requirements. Users can enter their specific water quality requirement in the iDST.

Table 2. Hydraulic fracturing water quality requirements

Hydraulic fracturing system	Crosslink gel system	Slickwater system
pH	6.0 - 8.0	> 5
Hardness (Ca+Mg)	< 2,000 mg/L as CaCO ₃	-
Iron	< 20 mg/L	-
Sulfate	200 - 1,000 mg/L	-
Chloride	< 40,000 mg/L	-
Bicarbonate	< 1,000 mg/L	-
Boron	< 10 mg/L	-
Multivalent Ions	-	< 5,000 mg/L
TDS	-	< 40,000 mg/L

Note: The water quality requirements for hydraulic fracturing vary and depend on the formation, fracturing methods and chemicals added to the fracturing fluids.

4.4 Case study assumptions

User score input, which indicates the importance of each parameter, was set to default values for this case study, as shown in Fig. 5a. With no preference in specific treatment technologies, user preference input was not changed, indicating that no specific treatment technology was included or excluded, as shown in Fig. 5b. Economic assumption of the case study utilizes values pre-stored in the iDST as shown in Fig. 6.

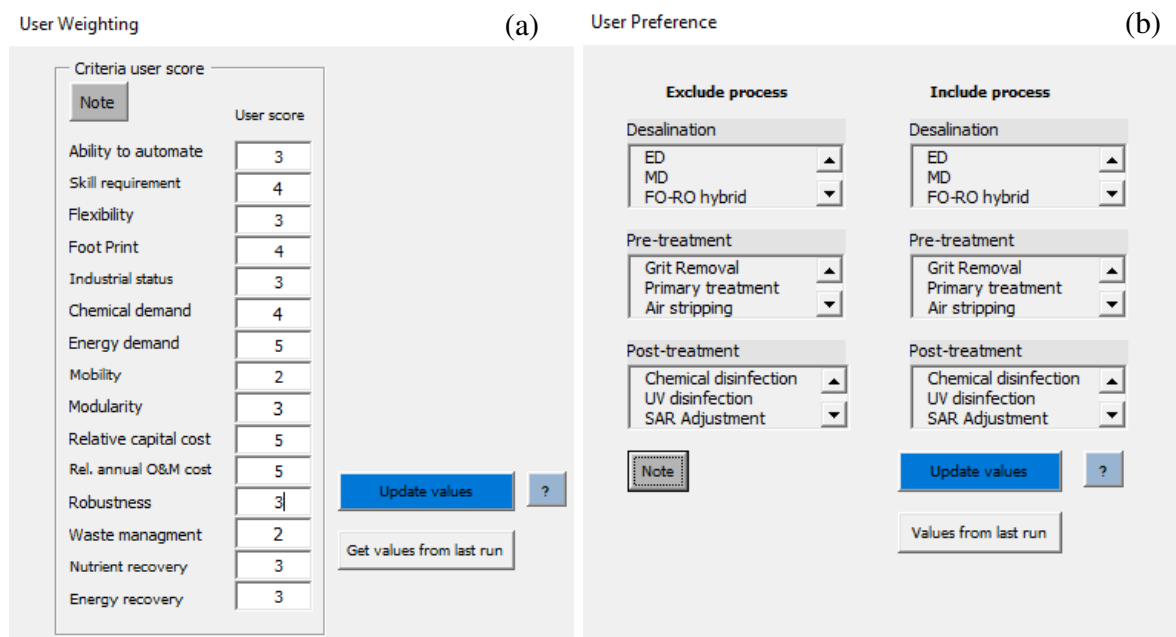


Fig. 5. iDST screenshots of (a) user scores containing default values, and (b) user preference.

Economic inputs

General

Location: Denver, CO

Project Life: 15

Interest Rate: 0.085

Cost esc. factor: 1.1

Area (acres): 10

Operation (%/yr): 1

Energy data

Base demand (kwh/m3): 0.23

Energy unit cost

Electrical: 0.08

Other source: 0.08

Energy source

Other purpose % of treat.: 0.05

Disposal (Kwh/bbl): 1

Labor

a: 0.76

b: 2.12

Multiplier: 1

Labor 1 [#]: 2.272

Cost [\$ /yr]: 40000

Labor 2 [#]: 0

Cost [\$ /yr]: 40000

Buildings, BU & sewer service life \$ cost

	Year	Cost	
Covey. pipelines (BU)	50	10	\$/in dia.
Transfer & Dist. (BU)	50	2000	\$/hp
Coveyance	50	10	\$/in dia.
Transfer & Dist	50	2000	\$/hp
Buildings	50	0	\$/sqft

BU & WW storage

BU data

Steel Tank

Steel (yr): 50

Concrete (yr): 50

Plastic (yr): 50

Pond (yr): 50

Pond (\$ /acre): 40000

Peak flow days: 1

WW data

Steel Tank

Steel (yr): 50

Concrete (yr): 50

Plastic (yr): 50

Other (yr): 50

Other unit cost: 40000

Peak flow days: 1

Terrain data

Trans. to BU at site: CTP to Site i

Transport to BU: CTP/TPi to Bu i

Raw WW transport: Site i to TP i

Energy demand: Stair lift data

Control system cost as %

Manual control only

SCADA- High Tech: 0.20

Remote-Low Tech: 0.15

Electrical-Manual: 0.10

Other \$ - frac. of Cap

Site Dev't: 0.05

Yard Piping: 0.05

Add. mat. &: 0.015

Taxes: 0.029

Bonds/permits: 0.05

Overhead & prof.: 0.15

Contingency: 0.3

Eng.Const. mgmt: 0.3

Legal: 0.08

Administrative: 0.05

Abandon. cost: 0.1

Pump efficiency: 0.75

Peak flow store.: 1

% capital taxed: 0.4

Chemical

	\$/lb	lb/MG
Base	0.25	0
Acid	0.10	0
Antiscalant	1.29	0
Oxidizer	0.5	0
Disinfectant	0.5	200
Other	0.0	0

New BU structure

Discharge Facility to Stream: \$/mgd

200000

Soilds or wastewater disposal: acre

g/m3	g/m3	\$/ton	\$/mil gal
50	120	200	1

w/E&N w/o E&N

Energy [E] Recovery

Capital Costs (\$/MG): 1000

O & M Cost (\$/MG): 500

Energy [E] input (Kwh/MG): 400

[E] output (Kwh/MG): 600

[E] trans. cap. cost (\$/MG/mile): 500

[E] trans. O&M cost (\$/MG/mile): 300

Nutrient [N] Recovery

Capital Costs (\$/MG): 1000

O & M Cost (\$/MG): 500

Energy input (Kwh/MG): 100

Energy output (Kwh/MG): 0

[N] trans. cap. cost (\$/MG/mile): 500

[N] trans. O & M (\$/MG/mile): 400

Material recovered (MT/MG): 0.5

Price per MT: 500

Land

Leased from BLM

Purchase (\$/ac): 20000

Lease (\$/acre): 10000

% aquisition: 0.02

Mitigation Costs: 50000

Benefits

Economic: Avg

Environment: Avg

Social: Avg

Other: Avg

Update values

Fig. 6. An iDST screenshot with economic inputs containing default values.

5 Case study results

5.1 Marcellus Shale

5.1.1 Produced water quality in Tioga and Washington counties

The TDS concentration of produced water in Tioga County ranges from 746 mg/L to 358,000 mg/L with an average of 88,500 mg/L, much higher than most beneficial use water quality requirements. Average TSS concentration is 468 mg/L, alkalinity 114 mg/L as CaCO₃, total hardness (sum of Ca²⁺ and Mg²⁺) 768 mg/L as CaCO₃, and pH 7.4 (Table A2 in Supplementary Content).

The average concentrations of TDS and major ions of produced water in Washington County are higher than in Tioga County (Fig. 7). It should be noted that the concentrations used in the study were the average values from the USGS produced water quality database. The TSS

concentration, unlike other parameters, is three times lower than that of the produced water in Tioga County. This produced water quality difference would lead to a higher treatment cost for beneficial use of produced water in Washington County due to higher concentrations of sodium, chloride, and hardness.

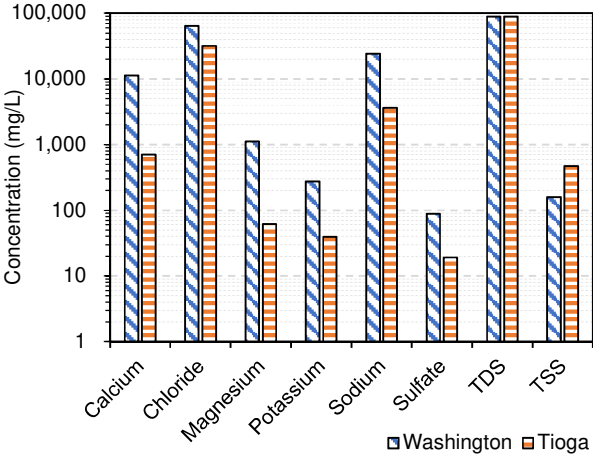


Fig. 7. Major produced water quality parameters in Washington and Tioga Counties.

5.1.2 Selected produced water treatment technologies

For Tioga County produced water, no desalination is required for hydraulic fracturing using gel system, as it does not have a limit on TDS concentration. The treatment trains selected by the iDST are summarized in Table 3. Treatment is required to remove suspended solids, sparingly soluble salts, and inactivate microorganisms. Hydraulic fracturing using slickwater method requires removal of suspended solids, sparingly soluble salts, and TDS by desalination because of its 40,000 mg/L TDS limit and other ion concentration requirements. Reuse for hydraulic fracturing requires disinfection because bacteria present in the fracturing fluid will sour the well, producing organic acids and increasing operational expenses as a result of the corrosion (e.g., H₂S pitting, stress cracking) in both surface equipment and subsurface pipes. Mechanical vapor compression (MVC) distillation was selected by the iDST as the desalination technique for the produced water with feed salinity of 88,500 mg/L.

Table 3. Selected treatment trains for produced water in Tioga and Washington Counties

Beneficial use	Treatment train
<i>Tioga County produced water</i>	
Gel fracking	Chemical precipitation - Media filter - Chemical disinfection
Slickwater fracking	Chemical precipitation - Media filter – MVC – Blending
Class B irrigation	Chemical precipitation - Media filter - MVC – Blending
<i>Washington County produced water</i>	
Gel and slickwater fracking and Class B Irrigation	Chemical softening and precipitation - Media filter – MVC - Blending

For Washington County produced water, the selected treatment processes for the three reuse options are the same, starting with chemical softening and precipitation, followed by media filtration to remove particulate matters including suspended petroleum hydrocarbons. Although salinity level is not required for hydraulic fracturing using gel system, MVC was adopted to reduce chloride concentration to lower than 40,000 mg/L. The product water is required to blend with filtered produced water to meet water quality requirements. MVC was also selected for hydraulic fracturing using slickwater system and for irrigation, to reduce salinity level to the required concentration. The MVC product water is blended with filtered produced water to meet the water quality requirement for different beneficial use purposes.

5.1.3 Screening-level estimated project costs for produced water treatment

5.1.3.1 Tioga County produced water

According to the Pennsylvania State Impact Project, there were 640 active shale gas wells in Tioga County owned by 9 operators [37]. The produced water production in Tioga County was projected for the next 15 years based on Equation 2 and the number of existing wells in the county. In this case study, shale gas wells were grouped by operators, that is, produced water from all the wells operated by the same operator would be collected, treated by clustered treatment facilities, and reused. Produced water quantity for each operator was assumed to be proportional to the number of wells they own. Two companies that own the most wells (386) and the least well (one) in Tioga County were chosen to represent two extreme production conditions. Company A represents the scenario of clustered produced water treatment collected from 386 wells with a high flow rate of 0.394 million gal/day (MGD) (9,373 bbl/day; 1,490 m³/day) while Company B with only one well represents wellhead treatment with a flow rate of 320 gal/day (7.7 bbl/day; 1.2 m³/day). The capital cost of a wellhead treatment train would be much lower

than that of clustered treatment due to small size of the facilities due to low flow rate requirement. However, the unit cost, in terms of dollars per gallon, would be much higher for wellhead treatment because of elevated capital investment and labor costs normalized by gallon of treated water. The economic scale of costs of the wellhead treatment is extremely low due to small flow rate.

The treatment costs and energy demand for the treatment trains selected by the iDST are summarized in Table 4. Among the three beneficial use scenarios, hydraulic fracturing using gel system had the lowest capital and O&M costs because of its low product water quality requirement, especially no TDS limit. Hydraulic fracturing using slickwater system was ranked the second; it had higher electrical energy demand, and the desalinated water would be blended with filtered water to meet the water quality requirement. For all the case studies, the lifetime of treatment facilities was assumed to be 10 years. Capital and O&M costs for the three beneficial use options did not differ considerably at low flow rate scenario (wellhead treatment), because of smaller facility size and less labor requirement. Total annualized costs of wellhead treatment options in Tioga County ranged from \$256,800/year to \$259,200/year. However, at high flow rate scenario the differences became significant. The annual O&M costs of reusing produced water for slickwater fracking and irrigation were approximately 2 times higher than those for gel system. Capital costs were approximately \$4.9 million for gel system, \$8.3 million for slickwater system, and \$8.3 million for irrigation use. For wellhead treatment for low flow rate, annual unit O&M costs were approximately \$1.9/gal (\$502/m³), while total annual unit costs were approximately \$2.2/gal (\$581/m³). Therefore, wellhead water treatment was deemed to be cost inhibitive due to small capacity *versus* the economic scale of costs. At high flow rate, gel system had the lowest O&M and total costs, \$0.003 and \$0.007/gal, respectively, while the costs for hydraulic fracturing using slickwater system and irrigation were estimated to be \$0.005 and \$0.011/gal, respectively.

Table 4. Screening-level estimated costs for produced water treatment in Tioga and Washington Counties

Beneficial use scenario	Capital cost (\$)	Unit O&M (\$/gal)	Total annualized unit cost (\$/gal)	Energy consumption (kWh/yr)
<i>Tioga County, low flow rate (320 gallons per day; 1.2 m³/day)</i>				
Gel frac	329,500	1.898	2.199	100
Slickwater frac	348,300	1.901	2.219	3,700
Irrigation	348,200	1.901	2.219	3,700
<i>Tioga County, high flow rate (0.394 MGD; 1,492 m³/day)</i>				
Gel frac	4,894,300	0.003	0.007	1,312,500
Slickwater frac	8,363,800	0.005	0.011	4,546,000
Irrigation	8,258,000	0.005	0.011	4,546,000
<i>Washington County, low flow rate (320 gallons per day; 1.2 m³/day)</i>				
Gel, Slickwater, Irrigation	353,300	1.738	2.034	4,100
<i>Washington County, high flow rate (0.394 MGD; 1,492 m³/day)</i>				
Gel, Slickwater, Irrigation	17,139,100	0.004	0.010	10,540,800

5.1.3.2 Washington County produced water

By 2014, there were 1094 shale gas wells in the Washington County owned by 10 operators [37]. The companies operating 748 wells and 1 well were chosen to simulate high and low produced water quantity scenarios, at 0.889 MGD (21,174 bbl/day; 3.36 million m³/day) and 350 gal/day (8.38 bbl/day; 1.3 m³/day), respectively.

Produced water flow rate over time for Washington County had similar trend as Tioga County. High flow rate scenario in Washington County had higher flow rate than in Tioga County, which led to lower unit costs. Operators with the least wells in both counties had 1 well, which makes their flow rates similar, thus almost same costs (Table 4). As the same treatment processes were selected to the three beneficial reuse options, the iDST estimated the same capital cost and O&M cost for different beneficial use scenarios - \$2.03/gal (\$536/m³) for low flow rate of 350 gal/day (1.3 m³/day), and \$0.01/gal (\$2.64/m³) for high flow rate of 0.889 MGD (3.36 million m³/day). Because the costs calculated in the iDST were at a screening-level, the cost estimate was not sensitive enough to reflect the amounts of chemicals used, such as lime and soda, to achieve different product water qualities. However, the iDST allows users to enter chemical uses for more accurate cost estimate. The difference of costs between low flow scenario and high flow scenario was significant. Low flow scenario required much lower capital

cost and annual energy consumption but had a much higher unit cost (Table 4).

5.1.4 Cost comparison of beneficial uses, deep well injection, and transportation

Deep well injection is the most commonly used disposal method for shale gas produced water because of its low cost. In Pennsylvania, the number of injection wells is very limited because of the geological condition of the formation. Among the five active injection wells that accept wastewater from the O&G industry, the nearest one is over 120 miles from Tioga County, which makes transportation cost significantly high. An average \$8/bbl (\$0.19/gal; \$50.3/m³) hauling cost of produced water was estimated for Tioga County [21]. Injection cost generally ranges from \$0.5/bbl to \$2.5/bbl (\$0.0119-0.0595/gal; \$3.15-15.7/m³). Considering the supply and demand relationship in Pennsylvania, \$2/bbl (\$0.0476/gal; \$12.6/m³) of injection cost was assumed for Tioga County, resulting in an overall disposal cost, including deep well injection and transportation, of \$10/bbl (\$0.238/gal; \$62.9/m³). It was estimated that a produced water flow rate of 170 bbl/day (27 m³/day) would be required to breakeven disposal cost with treatment cost for gel system. Assuming a produced water flow rate of 2-3 bbl/day per well, reuse of produced water for a group of 60-100 wells would be more cost-efficient than disposal. Considering all operators in Tioga County, 3 out of 8 operators own more than 60 wells, while all others own less than 30 wells. Centralizing and treating produced water from multiple operators would be recommended to small operators to minimize treatment costs.

The nearest injection well that accepts O&G wastewater from Washington County is approximately 50 miles away in Pennsylvania. Injection wells in Ohio were not included in this case study because of limited information. An estimated hauling cost of \$4/bbl (\$0.0952/gal; \$25.2/m³) was adopted, while \$2/bbl (\$0.0476/gal; \$12.6/m³) injection cost was added to the total cost of \$6/bbl (\$0.143/gal; \$37.8/m³) for disposal using deep injection wells, which is 40% less than that in Tioga County. Using the breakeven approach to balance with the disposal cost, produced water from at least 100-165 wells needs to be collected and treated at a clustered facility. In Washington County, only two operators own more than 100 wells and can make beneficial use cost-efficiently by themselves. Other operators are recommended to collectively treat produced water and develop clustered treatment systems to decrease the costs. It should be noted that the cost for purchasing fresh water for hydraulic fracturing was not included in the cost analysis; taking into account the fresh water costs would further offset the costs for reusing

flowback and produced water.

5.1.5 Flowback water in Marcellus Shale, Pennsylvania

Hydraulic fracturing flowback water quality and quantity were retrieved from the Marcellus Shale Coalition Produced Water Database [18]. Among the 19 wells in the database, the well J is located in Tioga County, and the wells B and F are located in Washington County. The water quality for days 1, 5, 14, and 15 was chosen to represent flowback water. The weighted average of water quality based on daily flow rate was calculated in the iDST (Table 5). The flowback water flow rate for Tioga County was taken as the average value of the 19 wells (878 bbl/day; 140 m³/day). For Washington County, the average flow rate for wells B and F was assumed to be 930 bbl/day (148 m³/day).

Table 5. Summary of major constituents in flowback water. All concentrations (except pH) are in mg/L.

Water quality	Tioga County	Washington County
Alkalinity (as CaCO ₃)	138	90
Calcium	981	8,188
Chloride	12,307	58,815
Magnesium	86	843
Potassium	58	273
Sodium	5,243	22,783
Sulfate	15	90
TDS	24,297	97,104
Total hardness (as CaCO ₃)	3,987	29,441
TOC	36	57
TSS	516	94
pH	6.93	6.42

The treatment trains for the two counties selected by the iDST are summarized in Table 6. Iron (III) and total hardness were required to be removed by chemical softening and precipitation in both counties to prevent scaling and fouling. Because of the low TDS in flowback water in Tioga County, beneficial reuse for hydraulic fracturing using gel and slickwater systems did not require desalination, which significantly reduced the costs. Only chemical disinfection was required to inactivate microorganisms. Brackish water reverse osmosis (BWRO) was selected to desalinate flowback water in Tioga County for irrigation. For flowback water in Washington County, MVC was selected for the higher TDS water.

Table 6. Treatment trains for reusing flowback water in Tioga and Washington County

Beneficial Use	Treatment Train
<i>Tioga County</i>	
Gel fracking	Chemical softening - Media filter - Chemical disinfection
Slickwater fracking	Chemical precipitation - Media filter - Chemical disinfection
Class B Irrigation	Chemical precipitation - Media filter - BWRO - Blending
<i>Washington County</i>	
Gel and slickwater fracking, and Class B Irrigation	Chemical softening - Media filter - MVC - Blending

The estimated treatment costs for flowback water are summarized in Table 7. Unit costs for reusing flowback water in Tioga County were much lower than those for Washington County because of better flowback water quality in Tioga County. Without desalination processes required, reuse of flowback water for hydraulic fracturing using gel and slickwater systems in Tioga County had the lowest costs.

Table 7. Treatment costs for reusing flowback water in Tioga and Washington Counties

	Capital cost (\$)	Unit O&M (\$/gal)	Total annualized unit cost (\$/gal)	Energy consumption (kWh/yr)
<i>Tioga County (878 bbl/day; 140 m³/day)</i>				
Gel fracking	798,300	0.0173	0.0238	25,900
Slickwater fracking	700,900	0.0172	0.0229	14,100
Class B Irrigation	1,299,400	0.0178	0.0289	108,500
<i>Washington County (930 bbl/day; 148 m³/day)</i>				
Gel and slickwater fracking, and Class B Irrigation	531,300	0.1591	0.2009	46,200

Note: cost of solid waste management is not included in the economics analysis.

5.2 Barnett Shale

The case study for the Barnett Shale adopted similar approach as for the Marcellus Shale. Water quality and quantity data were collected, analyzed, and projected for the future 15 years. The iDST was utilized to select the optimal treatment trains based on user preference and estimate screening-level treatment costs for various reuse scenarios. The costs were then compared with disposal costs through deep injection wells, and recommendations were made for operators in the Barnett Shale based on the site-specific conditions. The flowback and produced

water quality in Barnett Shale is summarized in Table 8.

Table 8. Flowback and produced water quality in Barnett Shale

Parameter	Average concentration (mg/L)	
	<i>Flowback</i> ¹	<i>Produced water</i> ²
Alkalinity (as CaCO ₃)	852	237
Ammonia	244	
Barium		42
Calcium	1,082	2,242
Chloride	23,052	38,149
Magnesium	172	253
Iron(III)	24	33
Potassium	213	
Sodium	13,327	12,453
Sulfate	689	60
TDS	37,800	67,285
Total Hardness (as CaCO ₃)	4,000	
TSS	197	
pH	7.13	

Note: ¹[32]; ²[28, 33]

5.2.1 Flowback water reuse scenario

In this case study, the average flow rate of the treatment facility was designed to be 1,300 bbl/day (54,600 gal/day; 207 m³/day), assuming flowback water, wellhead treatment for the Barnett Shale. All beneficial uses require the removal of suspended solids and hardness using chemical softening and coagulation. To reuse the flowback water for hydraulic fracturing using gel system, although TDS removal is not required, MVC was selected by the iDST to remove chloride that exceeded the required limits. MVC was also selected for irrigation to reduce TDS concentration (Table 9). As the salinity of Barnett Shale flowback water is lower than the requirement of slickwater hydraulic fracturing liquid, only disinfection was needed to eliminate microorganisms. Slickwater hydraulic fracturing is the most favorable beneficial use option with the lowest costs and energy consumption (Table 10).

Table 9. Treatment trains for reusing flowback water in Barnett Shale

Beneficial Use	Treatment Train
Gel fracking	Chemical coagulation - Media filter - MVC - Chemical disinfection
Slickwater fracking	Chemical coagulation - Media filter - Chemical disinfection

Class B Irrigation	Chemical coagulation - Media filter - MVC - Chemical disinfection
--------------------	---

Table 10. Cost summary for flowback water reuse in Barnett Shale

	Capital Cost (\$)	Unit O&M (\$/gal)	Total Annualized Unit Cost (\$/gal)	Energy Consumption (kWh/yr)
Gel fracking	1,952,700	0.015	0.026	641,600
Slickwater fracking	854,200	0.012	0.017	28,000
Class B irrigation	1,938,000	0.015	0.026	641,600

Note: cost of solid waste management is not included in the economics analysis.

There are approximately 144,000 Class II wells in the United States, of which 20% is SWD wells [21]. In Texas, approximately 12,000 SWD wells are currently available for flowback and produced water disposal at a cost of \$0.5-\$2.5/bbl (\$3.15-\$15.75/m³) [21]. Based on supply and demand, the disposal cost was assumed to be \$0.5/bbl (\$3.15/m³) in the Barnett Shale for this case study [21]. An average trucking cost of \$0.75/bbl (\$4.7/m³) was estimated. The overall cost to dispose flowback and produced water through SWDs was estimated to be \$1.25/bbl (\$7.9/m³; \$0.0298/gal), which is close to the cost to reuse the Barnett Shale flowback water for slickwater hydraulic fracturing. Compared with the flowback water scenarios in Pennsylvania, the cost of reuse is much lower in the Barnett Shale, as well as disposal costs. Moreover, the Barnett Shale has a higher density of producing wells and therefore it is easier for the operators to develop clustered or centralized treatment to increase the flow rate and reduce the economic scale of costs.

5.2.2 Produced water reuse scenario

Two producers in the Barnett Shale were chosen to represent the most and least wells with the high and low flow rate scenarios of 8,554 bbl/day (0.36 MGD; 1,363 m³/day) and 2 bbl/day (84 gal/day; 0.32 m³/day), respectively. All reuses require chemical coagulation and media filtration. No desalination is required to reuse the produced water for hydraulic fracturing using gel system. MVC was selected to reduce TDS level to reuse produced water for hydraulic fracturing using slickwater system and for irrigation (Table 11). The product water needs to be blended with filtered produced water to use for irrigation and hydraulic fracturing using slickwater system to achieve desired water quality and to reduce overall costs.

The low flow rate scenario led to a very high unit cost to reuse produced water at \$8.8/gal (\$2,325/m³) for all reuse options (Table 12). The unit costs for the high flow rate scenario were estimated to be \$0.005/gal (\$1.32/m³) for gel system hydraulic fracturing to \$0.012/gal (\$3.17/m³) for slickwater fracturing and irrigation. Reusing produced water for hydraulic fracturing using gel system is the more economic option with low cost and energy consumption because no desalination is required.

Table 11. Treatment trains for reusing produced water in Barnett Shale

Beneficial Use	Treatment Train
Gel fracking	BAF - Media filter - Zeolite - Chemical disinfection
Slickwater fracking	BAF - Media filter - Zeolite - MVC - Chemical disinfection
Class B Irrigation	BAF - Media filter - Zeolite - MVC - Chemical disinfection

Table 12. Cost summary for produced water reuse in Barnett Shale

	Capital cost (\$)	Unit O&M (\$/gal)	Total annualized unit cost (\$/gal)	Energy consumption (kWh/yr)
<i>Low flow rate (84 gal/day; 0.32 m³/day)</i>				
Gel fracking	325,800	7.59	8.78	50
Slickwater fracking	332,100	7.59	8.80	900
Irrigation	332,100	7.59	8.80	900
<i>High flow rate (0.36 MGD; 1,363 m³/day)</i>				
Gel fracking	3,841,500	0.0021	0.0054	142,500
Slickwater fracking	8,677,000	0.0046	0.0124	4,147,900
Irrigation	8,580,500	0.0046	0.0123	4,147,900

Note: cost of solid waste management is not included in the economics analysis in the iDST.

To break even with the cost for disposal through injection wells, it requires at least 1,550 bbl/day (246 m³/day; 0.065 MGD) treatment capacity for reusing produced water for gel hydraulic fracturing. Using the same assumption as in the Marcellus Shale, it requires to treat produced water collected from at least 517 to 1,275 wells for gel hydraulic fracturing to break even with the costs for disposal. Under the current production conditions in the Barnett Shale, reusing produced water is not economically competitive as compared to disposal through injection wells because of the requirements for large number of wells, cooperation between producers, and collection and treatment systems.

6 Conclusion

Unconventional O&G development increased rapidly during the past decade, which leads to an increasing demand on fresh water for hydraulic fracturing and better management of wastewater. Treating flowback and produced water for beneficial reuse has become an attractive option; however, reusing flowback and produced water is challenging because of poor water quality, complexity in selecting treatment technologies, and highly variable wastewater quality and quantity.

The iDST provides a comprehensive decision-support framework integrated with multiple criteria, functions, objectives, and constraints to optimize the selection of treatment technologies for beneficial use of hydraulic fracturing flowback and produced water. The case studies in the Marcellus Shale and Barnett Shale demonstrated that flow rate and water quality are the two primary factors affecting the costs and feasibility of treating and beneficial use of these wastewaters. Higher flow rate leads to higher total capital cost and annual O&M cost (\$/yr) because of higher plant capacity and more labor requirement, but lower unit costs (\$/gal or \$/m³). Costs for well-head treatment are much higher than centralized treatment options. Meanwhile better water quality reduces the need of treatment processes, thus reducing costs. Reusing for hydraulic fracturing requires the least treatment processes, especially avoiding desalination technologies thus resulting in lower treatment cost. For example, reusing flowback water in Tioga County for crosslink gel system fracturing requires minimal treatment, which leads to \$7/kgal total unit cost, compared with \$28.9/kgal for reusing produced water in Tioga County, that requires treatment with BWRO. In addition, onsite reuse for hydraulic fracturing is highly favorable because of reduced water transportation costs. The case studies demonstrate that the iDST is a useful screening tool to select treatment trains and estimate screening-level costs for reuse scenarios from current practice of hydraulic fracturing to potential uses such as irrigation.

Due to the limited number of injection wells and high disposal cost, beneficial use of fracturing flowback and produced water is very attractive in the Marcellus Shale. Clustered treatment systems are recommended considering the economic scale of treatment costs. Reusing flowback water in the Barnett Shale would be the most cost-efficient for hydraulic fracturing. Reusing produced water in the Barnett Shale is currently not economically favorable because of the low disposal cost through SWD wells. However, the rapid development of unconventional O&G industry would result in more intensive water demand, which further leads to a higher

potential of flowback and produced water beneficial reuse.

Acknowledgments

The authors thank the Research Partnership to Secure Energy for America program administered by the U.S. Department of Energy's National Energy Technology Laboratory (DE11122-53) for financial support of the project. The authors also thank the participating producers and institutes for their technical assistance, support, and contributions of water quality and quantity data.

Supplementary Content

- A Supplementary Content file is available free of charge on the web.
- A copy of the iDST spreadsheet is available on the web at:
http://aqwatec.mines.edu/produced_water/tools/download/

Acronyms

bbl – Barrel (1barrel = 42 gallons = 159 liters)

BEM – Beneficial Use Economic Module

BOD – Biochemical oxygen demand

BSM – Beneficial Use Screening Module

BWRO – Brackish water reverse osmosis

CBM – Coalbed methane

iDST – Integrated decision support tool

kWh – Kilowatt-hour

MCDA - Multi-criteria decision analysis

MGD – Million gallons per day

MVC – Mechanical vapor compression (distillation)

O&G – Oil and gas

O&M – Operation and maintenance

QA/QC – Quality assurance and quality control

SWD – Salt water disposal

TDS – Total dissolved solids

TOC – Total organic carbon
TOX – Total organic halogens
TSM – Treatment Selection Module
TSS – Total suspended solids
USEPA – US Environmental Protection Agency
WQM – Water Quality Module

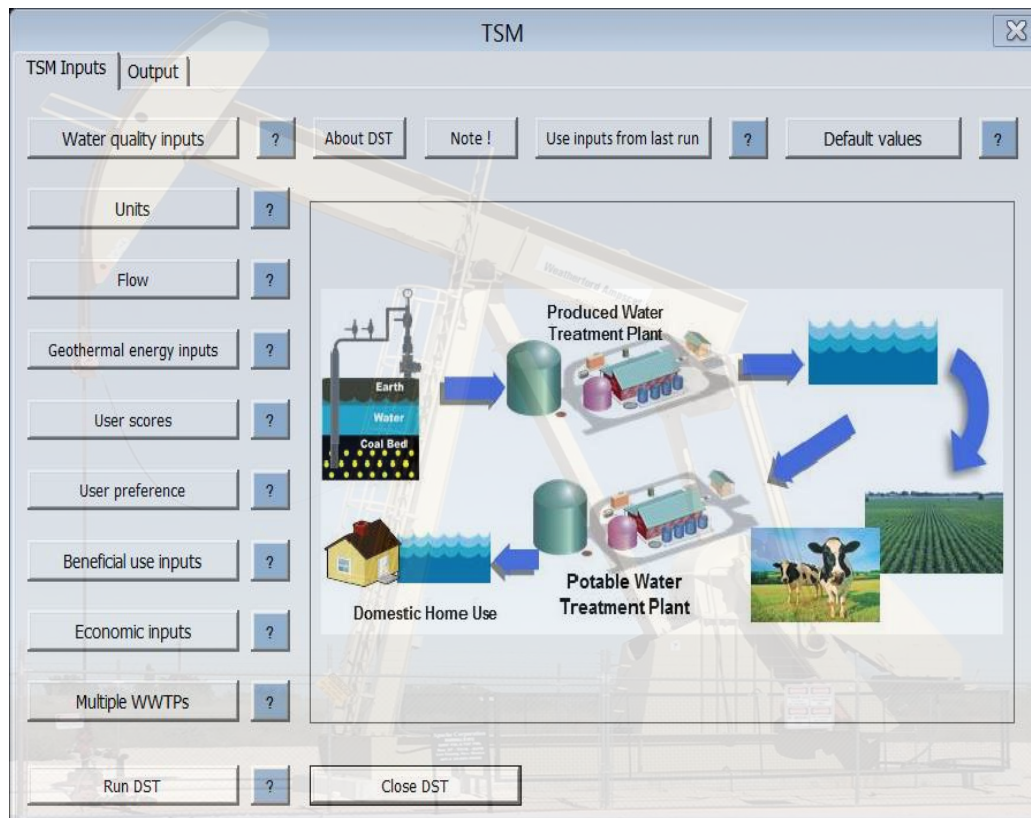
References

- [1] J. Veil, U.S. Produced Water Volumes and Management Practices in 2012, 2015, Ground Water Protection Council, http://www.veilenvironmental.com/publications/pw/prod_water_volume_2012.pdf
- [2] P. Folger, M. Tiemann, Human-Induced Earthquakes from Deep-Well Injection: A Brief Overview, 2016, Congressional Research Service, <https://fas.org/sgp/crs/misc/R43836.pdf>
- [3] D.M. Akob, A.C. Mumford, W. Orem, M.A. Engle, J.G. Klinges, D.B. Kent, I.M. Cozzarelli, Wastewater disposal from unconventional oil and gas development degrades stream quality at a West Virginia injection facility, *Environmental Science & Technology* 50 (2016) 5517-5525.
- [4] C.D. Kassotis, L.R. Iwanowicz, D.M. Akob, I.M. Cozzarelli, A.C. Mumford, W.H. Orem, S.C. Nagel, Endocrine disrupting activities of surface water associated with a West Virginia oil and gas industry wastewater disposal site, *Science of The Total Environment* 557-558 (2016) 901-910.
- [5] US Geological Survey, Evidence of Unconventional Oil and Gas Wastewater Found in Surface Waters near Underground Injection Site, 2016, <https://www.usgs.gov/news/evidence-unconventional-oil-and-gas-wastewater-found-surface-waters-near-underground-injection>
- [6] T.J. Gallegos, B.A. Varela, S.S. Haines, M.A. Engle, Hydraulic fracturing water use variability in the United States and potential environmental implications, *Water Resources Research* 51 (2015) 5839–5845.
- [7] R. Ashleya, D. Blackwoodb, D. Butlerc, P. Jowittd, J. Daviese, H. Smithf, D. Gilmourg, C. Oltean-Dumbravah, Making asset in investment decisions for wastewater systems that include sustainability, *Journal of Environmental Engineering* 134 (2008) 200-209.
- [8] T.L. Saaty, L.G. Vargas, *Models, Methods, Concepts & Applications of the Analytic Hierarchy Process*, Springer, New York, NY, 2001, 978-1-4614-3597-6.

- [9] F. Akinmolayan, N. Thornhill, E. Sorensen, A detailed mathematical modelling representation of clean water treatment plants, *Computer Aided Chemical Engineering* 37 (2015) 2537-2542.
- [10] F. Capitanescu, A. Marvuglia, E. Benetto, A. Ahmadi, L. Tiruta-Barna, Linear programming-based directed local search for expensive multi-objective optimization problems: Application to drinking water production plants, *European Journal of Operational Research* 262 (2017) 322-334.
- [11] M. Kermani, Z. Périn-Levasseur, M. Benali, L. Savulescu, F. Maréchal, An improved linear programming approach for simultaneous optimization of water and energy, *Computer Aided Chemical Engineering* 33 (2014) 1561-1566.
- [12] M.N. Koleva, C.A. Styan, L.G. Papageorgiou, Optimisation approaches for the synthesis of water treatment plants, *Computers & Chemical Engineering* 106 (2017) 849-871.
- [13] K.G. Dahm, K.L. Guerra, P. Xu, J.E. Drewes, Composite geochemical database for coalbed methane produced water quality in the Rocky Mountain region, *Environmental Science & Technology* 45 (2011) 7655–7663.
- [14] M.H. Plumlee, J.-F.β. Debroux, D. Taffler, J.W. Graydon, X. Mayer, K.G. Dahm, N.T. Hancock, K.L. Guerra, P. Xu, J.E. Drewes, T.Y. Cath, Coalbed methane produced water screening tool for treatment technology and beneficial use, *Journal of Unconventional Oil and Gas Resources* 5 (2014) 22-34.
- [15] M. Geza, G. Ma, H. Kim, T.Y. Cath, P. Xu, iDST: An integrated decision support tool for treatment and beneficial use of non-traditional water supplies – Part I. Methodology, *Journal of Water Process Engineering* (2018) in review.
- [16] M.S. Blondes, K.D. Gans, M.A. Engle, Y.K. Kharaka, M.E. Reidy, V. Saraswathula, J.J. Thordsen, E.L. Rowan, E.A. Morrissey, U.S. Geological Survey National Produced Waters Geochemical Database v2.3 (PROVISIONAL), 2017, U.S. Geological Survey, <https://energy.usgs.gov/EnvironmentalAspects/EnvironmentalAspectsofEnergyProductionandUse/ProducedWaters.aspx#3822349-data>
- [17] M. Cather, D. Chen, Improving and Updating of the NM Produced Water Quality Database: Summary of New Mexico Produced Water Database and Analysis of Data Gaps, 2016, New Mexico Water Resources Research Institute and New Mexico Environment Department, <https://nmwri.nmsu.edu/wp-content/uploads/ProducedWater-Reports/Reports/Cather%20et%20al%202016%20-%20Improving%20and%20Updating%20of%20the%20NM%20Produced%20Water%20Quality%20Database%20Summary%20of%20NM%20PW%20Database%20and%20Analysis%20of%20Data%20Gaps.pdf>

- [18] T. Hayes, Sampling and Analysis of Water Streams Associated with the Development of Marcellus Shale Gas. Prepared for Marcellus Shale Coalition, 2009, Gas Technology Institute, <https://www.bucknell.edu/script/environmentalcenter/marcellus/default.aspx?articleid=14>
- [19] New Mexico Oil Conservation Division, Produced Water Data Search (2015) <http://gotech.nmt.edu/gotech/Water/producedwater.aspx>
- [20] J. Veil, Shale Gas Water Management – Experiences from North America, 2014, Society of Petroleum Engineers, Distinguished Lecturer Program, <http://www.spe.org/dl/docs/2014/Veil.pdf>
- [21] R. McCurdy, Underground Injection wells for produced water disposal, 2011, EPA hydraulic fracturing study technical workshop #4: water resources management, https://www.epa.gov/sites/production/files/documents/21_McCurdy_-_UIC_Disposal_508.pdf
- [22] Railroad Commission of Texas, Barnett Shale Information, 2013, <http://www.rrc.state.tx.us/oil-gas/major-oil-and-gas-formations/barnett-shale-information/>
- [23] Railroad Commission of Texas, Oil and Gas Production Data Query System (PDQ), 2013, <http://www.rrc.state.tx.us/about-us/resource-center/faqs/oil-gas-faqs/faq-production-data-query-system-pdq/>
- [24] Railroad Commission of Texas, Water Use in Association with Oil and Gas Activities, 2013, <http://www.rrc.state.tx.us/about-us/resource-center/faqs/oil-gas-faqs/faq-water-use-in-association-with-oil-and-gas-activities/>
- [25] E. Hansen, D. Mulvaney, M. Betcher, Water resource reporting and water footprint from Marcellus shale development in west Virginia and Pennsylvania, 2013, Downstream Strategies and San Jose State University, San Jose. http://www.downstreamstrategies.com/documents/reports_publication/marcellus_wv_pa.pdf
- [26] B.D. Lutz, A.N. Lewis, M.W. Doyle, Generation, transport, and disposal of wastewater associated with Marcellus Shale gas development, *Water Resources Research* 49 (2013) 647-656.
- [27] C.W. Abdalla, J.R. Drohan, K.S. Blunk, J. Edson, Marcellus shale wastewater issues in Pennsylvania - current and emerging treatment and disposal technologies, 2011, Penn State University's Agriculture and Environment Center, [http://www.ohioenvironmentallawblog.com/uploads/file/marcellus_wastewater_fact_sheet\[1\]\(1\).pdf](http://www.ohioenvironmentallawblog.com/uploads/file/marcellus_wastewater_fact_sheet1.pdf)
- [28] M.E. Mantell, Produced water reuse and recycling challenges and opportunities across major shale plays, 2011, EPA hydraulic fracturing study technical workshop #4: water resources management, https://www.epa.gov/sites/production/files/documents/09_Mantell_-_Reuse_508.pdf

- [29] B. Bai, S. Goodwin, K. Carlson, Modeling of frac flowback and produced water volume from Wattenberg oil and gas field, *Journal of Petroleum Science and Engineering* 108 (2013) 383-392.
- [30] K. Oetjen, K.E. Chan, K. Gulmark, J.H. Christensen, J. Blotevogel, T. Borch, J.R. Spear, T.Y. Cath, C.P. Higgins, Temporal characterization and statistical analysis of flowback and produced waters and their potential for reuse, *Science of The Total Environment* 619-620 (2018) 654-664.
- [31] J. Rosenblum, E.M. Thurman, I. Ferrer, G. Aiken, K.G. Linden, Organic chemical characterization and mass balance of a hydraulically fractured well: From fracturing fluid to produced water over 405 days, *Environmental Science & Technology* 51 (2017) 14006-14015.
- [32] T. Hayes, B.F. Severin, Barnett and Appalachian Shale Water Management and Reuse Technologies, 2012, RPSEA, <https://www.netl.doe.gov/File%20Library/Research/Oil-Gas/Natural%20Gas/shale%20gas/08122-05-final-report.pdf>
- [33] H. Li, Produced water quality characterization and prediction for Wattenberg field, Colorado State University, Fort Collins, Colorado (2013). https://dspace.library.colostate.edu/bitstream/handle/10217/79104/Li_colostate_0053N_11585.pdf?sequence=1
- [34] US Department of Agriculture, Census of Agriculture, 2012 Census of Counties in Pennsylvania, 2012, https://www.agcensus.usda.gov/Publications/2012/Online_Resources/County_Profiles/Pennsylvania/
- [35] Pennsylvania Department of Environmental Protection, Reuse of treated wastewater guidance manual, 2012, <http://www.elibrary.dep.state.pa.us/dsweb/Get/Document-88575/385-2188-002.pdf>
- [36] L. Li, G.A. Al-Muntasheri, F. Liang, A review of crosslinked fracturing fluids prepared with produced water, *Petroleum*, 2 (2016) 313-323.
- [37] C. Amico, D. DeBelius, S. Detrow, M. Stiles, Shale Play Natural Gas Drilling in Pennsylvania, (2015) <http://stateimpact.npr.org/pennsylvania/drilling/>



Review

Analysis of Regulatory Framework for Produced Water Management and Reuse in Major Oil- and Gas-Producing Regions in the United States

Wenbin Jiang, Lu Lin, Xuesong Xu , Huiyao Wang and Pei Xu * 

Department of Civil Engineering, New Mexico State University, Las Cruces, NM 88003, USA; wbjiang@nmsu.edu (W.J.); linluedu@gmail.com (L.L.); xuesong@nmsu.edu (X.X.); huiyao@nmsu.edu (H.W.)
* Correspondence: pxu@nmsu.edu

Abstract: The rapid development of unconventional oil and gas (O&G) extraction around the world produces a significant amount of wastewater that requires appropriate management and disposal. Produced water (PW) is primarily disposed of through saltwater disposal wells, and other reuse/disposal methods include using PW for hydraulic fracturing, enhanced oil recovery, well drilling, evaporation ponds or seepage pits within the O&G field, and transferring PW offsite for management or reuse. Currently, 1–2% of PW in the U.S. is used outside the O&G field after treatment. With the considerable interest in PW reuse to reduce environmental implications and alleviate regional water scarcity, it is imperative to analyze the current regulatory framework for PW management and reuse. In the U.S., PW is subject to a complex set of federal, state, and sometimes local regulations to address the wide range of PW management, construction, and operation practices. Under the supervision of the U.S. Environment Protection Agency (U.S. EPA), different states have their own regulatory agencies and requirements based on state-specific practices and laws. This study analyzed the regulatory framework in major O&G-producing regions surrounding the management of PW, including relevant laws and jurisdictional illustrations of water rules and responsibilities, water quality standards, and PW disposal and current/potential beneficial reuse up to early 2022. The selected eastern states (based on the 98th meridian designated by the U.S. EPA as a tool to separate discharge permitting) include the Appalachian Basin (Marcellus and Utica shale areas of Pennsylvania, Ohio, and West Virginia), Oklahoma, and Texas; and the western states include California, Colorado, New Mexico, and Wyoming. These regions represent different regulations; climates; water quantities; quality diversities; and geologic, geographic, and hydrologic conditions. This review is particularly focused on the water quality standards, reuse practices and scenarios, risks assessment, knowledge gaps, and research needs for the potential reuse of treated PW outside of O&G fields. Given the complexity surrounding PW regulations and rules, this study is intended as preliminary guidance for PW management, and for identifying the knowledge gaps and research needs to reduce the potential impacts of treated PW reuse on the environment and public health. The regulations and experiences learned from these case studies would significantly benefit other states and countries with O&G sources for the protection of their environment and public health.

Keywords: produced water; water reuse; regulatory framework; water quality standards; Appalachian Basin; California; Colorado; New Mexico; Oklahoma; Texas; Wyoming



Citation: Jiang, W.; Lin, L.; Xu, X.; Wang, H.; Xu, P. Analysis of Regulatory Framework for Produced Water Management and Reuse in Major Oil- and Gas-Producing Regions in the United States. *Water* **2022**, *14*, 2162. <https://doi.org/10.3390/w14142162>

Academic Editors: Laura Bulgariu and Andrea G. Capodaglio

Received: 28 May 2022

Accepted: 2 July 2022

Published: 8 July 2022

Publisher's Note: MDPI stays neutral with regard to jurisdictional claims in published maps and institutional affiliations.



Copyright: © 2022 by the authors. Licensee MDPI, Basel, Switzerland. This article is an open access article distributed under the terms and conditions of the Creative Commons Attribution (CC BY) license (<https://creativecommons.org/licenses/by/4.0/>).

1. Introduction

A significant amount of produced water (PW) is brought to the land surface during oil and gas (O&G) exploration and production [1]. PW is primarily composed of reservoir water extracted from rock formation (i.e., formation water); it may also include a portion of the frac fluid returned to the surface after hydraulic fracturing (i.e., HF flowback water) or the water injected for enhanced oil recovery (EOR). PW contains the naturally occurring

constituents from the hydrocarbon-bearing strata, such as salts, minerals, metals, ammonia, hydrogen sulfide, organics (e.g., oil and grease, total petroleum hydrocarbons, volatile and semi-volatile organic compounds), radionuclides, and any chemicals added downhole or during well drilling, production, or maintenance processes (e.g., acid, biocide, breaker, clay stabilizer, corrosion inhibitor, crosslinker, friction reducer, gelling agent, and surfactant).

Because of the complex chemistry characteristics of PW [2–4], the primary disposal option for PW in the U.S. and Canada is deep well injection [5–7]. Other reuse or disposal methods include using PW for HF, EOR, well drilling, evaporation ponds or seepage pits within the O&G field, transferring PW offsite for disposal, and discharge or reuse after proper treatment [3,8–10]. The non-injection methods are especially used in areas that lack deep injection wells (e.g., Pennsylvania in the U.S., Europe, and China) due to geological structure or regulations. In the U.S., approximately 1–2% of PW is used outside of the O&G field [11–13]. Reuse of PW with lower salinity mainly occurs in the western U.S., such as in California and Wyoming, because of the severe droughts and applicable regulations. Approximately 20 billion barrels ($3180 \times 10^6 \text{ m}^3$) of PW will be generated by the onshore O&G activities in the U.S. in 2022. Approximately 41% of the PW will be reinjected for EOR, 47% will be disposed of using SWD wells, and 13% will be reused for fracking operations [8].

With the increased O&G development, underground disposal practices are not sustainable and have caused environmental concerns (e.g., seismicity activities and groundwater contamination) [14]. Further, because 38% of shale resources in the world are located in semi-arid or arid regions [15], the large amount of PW disposed of as waste has the potential to be treated and reused to alleviate regional chronic water scarcity [12,16]. It is recognized that PW reuse inside the O&G field, such as for HF, is the most promising approach because it requires minimal treatment and has relatively low risks of causing adverse effects on the ecosystem and human health [17,18]. However, the PW volume may exceed the water requirement for internal uses [19]. For example, it was estimated that the PW volume in the Delaware Basin, New Mexico, and Texas exceeded HF water demand by 3.7 times [20]. Thus, extra treated PW can be used outside of the O&G field for irrigation, livestock watering, land application, and other usages after proper treatment. The PW treatment methods are mainly based on water quality, such as suspended solids, total dissolved solids (TDS), metals, organic contaminants, and radionuclides. The commonly used methods include settling, filtration, coagulation, oxidation, distillation, and biological treatment [10,12]. The detailed PW characterization and treatment methods can be found in other reviews [3,10,21].

Another major concern for PW management is its possible contamination of soil, surface water, and groundwater through spills or leakages during its transportation for disposal, treatment, or recycling [6,22]. For example, 113 environmental spills of PW were reported in 2015 in the Duvernay shale region, Canada [23]. Moreover, recent studies raised concerns about the contamination of underground sources of drinking water due to acid stimulation and HF in the U.S., such as in the Pavillion Field, Wyoming [24], and the Permian Basin in West Texas [25]. Further, the laboratory data from the U.S. and Canada have shown that exposure to PW causes a series of problems, such as inhibiting the survival and reproduction of aquatic animals (e.g., zebrafish [26] and rainbow trout [27]), and results in functional impairment in exposed animals [28]. Another study assessed potential surface water impacts that could occur downstream of saltwater disposal well (SWD) injection facilities in West Virginia [29]. The study reported increased antagonist activities downstream of a SWD injection site, which could disrupt reproduction and/or development in aquatic animals [29].

Although numerous studies focused on the evaluation of reusing treated PW, the regulations for PW reuse from government agencies around the world are very limited [9]. Common water regulations or guidelines are focused on water applications, such as the United States Environmental Protection Agency (U.S. EPA) drinking water standards and guidelines for irrigation [30], and the European Union water quality directive for ground water (80/68/EEC). However, based on a study by Danforth et al. [31], more than

1000 chemicals in the PW have no U.S. EPA-approved analytical methods for detection or quantification in the regulatory context, which means the current regulations may not be sufficient to monitor treated PW quality to assure its safe reuse outside the O&G field. All these studies suggest that regulatory agencies should establish a comprehensive monitoring and evaluation program to assess the impacts and risks of reusing treated PW on groundwater, surface water, ecological systems, and potential public health before its reuse outside of the O&G field.

Critical review and analysis of PW management, regulations, and reuse scenarios (inside and outside the O&G field) in the major production regions in the U.S. would assist the O&G industry and regulators in better understanding the challenges for PW reuse, addressing the knowledge gap, and providing information to establish suitable regulations. The experiences learned from the case studies can be used by other states in the U.S. or countries and regions for establishing PW management and reuse programs. For example, in China, the study of the impact of the HF water cycle on the environment is in the early stage, and the research for solutions and regulations to achieve more sustainable unconventional O&G development has just emerged [9,32].

In the U.S., nearly every aspect of the PW cycle is subject to a complex set of federal, state, and sometimes local regulations to address the wide range of management, construction, and operation practices. Regulations are involved in permitting water sourcing (e.g., water rights), transportation (e.g., pipeline and trucking), storage (e.g., tank construction and secondary containment), disposition (e.g., discharge to surface water, wastewater treatment facilities, underground injection), and beneficial use within and outside of O&G fields. Figure 1 illustrates the key points for PW management and reuse.

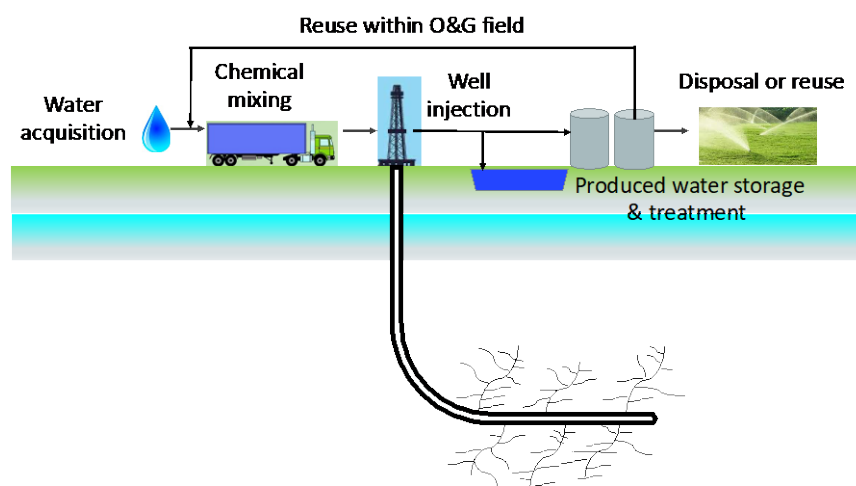


Figure 1. Schematic diagram of produced water management and reuse.

In the U.S., two federal regulatory programs are associated with PW management, as shown in Figure 2. The first federal regulation is the National Pollutant Discharge Elimination System (NPDES) program. Through the Clean Water Act (CWA), the U.S. Congress directs the U.S. EPA to create an NPDES permitting, compliance, and enforcement program that regulates discharges of PW to surface water bodies (e.g., rivers, lakes, and streams). The NPDES program also regulates PW discharged to a municipal wastewater treatment facility to meet the requirements for pretreatment and any additional standards imposed by the facility. PW discharged to a centralized wastewater treatment (CWT) facility must meet standards established in its NPDES or state discharge permit. NPDES water quality permits are either issued by the U.S. EPA or by states that have been delegated by the U.S. EPA to issue their own permits. Most PW in the east of the 98th meridian (Figure 3) cannot be discharged directly from an O&G well site. It can be treated offsite in a CWT facility, and then discharged if the facility has been issued an NPDES (or state-equivalent) permit [17]. In contrast, for the wells located in the west of the 98th meridian, the NPDES

exemption allows for the release of PW for beneficial uses such as wildlife or livestock watering or other agricultural uses if it is “of good enough quality”, meeting the minimum oil and grease limit of 35 mg/L and other parameters [33].

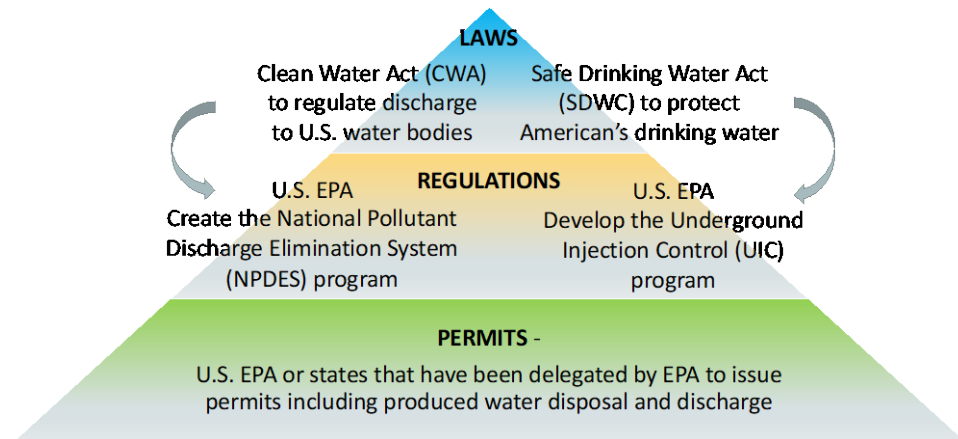


Figure 2. The U.S. legal and regulatory framework for produced water management.

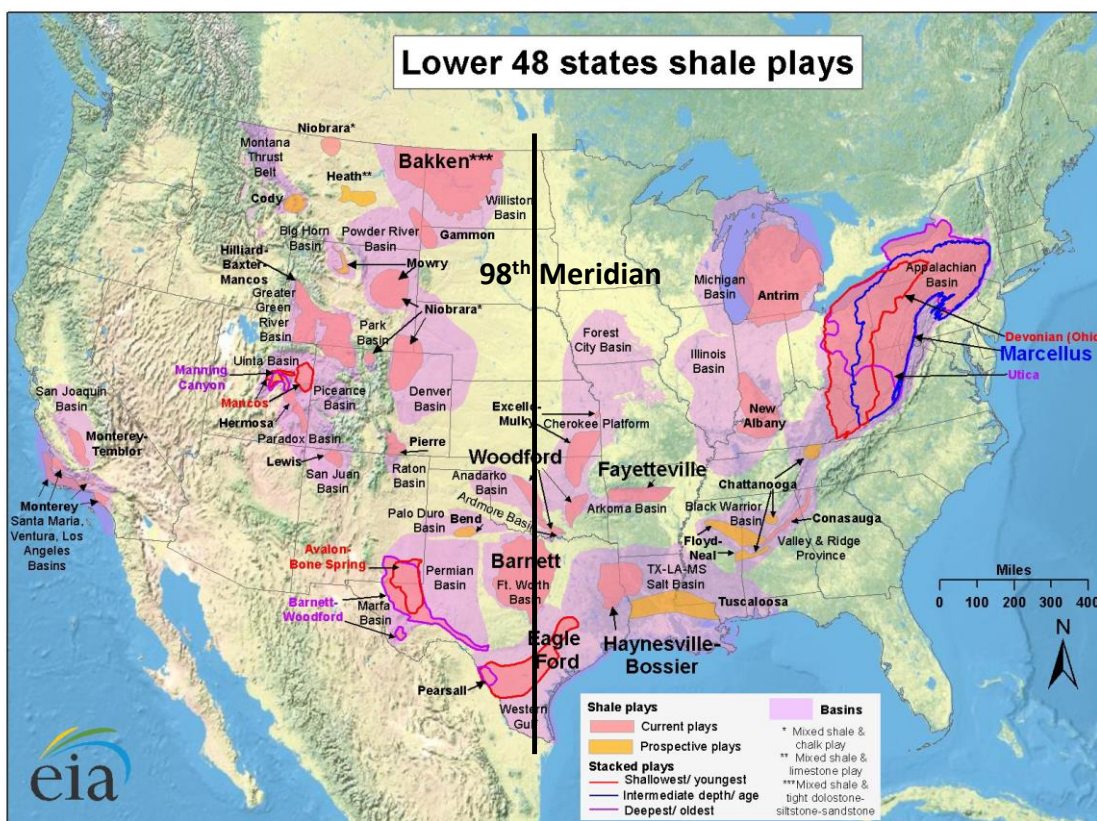


Figure 3. Major oil and gas production regions in the U.S. with 98th meridian. Source: U.S. Energy Information Administration [34].

The second federal regulation is the Underground Injection Control (UIC) program. Through the Safe Drinking Water Act (SDWA), the U.S. Congress directs the U.S. EPA to develop the UIC program to regulate disposal in injection wells to protect America’s drinking water sources. Most oil- and gas-producing states have received the authority to implement UIC under agreements with the U.S. EPA. The UIC program is designed to protect underground drinking water aquifers through the regulation of six classes of injection wells. Wells used for injecting PW are Class II wells, including Class II-R wells for

EOR and Class II-D wells for disposal in a formation below a drinking water aquifer and other than the producing formation.

PW is primarily regulated at the state level when the states receive primacy to administer the NPDES or UIC programs. The states can modify the regulatory programs based on state-specific practices and laws [33]. For example, some states do not allow moving water from one basin to another due to the constraints of water rights. Therefore, each of the 31 states with O&G production can have different regulations; they can be more restrictive than federal regulations, and can include regulations for activities not covered by federal regulations [33]. In addition to O&G agencies or state environmental protection agencies, public health agencies, state engineers, or regional water planning commissions may also be involved in regulating PW. Thus, in the U.S., it is imperative to analyze the current regulatory framework for PW management, which requires new levels of coordination and planning between federal and state agencies, inter-organizations, or across states for inter-state basins, such as the Permian and the Appalachian. The information and experience from different states can be used as references and guidelines for new PW reuse projects.

This study aims to provide an overview of current PW production, management practices with regulations, and reuse scenarios in the major production areas in the U.S. We analyzed the regulatory framework surrounding the management of PW, including relevant laws and jurisdictional illustrations of water rules and responsibilities, water quality standards, and PW disposal and beneficial reuse up to 2022. Given the complexity surrounding PW regulations and rules, this study is intended as preliminary guidance for PW management, and for identifying the knowledge gaps and research needs to reduce the potential impacts of PW reuse on the environment and public health. The establishment of regulations in the U.S. would significantly benefit other regions/countries with an interest to develop unconventional O&G.

2. Materials and Methods

The investigated production areas are selected based on the 98th meridian as shown in Figure 3. The 98th meridian has long been designated by the U.S. EPA as a tool to separate discharge-permitting under NPDES rules. The eastern states (east or on of the 98th meridian) include the Appalachian Basin (Marcellus and Utica shale areas of Pennsylvania, Ohio, and West Virginia), Oklahoma, and Texas; and the western states (west of the 98th meridian) include California, Colorado, New Mexico, and Wyoming. These regions are selected to represent different regulations; climates; water quantities; quality diversities; and geologic, geographic, and hydrologic conditions.

This study involves a comprehensive literature review from peer-reviewed manuscripts, technical reports, engineering contracts, government reports, news releases, databases of national and regional water resources and water quality, and information provided by the industry partners and regulatory agencies through the New Mexico Produced Water Research Consortium (NMPWRC). The NMPWRC was created by the New Mexico Environment Department (NMED) and New Mexico State University (NMSU) to develop a framework to fill scientific and technical knowledge gaps necessary to establish regulations and policies for the treatment and reuse of PW outside of the O&G fields. This study summarizes the existing regulatory framework, water quality standards, and risk assessment. It aims to identify the knowledge gaps to inform policy decisions for the potential safe reuse of treated PW outside of O&G fields.

3. Results and Discussion

Table 1 summarizes the PW regulatory agencies in the selected states with major O&G production activities. Table 2 summarizes the PW production and management practices in the selected states. The information in Tables 1 and 2 will be discussed in detail in each section. Water quality limits for reusing PW for irrigation, wildlife and livestock watering, discharge to surface water, road application, dust control, and groundwater standards are discussed. The detailed application standards are summarized in Supporting Information.

Table 1. Regulatory agencies for produced water management in the selected states.

State	Underground Injection Control Wells (Class II)	Reuse Inside of the O&G Fields	Commercial Facility	Discharge to Surface Water via NPDES
Pennsylvania	U.S. Environmental Protection Agency (EPA)	Pennsylvania Department of Environmental Protection (PADEP)	EPA	PADEP
Ohio	Ohio Department of Nature Resources (ODNR)	ODNR	ODNR	Ohio EPA Division of Surface Water (DSW)
West Virginia	West Virginia Department of Environmental Protection (WVDEP)	WVDEP	WVDEP	WVDEP
Texas	Railroad Commission of Texas (TRRC)	TRRC	TRRC	Texas Commission on Environmental Quality (TCEQ)
Oklahoma	Oklahoma Corporation Commission (OCC)	OCC	OCC	Oklahoma Department of Environmental Quality (ODEQ)
Wyoming	Wyoming Oil and Gas Conservation Commission (WOGCC)	WOGCC	WOGCC	Wyoming Department of Environmental Quality (WDEQ)
Colorado	Colorado Oil and Gas Conservation Commission (COGCC)	COGCC	COGCC	Colorado Department of Public Health and Environment (CDPHE)
New Mexico	New Mexico Oil Conservation Division (OCD)	OCD	OCD	U.S. EPA
California	California Geologic Energy Management Division (CalGEM)	California Waterboards (State water board and nine regional water boards)	California Waterboards	California Waterboards

Note(s): The U.S. EPA issues NPDES permits for federally owned facilities, on tribal lands, and in Massachusetts, New Hampshire, New Mexico, and the District of Columbia. Other permits are issued by state regulators if not issued by the U.S. EPA.

Table 2. Produced water production and management practices in the selected states.

Region	PW Production (2017)	PW Disposal (Deep Well Injection)	PW Reuse Inside O&G Field	PW Reuse for EOR	PW Reuse/ Dispose Outside O&G Field	Examples of PW Reuse Outside O&G Field
Appalachian Basin	105 MMbbls ($16.8 \times 10^6 \text{ m}^3$)	PA: 1.1%, WV: 56%, OH: 89%.	PA: 96%, WV: 29%, OH: 9.1%.	PA: n/a, WV: 14%, OH: 1.3%.	PA: 1.6%, WV: n/a, OH: n/a.	n/a
Oklahoma	2844 MMbbls ($455 \times 10^6 \text{ m}^3$)	41.7%	n/a	44.9%	13.4%	n/a
Texas	9895 MMbbls ($1583 \times 10^6 \text{ m}^3$)	36.2%	n/a	46.1%	17.6%	n/a
California	3100 MMbbls ($496 \times 10^6 \text{ m}^3$)	22.4%	5.1%	59.3%	11.1%	Irrigation
Colorado	310 MMbbls ($49.6 \times 10^6 \text{ m}^3$)	47.1%	8.9%	32.5%	11.5%	Dust control; aquifer recharge and recovery; pits and surface water discharge. Surface water discharge; groundwater injection; dust control and road application; irrigation; land application; impoundment.
Wyoming	1700 MMbbls ($272 \times 10^6 \text{ m}^3$)	14%	n/a	46%	37%	
New Mexico	1240 MMbbls ($196.9 \times 10^6 \text{ m}^3$, 2019)	51%	10%	40%	n/a	n/a

Note(s): PW: produced water; MMbbls: million barrels; PA: Pennsylvania; OH: Ohio; WV: West Virginia; n/a: not available.

3.1. PW Management in the East or on the 98th Meridian

For the eastern states, because the direct discharge of PW to the surface water is prohibited, PW is usually managed through reuse within the O&G field, injection for EOR, disposal through SWD, and treatment in CWT facilities. In Pennsylvania, because of the poor geology for underground injection, a high percentage (~90%, in 2017) of PW is reused, and the rest is either treated through CWT facilities or sent to West Virginia and Ohio for disposal. More PW was injected for disposal in West Virginia and Ohio, ~56% and ~89%, respectively, in 2017. Ohio usually accepts PW from nearby states (Pennsylvania, New York, and West Virginia) for deep well injection because it has more SWD wells [13]. Although PW can be reused outside of the O&G field in the west part of Oklahoma and Texas (states on the 98th meridian), the feasibility is still under the investigation phase in these two states. Oklahoma has ample freshwater resources and SWD wells; thus, a large amount of PW was managed through deep well injection (41.7%) and injected for EOR (44.9%) in 2017. However, the increased seismicity activities urged the state to find alternative methods for PW management. Texas has a similar situation as Oklahoma; 46.1% and 36.2% of PW were injected for EOR and for disposal in 2017, respectively. With the increased seismicity activities, and part of west Texas currently being under a drought condition, the reuse of PW outside of the O&G field would also significantly benefit the society [13].

3.1.1. Appalachian Basin

PW Production, Disposal, and Management in Appalachian Basin

The Appalachian formations of the Marcellus and Utica shale areas include Pennsylvania, Ohio, and West Virginia (Figure 3). In 2020, the Appalachian Basin produced approximately 24 million barrels (MMbbls) of oil and 12.3 trillion cubic feet (tcf) of natural gas, making it the highest gas-producing region in the U.S. [34]. The Appalachian Basin produced 105 MMbbls ($16.8 \times 10^6 \text{ m}^3$) of PW in 2017 [13]. One factor in accelerating PW management is the poor geology for disposal wells. Pennsylvania has limited the number of disposal wells, and so far, only has less than ten permitted disposal wells for PW. Due to limited disposal options and high disposal costs, Marcellus and Utica operators in Pennsylvania became early adopters of PW reuse. In the Appalachian Basin, flowback water is almost entirely recycled and reused to hydraulically fracture new wells because formation water can only provide a small fraction of the water needed for HF in this area. Generally, the PW in the basin is highly diluted with additional freshwater to make up the necessary volumes, thereby decreasing the treatment requirement of PW for HF. A small percentage of the flowback water is disposed of through underground injection wells regulated by the state/EPA, or treated to drinking water standards at state-permitted facilities [33,35].

The PW from the Marcellus Shale has a high TDS concentration (40,000–90,000 mg/L with long-term >120,000 mg/L), moderate-to-high scaling tendency (high Ca and Mg), but low total suspended solids (around 160 mg/L), which makes filtration reasonable. Hence, the PW quality in the Marcellus Shale is manageable and attractive for reuse. Most CWT facilities, such as Hillstone, HydroRecovery, and Reserved Environmental Services, still utilize chemical precipitation.

Sharing PW among producing companies is most common in Pennsylvania and West Virginia. PW may be transferred from one company without enough nearby completion operations to another company needing PW for reuse. Agreements to exchange water can reduce costs for both companies while reducing truck miles driven and water disposal. For example, Antero Resources had the largest desalination plant for PW reuse in the industry. The 60,000 barrels per day capacity plant in West Virginia costs approximately \$500 million. The company has a water system to gather PW and distribute the treated water for reuse. Yet, Antero's Clear Water facility was shuttered in 2019 due to the current low commodity price environment and operation challenges. The company was conducting an evaluation to look at all options to determine the most cost-effective ways for operations. Those options included resumption of the water cleaning efforts at the facility, blending with fresh water, and reusing or trucking water to injection wells [36].

However, concerns have arisen about whether surface owners may make a monetary claim on water transferred among operators. A second concern is whether the liability for spills is fully passed to the receiving company. An example is that the Hillstone Central Station Facility takes the water title once it enters the facility from the truck. The client takes the title of the treated water as it exits the facility and enters their vehicle. If any spills occur between the inlet or outlet of the facility, the midstream company is responsible. Despite these concerns, water sharing among producers smooths out the peaks and valleys of individual company water demands [33].

Based on the 2017 data [13], in Pennsylvania, approximately 96% of PW was reused within the O&G industry, 1.6% was discharged to surface water through CWT facilities, and 1.1% was injected for disposal. In West Virginia, around 29% of PW was reused within the O&G industry, 14% was injected for EOR, and 56% was injected for disposal. In Ohio, around 89% (46% from Ohio wells and 43% from out-of-state wells) of PW was injected for disposal, 9.1% was reused within the O&G industry, and 1.3% was injected for EOR. Underground injection mainly occurs in Ohio because it has much more PW injection wells (217 wells) in the Appalachian area. In 2019, Ohio Class II Underground Injection wells received a total of 43.4 million barrels of PW. Among these, 25.3 million barrels (58%) were from Ohio and 18.2 million barrels (42%) were from outside of Ohio (Pennsylvania, West Virginia, and New York) [37]. The Pennsylvania Department of Environmental Protection (DEP) data suggest that exploration and production (E&P) only sent 4.8 million barrels PW to injection [37]; much of the remainder was sent by centralized processing facilities. If the facilities did not have an outlet for recycled water, they would pay shipment for disposal to make room for more E&P water. Pennsylvania regulations do not require tracking the water after it is dropped off at a centralized processing facility, making recycle volumes look artificially higher than they are.

Discharges of treated PW may occur through CWT facilities offsite from O&G operations under industrial effluent limitation guidelines in 40 CFR Part 437 (65 Fed. Reg. 81300 (22 December 2000)). The U.S. EPA released a report in May 2018 listing the facilities in the region of the Marcellus and Utica plays with the permit to discharge treated PW [38]. However, not all discharge permits are issued by the U.S. EPA. Some are permitted under Part 437, and some of them are not currently permitted under Part 437, but the revised permit is expected to contain Part 437 limitations, and there are some other discharge permits issued by state agencies.

In Pennsylvania, the NPDES water discharge permit is issued by the Pennsylvania DEP, whereas the UIC program is regulated by the U.S. EPA [33]. In Ohio, the storage, recycling, treatment, processing, and disposal of brine and other waste substances are regulated by the Ohio Department of Nature Resources (ODNR) [33]. PW discharge in West Virginia is regulated by the West Virginia DEP [39], and the UIC program is managed by the Office of Oil and Gas under West Virginia Code Chapter 22 "Environmental Resources" [40].

PW Reuse Standards and Case Studies in Appalachian Basin

In Ohio, relators seek a writ of mandamus to compel the Respondents State of Ohio, its Governor, and officers within ODNR to comply with ORC § 1509.22(C) by promulgating rules and regulations prior to issuance of so-called "Chief's Orders." Chief's Orders are used by the ODNR to allow the operation of privately-owned facilities for the storage, recycling, treatment, processing, and disposal of brine and other waste substances associated with O&G drilling [41].

West Virginia does not have a specific process for centralized treatment facilities; instead, they must seek input from the West Virginia DEP. For example, the Hillstone Central Station Facility had to demonstrate a zero liquids discharge status to the water department. All process liquids and any precipitation that come into contact with O&G contamination should be directed to the facility for treatment and beneficial reuse. An air permit is also required because rich volatile organic compounds (VOCs) content in the PW could emit over-regulated values.

In January 2021, the Pennsylvania DEP renewed the General Permit WMGR123—Processing and Beneficial Use of Oil and Gas Liquid Waste (First issued in 2012), which was issued under the Bureau of Waste Management Authority. For wastewaters with low TDS (i.e., less than 500 mg/L) that comply with standards found in the permit (Supporting Information, Table S1), which was derived from drinking water standards, the operator does not have to manage the waste as residual waste, and should utilize existing designs for impoundments and handling of the water. This approach would work for water generated at a well site and stored before transport to a recycling facility, and for recycled water treated and transported to a well site for reuse. These wastewaters with low TDS no longer have to be transported as residual waste. However, for high-TDS wastewater, which does not comply with the General Permit WMGR123, as shown in Table S1, it must be managed as residual waste. Both the generators and users of the recycled water should comply with the regulations on storage and transportation found at 25 PA Code § 299 and the permitting and design requirements for impoundments found in 25 PA Code Section 299.141 through 299.145. If either the generator of the waste or the party beneficially reusing the waste wishes to store the waste before either shipment or reuse, they need to comply with storage requirements that are generally more stringent than the requirements under the O&G regulations. Moreover, the permit holder must comply with several other requirements associated with the general permit. They include a bonding requirement, sampling requirements to determine whether the wastewaters comply with Table S1, facility siting requirements, and inspection and records requirements.

The Marcellus and Utica region has led other basins in the development of commercial water treatment plants. The commercial plants, some starting operations as early as 2010, typically take water from multiple producers. The plants treat and may store the water until it is needed for reuse. For instance, Eureka Resources has three commercial water treatment plants in Pennsylvania, which have served unconventional O&G producers in the Marcellus Shale for ten years. Although two of the plants have a permit to discharge treated water to the Susquehanna River, most of the water is reused for other O&G operations. The plants have a treatment capacity of 10,000 barrels per day (1590 m³/day). The treatment process generates little to no disposal of liquids. In addition to treating the water, one plant is also removing methanol from the water and reselling it for natural gas operations in the area. Another Eureka plant recovers sodium chloride and calcium chloride for industrial sales, establishing marketing and sales channels for co-product sales and revenue generation. Eureka Resources possesses a US patent for treating wastewater and recovering the salts. The method includes the steps of receiving wastewater, screening the wastewater to determine the optimal treatment approach, and pretreating the wastewater to an acceptable quality for thermal–mechanical crystallization/evaporation. Another embodiment is applied to recovering calcium chloride and lithium carbonate from the fluid; it includes processing the fluid through a second stage thermal–mechanical evaporation/crystallization unit. This unit is configured to generate high-purity CaCl₂, distilled water, and a mixed reject stream [42]. According to Eureka Resources, a 50,000 barrel per day Eureka facility would produce ~250,000 metric tons (MT) per year of high-purity NaCl, ~20,000 MT per year of CaCl₂, and 1250 MT per year of LiCl. Recovering minerals from PW is anticipated to provide economic benefits to offset PW treatment costs and environmental benefits by eliminating mining and minimizing waste disposal [43].

Besides centralized facilities, onsite treatment using portable units stationed on well sites can significantly reduce the truck traffic carrying wastewater. For example, Aquatech tested evaporation/distill technology to treat PW in southwestern Pennsylvania to provide recycled distilled water at Marcellus Shale drilling sites [44]. Aquatech’s mobile treatment unit treats water to a TDS of less than 500 mg/L.

Technologically Enhanced Naturally Occurring Radioactive Material Management and Waste Disposal in Appalachian Basin

PW may contain different levels of naturally occurring radioactive materials (NORM). The Marcellus shale, underlying Ohio, Pennsylvania, West Virginia, and New York, has been tested, showing high NORM [45]. Tanks, filters, pumps, pipes, hoses, and trucks that brine touches can all become contaminated, with the radium building up into a hardened “scale,” concentrating as high as 400,000 picocuries (pCi) per gram [45]. With fracking, which involves sending pressurized fluid deep underground to break up shale layers, there is dirt and shattered rock, called drill cuttings, that can also be radioactive.

There have been discussions about the Technologically Enhanced Naturally Occurring Radioactive Material (TENORM) management and waste disposal in the Appalachian Basin. Ohio can only accept waste that is 6.99 pCi/g combined radium 226/228 above background levels. West Virginia can accept up to 50 pCi/g combined (plus uncertainty), but requires testing on a per box basis. However, lab testing relies on a 21-day ingrowth, so there is a general lack of rapid TENORM management testing. Pennsylvania landfills can receive TENORM levels that are below the Department of Transportation hazard classification. Still, each landfill is limited on a monthly tonnage managed by the Pennsylvania DEP. Virtually all lower level (less than 50 μ R/h, microrentgen/hour) TENORM waste generated in the Appalachian Basin is disposed of in Pennsylvania landfills. The waste over 50 μ R/h is sent to the Austin Masters Services or sent out west to facilities that can accept higher levels. The cost and regulatory burden of TENORM waste management in the Appalachian Basin are high, which can be as much as \$350 per ton [46,47].

Summary

PW treatment and reuse are extensively implemented in the Appalachian Basin due to limited disposal options, high disposal cost, and environmental concerns about the impacts on the ecosystem and human health. Sharing PW among producing companies is most common in Pennsylvania and West Virginia, whereas Ohio has much more injection wells for PW from inside and outside of the state. Centralized facilities often treat PW to drinking water or distillate quality standards. The water is then reused for well completions, injected into the hydrogeological cycle for EOR, or sent to industrial and municipal facilities to be combined with wastewater for discharge.

In Ohio, Chief’s Orders are used by ODNR to allow the operation of privately-owned facilities for the storage, recycling, treatment, processing, and disposal of brine and other waste substances associated with O&G drilling. West Virginia does not have a specific process for centralized treatment facilities; instead, they seek input from the West Virginia DEP. The Pennsylvania DEP renewed General Permit WMGR123—Processing and Beneficial Use of Oil and Gas Liquid Waste. Owing to high radioactive signatures detected in the brine, there has been a long and detailed discussion about TENORM management and waste disposal in the Appalachian Basin.

3.1.2. Oklahoma

PW Production, Disposal, and Management in Oklahoma

Oklahoma has about 5% and 8% of the U.S. proved crude oil reserves and natural gas reserves, respectively. The state was the fourth-largest onshore crude oil producer; it produced 171 MMbbls of oil and 2.8 tcf of gas in 2020 [34]. The primary producing plays in Oklahoma are principally located in the state’s Anadarko Basin, as shown in Figure 3.

The Anadarko Basin in western Oklahoma has been the site of increased oil production in recent years [48]. PW across the state has different characteristics based on the plays, such as water quantity and quality (salinity). For example, the Mississippi Lime has a high water-to-oil ratio, and the water has the highest salinity in the state; the Granite Wash and Tonkawa areas produce less water with lower salinity. Detailed information regarding the PW volumes injected and the TDS by county in Oklahoma can be found in “Oklahoma Water for 2060 PW Reuse and Recycling, Table 2-1”.

In Oklahoma, freshwater is available and relatively inexpensive; most of PW is disposed into UIC Class II wells. In 2014, nearly 1500 MMbbls ($240 \times 10^6 \text{ m}^3$) of PW were disposed of underground in Oklahoma. In 2016, the underground injection of PW was reduced due to the Oklahoma Corporation Commission (OCC) regulations in critical areas to limit the volume of injections correlated with the seismic events in Oklahoma [18]. In 2017, 2844 MMbbls ($455 \times 10^6 \text{ m}^3$) of PW were generated in Oklahoma; 1185 MMbbls (41.7%, $192 \times 10^6 \text{ m}^3$) of PW were disposed of through underground injection, 44.9% was injected for EOR, and 13.4% was managed through offsite commercial disposal [13].

Based on the U.S. Geological Survey (USGS) information [49], the number of earthquakes in the central U.S. has increased dramatically from 2009 to 2016. There was an average of 25 earthquakes of M 3.0 and larger in the center and the eastern U.S. between 1973–2008. Since 2009, at least 58 earthquakes of this size have occurred each year, and at least 100 earthquakes of this size have occurred every year since 2013. The rate peaked in 2015, with 1010 M 3+ earthquakes. Oklahoma is the most affected region, including the M 5.8 and M 5.0 Cushing Oklahoma earthquakes that occurred in 2016. Many studies have indicated that the increased earthquakes were induced by HF [14] and wastewater injection [50,51].

PW Reuse in Oklahoma

To reduce the number of induced earthquakes, PW management in Oklahoma has become an imperative task. In December 2015, Oklahoma Governor Mary Fallin launched a project to study and recommend alternatives to manage PW from O&G operations in Oklahoma. The Oklahoma Water Resources Board led the project, and 17 expert members formed the Produced Water Working Group (PWWG). In April 2017, the final report, “Oklahoma Water for 2060 PW Reuse and Recycling,” was published. The report was designed to evaluate the data, issues, and opportunities with PW in Oklahoma. It had two objectives: (1) to reduce the use of freshwater in O&G production; and (2) to reduce PW injection, potentially creating new water sources.

In the study, the PWWG investigated PW production in 66 counties and water quality in 29 counties in Oklahoma, the top 40 major water users in the state based on water permits, and the PW treatment costs for various volume levels and water quality levels for eight selected companies in Oklahoma. The PWWG identified a total of 17 scenarios based on the correlation between high PW volumes and entities requiring significant volumes of non-potable water for irrigation, power, mining, O&G use, industrial use, aquifer storage and recovery (ASR), and surface water discharge, as shown in Table S2. The PWWG further evaluated the primary advantages and disadvantages of each PW reuse alternative, and then developed ten representative cases of PW reuse or recycling in Oklahoma with potential treatment and disposal costs ranging from \$0.57/barrel (\$3.59/ m^3) of water to over \$7/barrel (\$44/ m^3) of water, as shown in Table S3. Potential uses of PW for agriculture/irrigation, ASR, and mining were determined unfeasible in Oklahoma due to the cost, seasonality, and regulation challenges. Thus, these scenarios were excluded from the cost estimation [18].

In addition, the U.S. EPA’s report for PW management, “Final Report: Summary of Input on Oil and Gas Extraction Wastewater Management Practices Under the Clean Water Act”, was published in May 2020. The industry indicated that unless PW has TDS concentrations of less than a few thousand mg/L, treatment using membranes (e.g., reverse osmosis) or distillation would be necessary to generate water suitable for agricultural uses or discharge to surface waters. The cost of such treatment is not currently competitive, whereas other wastewater management options are available [17]. The key findings from the Oklahoma 2017 report include:

PW reuse by the O&G industry is the most viable, cost-effective alternative due to minimal water treatment needs and low treatment costs. Over time, expanding the water distribution systems would reduce conveyance costs and further facilitate PW use for HF. An increase in inter-organizational planning and sharing of resources to improve reuse viability is required.

The PWWG evaluated a particular case of using surplus PW from the Mississippi Lime play area around Alfalfa County. The surplus could be gathered and conveyed to Blaine County sites for O&G reuse. The analysis showed it has the potential to be financially competitive with the underground injection, although the project could be technically and commercially complex.

Water treatment and desalination techniques of PW should be further investigated and developed. For example, low-cost evaporation techniques should be developed that can potentially limit water conveyance and provide a viable alternative to disposal.

PW Regulations in Oklahoma

In December 2018, the Oklahoma Department of Environmental Quality (ODEQ) applied for authorization from the U.S. EPA to take over NPDES primary enforcement authority for certain wastewaters discharges, including PW. The application could give ODEQ the authorization to issue permits that would allow oil producers to dispose of oil field PW in above-ground waterways, and the application has been approved by the U.S. EPA.

In May 2020, Oklahoma Governor Kevin Stitt signed the “Oil and Gas Produced Water and Waste Recycling and Reuse Act” into law (S.B.1875), and it became effective on 1 November 2020. The Act designates who owns and is responsible for PW and waste from oil and natural gas drilling and production operations; it encourages PW recycling and reuses in Oklahoma by alleviating much of the uncertainty regarding ownership of PW, which will reduce freshwater demand and lower saltwater injection volumes.

Summary

Most of the PW was disposed of through deep well injection in Oklahoma because of the availability of freshwater and Class II disposal wells. However, the increased number of seismic events induced by HF and PW disposal raised concerns regarding PW management. In 2017, the final report, “Oklahoma Water for 2060 PW Reuse and Recycling”, was published. The report suggested that PW reuse in the O&G field is the most viable, cost-effective alternative, and evaporation techniques need further investigation and development. In 2020, the Oklahoma Governor signed the “Oil and Gas PW and Waste Recycling and Reuse Act” into law (S.B.1875). The Act designates who owns and is responsible for PW and waste from oil and natural gas drilling and production operations. It encourages the efforts of PW recycling and reuses in Oklahoma by alleviating much of the uncertainty regarding ownership of PW, which would reduce freshwater demand and lower saltwater injection volumes in the future.

3.1.3. Texas

PW Production, Disposal, and Management in Texas

Texas is a leader in oil production in the U.S. and a significant contributor to increasing gas supplies. It produced 1782 MMbbls of oil and 10 tcf of gas in 2020 [52]. The production areas in Texas are shown in Figure 3, including the Permian Basin in West Texas; the Anadarko Basin/Granite Wash and Palo Duro (or Bend) Basins in the Panhandle; the Barnett Shale in the Fort Worth Basin; the Western Gulf Coast Basin in southwest Texas (which includes the Eagle Ford Shale); and the historic East Texas Field, which contains the Haynesville–Bossier Shale [53].

The average water-to-oil ratio in Texas is estimated to be 7:1 [52]. In 2017, 9895 MMbbls ($1583 \times 10^6 \text{ m}^3$) of PW were generated in Texas, and PW was primarily managed through injection for EOR (46.1%) or disposal through SWD (36.2%). The Railroad Commission of Texas (RRC) and Texas Commission on Environmental Quality (TCEQ) were delegated the authority to regulate the UIC wells in 1982. Monthly reporting of volumes and pressures began in Texas on 1 January 1983. Over the decades, Texas has issued more than 54,700 permitted O&G injection and disposal wells, with approximately 34,200 currently active as of July 2015. Of these 34,200 active injection and disposal wells, about 8100 are wells that are used for disposal; the remainder (about 26,100) are injection wells [54].

Regulations on PW Discharge and Reuse in Texas

The data of current PW volumes for treatment, recycling, and reuse in Texas are variable and difficult to verify. Based on the IHS Markit, approximately 4–5% of PW is “treated and recycled” in the industry, and this number is expected to increase by nearly 16% over the next 4–5 years [55]. The 2019 Groundwater Protection Council report also provided PW reuse data for key basins across the US, showing that PW reuse is over 10% in the Permian Basin, but only 1% in the Eagle Ford Basin and negligible in the Haynesville Basin [33].

Statewide Rule 8 and Chapter 4, Subchapter B (Commercial Recycling), have been written and amended to encourage recycling in the oil field. The Commercial Recycling rules are divided into six separate divisions based on the type of O&G waste being treated, and the location and duration of the treatment operations. The Commercial Recycling rules focus on recycling drilling fluids and drilling muds for reuse in the well completion process, and recycling drilling solids for reuse as road base [56]. PW is regulated by Division 5 and 6. Off-Lease Fluid Recycling is limited to any location for a maximum of two years. The information must be submitted in the permit application, including but not limited to a diagram of the facility processing information, storage, and liner information. Stationary Fluid Recycling facilities are permitted for one location for up to five years. After five years, renewal of the permit may be requested [57].

The Texas legislature passed HB 3246 in May 2019 to address the recycling of fluid oil field waste (PW). The bill states that when fluid O&G waste is produced and used by or transferred to a person who takes possession of that waste for treating the waste for subsequent beneficial use, the waste is considered the property of the person who takes possession of it for treating the waste for subsequent beneficial use until the person transfers the waste or treated waste to another person for disposal or use. The legislation focuses on waste regulation and ensures that PW can be readily recycled by O&G operators and service companies unless otherwise expressly provided by a legally binding document.

Texas has over 100 facilities that provide waste treatment from O&G fields for storage, reclamation, treatment, or disposal of fluids or solid wastes transported to the facility. In 2018, only two facilities listed specifically handle “Fluids Recycling,” and they were both located in the RRC District (Midland) [53]. Large, centralized systems can treat large quantities of PW per day, thus providing an opportunity for PW treatment and reuse.

The treatment processes for PW depend on the application purpose. For subsequent fracturing operations, the treatment processes only include necessary chemical and mechanical treatment to eliminate oils and suspended solids, with the additional biocide or oxidizer to remove dissolved substances and biologics that may damage wells. Further treatment is necessary if the product water will be released into the environment. This additional treatment level may include the removal of organics, dissolved solids, and heavy metals [53].

Due to the existing federal NPDES requirements for onshore O&G operations in Texas, few discharges of PW are authorized. Any discharge would require both federal and state agency permits. In 2018, TCEQ issued a permit for PW discharges of onshore O&G operation (NPDES Permit No. TX0134061). These activities are subject to the Oil and Gas Extraction Point Source Category (40 CFR Part 435). Agricultural and Wildlife Water Use Subcategory allows the discharge of PW from facilities west of the 98th meridian for agricultural and wildlife propagation. To ensure that this discharge is of sufficient quality for livestock and wildlife water use, and, therefore, meets the requirements, some permits established a more stringent oil and grease limit of 10 mg/L monthly average, with a daily maximum limit of 15 mg/L. The limit is based on best professional judgment in accordance with 40 CFR 125.3(h) (1) and is consistent with other PW permits issued by other EPA regions. The EPA has established average monthly oil and grease limitations of 15 mg/L for these draft permits based on the region’s long-standing use of the 15 mg/L standards to represent the concentration at which a visible oil sheen is likely to occur [58]. The criterion for pH is between 6.5 and 9.0 for the water segment under Texas Administrative Code Title 30, Chapter 307. The prohibition of the discharge of floating solids or visible foam other than trace amounts is established in the

permit. In addition, there shall be no discharge of visible films of oil, globules of oil, grease, or solids in or on the water, or coatings on stream banks [59].

The 98th meridian bisects Texas into land roughly east or west of Dallas. Under the current federal regulatory scheme, onshore discharges east of the 98th meridian are typically not authorized. In the report by the Texas Alliance of Energy Producers and the Independent Petroleum Association of America, it is suggested, “Some may consider this division anachronistic and not reflective of the current technological advances in recycling nor the need for site-specific permit conditions independent of broad national controls” [53].

In May of 2019, the Texas legislature passed HB 2771, which transferred duties and authority to TCEQ upon NPDES delegation from the U.S. EPA, as opposed to the RRC, for issuing permits for the discharge of PW, hydrostatic test water, and gas plant effluent resulting from certain O&G activities. It also directs the TCEQ to submit a request to the U.S. EPA to seek federal NPDES delegation to Texas of these types of discharges, eliminating the duplication of federal and state oversight. On 15 January 2021, the U.S. EPA approved the request.

PW Reuse in Texas

The reuse of PW outside of Texas’s O&G sector is still in the research phase. A cotton-growing project was conducted in Pecos using recycled PW from nearby oil and natural gas activity in the Delaware Basin [60]. This project’s coalition included the RRC, Texas A&M AgriLife Research, and Anadarko Petroleum Corporation. This study evaluated cotton growth and yield response to irrigating with treated PW blended with groundwater (1:4 ratio), and investigated the effect of treated PW on soil chemical properties. The TDS concentration of groundwater was 3200 mg/L, and treated PW with 98 mg/L TDS concentration. After blending, the irrigation water had a TDS concentration of 2470 mg/L with sodium 766 mg/L, chloride 1450 mg/L, calcium 127 mg/L, magnesium 40 mg/L, and bicarbonate 122 mg/L. Boron concentration in the treated PW was 4 mg/L and diluted to 0.8 mg/L after blending with groundwater. The sodium adsorption ratio of the groundwater, treated PW, and blended water was 17.4, 4.9, and 15.2, respectively. The results suggested that irrigating with treated PW blended with groundwater did not reduce cotton yield or lint quality. In addition, compared to groundwater irrigation, the blended PW reduced soil salinity parameters, such as conductivity, sodium, and chloride. Further studies are still required for the agricultural reuse of PW.

To provide a new water source for beneficial use in Texas, House Bill 2545 [61] was introduced to incentivize water desalination by providing a franchise tax credit to desalination operators who treat high-salinity water. The proposed franchise tax credits are \$1 for every 1000 gallons ($\$0.26/\text{m}^3$) of source water treated by the permit holder if TDS is more than 3000 mg/L, and \$5 and \$17 per 1000 gallons ($\$1.32/\text{m}^3$ – $\$4.49/\text{m}^3$) if at least 50% of the source water is over 70,000, 90,000 mg/L TDS. The proposed franchise tax credit may then be transferred to another eligible tax liability for credit only after the original tax credit recipient has satisfied its qualified tax obligation(s). The tax credit recipient may carry forward its credit for five consecutive reports (i.e., six years). However, this bill did not pass in 2019.

In June 2021, the Texas Produced Water Consortium (TxPWC) was established by Senate Bill 601 to study the economics and technologies related to beneficial uses of PW, and provide guidance for establishing PW permitting, regulations, and rules to better enable the use of PW in Texas.

Summary

The large volume of PW generated in Texas is injected for EOR or disposed of through SWD. Statewide Rule 8 and Chapter 4, Subchapter B, Commercial Recycling, have been written and amended to encourage recycling of PW in the O&G field. The legislation was passed to amend the Natural Resources Code that specifies that a person will not be liable for a recycled product that has been transferred to another person with the contractual

understanding that the treated product will be used in connection with the drilling for, or production of, oil or gas.

Due to the existing federal NPDES requirements for onshore O&G operations, few PW discharges are authorized. In 2019, the Texas legislature passed HB 2771, which transferred duties and authority to TCEQ upon NPDES delegation from the U.S. EPA, as opposed to the RRC, for issuing permits for the discharge of PW resulting from certain O&G activities. In 2021, the EPA approved Texas' request to administer the NPDES program for PW discharges, hydrostatic test water, and gas plant effluent or O&G discharges within the state of Texas. In the same year 2021, the TxPWC was established to study the economics, technologies, and environmental and public health considerations related to the beneficial uses of PW, and to provide guidance for establishing PW permitting and regulations in Texas.

3.2. PW Management in the West of the 98th Meridian

The western U.S. has been under severe and chronic drought, and the water used for O&G well development aggravated the drought problem. The treatment and reuse of PW inside and outside of the O&G field would significantly benefit arid and semiarid regions in the west of the U.S. [12]. Based on the Oil and Gas Extraction Effluent Guidelines and Standards (40 CFR Part 435 Subpart E), the discharge of treated PW to surface water for agriculture or wildlife beneficial reuse is allowed in the west of the 98th meridian in the U.S., including California, Colorado, New Mexico, and Wyoming.

These western states are either using or working actively to investigate the feasibility of reusing PW outside of the O&G fields. Currently, PW reuse for agriculture is primarily occurring in California and Wyoming. PW reuse in California is predominantly in the San Joaquin Valley due to low salinity in PW; around 11% of PW was used outside of the O&G field in California, 2017 [13]. Research has proved that treated PW can be safely used for agriculture without harming crops [62]. PW generated from coalbed methane (CBM) in Wyoming usually has low salinity, and 37% was discharged to surface water in 2017 [13]. A lesser percentage (5.5%) of PW was reused outside of the O&G field in Colorado, 2017. The use of treated PW for agriculture is under active investigation in Colorado. However, some research found adverse effects of treated PW for the soil and plants [63–65]. These results suggested that more treatments and toxicity studies are required for PW before it can be used for irrigation; some advanced treatment methods, such as membrane-based techniques, are required. For New Mexico, approximately 10% of PW was reused inside the O&G field, and currently, there is no PW reused outside of the O&G field [66]. New Mexico regulatory agencies are working with academia, environmental groups, and the industry to find suitable methods to reuse treated PW outside of the O&G field [67].

Further, more regulation agencies are involved in monitoring PW quality and quantity in these western states compared to the eastern states because of the reuse potential of PW outside of the O&G field.

3.2.1. California

PW Production, Disposal, and Management in California

California ranked seventh among the U.S. for oil production and produced 144 MMbbls of oil and 0.17 tcf of gas in 2020 [34]. California has about 76,000 active O&G production wells; more than half are in Kern County, one of the top oil-producing counties in the U.S. [68].

California Geologic Energy Management Division [69,70] has primary responsibility for ensuring the safe and environmentally protective development and recovery of energy resources. Following the passage of Senate Bill 1281 in 2014 [71], the California water boards (the State Water Resources Control Board (SWRCB) and the nine Regional Water Quality Control Boards (RWQCB), including the Central Valley Regional Water Quality Control Board (CVRWQCB)) have been increasingly allocated the resources necessary to provide active water quality oversight related to oil production activities in California, thereby providing a clearer picture of PW management.

On average, California's O&G fields produce fifteen times as much water as oil [72]. In 2017, around 3100 MMbbls ($496 \times 10^6 \text{ m}^3$) of PW were generated in California. PW management in California can be classified as: (1) injection for EOR (59.3%); (2) underground injection for disposal (22.4%); (3) reuse outside of the O&G industry (10.0%); (4) reuse inside of the O&G industry (5.1%); (5) surface discharge and evaporation (1.1%) [13]. California has 1219 pits, of which, 587 are active; most of the pits (1062 total, 476 active) are in the Central Valley, primarily in Kern County.

PW Reuse for Agricultural Irrigation in California

In California, the SWRCB and the nine RWQCB are responsible for protecting California's waters. Among their many functions and duties, the SWRCB sets statewide policy, and the Regional Boards adopt Water Quality Control Plans or Basin Plans. According to the Waste Discharge Requirements General Order for oil field discharge to land, the PW discharge cannot exceed the Basin Plan's maximum salinity limits for electrical conductivity (EC, 1000 $\mu\text{mhos/cm}$), chloride (200 mg/L), and boron (1 mg/L) [73]. The RWQCB, including the CVRWQCB, have also been given the authority to gather additional information by requiring reporting of all additives used or supplied to operators who operate wells that supply treated PW for reuse within the region to further inform analysis of the practice (California Water Code §13267.5). Public concerns about using PW in agriculture have also prompted the CVRWQCB to establish a Food Safety Expert Panel consisting of academics, regulators, and consulting scientists to review the practice, assess risk, and make recommendations [74]. California regulators prohibited PW from fracking for irrigation; only PW from conventional oil drilling can be applied for irrigation [75,76].

As described in the "Final Report: Task 1" prepared by GSI International for the CVRWQCB [62], "from December 2017 through September 2018, CVRWQCB staff issued Orders under California Water Code sections 13267 and 13267.5 to oil companies and chemical manufacturers and distributors. These Orders required, under penalty of perjury, each recipient to submit the chemical make-up of additives used during petroleum exploration, production, and treatment at facilities that use PW for irrigation of crops for human consumption." The receipt of this data aided the preparation of a report by the Food Safety Expert Panel with the mission of preparing a report describing risks associated with the use of treated PW for the irrigation of edible crops, with a focus on crops irrigated in the Kern Sierran Foothills Subregion.

PW reuse in California is predominantly in the San Joaquin Valley due to low salinity in PW. The discharges of PW in this area are regulated by the Waste Discharge Requirements that conditionally allow the water to be used for irrigation and require monitoring. Examples of PW treatment in Kern County include mechanical separation, sedimentation, air floatation, and filtration (walnut hull vessels). These processes can remove and reduce petroleum hydrocarbons and other chemicals used during oil production activities before delivery to a water district. Another example of PW reuse is in the Arroyo Grande Oil Field [77]. The Arroyo Grande PW Reclamation Facility treats PW from a nearby oil field. The product water from the facility goes to irrigation use, whereas the unused treated water is discharged into nearby Pismo Creek, with volumes not to exceed 0.84 million gallons per day, according to an NPDES permit.

Risk Assessment of PW Reuse in California

Given California's severe and persistent drought, reclaimed PW is recognized as a viable water source for beneficial use that can be expanded to supplement surface and groundwater resources. Therefore, risk assessment tools should be applied to rapidly identify PW quality suitable for blending with other freshwater sources to be used as irrigation water. A study of PW in the Cawelo Water District near Bakersfield was conducted to evaluate whether chemical components found in the district's irrigation waterfall are within acceptable health and safety levels for its intended agricultural use. There were over 70 chemicals tested, including petroleum hydrocarbons, heavy metals, and radioisotopes. The results suggested

that all the tested 70 chemicals were found at concentrations well within drinking water standards, and do not threaten irrigated plants, food safety, or human health [78]. Risk assessment used to develop the risk-based comparison (RBC) evaluated the potential for human health effects from potential exposure to chemicals of interest (COIs) in crops because of deposition from irrigation water into the soil and subsequent uptake from the soil into plant tissues. According to the SWRCB, no studies to date have shown that irrigating food crops with reclaimed PW poses any threat to public health [78].

A recent report in 2020 from the CVRWQCB Food Safety Expert Panel presents the results of a human health risk assessment performed to establish RBC levels of COIs in irrigation water containing reclaimed PW [79]. To establish RBC levels, a screening process was conducted to identify COIs based on their potential toxicological significance, with other COIs added at the request of the state regulatory agency that approves the use of reclaimed PW for irrigation. The assessment derived the recommended RBC levels for blended irrigation water using the most stringent target risk thresholds applied by the U.S. EPA and the state regulatory agency: a theoretical upper-bound incremental cancer risk of 1×10^{-6} , which is 100 times lower than the upper end of the acceptable risk range applied by the U.S. EPA and other agencies. The recommended irrigation water RBC levels are listed in Table S4 (Original Report Table 15 [79]). Concentrations above the recommended RBC levels in irrigation water would warrant further assessment to determine whether they fall within the U.S. EPA and other agencies' acceptable risk range. Data available from the California RWQCB dataset in fall 2015 show that measured concentrations of the COIs in blended irrigation water are all below the recommended RBC levels, indicating that the crops (almonds, pistachios, citrus, grapes, potatoes, and carrots) are suitable for human consumption under the regulatory agency's recommended target risk thresholds [79].

The injection of PW from O&G activities into groundwater aquifers is in the process of being exempted in California. Independent scientific studies of HF and well stimulation in California reported a potential risk on groundwater quality in the San Joaquin Valley and the Los Angeles Basin [80–82]. It is suggested that the criteria from Underground Sources of Drinking Water in the EPA's UIC Program should be used as a baseline to protect fresh and brackish groundwater in all states [80,83].

In 2016, Shonkoff et al. evaluated the list of 173 chemicals reported as used in oil fields from which PW is deployed for irrigation, watering livestock, and recharging groundwater in the San Joaquin Valley of California [84]. In 2020, GSI Environmental Inc. conducted subsequent technical work under the oversight of the California CVRWQCB [85]. GSI reviewed 399 known chemical additives and naturally occurring chemicals in PW, and selected 143 COIs for further evaluation in the context of PW reuse in agriculture irrigation and other potential sources of these chemicals in the agricultural water supply. The report from GSI stated that there did not appear to be significant differences between blended irrigation water and known levels in other sources of surface or groundwater and other sources of these chemicals. The sampling and chemical analysis of all crops irrigated with PW in the Central Valley showed 30 analytes detected. Although there did not appear to be any evidence of a difference between treated and control samples that can be attributed to PW, there is a need to conduct more research to monitor and evaluate the long-term impact of using treated PW for agricultural uses regarding a full spectrum of organic, inorganic, and other chemicals of concern in plants, soil, wildlife, and groundwater.

Summary

California's O&G fields produce fifteen times as much water as oil. PW management can be classified into underground injection, EOR, reuse inside and outside of O&G fields, and surface discharge and evaporation. In California, only PW from conventional oil drilling is permitted for irrigation, and PW from fracking is prohibited for agricultural uses. A small portion of PW has been applied for local agricultural irrigation, primarily in the Kern Sierran Foothills Subregion. The discharges of PW to these districts are regulated by

the Waste Discharge Requirements that conditionally allow the water used for irrigation and require monitoring.

The CVRWQCB applied risk assessment tools to identify O&G fields with PW quality suitable for blending with irrigation water. A study suggested that the detected 70 chemicals were found at concentrations well within drinking water standards and were evaluated as not posing a threat to irrigated plants, food safety, or human health. Although some studies indicated that detected chemicals in PW might have potential risks for human health, the research result from GSI Environmental Inc. suggested that there did not appear to be any evidence of a difference between treated and control samples attributed to PW. However, more independent, third-party studies should be conducted to assure the safeness of the reuse of treated PW for irrigation.

3.2.2. Colorado

PW Production and Disposal in Colorado

Colorado ranked 7th in natural gas production, with the sixth-largest natural gas reserve and one-fourth of economically recoverable CBM reserves in the nation [34]. The state also holds nearly 4% of the nation's crude oil reserves, and 90% of the oil production was in the Niobrara Denver-Julesburg Basin in 2018 (Figure 3) [86]. Colorado's annual crude oil and gas production was 165 MMbbls and 2 tcf in 2020, respectively [34]. In 2017, Colorado generated 310 MMbbls ($49.6 \times 10^6 \text{ m}^3$) of PW, and around 32.5% was injected for EOR, 47.1% was disposed of by injection, 5.5% was discharged to surface water, 6.0% was disposed through evaporation, and 8.9% was reused within the O&G industry [13].

PW Regulations in Colorado

Colorado has a unique water rights system in the west, with its own water court system [87]. The management of the O&G industry involves multiple state agencies, including the Colorado Oil and Gas Conservation Commission (COGCC), the Colorado Division of Water Resources (CDWR), the Water Quality Control Commission (WQCC), and the Water Quality Control Division (WQCD). After passing the amended SB 19-181 in April 2019, local government control has been notably increased to regulate O&G development in Colorado, enabling the power of land-use authority to enact and manage more restrictive "necessary and reasonable" regulations than the state does within its jurisdiction.

According to the Colorado Oil and Gas Conservation Act, the COGCC is directed to "Regulate the development and production of the natural resources of oil and gas in the state of Colorado in a manner that protects public health, safety, and welfare, including protection of the environment and wildlife resources." Regulating O&G drilling, production, treatment, and disposal of waste (except commercial disposal facilities) falls into the jurisdiction of the COGCC. The COGCC has jurisdiction over permitting the Class II UIC wells (22 wells approved in 2019), pits (three pits approved in 2019), and non-commercial centralized waste management facilities accepting waste from the O&G field (two new approved and 54 active facilities in 2019) [88]. Pursuant to the Commission Rule 205A of COGCC, mineral developers must disclose chemical additives for HF to FracFocus, within 60 days after the conclusion of HF treatment and no more than 120 days after commencement.

The WQCC is responsible for implementing water quality classifications and standards for surface water and groundwater, and developing specific state water regulations and quality policies. The WQCD enforces such regulations, regulates discharge permitting, and provides oversight of commercial waste disposal facilities. Generally, the CDWR has jurisdiction over water rights (i.e., appropriation and distribution) adjudicated by the water courts and determination of their beneficial use. The construction of groundwater wells requires a permit from the CDWR to prevent pollution to state waters. The extraction of groundwater from CBM wells is considered beneficial and requires a permit from the CDWR, regardless of a tributary or non-tributary status. Subsequent beneficial use of extracted CBM water requires a well permit from the CDWR, justifying its appropriation of

a water right. The CDWR well-permitting of withdrawal and beneficial use of groundwater for CBM wells and non-CBM wells is exhibited in Table S5.

PW Management in Colorado

Mitigation of groundwater contamination. Spills of PW onto surface land have often been caused by equipment malfunction or human error [22]. The COGCC uses an electronic form-filling system, including a Spill/Release Report (Form 19), to collect spill incidents in Colorado. Operators shall, immediately upon discovery, control and contain all spills/releases of exploration and production waste, gas, or produced fluids. A spill of more than five barrels (0.79 m^3), regardless of whether it is within containment or outside of containment, and more than one barrel (0.16 m^3) spill out of secondary containment, shall be reported within 24 h after detection of the spill (CO CRS §34-60-130). Regarding spill/release prevention in Colorado, a secondary containment shall be installed around all PW tanks containing PW with TDS more than 3500 mg/L (CO CRS §34-60-603).

The evaluation of PW generation and PW spilled in Weld County demonstrated that the total surface of PW spill has a linear correlation with the scale of drilling production [89]. To understand and monitor potential groundwater contamination from drilling, mainly a result of surface spills and well casing failures [90,91], the COGCC sets concentration levels for both shallow (unconfined) and deep (confined) aquifers, along with the WQCC standards and classifications, to ensure compliance with groundwater standards (Table S6) and adjacent soils standards (Table S7).

Underground Injection Control (UIC). The COGCC, delegated by the U.S. EPA, has the authority to regulate Class II UIC wells by permitting and monitoring PW injection as “dedicated injection wells” for disposal or EOR. Thirty and twenty-two UIC well permits were issued in 2018 and 2019, respectively. The COGCC works closely with the WQCD to prevent groundwater contamination from UIC wells and, in union with the U.S. Geological Survey Earthquake Notification Service, to continuously monitor the potential local seismicity related to the PW injection. In 2017 and 2018, approximately 50% of PW was injected into Class II UIC wells either for disposal or EOR, and the percentage increased to 70% in 2019.

Dust Control. As industrial reuse of PW is generally viewed as a viable use in the Colorado Water Law system, the use of PW (TDS < 3500 mg/L and excluding flowback fluids) in dust and ice control, viewed as disposal, is allowed in the same geologic basin on operators’ lease roads without a permit, as long as it is from a non-tributary basin (CO CRS § 37-90-137). It is worth mentioning that the average TDS concentrations of CBM and the unconventional Niobrara Denver-Julesburg basin PW usually have TDS greater than 3500 mg/L, which is not suitable for land application or dust control. A relatively small amount of PW for dust suppression was reported in 2017 and 2018 on the O&G lease roads. The adjacent soil around the roads must meet the qualification requirements listed in Table S7 (CO CRS §34-60-910). Samples from comparable, nearby non-impacted native soil must be collected and analyzed for purposes of establishing background soil conditions, including pH and EC. Where the EC of the impacted soil exceeds 4 mS/cm or $2 \times$ background (Table S7), the sodium adsorption ratio (SAR) must also be determined.

Pits and surface water discharge. Most of the PW that is not injected through UIC wells is disposed of in pits through evaporation/percolation, with pretreatment to prevent crude oil and condensate from entering the properly permitted lined or unlined pit or surface discharge. Unlined pits have been restricted to a certain date (Rule 904a) and in certain conditions (Rule 902). Unlined pits shall not be constructed in areas where pathways for communication with groundwater or surface water are likely to exist, except as allowed under Rule 902. Permitting pits may be allowed on-site for various purposes, e.g., to contain drill cuttings and PW, and for reuse and recycling of PW. The COGCC is responsible for permitting (Form 15), monitoring and evaluation, and overseeing the closure of pits. New pit applications have significantly decreased (only two and three new approvals for 2018 and 2019, respectively), in coincidence with decreased O&G activities in areas with a

tradition of PW disposal using pits, and the adoption of “pitless” drilling and completion activities in Colorado.

PW may also be discharged into state surface water bodies under a Colorado Discharge Permit System (CDPS) under the jurisdiction of the WQCD, in accordance with the national 40 CFR 435 and 437 standards. The CDPS general permit COG-840000 covers only PW (from conventional and CBM production) discharge to surface waters from the Centralized Exploration and Production Waste Management Facility, used exclusively by one owner/operator or by more operators under an operating agreement, and the Commercial Disposal Facility (offsite). The numerical limitations and monitoring are determined on a site-specific basis. The effluent limits (numeric and narrative) are based on several guidelines, including the 40 CFR 435 standards, the water quality standards of the receiving water, site-specific review of the disposal facility information, the state’s basic standards and methodologies for surface water, and the WQCD’s policies and guidelines. The applicable numeric limits are either statewide or site-specific, including general parameters, organic compounds, metals, radionuclide parameters, and other pollutants that are applicable, whereas the narrative water quality limits are mainly for the protection of irrigated crops, livestock watering (TDS < 3500 mg/L), and aquatic life (Whole Effluent Toxicity testing). *Reuse of PW outside of the O&G fields.* PW has been widely reused inside the O&G fields in Colorado, including for EOR and drilling. The CDWR has jurisdiction over appropriations of water for various beneficial uses. The first beneficial reuse of PW outside of the O&G field was reported in Wellington [92]. The treated PW was used to augment the shallow aquifer to ensure adequate drinking water resources for a nearby city. Three major steps were required to secure the water right of PW reuse: (1) obtain a beneficial use permit from the CDWR (confirmed PW as non-tributary in this case); (2) pass preliminary effluent limit determination for surface discharge in WQCD, and obtain a discharge permit from the COGCC; and (3) obtain a vested water right from the water court.

Though using PW for irrigation purposes has not been adopted in Colorado, studies assessing such feasibility have been investigated [93]. A study investigated the utility and feasibility of treated PW from the Niobrara Denver-Julesburg basin as irrigation water for salt-tolerant crops, e.g., switchgrass and rapeseed. The results showed that treated PW with TDS < 3500 mg/L and relatively low organic content are necessary to maintain biomass yield and plant health [94].

Summary

The COGCC, WQCC, WQCD, and CDWR shared jurisdiction with local governments for the management of PW in Colorado. Groundwater contamination associated with PW is a primary environmental concern in Colorado, with its monitoring and mitigation administrated by the COGCC. The disposal of PW occurs primarily through Class II UIC well injection, pits, and surface discharge, plus a small fraction for dust suppression applied on the O&G lease roads. Colorado recognizes the reuse of PW as a viable beneficial use, e.g., aquifer recharge. Currently, the application of PW for agricultural irrigation is under active investigation.

3.2.3. Wyoming

CBM PW Production in Wyoming

Wyoming is in a semiarid climate and occasionally experiences water shortage in some areas affected by the current drought cycle. Wyoming’s annual crude oil and gas production was 89 MMbbls and 1.4 tcf in 2020, respectively [34]. CBM wells are treated separately from conventional natural gas production. According to the Wyoming State Geological Survey, the total recoverable CBM resources are estimated at 31.7 tcf, equal to one-third of the total recoverable CBM resources in the U.S. [95]. PW from coal seams has been a vital groundwater resource suitable for beneficial reuse. The relatively low TDS content of the CBM PW in Wyoming often enables subsequent discharge into surface streams or beneficial reuse, such as agricultural irrigation, aquifer recharge, and land application.

In 2017, 1700 MMbbls ($272 \times 10^6 \text{ m}^3$) of PW were generated in Wyoming, and 46% was injected for EOR, 14% was injected for disposal, 37% was discharged to surface water, and the rest was managed by evaporation or offsite commercial disposal [13].

CBM PW Regulations in Wyoming

The O&G industry is under the oversight of the Wyoming Oil and Gas Conservation Commission (WOGCC). The WOGCC holds the authority to regulate drilling and plugging wells to protect O&G formation from water intrusion, prevent contamination of freshwater resources, and regulate PW containment, storage, treatment, and disposal inside O&G fields. In Wyoming statutes, PW includes formation water from the O&G reservoir, injected water, and any chemical additives added during the production and treatment process.

The Wyoming State Engineer's Office (WSEO) supervises the allocation of water resources (quantity). The CBM PW has been designated as a beneficial use of groundwater in Wyoming for decades, and follows the same application process for groundwater within the jurisdiction of WSEO to appropriate the groundwater, in conjunction with a permit from the WOGCC for CBM production. The WSEO must approve the application for a Permit to Appropriate Ground Water (Form U.W.5) before drilling any CBM well. It details specific management scenarios of CBM PW when it is further used as a direct source for another beneficial use, such as water production for CBM only (no additional permit required); for stock watering; for discharge into surface reservoir directly; for O&G well drilling and stimulation/enhancement, dust control, and compaction; for industrial processes; for irrigation; and for aquifer and recovery wells. If not proposed for further beneficial use by any developer, CBM PW is considered as surface supply (i.e., discharge to surface or to new/existing reservoir), and is governed by laws about surface water, which requires additional permitting requirements from the WSEO Surface Water Division. Once CBM PW becomes the water of the state (passed an NPDES discharge point), no permit is required for land applications.

The Wyoming Department of Environmental Quality (WDEQ) also participates in the discharge and use of all PW (quality). A discharge permit from WDEQ is required for the O&G production facility to meet specific standards and requirements. Moreover, the discharge of treated PW must comply with the U.S. EPA effluent guidelines and NPDES standards. After the discharge point, treated PW is considered the property of the state. In the western states, the split of property regimes is common, where land ownership (surface) and estate minerals (underlying) belong to separate entities [96,97], which expands the number of stakeholders involved during O&G development [98]. A legal contract including a description of surface use and damage agreements is required in Wyoming between the surface owner and mineral developer, which highlights the prominent role of landowners during O&G activities [98].

Only Colorado and Wyoming in the Rocky Mountain states require water rights for CBM production. The water rights system in Wyoming focuses on permitting to protect prior appropriation (ensuring senior water rights are not interfered with by CBM PW production). It allows simple disposal for O&G producers once the water reaches the surface [99], whereas further beneficial use of CBM PW or reservation/storage for future use is viewed as a disposal option for producers, and has been a challenge. In doing so, most of the PW extracted has been wasted/disposed of after CBM production, which, if appropriately reused, could preserve household and livestock well capacities for future beneficial use [100].

CBM PW Management and Reuse in Wyoming

The quality of CBM PW in the PRB declines from the south and east basin edges, with water quality close to drinking water level and EC and SAR suitable for irrigation. The west and north regions have relatively low water quality, including one or more water quality parameters exceeding reuse standards (e.g., TDS for drinking, EC for irrigation of sensitive

plants, and SAR for irrigation) [95,101]. In practice, surface discharge and irrigation are executed in eastern PRB.

Surface water discharge. The discharge of CBM PW into surface streams is allowed in Wyoming as long as it bears “good enough quality” for watering livestock or wildlife. Effluent limits are required for CBM PW surface discharge to protect livestock and wildlife consumption, including chloride 2000 mg/L, sulfate 3000 mg/L, specific conductance 7500 $\mu\text{S}/\text{cm}$, oil and grease 10 mg/L, pH 6.5–9.0, and total recoverable radium 226 of 60 pCi/L.

The WDEQ can grant a temporary surface discharge of CBM PW under two conditions: less than a six-month discharge (additional one-time six-months extension/renewal) into a reservoir for livestock watering, as emergency water to livestock; or a 15-day discharge permit for CBM PW characterization, which must occur greater than 0.5 miles from a perennial water body with a discharge rate less than 0.5 cubic feet per second. The effluent limits include 1000 $\mu\text{g}/\text{L}$ dissolved iron, pH 6.5–9, chloride 2000 mg/L, total recoverable arsenic 150 $\mu\text{g}/\text{L}$, and specific conductivity 7500 $\mu\text{S}/\text{cm}$.

Groundwater injection. The CBM PW can be injected into shallow aquifers bearing $\text{TDS} < 10,000 \text{ mg}/\text{L}$ or $< 5000 \text{ mg}/\text{L}$ through UIC Class V wells by mineral developers administered by the WDEQ. Rules and regulations in chapter sixteen of the Wyoming Water Quality Division must be met to obtain the injection permit to construct and operate a CBM PW injection well. The injection is not common in the PRB due to the complex management of multiple producing zones and numerous mineral developers [102], except in the city of Gillette, which uses CBM PW for partial replenishment of the city’s potable water resource [103].

Dust control and road application. Although no permit was required under the NPDES program for the application of CBM PW for dust control, approval from the WOGCC must be obtained. CBM PW spreading on roads for dust control is usually mixed with magnesium chloride. In addition, dust control activities on public lands must comply with applicable Bureau of Land Management requirements and local government requirements.

WDEQ also stated that “When no other alternative is reasonably available for disposal of limited quantities of wastewater or exploration and production exempt oily wastes, a Road Application of Waste or Wastewater permit may be requested.” The water quality analysis of PW and PW-contaminated soils includes radium 226, benzene, TDS, arsenic, total metals, and other constituents determined to be appropriate by the WOGCC (Table S8).

Irrigation. Due to the continuous drought in the PRB, irrigation using CBM PW is encouraged. Most of the CBM PW directly used for agricultural irrigation does not satisfy sustainability criteria for irrigation water, and, therefore, a managed irrigation system is required [104]. Table S9 summarizes the scenarios of CBM PW used for irrigation in Wyoming.

The WDEQ has set up a permitting guideline in the PRB for the discharge of CBM PW to irrigated lands under different scenarios. SAR and salinity are the primary concerns, particularly for the ephemeral channel (SAR limit 3–10) (Table S9). Scenario 3 in Table S9 provides guidelines for ephemeral streams that previously conveyed flood irrigation water that leached salts out of the soil. Turning an ephemeral stream into a perennial stream by CBM PW discharge may adversely affect the soil and plants (i.e., salt mobilization from poor quality soil, bank erosion, disruption to the existing ecosystem) [99]. A significant increase in EC, SAR, and exchangeable sodium percent was reported in fine-textured soil after 1~4 years of irrigation of CBM PW [105]. Therefore, the EC threshold is calculated by dividing the median value tested or the published soil EC threshold value by 1.5 (Table S9).

CBM PW treatment and soil amendment are general approaches for the managed irrigation system, e.g., lowering Na^+ content, SAR, and alkalinity in CBM water; application of gypsum (exchange Na^+) and sulfur (alkalinity reduction) to soil [106]. Gypsum can increase Ca^{2+} content in the soil system, competing for exchange sites on a clay surface, with Na^+ to be leached out by flooding and irrigation events [107]. The application of elemental sulfur can decrease the soil pH and promote the dissolution of calcite to release Ca^{2+} .

Land application. A land application permit is required for each site, along with the landowner’s approval in Wyoming. The land application of CBM PW was reported to

increase forage production and enhance recharging shallow groundwater aquifers [102]. However, multi-year direct land application of CBM PW can alter soil characteristics with a continuous increase of soil EC and SAR, and decrease native plant species [108,109]. The biological effects of CBM PW land applications were complex and site-specific, indicating site-specific management approaches for land applications.

The previous land application permits focused on general water chemistry and inorganic constituents. The new permit (WDEQ Permit No. 19-283, issued to Encore Green, LLC, 2020), although specified for treated PW in Laramie County outside of PRB, signified a much more stringent trend, including a numeric limit on a total of 159 water constituents the treated PW shall not exceed before land applications: general, inorganic, and radionuclides (43); volatile organic compounds, semi-volatile organic compounds, and polyaromatic hydrocarbons (91); and pesticides (25). The new permit for land application in Wyoming added a substantial number of organic contaminants. The details of the constituents and permitted range/limit are summarized in Table S10.

Impoundment. The practice of impoundment is for the disposal of CBM PW through infiltration and evaporation, not genuinely constituting beneficial use [99], except occasionally for livestock watering. Impoundment must be approved by WOGCC and WDEQ; the CBM PW quality is regulated by the WDEQ's Wyoming Pollutant Discharge Elimination System. The potential pollution of groundwater has been identified due to unlined infiltration impoundment of CBM PW in Wyoming, primarily due to the infiltrating water acting as a solvent to leach constituents (e.g., sulfate salts, selenium) in the subsurface and transporting them into groundwater [95,110].

Summary

In the PRB, several management options have been executed, including impoundment, surface discharge, aquifer injection, road spreading, irrigation, and land application. The discharge of CBM PW into surface streams is allowed in Wyoming. The CBM PW can be injected into shallow aquifers through Class V wells, and no permit is required for road spreading. The direct use of CBM PW for irrigation may result in soil salinity and sodicity. The feasibility of using CBM PW for managed irrigation has been demonstrated with appropriate soil physical/chemical amendments. The direct land application of CBM PW does not meet irrigation water sustainability criteria and requires water, soil, and plant management. The new land application permit in Wyoming contains much more stringent requirements with a substantial number of water constituents.

The management of PW is three-fold in Wyoming, with WOGCC regulating activities inside the O&G field, the WSEO supervising appropriation and distribution (quantity), and the WDEQ managing the discharge and use of PW (quality).

3.2.4. New Mexico

PW Production, Disposal, and Management in New Mexico

New Mexico (NM) has more than 7% and 5% of the nation's proved crude oil reserves and natural gas reserves, respectively. It is the second-largest onshore oil-producing state and accounted for more than 9% of the nation's crude oil production [111]. In 2020, the total oil production of NM reached 380 MMbbls, which has increased more than five-fold since 2009 (61 MMbbls). In 2020, NM was the eighth-largest gas-producing state and produced more than 2.0 trillion cubic feet or about 5% of the U.S. gross withdrawals of natural gas [111]. The Permian Basin, located in the eastern NM and western Texas (Figure 3), is one of the most prolific petroleum-producing areas in the U.S. and the world [112].

Advanced drilling and oil recovery technologies have increased oil production in the Permian Basin. However, the large amount of water used for HF, along with the large volumes of PW generated during well production, has brought concerns in NM, a semiarid state that suffers from chronic droughts and water shortage [113]. It is estimated that up to 10 million gallons (38,000 m³) of water may be needed to frack one well, depending on several factors, such as its location, well type, and the operator [114,115]. In NM, freshwater

comes from either surface water or groundwater, e.g., the Pecos River and Ogallala Aquifer in the Permian Basin. In order to reduce stress on NM's water resources due to O&G production, effective on 13 October 2020, OCD Rule 19.15.16.19(B) requires that producers shall disclose water use (quantity for PW, freshwater, brackish water, and saline water) to the OCD within 45 days after completion, recompletion, or other HF of a well. According to the OCD Water Use Report Summary, as of 30 December 2021, the average freshwater use for HF was reduced from 20% in 2020 to 10% in 2021.

In the Permian Basin, three to four times of PW may be generated for every barrel of oil produced. In 2019, about 1203 MMbbls ($191 \times 10^6 \text{ m}^3$) and 37 MMbbls ($5.9 \times 10^6 \text{ m}^3$) of PW were generated in the NM Permian Basin and San Juan Basin, respectively [115,116]. However, in 2019, only about 10% of all PW generated in NM was being reused or recycled in O&G operations; eventually, all PW was treated as wastewater and was discharged through permitted UIC wells for EOR or disposal by SWD wells [117]. No PW has been permitted for use outside of O&G production activities in NM. With continued O&G development, underground disposal practices are not sustainable and have been linked to other environmental challenges (e.g., seismicity activities) [14]. Because freshwater supplies are dwindling, the reuse of the billions of gallons of treated PW may significantly benefit arid regions such as NM. One key factor that affects treated PW reuse is its quality, such as TDS, pH, organic contaminants, metals, naturally occurring radioactive material (NORM), chemicals added during HF, and toxicity [4]. The average TDS concentration varies based on the location and place, but is typically about 100,000–120,000 mg/L.

Produced Water Regulation in New Mexico

Under the Oil and Gas Act (Chapter 70 NMSA 1978), the Oil Conservation Division (OCD) within the Energy, Minerals and Natural Resources Department (EMNRD) regulates the handling and disposal of PW within the O&G industry in NM. This includes UIC wells for PW disposal, reuse through enhanced recovery operations, and recycling and reuse in O&G drilling operations. The OCD encourages the recycling and reuse of PW within the O&G industry by specifically exempting from permitting the disposition of PW for use in “drilling, completion, producing, secondary recovery, pressure maintenance or plugging of wells.”

New Mexico House Bill 546 (HB 546), which includes the Produced Water Act, went into effect on 1 July 2019. PW is defined in the Produced Water Act as “fluid that is an incidental byproduct from drilling for or the production of oil and gas.” The Produced Water Act addresses the reuse and recycling of PW and establishes that no water right is created from PW. “Recycled produced water” is defined as “produced water that is reconditioned by a recycling facility permitted by the oil conservation division of the energy, minerals and natural resources department.” PW recycling within the O&G industry reduces the use of freshwater for O&G applications. A key provision of HB 546 is that it removes obstacles related to the recycling of PW in NW, and encourages recycling by the industry while minimizing freshwater usage. Therefore, NM expects the volumes of PW recycled for oil production will increase in the coming years. The Produced Water Act also specifically directs the Water Quality Control Commission (WQCC) to “adopt regulations to be administered by the department of environment for the discharge, handling, transport, storage, recycling or treatment for the disposition of treated PW, including disposition in road construction maintenance, roadway ice or dust control or other construction, or in the application of treated PW to land, for activities unrelated to the exploration, drilling, production, treatment or refinement of oil or gas.” The Act provides that the WQCC “may adopt regulations to be administered by the department of environment for surface water discharges.”

Surface water discharges are currently regulated through EPA Region 6, and state-certified by the New Mexico Environment Department (NMED)'s Surface Water Quality Bureau because NM does not yet have primacy over the NPDES program. NMED's Ground Water Quality Bureau issues and manages discharge permits that have the potential to impact groundwater. The Office of the State Engineer (OSE) has no authority over PW, and no water right shall be established by the disposition of PW, recycled PW, or treated PW.

All PW that is produced from an O&G well is the responsibility of and under the control of the working interest owners and operators. However, a transferee shall have control of and responsibility for the PW when it is transferred, sold, or conveyed. Thus, the control of and responsibility of PW transfers with PW.

Implementation of Produced Water Act in New Mexico

To collect input from the public on the Produced Water Act, in the fall of 2019, NMED initiated and conducted public engagement activities across NM in coordination with EMNRD and OSE. The collected input is used to inform future regulatory and research efforts related to NMED's authority to regulate the treatment and use of PW outside of the O&G industry. In total, NMED generated a public input catalog containing 2296 statements. The public concern or opinion is roughly split between regulation needs (59%) and research needs (41%). Most input (56%) generally expressed concern regarding the unknowns surrounding PW use outside of O&G. The remaining (44%) either expressed direct support (6%) or opposition (38%) to one or more PW topics [66].

The level of treatment necessary to protect human health and the environment depends upon the intended end use of the treated PW. Emerging technologies to effectively treat PW are potentially making the PW reuse inside and outside of the O&G industry possible with targeted research and regulation. "Fit for purpose" research to support future regulations will address the range of factors that vary based on the end-use. In 2019, NMED and New Mexico State University (NMSU) launched the New Mexico Produced Water Research Consortium (NMPWRC) to assist the state in filling scientific and technical knowledge gaps necessary to establish regulations and policies for the treatment and reuse of treated PW. The NMPWRC leads an extensive research program to explore desalination and other technologies needed to adequately treat PW for potential fit-for-purpose reuse; characterize physical, chemical, and biological properties of PW and treated PW; assess the technical, societal, environmental, and economic effects of the use of treated PW, including risks and toxicity to public health and the environment; and develop public outreach and education programs to improve the public understanding of the potential impacts of using treated PW on public and environmental health and safety.

Summary

Currently, most of the PW was disposed of through deep well injection in NM, and no PW has been permitted for use outside of O&G production activities. However, to encourage the O&G industry to reuse and recycle the PW instead of relying on limited freshwater resources, the Produced Water Act was passed in 2019. The Produced Water Act clarified ambiguity regarding jurisdiction over PW reuse, and assigned it clearly to OCD when inside the O&G industry. The Act also clarified that the use of treated PW outside of the O&G industry is subject to the state Water Quality Act and must comply with the WQCC regulations administered by the NMED. The responsibility and liability for PW go with the water when it is transferred, and PW does not come with, nor does it affect, water rights. The NMPWRC was established to promote scientific research to fill scientific and technical knowledge gaps, necessary to develop regulations and policies for the treatment and reuse of PW.

4. Conclusions and Perspectives

This study analyzes the current regulatory framework for PW production, management, and reuse in the major oil and gas production areas in the U.S., including Appalachian Basin, California, Colorado, New Mexico, Oklahoma, Texas, and Wyoming. Most of the PW is injected either for EOR or by disposal wells. States in the east of the 98th meridian reuse more PW inside of the O&G fields due to the current U.S. EPA regulations. States in the west of the 98th meridian have been planning to reuse treated PW outside of the O&G fields because of the droughts and the exemptions from U.S. EPA regulations. Different states may need to develop their own regulations pertinent to their unique geographic locations, state-specific

practices and laws, and the differences between the PW quality and quantity. This review summarizes the PW regulations, examples of PW reuse practices, water quality standards, and risk assessment studies in different states, which can be used as guidelines and support regulatory development for other states or countries with proper modifications.

Recently, more regulations on PW management and reuse have been established by state regulators. Pennsylvania renewed the General Permit WMGR123 in 2021 to guide the reuse of PW inside the O&G field. The Oklahoma Governor signed the “Oil and Gas PW and Waste Recycling and Reuse Act” into law (S.B.1875) in 2020. The Act encourages the efforts of PW recycling and reuses in Oklahoma by alleviating much of the uncertainty regarding ownership of PW, which would reduce freshwater demand and lower saltwater injection volumes. In 2021, the U.S. EPA approved Texas’ request to administer the NPDES program for PW discharges within the state of Texas, and the Texas legislature passed HB 2771, which transferred duties and authority to TCEQ upon NPDES delegation from the U.S. EPA for issuing permits for the discharge of PW in 2019. NM passed HB 546 in 2019 to encourage the treatment, reuse, and recycling of treated PW within and outside of O&G fields.

Reuse of treated PW for agriculture mainly happens in California and Wyoming because of the “good” quality of the PW. Research from California suggested that the treated PW with high quality or after blending can be used for irrigation. Colorado recognizes the reuse of treated PW as a viable beneficial use, e.g., aquifer recharge. Currently, most of the PW was disposed of through deep well injection in NM, and no PW has been permitted for use outside of O&G production activities due to a lack of understanding of the risks associated with the reuse of treated PW. The NMPWRC was established to promote scientific research to inform future regulations and policies. A report from Wyoming demonstrated the feasibility of using CBM PW for managed irrigation with appropriate soil physical/chemical amendments. The feasibility of reusing treated PW for irrigation in Colorado, New Mexico, and Texas is under intensive investigation.

The treatment effectiveness for removing the chemical constituents in PW needs to be demonstrated to protect the environment and public health during beneficial use. Because of varying levels of oil residues, salts, suspended solids, petroleum hydrocarbons, metals, NORM, and other chemicals and potential toxins, PW must be treated to meet the water quality requirements for fit-for-purpose uses. There are many PW pre-treatment and treatment processes available that include modular and scalable components [118,119]. However, current treatment technologies are often not cost-competitive as compared to the options of SWD well disposal or water reuse for HF. Advancements in water treatment technology can create new and more cost-effective, energy-efficient opportunities to treat and reuse PW, such as using innovative, high-performance materials and technologies; selective removal and separation of constituents of concern; and the use of renewable energy and waste heat to reduce energy consumption and greenhouse gas emissions [120–123]. In addition, technologies are needed to achieve zero-waste-disposal and support the extraction or recovery of specific minerals in PW or treatment residuals as commodities [124,125].

A significant concern of reusing treated PW is the chemical additives put down wells during fracturing. Many chemical products are protected by patents that result in restrictions on the manufacturer providing useful information regarding the chemical formulation of the product. As manufacturers are unwilling to reveal key details about the chemical additives due to trade secrets, it makes it difficult to identify these chemicals and assess their associated risks during reuse. For risks and toxicology assessment, it is imperative that the chemical additives be disclosed, as well as the volume and frequency of their use. The CVRWQCB worked around this restriction by making it clear that O&G operations must disclose the chemical formulation if they were to receive a permit for discharging PW thereby providing the incentive to manufacturers for disclosing of product formulations. However, this was only accomplished with the CVRWQCB agreeing that they would review the formulations but that they also would maintain confidential any information regarding the formulation. This is an important issue that needs to be addressed by a standardized practice that will provide the required information to

regulators and for risk assessment but also will protect the economic interests of the party holding the product formulation patent, most likely the manufacturer.

It is also critical to investigate the chemicals' breakdown products during fracking. Chemicals are injected under high temperature and pressure into oil and gas reservoirs, where they interact with other compounds in the formation and may be transformed into other types of chemical constituents. Up to date, there are limited studies and no established tools to monitor these unknown transformation compounds and understand the toxicity effects of the chemical interactions during reuse applications. Currently, researchers and the industry are identifying greener chemical additives in HF and minimizing the use of chemicals with less-desirable environmental, safety, and health concerns. However, the proposed alternative chemicals also need to be evaluated regarding their potential impacts on public health and environmental risks, the efficacy and compatibility with other naturally occurring formation chemistries, operating conditions, as well as commercial availability and costs [126].

The U.S. EPA has developed the National Water Reuse Action Plan (WRAP) to support water security, sustainability, and resilience. Actions in the plan are intended to drive progress on reuse and address local and national barriers across a range of topics, including technical, institutional, and financial. To address the challenges of reusing treated PW outside of oil and gas fields, the U.S. EPA, in collaboration with partners in academia, state agencies, and the industry, leads a national program to study the safety of PW and develop cutting-edge analytical methods for evaluating the complex mixtures of contaminants, and for predicting the potential toxicological effects of PW and treated PW intended for reuse. The study includes targeted and nontargeted chemical analysis to identify the constituents and correlate molecular targets to identified chemical constituents using gene expression biomarkers and comparison with known targets examined in human cell lines. The study aims to fill the knowledge gaps in detecting and assessing risks to human and ecological health caused by chemicals in PW, and help identify fit-for-purpose reuse options outside of the oilfield. The program will provide valuable information and data to inform future permitting requirements by understanding the chemicals present and potential risks during reuse applications.

The reuse of PW inside and outside of the O&G fields would benefit society and the environment. However, the risks associated with reusing treated PW still require intensive research. Given PW is a new, non-traditional water source, and the water chemistry is complex with naturally occurring constituents and chemical additions during the well stimulation process, water quality standards for different reuse applications should consider the known and unknown chemicals and toxicological characteristics of PW and treated PW. Intensive research is needed to provide scientific and technical knowledge to establish science-based regulations and develop well-informed permitting programs for the safe reuse of treated PW outside of the O&G fields.

Supplementary Materials: The following supporting information can be downloaded at: <https://www.mdpi.com/article/10.3390/w14142162/s1>, Table S1: General Permit WMGR123 Appendix A (39 constituents) from Pennsylvania; Table S2: Alternative screening matrix for the produced water reuse in Oklahoma, prepared by the Produced Water Working Group; Table S3: Cost estimates for ten produced water use scenarios in Oklahoma, prepared by the Produced Water Working Group; Table S4: Recommended Irrigation Water Risk-Based Comparison (RBC) Levels (mg/L) in California; Table S5: Oil and Gas wells permitting in Colorado Division of Water Resources; Table S6: Groundwater standards in Colorado; Table S7: Soil quality criteria for road spreading of produced water in Colorado; Table S8: Regulatory guidelines for road application of waste and wastewater in Wyoming; Table S9: CBM permitting guideline for discharges to irrigated drainages of the Powder River Basin, Wyoming; Table S10. Wyoming Department of Environmental Quality parameter list for produced water for beneficial use for land application.

Author Contributions: Conceptualization, methodology, formal analysis, investigation, resources, writing—original draft preparation, writing—review and editing, W.J., L.L., X.X., H.W. and P.X.;

supervision and project administration, P.X. All authors have read and agreed to the published version of the manuscript.

Funding: The research was supported by the New Mexico Produced Water Research Consortium.

Data Availability Statement: Not applicable.

Acknowledgments: The authors acknowledge the New Mexico Produced Water Research Consortium and the New Mexico Environment Department for supporting this study and providing technical reviews of the case studies. The authors are also grateful to Karl Longley with Fresno State University for preparing and reviewing the California case study.

Conflicts of Interest: The authors declare no conflict of interest.

References

- Nicot, J.-P.; Scanlon, B.R. Water use for shale-gas production in Texas, US. *Environ. Sci. Technol.* **2012**, *46*, 3580–3586. [CrossRef] [PubMed]
- Khan, N.A.; Engle, M.; Dungan, B.; Holguin, F.O.; Xu, P.; Carroll, K.C. Volatile-organic molecular characterization of shale-oil produced water from the Permian Basin. *Chemosphere* **2016**, *148*, 126–136. [CrossRef] [PubMed]
- Jiang, W.; Lin, L.; Xu, X.; Cheng, X.; Zhang, Y.; Hall, R.; Xu, P. A Critical Review of Analytical Methods for Comprehensive Characterization of Produced Water. *Water* **2021**, *13*, 183. [CrossRef]
- Hu, L.; Jiang, W.; Xu, X.; Wang, H.; Carroll, K.C.; Xu, P.; Zhang, Y. Toxicological characterization of produced water from the Permian Basin. *Sci. Total Environ.* **2022**, *815*, 152943. [CrossRef]
- Jiang, W.; Xu, X.; Hall, R.; Zhang, Y.; Carroll, K.C.; Ramos, F.; Engle, M.A.; Lin, L.; Wang, H.; Sayer, M. Characterization of produced water and surrounding surface water in the Permian Basin, the United States. *J. Hazard. Mater.* **2022**, *430*, 128409. [CrossRef]
- Sun, C.; Zhang, Y.; Alessi, D.S.; Martin, J.W. Nontarget profiling of organic compounds in a temporal series of hydraulic fracturing flowback and produced waters. *Environ. Int.* **2019**, *131*, 104944. [CrossRef]
- U.S. EPA. Class II Oil and Gas Related Injection Wells. Available online: <https://www.epa.gov/uic/class-ii-oil-and-gas-related-injection-wells> (accessed on 18 June 2021).
- IHS Markit. Produced Water from Onshore US Oil and Gas Activities to Decline to Nearly 20 Billion Barrels Annually; Reach \$28 Billion in Value by 2022, IHS Markit Says. Available online: https://news.ihsmarket.com/prviewer/release_only/slug/2020-04-02-produced-water-from-onshore-us-oil-and-gas-activities-to-decline-to-nearly-20-billion-barrels-annually-reach-28-billion-in-value-by-2022-ihs-market-says (accessed on 10 February 2021).
- Zhong, C.; Zolfaghari, A.; Hou, D.; Goss, G.G.; Lanoil, B.D.; Gehman, J.; Tsang, D.C.; He, Y.; Alessi, D.S. Comparison of the hydraulic fracturing water cycle in China and North America: A critical review. *Environ. Sci. Technol.* **2021**, *55*, 7167–7185. [CrossRef]
- Chang, H.; Li, T.; Liu, B.; Vidic, R.D.; Elimelech, M.; Crittenden, J.C. Potential and implemented membrane-based technologies for the treatment and reuse of flowback and produced water from shale gas and oil plays: A review. *Desalination* **2019**, *455*, 34–57. [CrossRef]
- U.S. EPA. Summary of Input on Oil and Gas Extraction Wastewater Management Practices Under the Clean Water Act Final Report. 2020. Available online: <https://www.epa.gov/eg/summary-input-oil-and-gas-extraction-wastewater-management-practices-under-clean-water-act-final> (accessed on 7 April 2021).
- Jiang, W.; Pokharel, B.; Lin, L.; Cao, H.; Carroll, K.C.; Zhang, Y.; Galdeano, C.; Musale, D.A.; Ghurye, G.L.; Xu, P. Analysis and prediction of produced water quantity and quality in the Permian Basin using machine learning techniques. *Sci. Total Environ.* **2021**, 149693. [CrossRef]
- Veil, J.U.S. Produced Water Volumes and Management Practices in 2017. Available online: http://www.veilenvironmental.com/publications/pw/pw_report_2017_final.pdf (accessed on 12 August 2021).
- Skoumal, R.J.; Ries, R.; Brudzinski, M.R.; Barbour, A.J.; Currie, B.S. Earthquakes induced by hydraulic fracturing are pervasive in Oklahoma. *J. Geophys. Res. Solid Earth* **2018**, *123*, 10,918–910,935. [CrossRef]
- Reig, P.; Luo, T.; Proctor, J.N. Global Shale Gas Development: Water Availability & Business Risks; World Resources Institute. 2014. Available online: <https://www.wri.org/research/global-shale-gas-development-water-availability-business-risks#:~:text=This%20report%20reveals%20that%20lack,extremely%20high%20seasonal%20variability%3B%20and> (accessed on 12 July 2021).
- Scanlon, B.R.; Reedy, R.C.; Xu, P.; Engle, M.; Nicot, J.P.; Yang, Q.; Ikonnikova, S. Can we Beneficially Reuse Produced Water from Oil and Gas Extraction in the U.S.? *Sci. Total Environ.* **2020**, *717*, 137085. [CrossRef] [PubMed]
- U.S. EPA. Final Report: Summary of Input on Oil and Gas Extraction Wastewater Management Practices under the Clean Water Act; U.S. EPA. 2020. Available online: <https://www.epa.gov/sites/default/files/2020-05/documents/oil-gas-final-report-2020.pdf> (accessed on 21 July 2021).
- Strong, J.; Cunningham, J.; Dunkel, M. Oklahoma Water for 2060: Produced Water Reuse and Recycling; Okla. City. 2017. Available online: <https://www.owrb.ok.gov/2060/PWWG/pwwgfinalreport.pdf> (accessed on 21 July 2021).

19. Shaffer, D.L.; Arias Chavez, L.H.; Ben-Sasson, M.; Romero-Vargas Castrilloón, S.; Yip, N.Y.; Elimelech, M. Desalination and reuse of high-salinity shale gas produced water: Drivers, technologies, and future directions. *Environ. Sci. Technol.* **2013**, *47*, 9569–9583. [[CrossRef](#)] [[PubMed](#)]
20. Scanlon, B.R.; Ikonnikova, S.; Yang, Q.; Reedy, R.C. Will water issues constrain oil and gas production in the United States? *Environ. Sci. Technol.* **2020**, *54*, 3510–3519. [[CrossRef](#)] [[PubMed](#)]
21. Jiménez, S.; Micó, M.; Arnaldos, M.; Medina, F.; Contreras, S. State of the art of produced water treatment. *Chemosphere* **2018**, *192*, 186–208. [[CrossRef](#)] [[PubMed](#)]
22. Patterson, L.A.; Kunschik, K.E.; Wiseman, H.; Fargione, J.; Maloney, K.O.; Kiesecker, J.; Nicot, J.-P.; Baruch-Mordo, S.; Entrekin, S.; Trainor, A. Unconventional oil and gas spills: Risks, mitigation priorities, and state reporting requirements. *Environ. Sci. Technol.* **2017**, *51*, 2563–2573. [[CrossRef](#)] [[PubMed](#)]
23. Alessi, D.S.; Zolfaghari, A.; Kletke, S.; Gehman, J.; Allen, D.M.; Goss, G.G. Comparative analysis of hydraulic fracturing wastewater practices in unconventional shale development: Water sourcing, treatment and disposal practices. *Can. Water Resour. J./Rev. Can. Des Ressources. Hydr.* **2017**, *42*, 105–121. [[CrossRef](#)]
24. DiGiulio, D.C.; Jackson, R.B. Impact to Underground Sources of Drinking Water and Domestic Wells from Production Well Stimulation and Completion Practices in the Pavillion, Wyoming, Field. *Environ. Sci. Technol.* **2016**, *50*, 4524–4536. [[CrossRef](#)]
25. Rodriguez, J.; Heo, J.; Kim, K.H. The Impact of Hydraulic Fracturing on Groundwater Quality in the Permian Basin, West Texas, USA. *Water* **2020**, *12*, 796. [[CrossRef](#)]
26. He, Y.; Sun, C.; Zhang, Y.; Folkerts, E.J.; Martin, J.W.; Goss, G.G. Developmental toxicity of the organic fraction from hydraulic fracturing flowback and produced waters to early life stages of zebrafish (*Danio rerio*). *Environ. Sci. Technol.* **2018**, *52*, 3820–3830. [[CrossRef](#)]
27. He, Y.; Folkerts, E.J.; Zhang, Y.; Martin, J.W.; Alessi, D.S.; Goss, G.G. Effects on biotransformation, oxidative stress, and endocrine disruption in rainbow trout (*Oncorhynchus mykiss*) exposed to hydraulic fracturing flowback and produced water. *Environ. Sci. Technol.* **2017**, *51*, 940–947. [[CrossRef](#)] [[PubMed](#)]
28. Blewett, T.A.; Weinrauch, A.M.; Delompré, P.L.; Goss, G.G. The effect of hydraulic flowback and produced water on gill morphology, oxidative stress and antioxidant response in rainbow trout (*Oncorhynchus mykiss*). *Sci. Rep.* **2017**, *7*, 46582. [[CrossRef](#)] [[PubMed](#)]
29. Kassotis, C.D.; Iwanowicz, L.R.; Akob, D.M.; Cozzarelli, I.M.; Mumford, A.C.; Orem, W.H.; Nagel, S.C. Endocrine disrupting activities of surface water associated with a West Virginia oil and gas industry wastewater disposal site. *Sci. Total Environ.* **2016**, *557*, 901–910. [[CrossRef](#)]
30. US. EPA. *Guidelines for Water Reuse*; U.S. EPA; 2012. Available online: <https://www.epa.gov/sites/default/files/2019-08/documents/2012-guidelines-water-reuse.pdf> (accessed on 21 July 2021).
31. Danforth, C.; Chiu, W.A.; Rusyn, I.; Schultz, K.; Bolden, A.; Kwiatkowski, C.; Craft, E. An integrative method for identification and prioritization of constituents of concern in produced water from onshore oil and gas extraction. *Environ. Int.* **2020**, *134*, 105280. [[CrossRef](#)]
32. China National Energy Administration. National Energy Administration Circular on the Issuance of Shale Gas Development Plan (2016–2020); China National Energy Administration. Available online: <https://policy.asiapacificenergy.org/node/30502016> (accessed on 21 July 2021). (In Chinese)
33. GWPC. Produced Water Report: Regulations, Current Practices, and Research Needs. Available online: https://www.gwpc.org/sites/gwpc/uploads/documents/Research/Produced_Water_Full_Report___Digital_Use.pdf (accessed on 7 April 2020).
34. U.S. EIA. Lower 48 States Shale Plays. Available online: <https://www.eia.gov/analysis/studies/uss shalegas/> (accessed on 1 July 2022).
35. U.S. EPA. Study of Oil and Gas Extraction Wastewater Management under the Clean Water Act. 2019 EPA-821-R19-001. Available online: https://www.epa.gov/sites/production/files/2019-05/documents/oil-and-gas-study_draft_05-2019.pdf (accessed on 7 April 2020).
36. Sentinel, N.A. Clearwater Facility Idled for Evaluation. Available online: <https://www.newsandsentinel.com/news/local-news/2019/09/clearwater-facility-idled-for-evaluation/> (accessed on 20 June 2021).
37. PADEP. Pennsylvania Department of Environmental Protection. PA DEP Oil & Gas Reporting Website—Production/Waste Reports. Available online: <https://www.dep.pa.gov/DataandTools/Reports/Oil%20and%20Gas%20Reports/pages/default.aspx> (accessed on 5 April 2020).
38. U.S. EPA. Detailed Study of the Centralized Waste Treatment Point Source Category for Facilities Managing Oil and Gas Extraction Wastes. EPA-821-R-18-004. Available online: https://www.epa.gov/sites/production/files/2018-05/documents/cwt-study_may-2018.pdf (accessed on 3 October 2020).
39. West Virginia Department of Environmental Protection Office of Oil and Gas. General Water Pollution Control Permit Permit Number: GP-WV-1-07. Available online: <http://dep.wv.gov/oil-and-gas/Documents/Fact%20Sheet%20GP-WV-1-07.pdf> (accessed on 10 April 2020).
40. GWPC. State of West Virginia Class II UIC Program Peer Review. Available online: <http://www.gwpc.org/sites/default/files/West%20Virginia%20Class%20II%20Peer%20Review%20Report%20Final.pdf> (accessed on 10 April 2020).
41. FWAP. State of Ohio and FreshWater Accountability Project. In the Court of Appeals of Franklin County, Ohio. Available online: <https://fwap.org/wp-content/uploads/2014/11/Complt-FINAL-FINAL-complet.pdf> (accessed on 7 April 2020).

42. Ertel, D.J.; McManus, K.; Bogdan, J. Method and System for Treating Wastewater. US10202286B2, 2019. Available online: <https://patents.google.com/patent/US10202286B2/en> (accessed on 21 July 2021).
43. Office of Fossil Energy and Carbon Management. Produced Water: From a Waste to a Resource. 2020. Available online: <https://www.energy.gov/fecm/articles/produced-water-waste-resource> (accessed on 21 July 2021).
44. Jacobs, N.; Marcellus Shale Operators Ahead of the Game on Produced Water Management. EnergyInDepth Appalachian Basin. Available online: <https://www.energyindepth.org/marcellus-shale-operators-ahead-of-the-game-on-wastewater-management/> (accessed on 7 April 2020).
45. Nobel, J. America's Radioactive Secret. Available online: <https://www.rollingstone.com/politics/politics-features/oil-gas-fracking-radioactive-investigation-937389/> (accessed on 10 April 2021).
46. Allard, D.J. TENORM—PA Study & Regulatory Framework. Available online: <https://www.nrc.gov/docs/ML1727/ML17278A725.pdf> (accessed on 10 April 2020).
47. Tomastik, T.E.; Daniel, J. Challenges Facing Class II Disposal Well Operations in the Appalachian Basin. Available online: <http://www.gwpc.org/sites/default/files/event-sessions/Class%20II-VI%20-%20Tom%20Tomastik.pdf> (accessed on 10 April 2020).
48. U.S. EIA. Crude Oil and Natural Gas Production in Texas and Oklahoma's Anadarko Region Is Growing. 2017. Available online: <https://www.eia.gov/todayinenergy/detail.php?id=32672#:~:text=According%20to%20EIA%20T1%20textquoterights%20DPR%2C%20oil,over%20the%20next%2016%20months> (accessed on 10 June 2020).
49. USGS. Induced Earthquakes. Available online: https://www.usgs.gov/natural-hazards/earthquake-hazards/induced-earthquakes?qt-science_support_page_related_con=4#qt-science_support_page_related_con (accessed on 18 June 2020).
50. Keranen, K.M.; Weingarten, M.; Abers, G.A.; Bekins, B.A.; Ge, S. Sharp increase in central Oklahoma seismicity since 2008 induced by massive wastewater injection. *Science* **2014**, *345*, 448–451. [CrossRef]
51. Langenbruch, C.; Zoback, M.D. How will induced seismicity in Oklahoma respond to decreased saltwater injection rates? *Sci. Adv.* **2016**, *2*, e1601542. [CrossRef]
52. U.S. EIA. Petroleum & Other Liquids: Crude Oil Production. Available online: https://www.eia.gov/dnav/pet/pet_crd_crpdn_adc_mbbldpd_a.htm (accessed on 10 August 2021).
53. Lyons, B.; Tintera, J.; Wright, K. Sustainable Produced Water Policy, Regulatory Framework, and Management in the Texas Oil and Natural Gas Industry: 2019 and Beyond. Available online: <https://documentcloud.adobe.com/link/track/?uri=urn%3Aaaid%3Aascds%3AUS%3A2c7b5154-f581-47dc-9c19-314d82c8de05&pageNum=1> (accessed on 5 April 2020).
54. RRC. Railroad Commission of Texas. Injection and Disposal Wells. Available online: <https://www.rrc.state.tx.us/about-us/resource-center/faqs/oil-gas-faqs/faq-injection-and-disposal-wells/> (accessed on 30 October 2020).
55. Vaucher, D. Water Market for Upstream Oil and Gas Operations in the United States Worth an Estimated \$33.6 Billion in 2018. Energy & Natural Resources Research & Analysis. Available online: <https://ihsmarkit.com/research-analysis/water-market-for-upstream-oil-gas-operations-in-us.html> (accessed on 10 April 2020).
56. RRC. Railroad Commission of Texas. Recycling. Environmental Permit Types & Information. Available online: <https://www.rrc.state.tx.us/oil-gas/applications-and-permits/environmental-permit-types-information/recycling/> (accessed on 10 April 2020).
57. TOSS. Office of the Secretary of State. Texas Administrative Code. Available online: [https://texreg.sos.state.tx.us/public/readtac\\$ext.ViewTAC?tac_view=5&ti=16&pt=1&ch=4&sch=B](https://texreg.sos.state.tx.us/public/readtac$ext.ViewTAC?tac_view=5&ti=16&pt=1&ch=4&sch=B) (accessed on 10 February 2021).
58. U.S. EPA. NPDES General Permit to Discharge to Waters of the United States. Available online: <https://www3.epa.gov/region1/npdes/hydrogp/HydroGPFactSheet.pdf> (accessed on 18 June 2021).
59. U.S. EPA. NPDES Permit No. TX0134061 Fact Sheet. Available online: https://www.epa.gov/sites/default/files/2018-01/documents/tx0134061_fact_sheet.pdf (accessed on 3 October 2020).
60. Lewis, K.; Moore, J.; Weathersby, B. Agricultural Reuse of Treated Produced Water. Available online: https://www.owrb.ok.gov/2060/PWWG/Resources/Lewis_Katie.pdf (accessed on 10 April 2020).
61. Guillen, R.; Hinojosa, J. Texas HB No. 2545. 2019. Available online: <https://legiscan.com/TX/bill/HB2545/2019> (accessed on 10 April 2020).
62. Scofield, R.; Beckerman, B. Final Report: Task 1, Identification of Chemicals of Interest Related to the Reuse of Produced Water for Agricultural Irrigation of Edible Crops. Prepared by GSI Environmental for the California Central Valley Region Regional Water Quality Control Board. March 2020. Available online: https://www.waterboards.ca.gov/centralvalley/water_issues/oil_fields/food_safety/data/task1_report_final.pdf (accessed on 7 April 2020).
63. Sedlacko, E.M.; Jahn, C.E.; Heuberger, A.L.; Sindt, N.M.; Miller, H.M.; Borch, T.; Blaine, A.C.; Cath, T.Y.; Higgins, C.P. Potential for Beneficial Reuse of Oil and Gas-Derived Produced Water in Agriculture: Physiological and Morphological Responses in Spring Wheat (*Triticum aestivum*). *Environ. Toxicol. Chem.* **2019**, *38*, 1756–1769. [CrossRef]
64. Sedlacko, E.M.; Chaparro, J.M.; Heuberger, A.L.; Cath, T.Y.; Higgins, C.P. Effect of produced water treatment technologies on irrigation-induced metal and salt accumulation in wheat (*Triticum aestivum*) and sunflower (*Helianthus annuus*). *Sci. Total Environ.* **2020**, *740*, 140003. [CrossRef]
65. Miller, H.; Dias, K.; Hare, H.; Borton, M.A.; Blotvogel, J.; Danforth, C.; Wrighton, K.C.; Ippolito, J.A.; Borch, T. Reusing oil and gas produced water for agricultural irrigation: Effects on soil health and the soil microbiome. *Sci. Total Environ.* **2020**, *722*, 137888. [CrossRef]
66. New Mexico Environment Department. Summary of Initial Public Input on Produced Water. Available online: <https://www.env.nm.gov/new-mexico-produced-water/public-participation-2/> (accessed on 10 April 2021).

67. New Mexico Legislature. Fluid Oil & Gas Waste Act. Available online: <https://nmlegis.gov/Legislation/Legislation?Chamber=H&LegType=B&LegNo=546&year=19> (accessed on 10 June 2021).
68. CCST. California Council on Science & Technology, An Independent Scientific Assessment of Well Stimulation in California, Volume II: Potential Environmental Impacts of Hydraulic Fracturing and Acid Stimulations in the Oil and Gas Industry. Available online: <https://ccst.us/reports/an-independent-scientific-assessment-of-well-stimulation-in-california-volume-2/> (accessed on 7 April 2020).
69. CalGEM. California Department of Conservation: Geologic Energy Management Division. Available online: <https://www.conservation.ca.gov/calgem> (accessed on 7 April 2020).
70. CDC. California Announces New Oil and Gas Initiatives. Actions Reflect Expanded Mission and Vision for Regulators. News Release #2019-05. Available online: <https://www.conservation.ca.gov/index/Pages/News/California-Establishes-Moratorium-on-High-Pressure-Extraction.aspx> (accessed on 7 April 2020).
71. California Senate. California Senate Bill No. 1281, Pavley, Oil and Gas Production: Water Use: Reporting, (2013–2014). Available online: http://leginfo.legislature.ca.gov/faces/billNavClient.xhtml?bill_id=201320140SB1281 (accessed on 7 April 2020).
72. Shonkoff, S.B. Oil and Gas Wastewater Reuse in California: Considerations and Risks. Available online: <https://www.healthandenvironment.org/docs/SethShonkoffSlides2018-5-31.pdf> (accessed on 7 April 2020).
73. CRWQCB. California Regional Water Quality Control Board, Central Valley Region, Order R5-2017-0036. Waste Discharge Requirements General Order for Oil Field Discharges to Land General Order Number Three. Available online: https://www.waterboards.ca.gov/centralvalley/board_decisions/adopted_orders/general_orders/r5-2017-0036.pdf (accessed on 7 April 2020).
74. CVRWQCB. Central Valley Regional Water Quality Control Board. Food Safety—Oil Field Wastewater Reuse Expert Panel. Final Version. Available online: https://www.waterboards.ca.gov/centralvalley/water_issues/oil_fields/food_safety/information/offsep_charter.pdf (accessed on 7 April 2020).
75. Gross, L. California Regulators Banned Fracking Wastewater for Irrigation, but Allow Wastewater from Oil Drilling. Scientists Say There’s Little Difference. Available online: <https://insideclimatenews.org/news/24042022/california-produced-water/> (accessed on 15 May 2022).
76. California Regional Water Quality Control Board Central Valley Region. California Regional Water Quality Control Board Central Valley Region Order No. R5-2019-0024. Available online: https://www.waterboards.ca.gov/centralvalley/board_decisions/adopted_orders/kern/r5-2019-0024.pdf (accessed on 20 May 2022).
77. RWQCB. Waste Discharge Requirements for Plains Exploration and Production, Arroyo Grande Produced Water Reclamation Facility. Available online: https://www.waterboards.ca.gov/centralcoast/board_decisions/adopted_orders/2008/2008_0004_wdr_arroyo_grande_wrf.pdf (accessed on 10 April 2020).
78. Robles, H. Irrigation Water Quality Evaluation Report. 2016. Available online: <https://www.cawelwd.org/wp-content/uploads/2018/06/final-irrigation-water-quality-eval-report-07-april-2016.pdf> (accessed on 7 April 2020).
79. Navarro, L.; Jones, M.; NMulhearn, S. Development of Risk-Based Comparison Levels for Chemicals in Agricultural Irrigation Water. Sponsored by California Resources Corporation. Available online: https://www.waterboards.ca.gov/centralvalley/water_issues/oil_fields/food_safety/data/studies/erm_riskassrpt.pdf (accessed on 7 April 2020).
80. Jordan, P.; Brandt, A.; Ferrar, K.; Feinstein, L.; Phillips, S. A case study of the potential risks associated with hydraulic fracturing in existing oil fields in the San Joaquin basin. *Indep. Sci. Assess. Well Stimul. Calif.* **2015**, *3*, 267.
81. Shonkoff, S.; Jordan, P.; Brandt, A.; Ferrar, K.; Maddalena, R.; Greenfield, B. A Case Study of the Petroleum Geological Potential and Potential Public Health Risks Associated with Hydraulic Fracturing and Oil and Gas Development in the Los Angeles Basin. *Indep. Sci. Assess. Well Stimul. Calif.* **2015**. Available online: <https://ccst.us/wp-content/uploads/160708-sb4-vol-III-4.pdf> (accessed on 7 April 2020).
82. Stringfellow, W.T.; Camarillo, M.K.; Domen, J.K.; Shonkoff, S.B. Comparison of chemical-use between hydraulic fracturing, acidizing, and routine oil and gas development. *PLoS ONE* **2017**, *12*, e0175344.
83. DiGiulio, D.C.; Shonkoff, S.B.; Jackson, R.B. The need to protect fresh and brackish groundwater resources during unconventional oil and gas development. *Curr. Opin. Environ. Sci. Health* **2018**, *3*, 1–7. [[CrossRef](#)]
84. Shonkoff, S.B. *Hazard Assessment of Chemical Additives Used in Oil Fields that Reuse Produced Water for Agricultural Irrigation, Livestock Watering, and Groundwater Recharge in the San Joaquin Valley of California: Preliminary Results*; Technical Report; PSE Healthy Energy, Inc.: Oakland, CA, USA, 2016.
85. Scofield, R.; Beckerman, B. Assessment of Produced Water for Agricultural Irrigation of Edible Crops Progress Report. February 2020—Public Meeting of the Food Safety Expert Panel. Available online: https://www.waterboards.ca.gov/centralvalley/water_issues/oil_fields/food_safety/#docsreports%3E (accessed on 30 October 2020).
86. Kharaka, Y.; Gans, K.; Thordsen, J.; Blondes, M.; Engle, M. Geochemical data for produced waters from conventional and unconventional oil and gas wells: Results from Colorado, USA. In *E3S Web of Conferences*; EDP Sciences: Les Ulis, France, 2019; Volume 98, p. 03002.
87. McIntyre, W.C.; Mays, D.C. Roles of the water court and the state engineer for water administration in Colorado. *Water Policy* **2017**, *19*, 837–850. [[CrossRef](#)]
88. COGCC. Colorado Oil and Gas Conservation Commission (COGCC), 2019 Annual Report. 2019. Available online: <https://spl.cde.state.co.us/artemis/nrserials/nr1011internet/nr10112019internet.pdf> (accessed on 30 October 2020).

89. Shores, A.; Laituri, M. The state of produced water generation and risk for groundwater contamination in Weld County, Colorado. *Environ. Sci. Pollut. Res.* **2018**, *25*, 30390–30400. [CrossRef] [PubMed]
90. Li, H.; Son, J.-H.; Carlson, K.H. Concurrence of aqueous and gas phase contamination of groundwater in the Wattenberg oil and gas field of northern Colorado. *Water Res.* **2016**, *88*, 458–466. [CrossRef]
91. Sherwood, O.A.; Rogers, J.D.; Lackey, G.; Burke, T.L.; Osborn, S.G.; Ryan, J.N. Groundwater methane in relation to oil and gas development and shallow coal seams in the Denver-Julesburg Basin of Colorado. *Proc. Natl. Acad. Sci. USA* **2016**, *113*, 8391–8396. [CrossRef]
92. Produced Water Treatment and Beneficial Use Information Center. Produced Water Beneficial Use Case Studies. 2011. Available online: http://aqwaterc.mines.edu/produced_water/assessbu/case/ (accessed on 1 July 2022).
93. Dolan, F.C.; Cath, T.Y.; Hogue, T.S. Assessing the feasibility of using produced water for irrigation in Colorado. *Sci. Total Environ.* **2018**, *640*, 619–628. [CrossRef]
94. Pica, N.E.; Carlson, K.; Steiner, J.J.; Waskom, R. Produced water reuse for irrigation of non-food biofuel crops: Effects on switchgrass and rapeseed germination, physiology and biomass yield. *Ind. Crops Prod.* **2017**, *100*, 65–76. [CrossRef]
95. Coupal, R.; Lieske, S.N.; Miller, S.N.; Reddy, K. Water Production from Coalbed Methane Development in Wyoming: A Summary of Quantity, Quality, and Management. Available online: https://www.uwyo.edu/haub/_files/_docs/ruckelshaus/pubs/2005-cbm-water-final-report.pdf (accessed on 10 April 2020).
96. Jacquet, J.; Witt, K.; Rifkin, W.; Haggerty, J.H. A complex adaptive system or just a tangled mess? In *Governing Shale Gas: Development, Citizen Participation and Decision Making in the US, Canada, Australia and Europe*, 1st ed.; Routledge: Oxford, UK, 2018; p. 14.
97. Walsh, K.B. Split estate and Wyoming’s orphaned well crisis: The case of coalbed methane reclamation in the Powder River Basin, Wyoming. *Case Stud. Environ.* **2017**, *1*, 1–8. [CrossRef]
98. Walsh, K.B.; Haggerty, J.H. Social license to operate during Wyoming’s coalbed methane boom: Implications of private participation. *Energy Policy* **2020**, *138*, 111217. [CrossRef]
99. MacKinnon, A.; Fox, K. Demanding beneficial use: Opportunities and obligations for Wyoming regulators in coalbed methane. *Wyo. Law Rev.* **2006**, *6*, 369.
100. Valorz, N.J. Need for Codification of Wyoming’s Coal Bed Methane Produced Groundwater Laws. *Wyo. Law Rev.* **2010**, *10*, 115.
101. Jackson, R.E.; Reddy, K. Geochemistry of coalbed natural gas (CBNG) produced water in Powder River Basin, Wyoming: Salinity and sodicity. *Water Air Soil Pollut.* **2007**, *184*, 49–61. [CrossRef]
102. Vance, G.F.; Ganjgunte, G.K. Utilization of coalbed natural gas water: Issues, implications, and management. *Coalbed Methane Energy Environ.* **2010**, chapter 14. 303–336.
103. Robertson, J. Redefining CSG “waste” water: New opportunities for managed aquifer recharge. *Environ. Plan. Law J.* **2018**, *35*, 188–211.
104. Johnston, C.; Vance, G.; Ganjgunte, G. Soil property changes following irrigation with coalbed natural gas water: Role of water treatments, soil amendments and land suitability. *Land Degrad. Dev.* **2013**, *24*, 350–362. [CrossRef]
105. Ganjgunte, G.K.; King, L.A.; Vance, G.F. Cumulative soil chemistry changes from land application of saline–sodic waters. *J. Environ. Qual.* **2008**, *37*, S-128–S-138. [CrossRef]
106. Brinck, E.; Frost, C. Evaluation of amendments used to prevent sodification of irrigated fields. *Appl. Geochem.* **2009**, *24*, 2113–2122. [CrossRef]
107. Amezketa, E.; Aragüés, R.; Gazol, R. Efficiency of sulfuric acid, mined gypsum, and two gypsum by-products in soil crusting prevention and sodic soil reclamation. *Agron. J.* **2005**, *97*, 983–989. [CrossRef]
108. King, L.; Vance, G.; Ganjgunte, G. Use of coalbed natural gas (CBNG) waters: Soil and plant responses. In Proceedings of the 22nd National American Society of Mining and Reclamation Symposium Annual Meetings, Breckenridge, CO, USA, 19–23 June 2005; Barnhisel, R., Ed.; Raising Reclamation to New Heights: Lexington, KY, USA, 2005; pp. 607–622.
109. Phelps, S.; Bauder, J.W. *The Role of Plants in the Bioremediation of Coalbed Methane Product Water*; Department of Land Resources and Environmental Sciences, Montana State University: Bozeman, MT, USA, 2003.
110. Healy, R.W.; Bartos, T.T.; Rice, C.A.; McKinley, M.P.; Smith, B.D. Groundwater chemistry near an impoundment for produced water, Powder River Basin, Wyoming, USA. *J. Hydrol.* **2011**, *403*, 37–48. [CrossRef]
111. U.S. EIA. Petroleum & Other Liquids. Available online: <https://www.eia.gov/dnav/pet/hist/LeafHandler.ashx?n=pet&s=mcrfpnm1&f=a> (accessed on 20 October 2021).
112. Scanlon, B.R.; Reedy, R.C.; Male, F.; Walsh, M. Water issues related to transitioning from conventional to unconventional oil production in the Permian Basin. *Environ. Sci. Technol.* **2017**, *51*, 10903–10912. [CrossRef] [PubMed]
113. Riganti, C.U.S. Drought Monitor New Mexico. Available online: <https://droughtmonitor.unl.edu/CurrentMap/StateDroughtMonitor.aspx?NM> (accessed on 16 June 2021).
114. USGS. How Much Water Does the Typical Hydraulically Fractured Well Require? Available online: https://www.usgs.gov/faqs/how-much-water-does-typical-hydraulically-fractured-well-require?qt-news_science_products=0#qt-news_science_products (accessed on 10 February 2021).
115. Bruce, M.; Thomson, J.M.C. *Analysis of the Relationship Between Water, Oil & Gas in New Mexico: Investigation of Past and Future Trends*; New Mexico Water Resources Research Institute: Las Cruces, NM, USA, 2021. Available online: <https://www.worldcat.org/title/analysis-of-the-relationship-between-water-oil-gas-in-new-mexico-investigation-of-past-and-future-trends/oclc/1249753650> (accessed on 10 February 2021).

116. NMOCD. OCD Data and Statistics. Available online: <http://www.emnrd.state.nm.us/OCD/statistics.html> (accessed on 10 June 2021).
117. New Mexico Environment Department. Public Involvement Plan (PIP) for the Implementation of House Bill 546, the Produced Water Act. Available online: <https://www.env.nm.gov/wp-content/uploads/sites/16/2019/10/Produced-Water-PIP-20191015-FINAL.pdf> (accessed on 10 June 2021).
118. Geza, M.; Ma, G.; Kim, H.; Cath, T.Y.; Xu, P. iDST: An integrated decision support tool for treatment and beneficial use of non-traditional water supplies—Part I. Methodology. *J. Water Process Eng.* **2018**, *25*, 236–246. [[CrossRef](#)]
119. Ma, G.; Geza, M.; Cath, T.Y.; Drewes, J.E.; Xu, P. iDST: An integrated decision support tool for treatment and beneficial use of non-traditional water supplies—Part II. Marcellus and Barnett Shale case studies. *J. Water Process Eng.* **2018**, *25*, 258–268. [[CrossRef](#)]
120. Chen, L.; Xu, P.; Wang, H. Photocatalytic membrane reactors for produced water treatment and reuse: Fundamentals, affecting factors, rational design, and evaluation metrics. *J. Hazard. Mater.* **2022**, *424*, 127493. [[CrossRef](#)]
121. Sedlak, D.; Mauter, M.; Macknick, J.; Stokes-Draut, J.; Fiske, P.; Agarwal, D.; Borch, T.; Breckenridge, R.; Cath, T.; Chellam, S.; et al. *National Alliance for Water Innovation (NAWI) Master Technology Roadmap*; National Renewable Energy Lab. (NREL): Golden, CO, USA, 2021. [[CrossRef](#)]
122. Chen, L.; Xu, P.; Kota, K.; Kuravi, S.; Wang, H. Solar distillation of highly saline produced water using low-cost and high-performance carbon black and airlaid paper-based evaporator (CAPER). *Chemosphere* **2021**, *269*, 129372. [[CrossRef](#)] [[PubMed](#)]
123. Lin, L.; Jiang, W.; Chen, L.; Xu, P.; Wang, H. Treatment of Produced Water with Photocatalysis: Recent Advances, Affecting Factors and Future Research Prospects. *Catalysts* **2020**, *10*, 924. [[CrossRef](#)]
124. Hu, L.; Wang, H.; Xu, P.; Zhang, Y. Biomineralization of hypersaline produced water using microbially induced calcite precipitation. *Water Res.* **2020**, *190*, 116753. [[CrossRef](#)] [[PubMed](#)]
125. Hu, L.; Yu, J.; Luo, H.; Wang, H.; Xu, P.; Zhang, Y. Simultaneous recovery of ammonium, potassium and magnesium from produced water by struvite precipitation. *Chem. Eng. J.* **2020**, *382*, 123001. [[CrossRef](#)]
126. Harry, D.; Horton, D.; Durham, D.; Constable, D.J.C.; Gaffney, S.; Moore, J.; Todd, B.; Martinez, I. Grand Challenges and Opportunities for Greener Chemical Alternatives in Hydraulic Fracturing: A Perspective from the ACS Green Chemistry Institute Oilfield Chemistry Roundtable. *Energy Fuels* **2020**, *34*, 7837–7846. [[CrossRef](#)]



Contents lists available at [ScienceDirect](#)

Data in Brief

journal homepage: www.elsevier.com/locate/dib



Data Article

Datasets associated with the characterization of produced water and Pecos River water in the Permian Basin, the United States



Wenbin Jiang^a, Xuesong Xu^a, Ryan Hall^b, Yanyan Zhang^a,
Kenneth C. Carroll^c, Frank Ramos^d, Mark A. Engle^e, Lu Lin^a,
Huiyao Wang^a, Matthias Sayer^b, Pei Xu^{a,*}

^a Department of Civil Engineering, New Mexico State University, Las Cruces, NM 88003, United States

^b NGL Partners LP, Santa Fe, NM 87501, United States

^c Department of Plant and Environmental Science, New Mexico State University, Las Cruces, NM, United States

^d Department of Geological Sciences, New Mexico State University, Las Cruces, NM 88003, United States

^e Department of Earth, Environmental and Resource Sciences, The University of Texas at El Paso, El Paso, TX 79968, United States

ARTICLE INFO

Article history:

Received 18 May 2022

Revised 28 June 2022

Accepted 29 June 2022

Available online 4 July 2022

Dataset link: [Datasets associated with the characterization of produced water and Pecos River water in the Permian Basin \(Original data\)](#)

Keywords:

Water quality

Produced water characterization

Permian basin

Pecos river

Water reuse

ABSTRACT

The data in this report are associated with “Characterization of Produced Water and Surrounding Surface Water in the Permian Basin, the United States” (Jiang et al. 2022) and include raw data on produced water (PW) quality and Pecos River water quality in the Permian Basin, which is one of the major oil and gas producing areas in the U.S. The data include 46 samples for PW and 10 samples for Pecos River water. The data include wet chemistry, mineral salts, metals, oil and grease, volatile and semi-volatile organic compounds, radionuclides, ammonia, hydraulic fracturing additives, and per- and polyfluoroalkyl substances. The PW samples were collected from five different locations in the Permian Basin. Twenty-four of the PW samples and the ten Pecos River samples were analyzed by the authors. The information for the rest of PW samples (22 samples) was provided by industrial collaborators in the Permian Basin. Statistical analyses were performed on the combined data to obtain Mean, Max, Min,

DOI of original article: [10.1016/j.jhazmat.2022.128409](https://doi.org/10.1016/j.jhazmat.2022.128409)

* Corresponding author.

E-mail address: pxu@nmsu.edu (P. Xu).

<https://doi.org/10.1016/j.dib.2022.108443>

2352-3409/© 2022 The Author(s). Published by Elsevier Inc. This is an open access article under the CC BY license (<http://creativecommons.org/licenses/by/4.0/>)

NMOGA Exhibit 117

NMOGA_003334

25th percentile, 50th percentile, and 75th percentile of each analyte.

© 2022 The Author(s). Published by Elsevier Inc.
This is an open access article under the CC BY license
(<http://creativecommons.org/licenses/by/4.0/>)

Specifications Table

Subject	Water Science and Technology
Specific subject area	Produced water (PW) quality and surrounding river water quality related to unconventional oil and gas production
Type of data	Table
How the data were acquired	<p>To identify the chemicals of interest (COIs), the authors reviewed current PW management practices with regulations and reuse scenarios in the major production areas in the U.S. up to 2021. The investigated production areas include the Appalachian Basin (Marcellus and Utica shale areas of Pennsylvania, Ohio, and West Virginia), Oklahoma, Texas, California, Colorado, Wyoming, and New Mexico. The investigated beneficial reuse options include on-site reuse in the O&G field, irrigation, wildlife and livestock drinking water, discharge to surface water, groundwater recharge, road spreading, and land applications.</p> <p>Information of treated PW reuse in the O&G field was collected from the Pennsylvania case study [2]. Information of PW reuse for irrigation was derived from studies conducted in California [3–5], Colorado [6–8], and Texas [9]. Information of PW discharge to surface water and reuse for wildlife and livestock drinking water was from Texas [9], Colorado [10], and Wyoming [11]. Information of PW reuse for road spreading and land application was from Colorado [12] and Wyoming [13]. To ensure the thoroughness of the COIs list, it is compared to the United States Environmental Protection Agency (USEPA) drinking water standards, New Mexico groundwater standards [14], and New Mexico surface water standards [15]. The list of COIs was further reviewed by the New Mexico Produced Water Research Consortium.</p> <p>Gravimetric methods were used to measure total dissolved solids (TDS) and total suspended solids (TSS) concentrations. A Total Organic Carbon Analyzer (TOC-Vcsh, Shimadzu, Japan) was used to measure the concentrations of total organic carbon (TOC) and dissolved organic carbon (DOC). A benchtop multi-parameter meter (pH/con 300 Meter, Oakton Instruments, IL, USA) was used to measure pH. Hach COD test kits and alkalinity test kits (Hach, CO, USA) were used to measure chemical oxygen demand (COD) and alkalinity, respectively. A spectrophotometer (Hach DR6000, Hach, CO, USA) was used to measure ammonia. Ion chromatography (IC; Dionex ICS-2100, Thermo Fisher Scientific, CA, USA) was used to measure major ions. Inductively coupled plasma optical emission spectroscopy (ICP-OES; Optima 4300 DV, PerkinElmer, MA, USA) and inductively coupled plasma mass spectroscopy (ICP-MS; Elan DRC-e, PerkinElmer, MA, USA) were used to measure metals and trace elements. An alpha spectroscopy system (Mirion Technologies, Inc.) was used for the total alpha spectra acquisition and analysis. The system was equipped with 72 Passivated Implanted Planar Silicon detector which is connected to an Apex-Alpha software system [16]. A gamma spectroscopy with a broad Energy Germanium detector (BeGe, Mirion Technologies, Inc.) was used to measure radium activities [16].</p> <p>A spectrofluorometer (Aqualog-UV-800-C, Horiba Instruments, NJ, USA) was used to semi-quantitatively identify the organic compositions of PW with fluorescence Emission and Excitation Matrix (FEEM). A gas chromatography (GC, Agilent 6890) coupled with a quadrupole mass spectrometry (MS, Agilent 5973) was used to measure volatile organic compounds (VOCs) and semi-VOCs. A GC (Agilent 5890) coupled with a flame ionization detector was used to measure total petroleum hydrocarbons (TPH) and organic acids. A GC (Agilent 5890) coupled with an electron capture detector was used</p>

(continued on next page)

	to measure pesticides/herbicides. High performance liquid chromatography-tandem mass spectrometry (HPLC/MS/MS, SCIEX 5500) was used to measure per- and polyfluoroalkyl substances (PFAS). A high-resolution GC/MS (Thermo DFS) was used to measure Dioxins.
Data format	Raw
	Analyzed
Description of data collection	Samples for wet chemistry and inorganic analyses were collected in sterile plastic bottles. Samples for organic analyses were collected in method-specific bottles. All samples were stored at 4°C after collection and transported under chain of custody. All sample preparation and analyses followed the USEPA guidance and standard practices.
Data source location	Institution: New Mexico State University Region: Permian Basin Country: United States
Data accessibility	Repository name: Mendeley Data Data identification number: DOI: 10.17632/pfrxnjd7mw.4 Direct URL to data: https://data.mendeley.com/datasets/pfrxnjd7mw/4
Related research article	https://doi.org/10.1016/j.jhazmat.2022.128409

Value of the Data

- These data provide the quality information of 46 PW samples and 10 Pecos River samples from the Permian Basin in New Mexico and Texas. These data are valuable for a better understanding of PW and surface water quality in the Permian Basin.
- Beneficiaries of these data include researchers, engineers, oil and gas industry, water resource managers and regulators, and other stakeholders interested in PW and surface water quality.
- These data provide the first step for risk-based assessment and designing optimal methods for treatment and potentially beneficial use of treated PW within and outside the oil and gas industry in the Permian Basin.

1. Data Description

The data in “Produced water and Pecos River quality.xlsx” include five tabs:

- “1 Produced Water samples (PW)” includes the concentrations of 91 detected analytes in the 46 PW samples and the statistical results (Mean, Max, Min, 25th percentile, 50th percentile, and 75th percentile).
- “2 Compounds not detected in produced water (PW)” includes the names of 218 analytes that were not detected in the PW samples.
- “3 Pecos River sample (RW)” includes the concentrations of 67 detected analytes in the ten Pecos River water samples and the statistical results (Mean, Max, Min, 25th percentile, 50th percentile, and 75th percentile).
- “4 Compounds not detected in Pecos River (RW)” includes the names of 242 analytes that were not detected in the Pecos River water samples.
- “5 PW Sampling points” includes the information of PW samples based on the sampling point in [Fig. 1](#).
- “6 RL and MDL” includes reporting limit (RL) and minimal detection limit (MDL) for the analytes in this study.

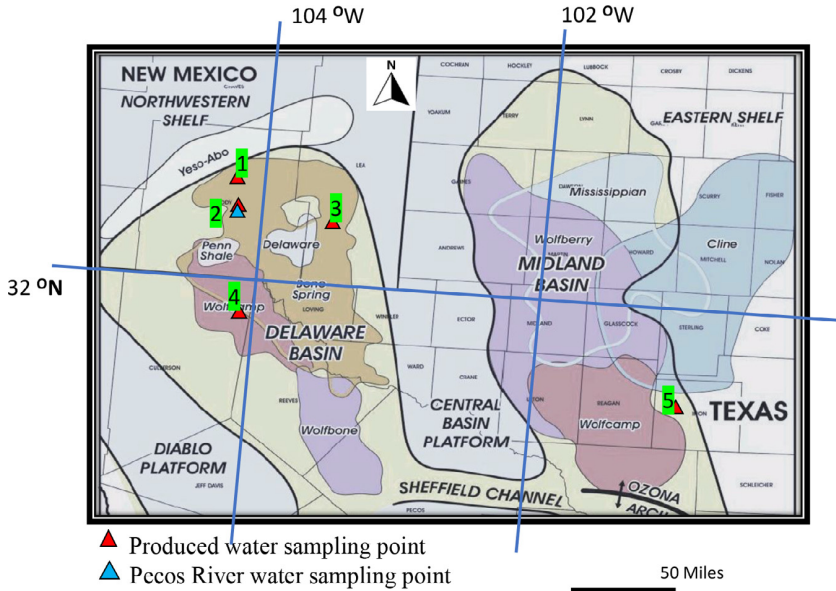


Fig. 1. Sampling points of produced water and Pecos River water [1]. Permian Basin County map is cited from [17]. Sampling points coordinates (estimated), Point 1: 32.83, -104.3; Point 2: 32.31, -104.0; Point 3: 32.10, -103.2; Point 4: 31.49, -103.7; Point 5: 31.32, -101.1.

2. Experimental Design, Materials and Methods

TDS and TSS were measured at the same time based on EPA method 2540C and 2540 D, respectively. A water sample was first filtered through a weighed 0.15 μm glass fiber filter. The filter was dried to a constant weight at 103 to 105 $^{\circ}\text{C}$; TSS was then measured by the increased filter weight. The filtrate was dried to a constant weight at 180 $^{\circ}\text{C}$ in a weighed dish; the dish weight increase was used to calculate TDS concentration. TOC and DOC analyses were based on EPA method 415.3. HCl was used to acidify the samples to $\text{pH} < 2$ to remove the inorganic carbon (carbonate and bicarbonate). Then the samples were analyzed by a TOC analyzer. Samples were filtered by a 0.45 μm filter for DOC analysis based on the procedure requirement. Alkalinity, COD, and ammonia were analyzed by following the protocols that come with the Hach test kits, respectively. Radium-226 was determined directly by measuring the 186.2 keV gamma photopeak (3.28% abundance). Radium-228 was determined indirectly by measuring Actinium-228 ($t_{1/2} = 6.1$ h) using 911 and 969 keV gamma photo peaks [16]. EPA method 900.0. was used for Gross Alpha and Gross Beta counts.

Organic analyses were performed by a commercial lab, Eurofins Test America. Unfiltered samples were used for the analyses. VOCs and SVOCs were measured based on EPA method 8260C and 8270D, respectively. TPH and organic acid were analyzed based on EPA method 8015D. Pesticide/herbicides were analyzed based on EPA method 8081B. PAFS were analyzed based on a modified EPA method 537. Dioxins were analyzed based on EPA method 1613B. Quantification was performed by using blank samples and external/internal standard calibration. Isotopic dilution was used for PFAS and dioxin quantitation.

The results for each sample were calculated for charge balance and mass balance. Then all the water samples were compiled together for statistical analysis. Statistical analyses were performed by using Excel to get Mean, Max, Min, 25% percentile, 50% percentile, and 75% percentile values for each analyte.

Ethics Statements

This study followed the ethical guidelines that all authors must comply with.

Declaration of Competing Interest

The authors declare that they have no known competing financial interests or personal relationships that could have appeared to influence the work reported in this paper.

The authors declare the following financial interests/personal relationships which may be considered as potential competing interests.

Data Availability

Datasets associated with the characterization of produced water and Pecos River water in the Permian Basin (Original data) (Mendeley data).

CRediT Author Statement

Wenbin Jiang: Methodology, Investigation, Formal analysis, Writing – original draft, Writing – review & editing; **Xuesong Xu:** Methodology, Investigation, Formal analysis, Writing – original draft, Writing – review & editing; **Ryan Hall:** Methodology, Investigation, Formal analysis, Writing – original draft, Writing – review & editing, Supervision, Funding acquisition; **Yanyan Zhang:** Writing – review & editing, Supervision, Funding acquisition; **Kenneth C. Carroll:** Writing – review & editing, Supervision, Funding acquisition; **Frank Ramos:** Methodology, Investigation, Formal analysis, Writing – original draft, Writing – review & editing; **Mark A. Engle:** Methodology, Investigation, Formal analysis, Writing – original draft, Writing – review & editing; **Lu Lin:** Methodology, Investigation, Formal analysis, Writing – original draft, Writing – review & editing; **Huiyao Wang:** Writing – review & editing, Supervision, Funding acquisition; **Matthias Sayer:** Writing – review & editing, Supervision, Funding acquisition; **Pei Xu:** Methodology, Investigation, Formal analysis, Writing – original draft, Writing – review & editing, Supervision, Funding acquisition.

Acknowledgments

The study is funded by the New Mexico Water Resources Research Institute and New Mexico State University, the United States. We are very grateful to the New Mexico Produced Water Research Consortium for technical support and data shared by the Consortium members. We thank Dr. Punam Thakur with the Carlsbad Environmental Monitoring & Research Center for the analysis of radionuclides.

References

- [1] W. Jiang, X. Xu, R. Hall, Y. Zhang, K.C. Carroll, F. Ramos, M.A. Engle, L. Lin, H. Wang, M. Sayer, Characterization of produced water and surrounding surface water in the Permian Basin, the United States, *J. Hazard. Mater.* 430 (2022) 128409.
- [2] Pennsylvania Department of Environmental Protection, GENERAL PERMIT WMGR123, Pennsylvania Department of Environmental Protection, 2021 https://files.dep.state.pa.us/Waste/Bureau%20of%20Waste%20Management/WasteMgtPortalFiles/SolidWaste/Residual_Waste/GP/GENERAL_PERMIT_WMGR123_FINAL_1_4_21.pdf. Accessed April 20, 2021.
- [3] R. Scofield, B. Beckerman, Final Report: Task 1, identification of chemicals of interest related to the reuse of produced water for agricultural irrigation of edible crops. Prepared by GSI environmental for the California central valley region regional water quality control board. March 2020. https://www.waterboards.ca.gov/centralvalley/water_issues/oil_fields/food_safety/data/task1_report_final.pdf, 2020. Accessed April 7, 2020.

- [4] L. Navarro, M. Jones, S. Mulhearn, Development of risk-based comparison levels for chemicals in agricultural irrigation water. Sponsored by California resources corporation. https://www.waterboards.ca.gov/centralvalley/water_issues/oil_fields/food_safety/data/studies/erm_riskassrpt.pdf, 2016. Accessed April 7, 2020.
- [5] R. Scofield, B. Beckerman, Assessment of Produced Water for Agricultural Irrigation of Edible Crops Progress Report. February 2020, Proceedings of the Public Meeting of the Food Safety Expert Panel, 2020 https://www.waterboards.ca.gov/centralvalley/water_issues/oil_fields/food_safety/#docsreports%3E. Accessed October 30, 2020.
- [6] E.M. Sedlacko, J.M. Chaparro, A.L. Heuberger, T.Y. Cath, C.P. Higgins, Effect of produced water treatment technologies on irrigation-induced metal and salt accumulation in wheat (*Triticum aestivum*) and sunflower (*Helianthus annuus*), *Sci. Total Environ.* 740 (2020) 140003.
- [7] E.M. Sedlacko, C.E. Jahn, A.L. Heuberger, N.M. Sindt, H.M. Miller, T. Borch, A.C. Blaine, T.Y. Cath, C.P. Higgins, Potential for Beneficial reuse of oil and gas-derived produced water in agriculture: physiological and morphological responses in spring wheat (*Triticum aestivum*, *Environ. Toxicol. Chem.* 38 (8) (2019) 1756–1769.
- [8] H. Miller, K. Dias, H. Hare, M.A. Borton, J. Blotevogel, C. Danforth, K.C. Wrighton, J.A. Ippolito, T. Borch, Reusing oil and gas produced water for agricultural irrigation: effects on soil health and the soil microbiome, *Sci. Total Environ.* 722 (2020) 137888.
- [9] M.P.T. Pham, J.W. Castle, J.H. Rodgers, Application of water quality guidelines and water quantity calculations to decisions for beneficial use of treated water, *Appl Water Sci* 1 (3) (2011) 85–101.
- [10] Water Quality Control Division, CDPS general permit for discharges associated with produced water treatment facilities Colorado discharge permit system. https://assets.vbt.io/public/files/6975/CO_Resources_Industrial/CO_-WQ-COG840000-_CDPS_General_Permit_-_Produced_Water_Treatment_Facilities.pdf, 2012. Accessed January 5, 2021.
- [11] Wyoming Department of Environmental Quality, Permit Regulations for Discharges to Wyoming Surface Waters, Wyoming Department of Environmental Quality, 2015 Ref. Number: 020.0011.2.03232015. Appendix H. https://rules.wyo.gov/DownloadFile.aspx?source_id=9763&source_type_id=81&doc_type_id=110&include_meta_data=Y&file_type=pdf&filename=9763.pdf&token=137154168010112251023075038252050235157169217097. Accessed January 5, 2021.
- [12] Colorado oil and gas conservation commission, Colorado exploration and production waste management. https://assets.vbt.io/public/files/6975/CO_Resources_Industrial/CO_-WQ-COG840000-_CDPS_General_Permit_-_Produced_Water_Treatment_Facilities.pdf, 2020. Accessed October 5, 2021.
- [13] Wyoming Department of Environmental Quality, Permit to construct. Permit NO. 19-283. <https://static1.squarespace.com/static/5c40e70a50a54fba6f8451d9/t/5e46d0532446a349db582540/1581699197696/Pine+Bluffs+Project+DEQ+Permit.pdf>, 2020. Accessed January 10, 2021.
- [14] New Mexico Water Quality Control Commission, Environmental Protection Water Quality Ground and Surface Water Protection, New Mexico Water Quality Control Commission, 1995 <https://www.srca.nm.gov/wp-content/uploads/attachments/20.006.0002.pdf>. Accessed January 10, 2021.
- [15] New Mexico Water Quality Control commission, Environmental protection water quality standards for interstate and intrastate surface waters. <https://www.epa.gov/sites/default/files/2014-12/documents/nmwqs.pdf>, 2000. Accessed January 10, 2021.
- [16] P. Thakur, A.L. Ward, T.M. Schaub, Occurrence and behavior of uranium and thorium series radionuclides in the Permian shale hydraulic fracturing wastes, *Environ. Sci. Pollut. Res.* 29 (28) (2022) 43058–43071.
- [17] Shalexperts, Permian basin geologic breakdown. <https://www.shalexperts.com/plays/wolfcamp-shale/Overview>. Accessed September 24, 2021.

Review

Treatment of Produced Water with Photocatalysis: Recent Advances, Affecting Factors and Future Research Prospects

Lu Lin , Wenbin Jiang, Lin Chen, Pei Xu  and Huiyao Wang *

Department of Civil Engineering, New Mexico State University, Las Cruces, NM 88003, USA; lulin@nmsu.edu (L.L.); wbjjiang@nmsu.edu (W.J.); chenlin@nmsu.edu (L.C.); pxu@nmsu.edu (P.X.)

* Correspondence: huiyao@nmsu.edu

Received: 12 July 2020; Accepted: 10 August 2020; Published: 12 August 2020



Abstract: Produced water is the largest byproduct of oil and gas production. Due to the complexity of produced water, especially dissolved petroleum hydrocarbons and high salinity, efficient water treatment technologies are required prior to beneficial use of such waste streams. Photocatalysis has been demonstrated to be effective at degrading recalcitrant organic contaminants, however, there is limited understanding about its application to treating produced water that has a complex and highly variable water composition. Therefore, the determination of the appropriate photocatalysis technique and the operating parameters are critical to achieve the maximum removal of recalcitrant compounds at the lowest cost. The objective of this review is to examine the feasibility of photocatalysis-involved treatment for the removal of contaminants in produced water. Recent studies revealed that photocatalysis was effective at decomposing recalcitrant organic compounds but not for mineralization. The factors affecting decontamination and strategies to improve photocatalysis efficiency are discussed. Further, recent developments and future research prospects on photocatalysis-derived systems for produced water treatment are addressed. Photocatalysis is proposed to be combined with other treatment processes, such as biological treatments, to partially reduce total organic carbon, break down macromolecular organic compounds, increase biodegradability, and reduce the toxicity of produced water.

Keywords: photocatalysis; produced water; water reuse; water treatment; affecting factors; future prospects

1. Introduction

Produced water, a byproduct of oil and gas production, is water in underground formations that is brought to the surface during oil and gas production. The methods used for produced water treatment include basic separation technologies designed for the removal of total suspended solids, oil and grease, and advanced treatment technologies designed for the removal of dissolved organic compounds, inorganic ions, and radioactive materials [1–10]. Phase separation underlies basic separation technologies, such as flotation, media filtration, coagulation/flocculation, centrifugation, and hydrocyclone. These basic separation technologies are in most cases incapable of producing an effluent compatible with higher standards for beneficial water reuse [11,12].

The commonly used advanced technologies for produced water treatment consist of membrane filtration, thermal distillation, adsorption, ion exchange, and advanced oxidation processes (AOPs). Nanofiltration and reverse osmosis (RO) are employed for the removal of the majority of organic and inorganic constituents from produced water with total dissolved solids (TDS) concentrations typically below 40 g/L [13,14]. Other technologies such as thermal distillation are required for produced water

with higher TDS, such as up to 200 g/L [3]. Sorption to activated carbon, biological treatments and AOPs are used for the removal of dissolved organic carbon (DOC) and are often combined with desalination processes to reduce fouling and polish water quality [15].

The removal of dissolved organic compounds in produced water using different treatment technologies was recently reviewed and identified as a bottle-neck for produced water reuse because the organic compounds were not eliminated efficiently [1,16,17]. For example, the biological treatment is used to remove organic constituents, especially in the downstream oil and gas industry [18], yet the efficiency of the bioprocess could be severely impeded with the presence of highly toxic recalcitrant compounds, such as benzene, toluene, ethylbenzene, and xylene [19]. The complexity of produced water and the diverse requirements for fit-for-purpose applications (e.g., for generation of high-quality water for steam production, irrigation or aquifer recharge) mandate the development of a multi-step, integrated treatment train, i.e., the combination of different processes, to remove a broad range of constituents. These technologies include pretreatment involving basic separation technologies, treatment using desalination processes, and post-treatment to further polish water quality with AOP, sorption, or re-mineralization. The detailed description of treatment technologies, their advantages and drawbacks, energy consumption and cost efficiency can be found in a number of reviews on produced water treatment [1–3,20–23].

Reactive oxygen or free radical species represent strong oxidants that can initiate AOPs in order to degrade pollutants to simple and nontoxic molecules. Free radical species are atoms or molecules containing at least one unpaired electron, such as hydroxyl radical ($\text{HO}\bullet$), and the superoxide anion radical ($\text{O}_2-\bullet$), with the $\text{HO}\bullet$ radical having attracted the most attention in this area [24]. AOPs are used in oil- and gas-produced water treatment for the removal of organic and some inorganic compounds, disinfection and the removal of odor and color [3]. Commonly used oxidants include ozone, hydrogen peroxide, chlorine, and Fenton's reagent (combination of hydrogen peroxide with ferrous iron). Produced water treatment technologies based on the combination of hydrodynamic cavitation, ozonation, acoustic cavitation and electrochemical oxidation have been studied for the removal of organic matter, bacteria and scalants, either for flowback reuse or as a pretreatment for RO [25]. The choice of AOPs mainly depends on the characteristics of the hydroxyl radicals ($\bullet\text{OH}$) generated, as they are highly reactive and have high oxidation potential. This fact enables these species to completely degrade DOCs into CO_2 and water, or at least partially into less toxic compounds [26]. The destruction of organic contaminants is the main advantage of AOPs in contrast to other processes such as active carbon, thermal and membrane technologies, which transfer the contaminants from one phase to another [19].

Photocatalytic water treatment is a promising AOP for environmental remediation [27]. Compared to traditional oxidation processes, photocatalytic oxidation operates at ambient conditions without a high temperature or high pressure, and many recalcitrant organic contaminants can be degraded without the addition of chemical oxidants [28]. Moreover, photocatalysis has been proven to be effective at transforming metallic ions and metalloids to less toxic species or species easier to be separated from the system in a subsequent treatment step [29,30]. Since chemical consumption and waste sludge production are one of the major concerns inhibiting produced water treatment, photocatalysis is an attractive technology in comparison with other technologies. However, studies on photocatalytic oxidation of produced water are quite limited, and there is lack of a comprehensive critical review on this field.

For produced water treatment, the efficiency of photocatalysis can be impacted by the different constituents present in a complex matrix composed by a high and heterogeneous concentration of salts [16]. A comprehensive review is needed for further development of AOPs in produced water treatment application. Therefore, this review focuses on evaluating the feasibility of photocatalysis on produced water treatment and the impact of water chemistry. The objective of this work is to examine the suitability of photocatalysis integrated in a multi-stage treatment train based on recent research since 2010.

2. Produced Water Characteristics, Treatment and Reuse

The United States produces an estimate of 890 billion gallons (3.37 billion m³) of produced water annually, making it the largest waste stream associated with oil and gas activities [31]. The amount of produced water generated every year keeps increasing with the expansion of unconventional oil and gas development, which produced more than 50% of crude oil and natural gas in 2019 [32]. The oil and gas production in the United States is mainly from seven key oil and gas basins: Appalachia including Marcellus and Utica (Pennsylvania, Ohio, and West Virginia), Bakken (North Dakota and Montana), Eagle Ford (South Texas), Haynesville (Louisiana and East Texas), Niobrara (Colorado and Wyoming), and the Permian basin (West Texas and southeast New Mexico) [33]. Produced water flow rate varies throughout the lifetime of an oil or gas well. Conventional oil and gas wells display little or no produced water at the beginning, with the flow rate increasing over time. Most unconventional hydraulically fractured wells display a high produced water flow rate initially due to the flowback of fracturing fluids, followed by a decay in flow rate until it levels off at a relatively steady lower level [34].

The physical and chemical properties of produced water vary considerably based on the geographic location of the field, the type of hydrocarbon product being extracted, the extraction method employed, and the minerals present in the bearing geologic formation. Since the water has been in contact with hydrocarbon-bearing formations for millennia, it generally contains some of the chemical characteristics of the formations and the hydrocarbons in those formations [35]. Produced water is typically saline with high TDS, including calcium, chloride, magnesium, sodium, and sulfate. Organic compounds are some of the main contaminants in produced water, including oil and grease (free, dispersed or emulsified); volatile and semi-volatile organics, such as benzene, toluene, ethylbenzene, and xylenes (BTEX); polycyclic aromatic hydrocarbons (PAHs); organic acids; and waxes. Contaminants in smaller amounts include dissolved gases (e.g., ammonia and hydrogen sulfide), chemical additives used to improve drilling and production operations, and naturally occurring radioactive materials leached from some formations or precipitated due to water mixing. Additionally, heavy metals and transformational byproducts that can form from the interaction between added chemicals and formation water have also been found in produced water [9,34,36]. When collecting data for its 2016 hydraulic fracturing study, the U.S. Environmental Protection Agency found literature reports of about 600 different chemicals in some produced water samples [37]. The concentrations of some select constituents in produced water are summarized in Table 1.

Table 1. Concentrations of select constituents in produced water [35].

Parameters	Range	Parameters	Range
pH	4.3–8.9	Ca (mg/L)	18–132,687
TDS (g/L)	1.0–470.3	Mg (mg/L)	4–18,145
TSS (mg/L)	2–21,820	Na (mg/L)	316–134,652
DOC (mg/L)	3.4–5960	K (mg/L)	8.6–14,649
Alkalinity (CaCO ₃ , mg/L)	6.1–2000	SO ₄ (mg/L)	0.5–7851
Total Ra (pCi/L)	0.2–18,045	Cl (mg/L)	1405–310,561
HEM (mg/L)	0.6–2000	HCO ₃ (mg/L)	1.9–7355
MBAS (mg/L)	0.01–54	Ba (mg/L)	0–22,400

HEM: Hexane extractable material; MBAS: methylene blue active substances (anionic surfactants); TOC: total organic carbon; TDS: total dissolved solids.

Currently, approximately 45% of produced water generated from onshore activities in the United States is reused within conventional oil and gas operations for enhanced recovery in conventional oil and gas operations, and well drilling and hydraulic fracturing operations in unconventional oil and gas production [34]. Enhanced recovery techniques include injecting water or steam into the formation to maintain pressure and help sweep more oil to the production wells. Another approach for produced water management is to reuse it outside of the energy sector, such as in irrigation,

municipal, and industrial sectors, or to discharge treated produced water to surface water or to recharge groundwater. Discharges for agriculture and wildlife propagation are taking place mainly in Wyoming with limited treatment such as settling and/or skimming. In Pennsylvania, produced water usually receives limited or no treatment prior to transfer to the publicly owned treatment works, while in the Marcellus and Utica shale areas of Pennsylvania, Ohio and West Virginia, produced water is disposed via centralized waste treatment facilities by receiving various levels of treatment, from simple physical/chemical treatments to advanced treatment utilizing membranes or distillation [37].

Beneficial uses of produced water outside the energy sector will require much more intensive water treatment than that required to support hydraulic fracturing where minimal treatment (clean brine for hydraulic fracturing) is sufficient [35]. The selection of appropriate technologies should consider the produced water quality, water quality requirements for reuse options, treatment economics, and minimize impacts to environment, local water resources, and public health [10,38]. To optimize produced water reuse, fit-for-purpose treatment will be essential to minimize costs.

3. Photocatalytic Treatment of Produced Water

Photocatalysis is a recognized AOP for a variety of pollution remediations. With the irradiation of UV or visible light, a semiconductor (e.g., TiO_2) can generate hydroxyl and superoxide anion radicals; then, these radicals can mineralize a wide range of organic compounds [39–42]. Equation (1) displays the general process for organic pollutant degradation by photocatalysis. It is generally accepted that electron–hole pairs are generated on the catalyst (TiO_2) upon light absorption with light energy higher than its bandgap (Equation (2)). An electron (e^-) in a conductive band and a positive hole (h^+) in the valence band are generated as described by Equation (3). After the dissociation of the exciton, the photogenerated electron and hole migrate to energetically favorable positions. The equilibrium of charge separation depends on diffusion and drift currents, and depends strongly on the rates of charge carrier generation and recombination. Surface water molecules can catch the hole and produce a reactive hydroxyl radical ($\text{OH}\cdot$) and H^+ that delocalizes on the nearby water molecules (Equation (4)). Further reaction can lead to the creation of hydrogen peroxide (Equations (5) and (6)), which also promotes the formation of hydroxyl radicals [43,44]. The hydroxyl radical and superoxide radical anions ($\text{HOO}\cdot$) are the primary oxidizing species that can lead to oxidation of the organic compounds [45]. Moreover, the volatile constituents in produced water such as methane can be oxidized by the generated hydroxide radicals, and the main product of the photo-induced methane transformation is hydrogen [46]. Recent studies on photocatalysis treatment of produced water are summarized in Table 2.

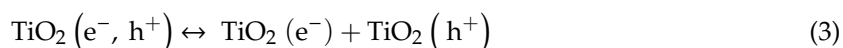


Table 2. Summary of recent studies on photocatalysis treatment of produced water.

Catalyst	System Setup	Test Solution	Characterization	Primary Results	Ref.
Photolysis/without catalyst	pH 5–9 UV 25 mL reactor	Synthetic PW Glutaraldehyde (0.1 mM) 0–300 g/L NaCl	GC–FID TOC HR–MS	■ 52–85% glutaraldehyde removal in 1 h, but majority of TOC remain	[47]
P25 TiO ₂	UVA pH 3 0.1–0.5 g/L of P25	Synthetic PW: toluene (10 mg/L), xylene (10 mg/L), naphthalene (3 mg/L), phenol (10 mg/L), acetic (150 mg/L), malonic acids (10 mg/L), seawater matrix (56 mS/cm), COD 262 mg/L, TOC 92 mg/L	TOC GC HPLC	■ <16% TOC removal in 4 h ■ No significant differences were observed in TOC removal with a higher P25 concentration	[19]
rGO-TiO ₂	slurry system 0.5 L UVA	Synthetic PW: acetic acid (150 mg/L), phenol (10 mg/L), toluene (10 mg/L), (o, m, p)-xylenes (10 mg/L) and naphthalene (3 mg/L)	TOC GC	■ Best weight ratio of rGO-TiO ₂ is 10%; 22% TOC removal in 5 h ■ Reaction rates: acetic acid < phenols < naphthalene < xylenes < toluene	[48]
ZnO	ZnO nanorod coated glass substrate	Synthesized PW: 25–150 mg/L petroleum hydrocarbons and partially hydrolyzed polyacrylamide (HPAM)	viscosity HPLC	■ The viscosity was reduced by 51% in 6 h treatment ■ 68%, 62%, 56% and 45% removal of 25, 50, 100 and 150 mg/L HPAM were measured by HPLC	[49]
TiO ₂	1.3 L UV pH 8–12 P25 3 g/L	Synthesized oil sands process waters: 100 mg/L naphthenic acids, 110 mg/L dissolved silicate, 91 mg/L colloidal SiO ₂ , 3920 mg/L NaCl	TOC	■ No difference from UV photolysis alone	[42]
TiO ₂	500 mL UVC TiO ₂ 0.1 g/L	PW: alkalinity 2.16 mg/L, PAHs 0.06 mg/L, Na 16.4 g/L, K 240 mg/L, Mg 417 mg/L, Ca 1.1 g/L, S 730 mg/L, pH 6.8, Turbidity 17.6 NTU, COD 1247 mg/L Synthesized solutions to simulate PW	GC–MS	■ A strong improvement with the addition of catalysts but the enhancement of photocatalysis was restricted by PW, particularly the aromatic compounds ■ The degradation of PAHs with high molecular weights was more sensitive to the variations of salinity and insoluble matter due to their lower solubility ■ The aromatic compounds worked as UV photon absorbers and competed with PAHs	[50]
Maghemite (γ-Fe ₂ O ₃)	pH 3–7 0–0.25 g/L catalyst 0–100 W UV 0–225 W visible light	synthetic PW: 600 mg/L BTEX	COD	■ pH has significant impact on COD removal, better performance at lower pH ■ Under pH 3, best efficiency was 95% in 5 days with visible light, 97% removal in 90 min with UV light	[51]

PW: produced water, COD: chemical oxygen demand, TOC: total organic carbon, GC–FID: gas chromatograph–flame ionization detector, HR–MS: high-resolution mass spectrometric, PAHs: polycyclic aromatic hydrocarbons, BTEX: benzene, toluene, ethyl benzene, xylene.

3.1. Decomposition and Mineralization

In the last decade, the study on photocatalytic treatment of produced water was quite limited, and most of the studies used synthetic produced water [19,42,47–50]. The target contaminants were focused on the main groups of contaminants usually present in produced water, including glutaraldehyde, toluene, xylene, naphthalene, phenol, acetic, etc. Some of them could be decomposed quickly, but the mineralization rates of all constituents remained slow. Jimenez et al. [19] investigated different AOPs (photocatalysis, Fenton, and ozonation) on synthetic produced water treatment. Among these techniques, photocatalysis was found to be the less effective for the treatment of produced water, as total organic carbon (TOC) removal was lower than 20% for the best scenario after 4 h treatment. No significant differences were observed in TOC removal at a higher P25 TiO₂ concentration. However, analysis using gas chromatograph–mass spectroscopy (GC–MS) confirmed the total abatement of smaller, volatile organic contaminants (i.e., toluene, xylene and naphthalene) and the decrease in phenol content (up to 99%). Similar comparison was conducted by Liang et al., they observed no significant reduction in TOC (for large molecular organic constituents such as oil and grease, and natural organic matter) for both TiO₂ photocatalysis and UV photolysis [42]. Graphene-like TiO₂ nanocomposites (rGO-TiO₂) exhibit higher photocatalytic activity than bare TiO₂ in the treatment of synthetic produced water containing high salinity levels and different compositions of recalcitrant dissolved organic matter. The photocatalytic reaction rates increased in the order of acetic acid < phenols < naphthalene < xylenes < toluene, but only 22% TOC removal in 5 h [48]. Partially hydrolyzed polyacrylamide (HPAM) is a commonly used polymer for enhanced oil recovery. Al-Sabahi et al. reported a new approach to use vertically aligned zinc oxide nanorods supported on substrates engineered for improving their visible light harvesting capacity for effective solar photocatalytic degradation of HPAM. After a 6 h treatment, 68%, 62%, 56%, and 45% removal of 25, 50, 100 and 150 mg/L HPAM, respectively, was reported. Mineralization was observed as 20% and 37% TOC reduction after 7 h and 14 h reaction times, respectively.

In summary, photocatalysis is demonstrated to be effective at decomposing recalcitrant organic compounds but not to achieve mineralization, which is consistent with other photocatalysis studies on water and wastewater [44,52]. For produced water treatment, it is recommended that multiple technologies be used in series operation to further reduce organic contaminants and intermediate products of photocatalysis. More attention should be paid for toxicity and biodegradability because these parameters significantly influence the design of subsequent treatment processes and overall product water quality.

3.2. Toxicity

Different approaches for acute and chronic toxicity evaluation have been applied for photocatalytically treated wastewater effluents such as bioassays with bacteria [53], seawater invertebrates [54], freshwater invertebrates [55], microalgae [53], plants (phytotoxicity) [56], and mammalian cells (genotoxicity) [57]. As reported in the majority of the studies, photocatalytic treatment is effective at decreasing toxicity of wastewater [44].

Even though the number of toxicity studies of photocatalysis increases, limited studies have mentioned toxicity evaluation for produced water treatment. The toxicity test is usually measured on the basis of the median effective concentration (EC₅₀), which is the concentration of a substance in an environmental medium expected to produce a certain effect in 50% of test organisms in a given population under a defined set of conditions. Jimenez et al. used *Vibrio fischeri* as test organisms to evaluate acute aquatic toxicity according to the basic test methodology. The results can be categorized into four classes depending on their toxicity using EC₅₀ values established by Calleja et al. [58]: class I (very toxic), EC₅₀ ≤ 25%; class II (toxic), when 25% < EC₅₀ < 75%; class III (slightly toxic), EC₅₀ = 75%; and class IV (non-toxic), EC₅₀ > 75%. The samples treated by photocatalysis ranged between 13 and 16%, which indicates that the effluent resulted somewhat less toxic than the initial produced water (EC₅₀ = 10%), in comparison with 40% for ozone and 57% for H₂O₂ [19].

Batch ozone-photocatalytic oxidation using $O_3/UV/TiO_2$ was performed in a laboratory-scale reactor to evaluate the efficiency of these processes in the degradation of contaminants and/or decrease in the ecotoxicity of produced waters of petroleum refineries [59]. The bacterial luminescence inhibition test using *Vibrio fischeri* and the fish toxicity test using juvenile guppies (*Poecilia vivipara*) were conducted in the testing laboratory. Acute toxicity tests showed a high toxicity of the raw effluents $EC_{50} < 1.55\%$, lower toxicity toward bacteria ($EC_{50} = 30.9\%$) after 60 min treatment but remained high in fish ($EC_{50} = 1.9\%$). This is because some toxics such as metals and ammonia compounds cannot be eliminated by the photocatalytic treatment, and the treated wastewater samples have significant toxicity toward the fish species, while the bacterial species was more tolerant to the photocatalytic-treated wastewater samples. Post-treatment, such as the biological treatment or the sorption process, is required for further removal of metals and ammonia compounds. Unfortunately, the study did not provide toxicity tests with single photocatalysis, as it is hard to distinguish the effect of photocatalysis from ozone, but it did demonstrate an efficient combination of photocatalysis with ozone to decrease produced water toxicity. More research on toxicity of produced water and photoinduced toxicity is needed to support the application of photocatalytic treatment technologies.

4. Factors Affecting Photocatalytic Performance

General factors affecting the photocatalytic activity, including pH, light wavelength and intensity, catalyst dosage, temperature, and concentration of salts and target contaminants, have been fully discussed in other photocatalysis reviews focusing on conventional water and wastewater treatment [43,52,60,61]. These factors either depend on the target contaminants or rely on the catalyst properties. Catalyst properties play a critical role for photocatalytic performance and, on account of limited data, they will be discussed in future research prospects (Section 5.5). Factors such as solution pH, catalyst dosage, temperature, and contaminant concentrations cannot be defined given the complexity of produced water and limited removal efficiency (as discussed in Section 2). Moreover, light wavelength and intensity are associated with the catalyst light absorption range and, in addition to high UV absorption of the aromatic compounds in the produced water (as discussed in Section 4.2), they further lower the impact of the light source on photocatalysis. Because the scope of the present work is focused on the factors affecting photocatalytic performance on treating produced water, we primarily discuss the factors that are associated with produced water chemistry.

4.1. Ionic Species in Produced Water

The presence of ionic species in produced water can affect the photocatalytic degradation [39,41]. Ionic substances such as chloride, carbonate, bicarbonate, nitrate, nitrite, and phosphate ions can affect photoelectrons generation, electron–hole recombination, and hydroxyl radical scavenging. The reaction of hydroxyl radical with chloride, carbonate and bicarbonate ions can be described in the following equations [43]:



Among these inorganic anions, chloride ions can play a detrimental effect on photocatalytic treatment by scavenging holes and hydroxyl radicals, given rise to the generation of less reactive chloride radical ($Cl\cdot$) and dichloride radicals (Cl_2^-) (Equations (10)–(12)) [62].



4.2. Organics in Produced Water

Organics are one of the prominent inhibitors for produced water treatment. Because photocatalysis is a combined process of adsorption and degradation, the existence of organics in produced water can affect removal efficacy of these two processes. The organic matter can prevent the breakdown of contaminants through site blockage, hydroxyl scavenging, and light absorption [63]. Recalcitrant compounds present in produced water, such as acetic acid and toluene, have a low reaction rate with radicals, which makes them refractory and hard to decompose [19]. Studies treating recalcitrant-to-OH-radicals components, such as acetic acid, phenol, and naphthalene, in produced water, are scarce and the removal efficiencies were reported to be low [48]. Catechol, dihydroxy benzenes, hydroquinone, and resorcinol were found to hinder severely photocatalytic reactions [64]. It was reported that some wastewater-derived organic matter could scavenge up to 95% of hydroxyl radicals [65]. The effects of insoluble particulate matter and organic composition of produced water on photocatalytic performance were evaluated by Liu et al. [50]. The organic composition was found the more likely factor retarding the breakdown of PAHs. In addition, the aromatic compounds played a key role in absorbing UV photons owing to their abundance and UV sensitivity. Moreover, the aromatic species can compete with PAHs for adsorption sites and activated species during the photocatalytic process. Hence, aromatic substances of high concentrations could significantly reduce the overall photocatalytic activity.

5. Future Research Perspectives

As shown in Figure 1, interests in photocatalytic treatment of produced water are growing remarkably, but only a few studies are employing photocatalysis into produced water treatment, as summarized in Table 2. Hence, more research is required to evaluate photocatalytic performance in produced water treatment. Future research directions are suggested in this section.

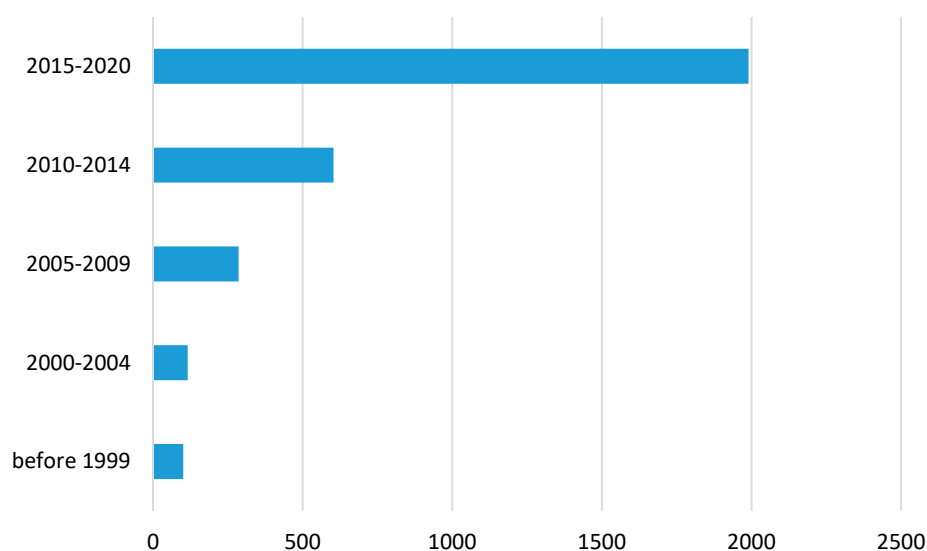


Figure 1. Number of publications mentioning photocatalysis and produced water. Data collected from Google Scholar.

5.1. Biodegradability Improved with Photocatalysis

As discussed in Section 3.1, photocatalysis could not achieve complete removal of TOC from produced water as a stand-alone treatment process. Photocatalysis can be coupled with other treatment processes such as the biological treatment to increase the treatment efficiency of both processes [60,66]. The nonselective reactivity of radicals on the non-biodegradable water-soluble pollutants determines that the photocatalytic process can be used effectively as a pre-treatment step to enhance biodegradation

of recalcitrant organic pollutants prior to biological water treatment. Hence, future work should focus more on demonstrating its efficiency in degrading a wide range of ambiguous refractory organics into readily biodegradable compounds, instead of achieving mineralization to innocuous carbon dioxide and water.

The biodegradability can be measured by the ratio of biochemical oxygen demand (BOD) and chemical oxygen demand (COD), where a low ratio represents low biodegradability of the organic compounds present in the solution. The BOD/COD ratio of produced water can be less than 0.1 [67], indicating the non-degradability properties of the produced water and the requirement of advanced treatment. The increase in biodegradability, i.e., a higher BOD/COD ratio, suggests macromolecular and bio-refractory organic matter could have been degraded to smaller molecules and become more biodegradable. The BOD/COD ratio can be used as a simple, straightforward indicator for photocatalysis to exhibit a great contribution to the biodegradability improvement of produced water, making the produced water more suitable for microbial growth.

5.2. Toxicity of Catalysts

The concerns regarding catalyst toxicity as engineered nanomaterials have risen in recent years towards the potential risks and toxicology to human health and the environment. This is associated with the fact that photocatalytic nanoparticles (e.g., TiO₂ nanoparticles) have been widely used in personal care products, such as sunscreens and chewing gums. There are increasing concerns regarding the potential risks of the nanoparticles to human health due to the direct and repeated exposure [68]. Debates are further powered by complaints and warnings from toxicologist and researchers all over the world that arise from the challenges related to the toxicity assessment of nanomaterials [68]. In addition, not all the synthesized materials have been considered in toxicity studies and the juvenility of nanotechnology impedes realistic exposure scenarios.

In the last decade, the number of publications studying toxicity of nanomaterials has increased continuously. TiO₂ nanoparticles have shown a toxic effect on numerous organisms and cell lines, including algae [69,70], bacteria [71–73], fungi [74], human keratinocytes [75,76], and water organisms like *Daphnia magna* [77,78] and fish [79,80]. In most of the studies, toxicity relied on nanoparticle concentration as well as irradiation intensity and duration. Phototoxicity was also reported on CuO [81], ZnO [69], and CdSe/ZnSe quantum dots [82] when they were irradiated with UV-containing light.

Friehs et al. reviewed photocatalytically active nanoparticles extensively for numerous environmental and energy related applications [68]. They summarized two main mechanisms of phototoxic effect on living organism: the production of reactive oxygen species and the dissolution of metal ions [83]. However, most phototoxicity studies are focused on TiO₂, mainly P25, and there was also a limited species diversity in nanotoxicity studies [84]. Only a small amount of the materials and the respective doping, coatings or other modifications that alter their physicochemical properties have been studied. Moreover, the high number of parameters that can influence the outcome of experiments may lead to inconsistent and conflicting data [85], thereby not allowing meaningful extrapolation of the conclusions to other nanomaterials. Therefore, toxicity of catalysts should be carefully investigated to ensure safe application of photocatalysis and other AOPs to produced water treatment.

5.3. Photoinduced Intermediates

To evaluate the suitability and niche of photocatalysis in produced water treatment trains, there is a great need to understand the toxicity of the intermediates generated during photocatalysis. Meanwhile, the identification of key photoinduced intermediates can help fully elucidate the reaction mechanism. The detection of intermediates can be achieved by conducting high-performance liquid chromatography with tandem mass spectrometry (LC–MS/MS) analysis, which can qualitatively and quantitatively determine the organic intermediates even at trace concentrations. Several research groups have studied the photochemical and photocatalytic degradation of various organic contaminants, including pharmaceuticals (e.g., ibuprofen, metoprolol) [40,86], insecticide (e.g., thiacloprid) [87], phenol [88],

4-chlorophenol [89], etc. To the best of our knowledge, to date, there is no study on the detection of intermediate products for produced water treatment.

Intensive attention has been devoted to the characterization of organic compounds in produced water in recent years. There are several advanced analytical techniques for characterizing and quantifying dissolved organic matter, including gas chromatography coupled with flame ionization detector (GC-FID), thermal conductivity detector (GC-TCD) or mass spectrometry (GC-MS) and liquid chromatography (LC) coupled with UV diode array detector (LC-UV), organic carbon detection (LC-OCD) or mass spectrometry (LC-MS). GC-based methods are extensively used for analysis of volatile and semivolatile compounds, including natural gas constituents (methane and ethane), BTEX (benzene, toluene, ethyl benzene, xylene), and diesel-range semivolatile organics. LC-based techniques are more suitable for non-volatile organic compounds, such as surfactants, fatty amines, and high molecular weight ionic polyacrylamide friction reducers [90]. Mass spectrometry (MS) is the most powerful detector to characterize complex fluids and has been extensively used for PW analysis. It can provide qualitative and quantitative information about the analytes with the help of standards or mass spectral libraries. Tandem high-resolution mass spectrometry (HRMS/MS) can provide crucial information to elucidate the elemental composition and structure of the compounds in the sample. The mostly widely used HRMS/MS includes quadrupole-time of flight mass analyzer (Q-ToF), orbitrap mass analyzer, and Fourier transform ion cyclotron resonance mass spectrometry (FT-ICR-MS).

Nontarget analysis is a critical tool to identify the intermediates due to their “unknown” property. Nontarget analysis heavily relies on HSMS/MS, such as Q-ToF, Orbitrap mass analyzer, and FT-ICR-MS. This approach requires no prior information about the unknown chemicals in the sample. The basic procedure for nontarget analysis is first to collect the mass spectra of unknown chemicals, and data processing techniques are used to assign potential molecular formula [91,92]. Chemical structure identification is achieved by database spectra-searching or matching the MS/MS spectra and retention time with reference standards. HSMS/MS has been used to identify the degraded products of organic compounds in produced water during hydraulic fracturing and biological treatments [93,94].

5.4. Photo-Detoxication of Heavy Metals

Photocatalysis has been demonstrated to convert the ionic species into their metallic solid form and deposit them over the semiconductor surface or transform them into less toxic soluble species. When a transformation to the zero-valent state is possible, this allows the recovery of the metal from the water, with an economic return [29,30]. Produced water contains heavy metals such as mercury and lead, as well as metalloids such as arsenic, in varied concentrations depending on formation geology and age of the well [1,95]. Concentrations of heavy metals in produced water are usually higher than those found in sea water; commonly studied metals include Ba, Cd, Cr, Cu, Pb, Hg, Ni, Ag, and Zn [3,95,96]. Produced water contains other trace metals, including Al, B, Fe, Li, Mn, Se, and Sr. Certain metals are of particular environmental concern as they may bioaccumulate and/or be toxic [96]. Although heavy metals are not primary contaminants of produced water, photo-detoxication of heavy metals can reduce the toxicity of produced water and facilitate reuse applications.

Heavy metals such as hexavalent chromium (Cr(VI)) present the highest environmental threat due to their toxicity for biological organisms together with their high solubility and mobility, while Cr(III) is considered non-toxic or of very low toxicity, and their mobility is lower than those of Cr(VI) [97]. The removal of Cr(VI) by photocatalytic-induced reduction reaction is highly efficient and environmentally friendly. A number of studies have been published on the photocatalytic reduction in Cr(VI) employing TiO₂, modified TiO₂, and other semiconductors, such as ZnO, CdS, ZnS, and WO₃, which have already been described in other reviews [98–100]. Another example of metalloids is arsenic, which mainly comes from natural sources due to dissolution of minerals in surface or groundwaters or volcanic processes [101,102]. Previous studies demonstrated that photocatalytic treatment is an efficient approach to promote oxidation of arsenite(III) to arsenate(V) [103]. Transformation to As(V) makes it easier to use conventional technologies, e.g., ion exchange and adsorption [30]. Nevertheless,

to date, limited research on heavy metal treatment from produced water has been reported. The toxicity of heavy metals in produced water is another concern for future produced water management.

5.5. Catalysts

As shown in Table 2, almost all photocatalytic treatments of produced water have been reported to be low in efficiency and require a longer reaction time (e.g., in hours). Various strategies have been adopted to improve the electron–hole pair recombination and narrow the band gap to widen the absorbance from UV to visible light range. However, the main reasons for low photocatalytic efficiency in produced water could be attributed to low efficiency of illumination and quick poisoning of catalysts. Given the complex composition of produced water, light transfer could be limited by the suspended solids and absorbing and scattering liquid to the catalyst. In addition, a large number of constituents could accumulate on the catalysts surface and further reduce the light reaching the catalysts, resulting in low efficiency and catalyst inactivation. Therefore, photocatalysis is not effective when applied to raw produced water and requires a certain level of pre-treatment.

Another option is to enhance the surface area of catalysts that provides a larger illuminated surface to absorb light. The suspended configuration is related to a high volumetric generation rate of reactive oxygen species in proportion to the active sites of catalysts used in suspension [103]. Still, a supplementary system to separate catalysts from the treated water needs a new process to overcome catalyst loss and its introduction into the environment. Immobilized configuration eliminates the subsequent separation system, but the light reflection by the photocatalyst support and the reduced amount of the active site together with the enlarged mass transfer limitation poses a serious concern that needs to be addressed.

A third option is to eliminate the constraints associated with operating parameters. Since the chemical composition and pH of produced water varies considerably from formation to formation and well to well, efforts should be made in the area of catalyst modification for a wide range of operating conditions, such as temperature, pH and contaminant concentrations. The impact of modification methods on catalyst properties cannot be ignored. The hydrothermally prepared catalysts often contain physisorbed and lattice water, which may contribute to the efficiency of photocatalysts, and lattice water may help the separation of the electron–hole pairs [104,105]. It has also been reported that there are cationic impurities in the lattice on the electronic properties of synthesized catalysts [106,107]. Practice reveals the controversial results of metal-doping catalysts, which can be explained by the competing processes of photogeneration and recombination of electron and hole pairs [104,108]. Additionally, research should also be conducted on semiconductor modifications to achieve a self-cleaning capability. Modification of catalysts can optimize interactions of catalyst particles and organic pollutants, thus resisting contaminant accumulation on the catalyst's surface and reducing the risk of catalyst poison.

6. System Integration

High concentrations of ionic species and recalcitrant organics in produced water require a holistic treatment solution with the consideration of an integrated multiple processes approach. Light absorption and scattering in produced water can significantly reduce the irradiation reception of a catalyst. In order to enhance the photocatalytic performance in treating produced water, physical separation processes, such as an oil–water separator, a coalescer or hydrocyclones, are required to eliminate suspended solids, oil and grease [109].

After physical separation, biological processes can be employed to further reduce organic constituents in produced water effluent [110]. However, due to the complexity of produced water, some constituents are difficult to be removed biologically and often persist after a conventional secondary biological treatment. Photocatalysis can breakdown residual compounds in many industrial wastewaters that are hardly biodegradable [111]. Therefore, a combination of photocatalysis with

the biological treatment is suggested to minimize treatment costs and improve the overall treatment efficiency, as shown in Figure 2.

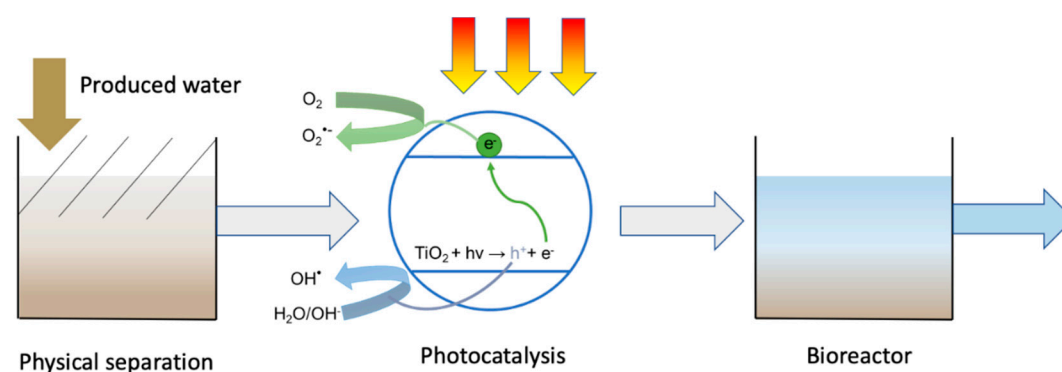


Figure 2. Proposed produced water treatment train.

Although the combination of photocatalysis and biodegradation has been proved to be effective in wastewater treatment [111–114], the application in produced water is still quite limited with only one reported study thus far. Correa et al. investigated the efficiency of an ozone-photocatalyzed $O_3/UV/TiO_2$ oxidation process followed by biological remediation for produced water treatment. The result was promising—after a 5 min $O_3/UV/TiO_2$ oxidation process, phenol concentration decreased by 99.9%, sulfide by 53.0%, COD by 37.7%, oil and grease by 5.2%, and ammonia by 1.9%, while after 60 min of oxidation treatment, the removal efficiency increased to 99.9% for phenols, 98.2% for oil and grease, 97.2% for sulfide, 89.2% for COD, and 15% for ammonia. The acute toxicity tests with the bacterium *Vibrio fischeri* and the fish *Poecilia vivipara* revealed that produced water presented a high toxicity ($EC_{50} < 1.55\%$ for both species). The combined oxidation and biological process showed a significant toxicity reduction with $EC_{50} = 89.2\%$ for bacteria and $EC_{50} = 85.7\%$ for fish [59].

The concept of a physical separation (photocatalysis) biotreatment would not only improve the activity of the biological treatment, but also improve the water quality of product water by toxicity reduction. In addition, photocatalysis can be also used as a post-treatment to polish the product water quality by degrading organic residuals. More research is required to further prove the feasibility of the combined system for produced water treatment.

7. Conclusions

In order to meet the needs of environmental regulations as well as reuse and recycling of produced water, extensive efforts have been devoted to investigating produced water treatment technologies. In produced water treatment, no single technology can meet suitable water quality requirements, therefore, multiple technologies have to be used to remove a wide range of contaminants. Choice of the best technology depends on the chemistry of the produced water, cost effectiveness, space availability, reuse and discharge plans, durable operation, and byproducts. Photocatalysis is a promising destructive technology due to low or no chemical consumption and no waste sludge production during the treatment. Studies on photocatalytic oxidation of produced water are quite limited, and there is a lack of a comprehensive understanding of the applicability of photocatalysis and the strategies to improve the treatment efficacy. The objective of the present work is to critically review the feasibility of photocatalysis-involved treatment solutions and factors affecting produced water treatment.

Photocatalytic activity can be significantly impacted by the aqueous chemistry of produced water. Ionic substances, such as chloride, carbonate, bicarbonate, nitrate, nitrite, and phosphate ions, can affect photoelectrons generation, electron–hole recombination and hydroxyl radical scavenging. However, ionic strength caused by chloride, calcium, magnesium, and sulfate can change the type and concentration of adsorption sites and the electrostatic interactions in the interface of a solution

and catalyst. High organic contents are one of the prominent inhibitors for produced water treatment through site blockage, hydroxyl scavenging, and light adsorption. In order to enhance the photocatalytic performance in treating produced water, conventional physical separation processes are required to eliminate suspended solids, oil and grease.

Research on photocatalytic treatment of produced water is very limited, and most studies used synthetically produced water. The results revealed that photocatalysis was effective at decomposing recalcitrant organic compounds but not for achieving mineralization. Therefore, photocatalysis can be used as a pretreatment with other treatment processes such as biological treatments to partially reduce TOC, break down macromolecular organic compounds, increase biodegradability, and reduce the toxicity of produced water. Photocatalysis can be also used as a post-treatment to polish the product water quality by removing contaminant residuals. In addition, there is a research need for the modification of photocatalysts that are adaptive and flexible for a wide range of operating conditions, with an improved specific surface area and self-cleaning capability.

Author Contributions: L.L., W.J., L.C., P.X. and H.W. wrote the original draft and reviewed and edited the manuscript. H.W. and P.X. acquired research funding. H.W. managed the research project. All authors have read and agreed to the published version of the manuscript.

Funding: The authors thank the United States Bureau of Reclamation Desalination and Water Purification Research and Development Program (Agreement No. R19AC00109) and ExxonMobil Upstream Research Company for financial support of the research.

Conflicts of Interest: The authors declare no conflict of interest. The funders had no responsibility in the design of the study; in the collection, analyses, or interpretation of data; in the writing of the manuscript, or in the decision to publish the results.

References

1. Fakhru’L-Razi, A.; Pendashteh, A.; Abdullah, L.C.; Biak, D.R.A.; Madaeni, S.S.; Abidin, Z.Z. Review of technologies for oil and gas produced water treatment. *J. Hazard. Mater.* **2009**, *170*, 530–551. [[CrossRef](#)]
2. Arthur, J.D.; Langhus, B.G.; Patel, C. *Technical Summary of Oil & Gas Produced Water Treatment Technologies*; All Consulting, LLC: Tulsa, OK, USA, 2005.
3. Igunnu, E.T.; Chen, G.Z. Produced water treatment technologies. *Int. J. Low Carbon Technol.* **2012**, *9*, 157–177. [[CrossRef](#)]
4. Xu, P.; Drewes, J.E. Viability of nanofiltration and ultra-low pressure reverse osmosis membranes for multi-beneficial use of methane produced water. *Sep. Purif. Technol.* **2006**, *52*, 67–76. [[CrossRef](#)]
5. Xu, P.; Drewes, J.E.; Heil, D. Beneficial use of co-produced water through membrane treatment: Technical-economic assessment. *Desalination* **2008**, *225*, 139–155. [[CrossRef](#)]
6. Hickenbottom, K.L.; Hancock, N.T.; Hutchings, N.R.; Appleton, E.W.; Beaudry, E.G.; Xu, P.; Cath, T.Y. Forward osmosis treatment of drilling mud and fracturing wastewater from oil and gas operations. *Desalination* **2013**, *312*, 60–66. [[CrossRef](#)]
7. Stoll, Z.A.; Forrestal, C.; Ren, Z.J.; Xu, P. Shale gas produced water treatment using innovative microbial capacitive desalination cell. *J. Hazard. Mater.* **2015**, *283*, 847–855. [[CrossRef](#)]
8. Hu, L.; Yu, J.; Luo, H.; Wang, H.; Xu, P.; Zhang, Y. Simultaneous recovery of ammonium, potassium and magnesium from produced water by struvite precipitation. *Chem. Eng. J.* **2020**, *382*, 123001. [[CrossRef](#)]
9. Rodriguez, A.Z.; Wang, H.; Hu, L.; Zhang, Y.; Xu, P. Treatment of Produced Water in the Permian Basin for Hydraulic Fracturing: Comparison of Different Coagulation Processes and Innovative Filter Media. *Water* **2020**, *12*, 770. [[CrossRef](#)]
10. Geza, M.; Ma, G.; Kim, H.; Cath, T.Y.; Xu, P. iDST: An integrated decision support tool for treatment and beneficial use of non-traditional water supplies—Part I. Methodology. *J. Water Process. Eng.* **2018**, *25*, 236–246. [[CrossRef](#)]
11. Dores, R.; Hussain, A.; Katebah, M.; Adham, S.S. Using Advanced Water Treatment Technologies to Treat Produced Water from the Petroleum Industry. In Proceedings of the SPE International Production and Operations Conference & Exhibition, Doha, Qatar, 14–16 May 2012.

12. Hussain, A.; Minier-Matar, J.; Janson, A.; Gharfeh, S.; Adham, S. Advanced technologies for produced water treatment and reuse. In Proceedings of the International Petroleum Technology Conference, European Association of Geoscientists & Engineers, Doha, Qatar, 19–22 January 2014; No. 1. pp. 1–11.
13. Munirasu, S.; Abu Haija, M.; Banat, F. Use of membrane technology for oil field and refinery produced water treatment—A review. *Process. Saf. Environ. Prot.* **2016**, *100*, 183–202. [[CrossRef](#)]
14. Alzahrani, S.; Mohammad, A.W. Challenges and trends in membrane technology implementation for produced water treatment: A review. *J. Water Process. Eng.* **2014**, *4*, 107–133. [[CrossRef](#)]
15. Boschee, P. Handling Produced Water from Hydraulic Fracturing. *Oil Gas Facil.* **2012**, *1*, 22–26. [[CrossRef](#)]
16. Jiménez, S.; Micó, M.M.; Arnaldos, M.; Medina, F.; Contreras, S. State of the art of produced water treatment. *Chemosphere* **2018**, *192*, 186–208. [[CrossRef](#)] [[PubMed](#)]
17. Butkovskiy, A.; Bruning, H.; Kools, S.A.; Rijnaarts, H.; Van Wezel, A.P. Organic Pollutants in Shale Gas Flowback and Produced Waters: Identification, Potential Ecological Impact, and Implications for Treatment Strategies. *Environ. Sci. Technol.* **2017**, *51*, 4740–4754. [[CrossRef](#)] [[PubMed](#)]
18. Pendashteh, A.; Fakhru’L-Razi, A.; Chuah, T.; Radiah, A.D.; Madaeni, S.; Zurina, Z. Biological treatment of produced water in a sequencing batch reactor by a consortium of isolated halophilic microorganisms. *Environ. Technol.* **2010**, *31*, 1229–1239. [[CrossRef](#)] [[PubMed](#)]
19. Jiménez, S.; Andreozzi, M.; Micó, M.M.; Álvarez, M.G.; Contreras, S. Produced water treatment by advanced oxidation processes. *Sci. Total Environ.* **2019**, *666*, 12–21. [[CrossRef](#)] [[PubMed](#)]
20. Saba, B. Potential Treatment Options for Hydraulic Fracturing Return Fluids: A Review. *ChemBioEng Rev.* **2014**, *1*, 273–279. [[CrossRef](#)]
21. Abousnina, R.M.; Nghiem, L.D.; Bundschuh, J. Comparison between oily and coal seam gas produced water with respect to quantity, characteristics and treatment technologies: A review. *Desalin. Water Treat.* **2014**, *54*, 1793–1808. [[CrossRef](#)]
22. Estrada, J.M.; Bhamidimarri, R. A review of the issues and treatment options for wastewater from shale gas extraction by hydraulic fracturing. *Fuel* **2016**, *182*, 292–303. [[CrossRef](#)]
23. Xu, P.; Stoll, Z.; Ma, G.; Geza, M.; Cath, T.Y.; Drewes, J. *Technical Assessment of Produced Water Treatment Technologies. An Integrated Framework for Treatment and Management of Produced Water*; Final Report to Department of Energy Project 11122-53; New Mexico State University-Colorado School of Mines: Las Cruces, NM, USA; Golden, CO, USA, 2016.
24. Kanakaraju, D.; Glass, B.D.; Oelgemöller, M. Advanced oxidation process-mediated removal of pharmaceuticals from water: A review. *J. Environ. Manag.* **2018**, *219*, 189–207. [[CrossRef](#)]
25. Ely, J.W.; Fraim, M.; Horn, A.D.; Jakhete, S.D. Game changing technology for treating and recycling frac water. In Proceedings of the SPE Annual Technical Conference and Exhibition, Denver, CO, USA, 30 October–2 November 2011.
26. Lin, L.; Wang, H.; Xu, P. Immobilized TiO₂-reduced graphene oxide nanocomposites on optical fibers as high performance photocatalysts for degradation of pharmaceuticals. *Chem. Eng. J.* **2017**, *310*, 389–398. [[CrossRef](#)]
27. Lin, L.; Wang, H.; Jiang, W.; Mkaouar, A.R.; Xu, P. Comparison study on photocatalytic oxidation of pharmaceuticals by TiO₂-Fe and TiO₂-reduced graphene oxide nanocomposites immobilized on optical fibers. *J. Hazard. Mater.* **2017**, *333*, 162–168. [[CrossRef](#)] [[PubMed](#)]
28. Lin, L.; Wang, H.; Luo, H.; Xu, P. Enhanced photocatalysis using side-glowing optical fibers coated with Fe-doped TiO₂ nanocomposite thin films. *J. Photochem. Photobiol. A: Chem.* **2015**, *307*, 88–98. [[CrossRef](#)]
29. Braslavsky, S.E.; Braun, A.M.; Cassano, A.E.; Emeline, A.V.; Litter, M.I.; Palmisano, L.; Parmon, V.N.; Serpone, N. Glossary of terms used in photocatalysis and radiation catalysis (IUPAC Recommendations 2011). *Pure Appl. Chem.* **2011**, *83*, 931–1014. [[CrossRef](#)]
30. Litter, M.I. Mechanisms of removal of heavy metals and arsenic from water by TiO₂-heterogeneous photocatalysis. *Pure Appl. Chem.* **2015**, *87*, 557–567. [[CrossRef](#)]
31. Veil, J. *U.S. Produced Water Volumes and Management Practices in 2012*; Ground Water Protection Council: Oklahoma City, OK, USA, 2015; Available online: http://www.veilenvironmental.com/publications/pw/final_report_CO_note.pdf (accessed on 1 August 2020).
32. U.S. EIA. *Annual Energy Outlook 2019: With Projections to 2050*; US Energy Information Administration Office of Energy Analysis, U.S. Department of Energy: Washington, DC, USA, 2019. Available online: <https://www.eia.gov/outlooks/aeo/pdf/aeo2019.pdf> (accessed on 1 August 2020).

33. U.S. EIA. *Drilling Productivity Report*; US Energy Information Administration Independent Statistics & Analysis: Washington, DC, USA, 2020. Available online: <https://www.eia.gov/petroleum/drilling/> (accessed on 1 August 2020).
34. Produced Water Report: Regulations, Current Practices, and Research Needs. 2019. Available online: <http://www.gwpc.org/sites/default/files/files/Produced%20Water%20Full%20Report%20-%20Digital%20Use.pdf> (accessed on 1 August 2020).
35. Scanlon, B.R.; Reedy, R.C.; Xu, P.; Engle, M.A.; Nicot, J.; Yoxtheimer, D.; Yang, Q.; Ikonnikova, S. Can we beneficially reuse produced water from oil and gas extraction in the U.S.? *Sci. Total Environ.* **2020**, *717*, 137085. [[CrossRef](#)]
36. Chaudhary, B.K.; Sabie, R.; Engle, M.A.; Xu, P.; Willman, S.; Carroll, K.C. Spatial variability of produced-water quality and alternative-source water analysis applied to the Permian Basin, USA. *Hydrogeol. J.* **2019**, *27*, 2889–2905. [[CrossRef](#)]
37. Study of Oil and Gas Extraction Wastewater Management under the Clean Water Act. 2019. Available online: https://www.epa.gov/sites/production/files/2019-05/documents/oil-and-gas-study_draft_05-2019.pdf (accessed on 1 August 2020).
38. Ma, G.; Geza, M.; Cath, T.Y.; Drewes, J.E.; Xu, P. iDST: An integrated decision support tool for treatment and beneficial use of non-traditional water supplies—Part II. Marcellus and Barnett Shale case studies. *J. Water Process. Eng.* **2018**, *25*, 258–268. [[CrossRef](#)]
39. Lin, L.; Jiang, W.; Nasr, M.; Bechelany, M.; Miele, P.; Wang, H.; Xu, P.; Lu, L. Enhanced visible light photocatalysis by TiO₂-BN enabled electrospinning of nanofibers for pharmaceutical degradation and wastewater treatment. *Photochem. Photobiol. Sci.* **2019**, *18*, 2921–2930. [[CrossRef](#)]
40. Lin, L.; Jiang, W.; Bechelany, M.; Nasr, M.; Jarvis, J.; Schaub, T.; Sapkota, R.R.; Miele, P.; Wang, H.; Xu, P. Adsorption and photocatalytic oxidation of ibuprofen using nanocomposites of TiO₂ nanofibers combined with BN nanosheets: Degradation products and mechanisms. *Chemosphere* **2019**, *220*, 921–929. [[CrossRef](#)]
41. Lin, L.; Wang, H.; Luo, H.; Xu, P. Photocatalytic Treatment of Desalination Concentrate Using Optical Fibers Coated With Nanostructured Thin Films: Impact of Water Chemistry and Seasonal Climate Variations. *Photochem. Photobiol.* **2016**, *92*, 379–387. [[CrossRef](#)] [[PubMed](#)]
42. Liang, X.; Zhu, X.; Butler, E.C. Comparison of four advanced oxidation processes for the removal of naphthenic acids from model oil sands process water. *J. Hazard. Mater.* **2011**, *190*, 168–176. [[CrossRef](#)] [[PubMed](#)]
43. Ahmad, R.; Ahmad, Z.; Khan, A.U.; Mastoi, N.R.; Aslam, M.; Kim, J. Photocatalytic systems as an advanced environmental remediation: Recent developments, limitations and new avenues for applications. *J. Environ. Chem. Eng.* **2016**, *4*, 4143–4164. [[CrossRef](#)]
44. Rueda-Marquez, J.J.; Levchuk, I.; Ibañez, P.F.; Sillanpää, M. A critical review on application of photocatalysis for toxicity reduction of real wastewaters. *J. Clean. Prod.* **2020**, *258*, 120694. [[CrossRef](#)]
45. Kiss, J.; Kukovecz, Á.; Kónya, Z. Beyond Nanoparticles: The Role of Sub-nanosized Metal Species in Heterogeneous Catalysis. *Catal. Lett.* **2019**, *149*, 1441–1454. [[CrossRef](#)]
46. László, B.; Baán, K.; Varga, E.; Oszkó, A.; Erdőhelyi, A.; Konya, Z.; Kiss, J. Photo-induced reactions in the CO₂-methane system on titanate nanotubes modified with Au and Rh nanoparticles. *Appl. Catal. B: Environ.* **2016**, *199*, 473–484. [[CrossRef](#)]
47. Hong, S.; Ratpukdi, T.; Sivaguru, J.; Khan, E. Photolysis of glutaraldehyde in brine: A showcase study for removal of a common biocide in oil and gas produced water. *J. Hazard. Mater.* **2018**, *353*, 254–260. [[CrossRef](#)]
48. Andreozzi, M.; Álvarez, M.; Contreras, S.; Medina, F.; Clarizia, L.; Vitiello, G.; Llorca, J.; Marotta, R. Treatment of saline produced water through photocatalysis using rGO-TiO₂ nanocomposites. *Catal. Today* **2018**, *315*, 194–204. [[CrossRef](#)]
49. Al-Sabahi, J.; Bora, T.; Claereboudt, M.; Al-Abri, M.; Dutta, J. Visible light photocatalytic degradation of HPAM polymer in oil produced water using supported zinc oxide nanorods. *Chem. Eng. J.* **2018**, *351*, 56–64. [[CrossRef](#)]
50. Liu, B.; Chen, B.; Zhang, B.; Jing, L.; Zhang, H.; Lee, K. Photocatalytic Degradation of Polycyclic Aromatic Hydrocarbons in Offshore Produced Water: Effects of Water Matrix. *J. Environ. Eng.* **2016**, *142*, 04016054. [[CrossRef](#)]
51. Sheikholeslami, Z.; Kebria, D.Y.; Qaderi, F. Investigation of photocatalytic degradation of BTEX in produced water using γ -Fe₂O₃ nanoparticle. *J. Therm. Anal. Calorim.* **2018**, *135*, 1617–1627. [[CrossRef](#)]

52. Ahmed, S.N.; Haider, W. Heterogeneous photocatalysis and its potential applications in water and wastewater treatment: A review. *Nanotechnology* **2018**, *29*, 342001. [CrossRef] [PubMed]
53. He, Y.; Gao, Y.; Zhang, X.; Dong, Y. Construction of the elements based on lifted multiwavelet and its applications. *Integr. Ferroelectr.* **2016**, *172*, 132–141. [CrossRef]
54. Hasegawa, M.C.; Daniel, J.F.D.S.; Takashima, K.; Batista, G.A.; Da Silva, S.M.C.P. COD removal and toxicity decrease from tannery wastewater by zinc oxide-assisted photocatalysis: A case study. *Environ. Technol.* **2014**, *35*, 1589–1595. [CrossRef] [PubMed]
55. Çifçi, D.I.; Meric, S.; Optimization of Suspended photocatalytic treatment of two biologically treated textile effluents using TiO₂ and ZnO catalysts. *Glob. NEST J.* **2015**, *17*, 653–663. Available online: https://journal.gnest.org/sites/default/files/Submissions/gnest_01715/gnest_01715_published.pdf (accessed on 1 August 2020).
56. Tsoumachidou, S.; Velegraki, T.; Antoniadis, A.; Poullos, I. Greywater as a sustainable water source: A photocatalytic treatment technology under artificial and solar illumination. *J. Environ. Manag.* **2017**, *195*, 232–241. [CrossRef]
57. Saverini, M.; Catanzaro, I.; Sciandrello, G.; Avellone, G.; Indelicato, S.; Marci, G.; Palmisano, L. Genotoxicity of citrus wastewater in prokaryotic and eukaryotic cells and efficiency of heterogeneous photocatalysis by TiO₂. *J. Photochem. Photobiol. B Biol.* **2012**, *108*, 8–15. [CrossRef]
58. Calleja, A.; Baldasano, J.M.; Mulet, A. Toxicity analysis of leachates from hazardous wastes via microtox and daphnia magna. *Environ. Toxicol. Water Qual.* **1986**, *1*, 73–83. [CrossRef]
59. Corrêa, A.X.; Tiepo, E.N.; Somensi, C.A.; Sperb, R.M.; Radetski, C.M. Use of ozone-photocatalytic oxidation (O₃/UV/TiO₂) and biological remediation for treatment of produced water from petroleum refineries. *J. Environ. Eng.* **2010**, *136*, 40–45. [CrossRef]
60. Chong, M.N.; Jin, B.; Chow, C.; Saint, C.; Saint, C. Recent developments in photocatalytic water treatment technology: A review. *Water Res.* **2010**, *44*, 2997–3027. [CrossRef]
61. Sundar, K.P.; Kanmani, S. Progression of Photocatalytic reactors and it's comparison: A Review. *Chem. Eng. Res. Des.* **2020**, *154*, 135–150. [CrossRef]
62. Sirtori, C.; Agüera, A.; Gernjak, W.; Malato, S. Effect of water-matrix composition on Trimethoprim solar photodegradation kinetics and pathways. *Water Res.* **2010**, *44*, 2735–2744. [CrossRef] [PubMed]
63. Katz, A.; McDonagh, A.; Tijng, L.D.; Shon, H.K. Fouling and inactivation of titanium dioxide-based photocatalytic systems. *Crit. Rev. Environ. Sci. Technol.* **2015**, *45*, 1880–1915. [CrossRef]
64. Rincón, A. Effect of pH, inorganic ions, organic matter and H₂O₂ on E. coli K12 photocatalytic inactivation by TiO₂ Implications in solar water disinfection. *Appl. Catal. B Environ.* **2004**, *51*, 283–302. [CrossRef]
65. Keen, O.; McKay, G.; Mezyk, S.; Linden, K.G.; Rosario-Ortiz, F.L. Identifying the factors that influence the reactivity of effluent organic matter with hydroxyl radicals. *Water Res.* **2014**, *50*, 408–419. [CrossRef]
66. Nogueira, A.A.; Bassin, J.P.; Cerqueira, A.C.; Dezotti, M. Integration of biofiltration and advanced oxidation processes for tertiary treatment of an oil refinery wastewater aiming at water reuse. *Environ. Sci. Pollut. Res.* **2016**, *23*, 9730–9741. [CrossRef]
67. Liu, P.; Ren, Y.; Ma, W.; Ma, J.; Du, Y. Degradation of shale gas produced water by magnetic porous MFe₂O₄ (M = Cu, Ni, Co and Zn) heterogeneous catalyzed ozone. *Chem. Eng. J.* **2018**, *345*, 98–106. [CrossRef]
68. Friehs, E.; AlSalka, Y.; Jonczyk, R.; Lavrentieva, A.; Jochums, A.; Walter, J.-G.; Stahl, F.; Scheper, T.; Bahnemann, D.W. Toxicity, phototoxicity and biocidal activity of nanoparticles employed in photocatalysis. *J. Photochem. Photobiol. C Photochem. Rev.* **2016**, *29*, 1–28. [CrossRef]
69. Lee, W.-M.; An, Y.-J. Effects of zinc oxide and titanium dioxide nanoparticles on green algae under visible, UVA, and UVB irradiations: No evidence of enhanced algal toxicity under UV pre-irradiation. *Chemosphere* **2013**, *91*, 536–544. [CrossRef]
70. Miller, R.; Bennett, S.; Keller, A.A.; Pease, S.; Lenihan, H.S. TiO₂ Nanoparticles Are Phototoxic to Marine Phytoplankton. *PLoS ONE* **2012**, *7*, e30321. [CrossRef]
71. Dalai, S.; Pakrashi, S.; Kumar, R.S.S.; Chandrasekaran, N.; Mukherjee, A. A comparative cytotoxicity study of TiO₂ nanoparticles under light and dark conditions at low exposure concentrations. *Toxicol. Res.* **2012**, *1*, 116. [CrossRef]
72. Adams, L.K.; Lyon, D.Y.; Alvarez, P. Comparative eco-toxicity of nanoscale TiO₂, SiO₂, and ZnO water suspensions. *Water Res.* **2006**, *40*, 3527–3532. [CrossRef] [PubMed]
73. Tong, T.; Binh, C.T.T.; Kelly, J.J.; Gaillard, J.-F.; Gray, K.A. Cytotoxicity of commercial nano-TiO₂ to Escherichia coli assessed by high-throughput screening: Effects of environmental factors. *Water Res.* **2013**, *47*, 2352–2362. [CrossRef] [PubMed]

74. Lipovsky, A.; Nitzan, Y.; Gedanken, A.; Lubart, R. Antifungal activity of ZnO nanoparticles—the role of ROS mediated cell injury. *Nanotechnology* **2011**, *22*, 105101. [[CrossRef](#)] [[PubMed](#)]
75. Simon, M.; Barberet, P.; Delville, M.-H.; Moretto, P.; Seznec, H. Titanium dioxide nanoparticles induced intracellular calcium homeostasis modification in primary human keratinocytes. Towards an in vitro explanation of titanium dioxide nanoparticles toxicity. *Nanotoxicology* **2010**, *5*, 125–139. [[CrossRef](#)]
76. Yin, J.-J.; Liu, J.; Ehrenshaft, M.; Roberts, J.E.; Fu, P.P.; Mason, R.P.; Zhao, B. Phototoxicity of nano titanium dioxides in HaCaT keratinocytes—generation of reactive oxygen species and cell damage. *Toxicol. Appl. Pharmacol.* **2012**, *263*, 81–88. [[CrossRef](#)] [[PubMed](#)]
77. Mansfield, C.; Alloy, M.; Hamilton, J.; Verbeck, G.; Newton, K.; Klaine, S.; Roberts, A.P. Photo-induced toxicity of titanium dioxide nanoparticles to *Daphnia magna* under natural sunlight. *Chemosphere* **2015**, *120*, 206–210. [[CrossRef](#)] [[PubMed](#)]
78. Kim, J.; Lee, S.; Kim, C.-M.; Seo, J.; Park, Y.; Kwon, D.; Lee, S.-H.; Yoon, T.H.; Choi, K. Non-monotonic concentration–response relationship of TiO₂ nanoparticles in freshwater cladocerans under environmentally relevant UV-A light. *Ecotoxicol. Environ. Saf.* **2014**, *101*, 240–247. [[CrossRef](#)]
79. Bar-Ilan, O.; Louis, K.M.; Yang, S.P.; Pedersen, J.A.; Hamers, R.J.; Peterson, R.E.; Heideman, W. Titanium dioxide nanoparticles produce phototoxicity in the developing zebrafish. *Nanotoxicology* **2011**, *6*, 670–679. [[CrossRef](#)]
80. Faria, M.; Navas, J.M.; Soares, A.; Barata, C. Oxidative stress effects of titanium dioxide nanoparticle aggregates in zebrafish embryos. *Sci. Total Environ.* **2014**, *470*, 379–389. [[CrossRef](#)]
81. Dasari, T.P.; Pathakoti, K.; Hwang, H.-M. Determination of the mechanism of photoinduced toxicity of selected metal oxide nanoparticles (ZnO, CuO, Co₃O₄ and TiO₂) to *E. coli* bacteria. *J. Environ. Sci.* **2013**, *25*, 882–888. [[CrossRef](#)]
82. Kim, J.; Park, Y.; Yoon, T.H.; Yoon, C.; Choi, K. Phototoxicity of CdSe/ZnSe quantum dots with surface coatings of 3-mercaptopropionic acid or tri-*n*-octylphosphine oxide/gum arabic in *Daphnia magna* under environmentally relevant UV-B light. *Aquat. Toxicol.* **2010**, *97*, 116–124. [[CrossRef](#)] [[PubMed](#)]
83. Kahru, A.; Dubourguier, H.-C.; Blinova, I.; Ivask, A.; Kasemets, K. Biotests and Biosensors for Ecotoxicology of Metal Oxide Nanoparticles: A Minireview. *Sensors* **2008**, *8*, 5153–5170. [[CrossRef](#)] [[PubMed](#)]
84. Bour, A.; Mouchet, F.; Silvestre, J.; Gauthier, L.; Pinelli, E. Environmentally relevant approaches to assess nanoparticles ecotoxicity: A review. *J. Hazard. Mater.* **2015**, *283*, 764–777. [[CrossRef](#)]
85. Bahadar, H.; Maqbool, F.; Niaz, K.; Abdollahi, M. Toxicity of Nanoparticles and an Overview of Current Experimental Models. *Iran. Biomed. J.* **2015**, *20*, 1–11. [[PubMed](#)]
86. Pinedo, A.; Lopez, M.; Leyva, E.; Zermeño, B.; Serrano, B.; Moctezuma, E. Photocatalytic Decomposition of Metoprolol and Its Intermediate Organic Reaction Products: Kinetics and Degradation Pathway. *Int. J. Chem. React. Eng.* **2016**, *14*, 809–820. [[CrossRef](#)]
87. Berberidou, C.; Kitsiou, V.; Lambropoulou, D.A.; Michailidou, D.; Kouras, A.; Poullos, I. Decomposition and detoxification of the insecticide thiacloprid by TiO₂-mediated photocatalysis: Kinetics, intermediate products and transformation pathways. *J. Chem. Technol. Biotechnol.* **2019**, *94*, 2475–2486. [[CrossRef](#)]
88. Trinh, D.T.T.; Le, S.T.T.; Channei, D.; Khanitchaidecha, W.; Nakaruk, A. Investigation of Intermediate Compounds of Phenol in Photocatalysis Process. *Int. J. Chem. Eng. Appl.* **2016**, *7*, 273–276. [[CrossRef](#)]
89. Kim, D.-H.; Lee, D.; Monllor-Satoca, D.; Kim, K.; Lee, W.; Choi, W. Homogeneous photocatalytic Fe³⁺/Fe²⁺ redox cycle for simultaneous Cr (VI) reduction and organic pollutant oxidation: Roles of hydroxyl radical and degradation intermediates. *J. Hazard. Mater.* **2019**, *372*, 121–128. [[CrossRef](#)]
90. Santos, I.; Hildenbrand, Z.L.; Schug, K.A. A Review of Analytical Methods for Characterizing the Potential Environmental Impacts of Unconventional Oil and Gas Development. *Anal. Chem.* **2018**, *91*, 689–703. [[CrossRef](#)]
91. Oetjen, K.; Giddings, C.G.; McLaughlin, M.; Nell, M.; Blotvogel, J.; Helbling, D.E.; Mueller, D.; Higgins, C.P. Emerging analytical methods for the characterization and quantification of organic contaminants in flowback and produced water. *Trends Environ. Anal. Chem.* **2017**, *15*, 12–23. [[CrossRef](#)]
92. Luek, J.L.; Gonsior, M. Organic compounds in hydraulic fracturing fluids and wastewaters: A review. *Water Res.* **2017**, *123*, 536–548. [[CrossRef](#)] [[PubMed](#)]
93. Akyon, B.; McLaughlin, M.; Hernandez, F.; Blotvogel, J.; Bibby, K. Characterization and biological removal of organic compounds from hydraulic fracturing produced water. *Environ. Sci. Process. Impacts* **2019**, *21*, 279–290. [[CrossRef](#)] [[PubMed](#)]

94. Sitterley, K.A.; Linden, K.G.; Ferrer, I.; Thurman, E.M. Identification of Proprietary Amino Ethoxylates in Hydraulic Fracturing Wastewater Using Liquid Chromatography/Time-of-Flight Mass Spectrometry with Solid-Phase Extraction. *Anal. Chem.* **2018**, *90*, 10927–10934. [[CrossRef](#)]
95. Pichtel, J. Oil and Gas Production Wastewater: Soil Contamination and Pollution Prevention. *Appl. Environ. Soil Sci.* **2016**, *2016*, 1–24. [[CrossRef](#)]
96. Ray, J.P.; Engelhardt, F.R. *Produced Water: Technological/Environmental Issues and Solutions*; Springer Science & Business Media: Berlin, Germany, 2012; Volume 46.
97. U.S. Environmental Protection Agency (EPA). *Integrated Risk Information System (IRIS) on Baygon*; National Center for Environmental Assessment, Office of Research and Development: Washington, DC, USA, 1999.
98. Litter, M.I.; Quici, N. New Advances in Heterogeneous Photocatalysis for Treatment of Toxic Metals and Arsenic. *Nanomater. Environ. Prot.* **2014**, 143–167. [[CrossRef](#)]
99. Litter, M.I. Treatment of Chromium, Mercury, Lead, Uranium, and Arsenic in Water by Heterogeneous Photocatalysis. *Chem. Eng. Renew. Convers.* **2009**, *36*, 37–67. [[CrossRef](#)]
100. Litter, M.I.; Morgada, M.E.; Bundschuh, J. Possible treatments for arsenic removal in Latin American waters for human consumption. *Environ. Pollut.* **2010**, *158*, 1105–1118. [[CrossRef](#)]
101. Bundschuh, J.; Litter, M.I.; Ciminelli, V.S.; Morgada, M.E.; Cornejo, L.; Hoyos, S.E.G.; Hoinkis, J.; Alarcón-Herrera, M.T.; Armienta-Hernández, M.A.; Bhattacharya, P. Emerging mitigation needs and sustainable options for solving the arsenic problems of rural and isolated urban areas in Latin America—A critical analysis. *Water Res.* **2010**, *44*, 5828–5845. [[CrossRef](#)]
102. Fostier, A.H.; Pereira, M.D.S.S.; Rath, S.; Guimarães, J.R. Arsenic removal from water employing heterogeneous photocatalysis with TiO₂ immobilized in PET bottles. *Chemosphere* **2008**, *72*, 319–324. [[CrossRef](#)]
103. Abdel-Maksoud, Y.; Imam, E.H.; Ramadan, A.R. TiO₂ Solar Photocatalytic Reactor Systems: Selection of Reactor Design for Scale-up and Commercialization—Analytical Review. *Catalysts* **2016**, *6*, 138. [[CrossRef](#)]
104. Kukovecz, A.; Kordas, K.; Kiss, J.; Konya, Z. Atomic scale characterization and surface chemistry of metal modified titanate nanotubes and nanowires. *Surf. Sci. Rep.* **2016**, *71*, 473–546. [[CrossRef](#)]
105. Bavykin, D.V.; Friedrich, J.M.; Walsh, F.C. Protonated Titanates and TiO₂ Nanostructured Materials: Synthesis, Properties, and Applications. *Adv. Mater.* **2006**, *18*, 2807–2824. [[CrossRef](#)]
106. Umebayashi, T.; Yamaki, T.; Itoh, H.; Asai, K. Analysis of electronic structures of 3d transition metal-doped TiO₂ based on band calculations. *J. Phys. Chem. Solids* **2002**, *63*, 1909–1920. [[CrossRef](#)]
107. Yu, H.; Irie, H.; Hashimoto, K. Conduction Band Energy Level Control of Titanium Dioxide: Toward an Efficient Visible-Light-Sensitive Photocatalyst. *J. Am. Chem. Soc.* **2010**, *132*, 6898–6899. [[CrossRef](#)]
108. Choi, W.; Termin, A.; Hoffmann, M.R. The Role of Metal Ion Dopants in Quantum-Sized TiO₂: Correlation between Photoreactivity and Charge Carrier Recombination Dynamics. *J. Phys. Chem.* **1994**, *98*, 13669–13679. [[CrossRef](#)]
109. Jiménez, S.; Micó, M.M.; Arnaldos, M.; Ferrero, E.; Malfeito, J.J.; Medina, F.; Contreras, S. Integrated processes for produced water polishing: Enhanced flotation/sedimentation combined with advanced oxidation processes. *Chemosphere* **2017**, *168*, 309–317. [[CrossRef](#)]
110. Mazzeo, D.E.C.; Levy, C.E.; Angelis, D.D.F.D.; Marin-Morales, M.A. BTEX biodegradation by bacteria from effluents of petroleum refinery. *Sci. Total Environ.* **2010**, *408*, 4334–4340. [[CrossRef](#)]
111. Oller, I.; Malato, S.; Pérez, J.S. Combination of Advanced Oxidation Processes and biological treatments for wastewater decontamination—A review. *Sci. Total Environ.* **2011**, *409*, 4141–4166. [[CrossRef](#)]
112. Waghmode, T.R.; Kurade, M.B.; Sapkal, R.T.; Bhosale, C.H.; Jeon, B.-H.; Govindwar, S.P. Sequential photocatalysis and biological treatment for the enhanced degradation of the persistent azo dye methyl red. *J. Hazard. Mater.* **2019**, *371*, 115–122. [[CrossRef](#)]
113. Parrino, F.; Corsino, S.F.; Bellardita, M.; Loddo, V.; Palmisano, L.; Torregrossa, M.; Viviani, G. Sequential biological and photocatalysis based treatments for shipboard slop purification: A pilot plant investigation. *Process. Saf. Environ. Prot.* **2019**, *125*, 288–296. [[CrossRef](#)]
114. Hamdi, H.; Namane, A.; Hank, D.; Hellal, A. Coupling of photocatalysis and biological treatment for phenol degradation: Application of factorial design methodology. *J. Mater.* **2017**, *8*, 3953–3961.



Article

Treatment of Produced Water in the Permian Basin for Hydraulic Fracturing: Comparison of Different Coagulation Processes and Innovative Filter Media

Alfredo Zendejas Rodriguez, Huiyao Wang, Lei Hu, Yanyan Zhang and Pei Xu * 

Civil Engineering Department, New Mexico State University, Las Cruces, NM 88003, USA; nahum@nmsu.edu (A.Z.R.); huiyao@nmsu.edu (H.W.); leihu@nmsu.edu (L.H.); zhangy@nmsu.edu (Y.Z.)

* Correspondence: pxu@nmsu.edu

Received: 2 January 2020; Accepted: 9 March 2020; Published: 11 March 2020



Abstract: Produced water is the largest volume of waste product generated during oil and natural gas exploration and production. The traditional method to dispose of produced water involves deep well injection, but this option is becoming more challenging due to high operational cost, limited disposal capacity, and more stringent regulations. Meanwhile, large volumes of freshwater are used for hydraulic fracturing. The goal of this study is to develop cost-effective technologies, and optimize system design and operation to treat highly saline produced water (120–140 g/L total dissolved solids) for hydraulic fracturing. Produced water was collected from a salt water disposal facility in the Permian Basin, New Mexico. Chemical coagulation (CC) using ferric chloride and aluminum sulfate as coagulants was compared with electrocoagulation (EC) with aluminum electrodes for removal of suspended contaminants. The effects of coagulant dose, current density, and hydraulic retention time during EC on turbidity removal were investigated. Experimental results showed that aluminum sulfate was more efficient and cost-effective than ferric chloride for removing turbidity from produced water. The optimal aluminum dose was achieved at operating current density of 6.60 mA/cm² and 12 min contact time during EC treatment, which resulted in 74% removal of suspended solids and 53–78% removal of total organic carbon (TOC). The energy requirement of EC was calculated 0.36 kWh/m³ of water treated. The total operating cost of EC was estimated \$0.44/m³ of treated water, which is 1.7 or 1.2 times higher than CC using alum or ferric chloride as the coagulant, respectively. The EC operating cost was primarily associated with the consumption of aluminum electrode materials due to faradaic reactions and electrodes corrosions. EC has the advantage of shorter retention time, in situ production of coagulants, less sludge generation, and high mobility for onsite produced water treatment. The fine particles and other contaminants after coagulation were further treated in continuous-flow columns packed with different filter media, including agricultural waste products (pecan shell, walnut shell, and biochar), and new and spent granular activated carbon (GAC). Turbidity, TOC, metals, and electrical conductivity were monitored to evaluate the performance of the treatment system and the adsorption capacities of different media. Biochar and GAC showed the greatest removal of turbidity and TOC in produced water. These treatment technologies were demonstrated to be effective for the removal of suspended constituents and iron, and to produce a clean brine for onsite reuse, such as hydraulic fracturing.

Keywords: produced water; beneficial reuse; filtration; electrocoagulation; chemical coagulation; hydraulic fracturing

1. Introduction

1.1. Challenges and Opportunities Associated with Produced Water

Produced water represents the largest waste stream generated during oil and gas production. When petroleum hydrocarbons are extracted, formation water is brought up to the surface contributing to produced water [1]. The composition of produced water varies considerably depending on the geographic location of the field, the type of hydrocarbons being extracted, the extraction method employed, and the minerals present in the bearing geologic formation [2–9]. Produced water is typically saline with high total dissolved solids (TDS; e.g., Na^+ , Ca^{2+} , Mg^{2+} , Cl^- , and SO_4^{2-}). Organic compounds are some of the main contaminants in produced water, including oil and grease (free, dispersed or emulsified); volatile and semi-volatile organics, such as BTEX (benzene, toluene, ethylbenzene, and xylenes); and PAHs (polycyclic aromatic hydrocarbons). Contaminants in small amounts include dissolved gases (e.g., ammonia and hydrogen sulfide), and chemical additives used to improve drilling and production operations. Additionally, heavy metals and naturally-occurring radioactive materials (NORMs) can be found in produced water.

The most common methods to manage produced water consist of disposal into permitted salt water disposal (SWD) wells within deep saline underground formations, or reinjection into conventional reservoirs for enhanced oil recovery operations [3,10]. However, deep well injection has become more challenging because of limited capacity and potential seismic hazard caused by anthropogenic fluid injections [11,12].

Millions of gallons of water are used for hydraulic fracturing with the addition of a complex mixture of chemical additives known as fracturing fluids that are injected to the ground to induce and maintain fractures in the geological formation. Produced water can be treated and reused for onsite hydraulic fracturing to reduce the use of fresh or brackish water for unconventional oil and gas operations and decrease the need for the deep well injection of produced water. Fracturing companies may have different water quality requirements depending on fracturing methods and chemical formula, but in general it requires low in suspended solids, organic matter, and multivalent metals (in particular Fe^{3+}), and bacteria counts. Hydraulic fracturing can use brackish water for its operation [13]. Therefore, desalination may not be needed or treated produced water can be blended with other water sources to meet the TDS requirement for fracturing.

Coagulation-flocculation-sedimentation-filtration processes can significantly remove suspended solids and colloidal particles from water. The most common chemical coagulants employed include aluminum sulfate (alum), ferric chloride, iron sulfate, and calcium hydroxide (lime) [14]. Wang et al. showed that flocculation of oilfield produced water using some of the most common coagulant agents was effective for trapping and removing suspended solids [14]. Dastgheib et al. combined two coagulants in different proportions to remove suspended solids in produced water with TDS values around 100,000 mg/L [15]. High turbidity removal was achieved by combinations of coagulants such as high alum–low lime, moderate alum–high lime, and moderate ferric chloride–low lime. When these chemicals were combined, pH was not impacted drastically [15]. Younker and Walsh reported a coagulation pretreatment employing ferric chloride reduced oil and grease concentration of produced water from 100 mg/L to below 30 mg/L [16]. Ferric chloride was used at a 10 mg/L concentration, and the salinity level of produced water was 32,000 mg/L. In the same study, Younker and Walsh also used organoclay adsorption as pretreatment for produced water and found that disperse oil could be greatly removed if the dose of organoclay increased up to 1000 mg/L and the mixing time was no less than 45 min. When combining coagulation with organoclay adsorption for removal of oil and grease from produced water, chemical coagulation played a significant role as pretreatment.

One of the main drawbacks of chemical coagulation (CC) is the large amount of residual sludge formed at the end of the process, because counterions are added to the solution along with the metal cations that serve to form the flocs. In addition, chemical coagulants contain very little coagulating agent on a mass basis. For example, 1 ton of alum as $\text{Al}_2(\text{SO}_4)_3 \cdot 18(\text{H}_2\text{O})$ contains only 81 kg of Al(III),

while 1 ton of ferric chloride $\text{FeCl}_3 \cdot 6(\text{H}_2\text{O})$ provides 210 kg of Fe(III). Therefore, chemical coagulation requires the handling of larger amounts of chemicals and sludge.

Electrocoagulation (EC) utilizes sacrificial anodes to generate active coagulants to remove contaminants by precipitation and flotation. The most common metals employed as electrodes for EC are aluminum and iron, because these are easily available (abundant), have a low cost, and are not toxic. The same metal is usually used for both the anode and cathode in an EC reactor. When electricity is applied, the anode is oxidized into cations, while in the cathode water is reduced into hydrogen gas and hydroxyl anions (Figure 1). The gas generated removes pollutants by flotation, and the coagulant agents generated in the anode cause floc formation and precipitation as sludge [17]. EC produces about half the sludge of CC.

EC is an attractive technology and has been used for treating different types of water and wastewater, such as surface water; tannery and textile wastewater; pulp and paper industry wastewater; oily wastewater; food industry wastewater; and other types of wastewater containing heavy metals, cyanide, and other contaminants [18]. EC can be directly powered by solar photovoltaic [19].

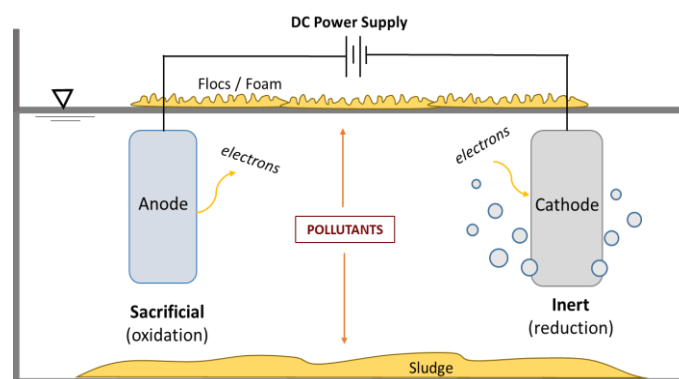


Figure 1. General schematic representation of electrocoagulation (EC).

EC efficiency depends on the conductivity and ionic content of water. Salinity, one of the most remarkable problems of produced water, can become an advantage for EC treatment [20,21]. EC has been reported to be effective at removing organic matter, turbidity, trace metals, and boron in produced water. Millar et al. demonstrated the treatment of coal seam produced water using EC with aluminum electrodes arranged in bipolar mode [20,21]. Higher current density, longer contact time and elevated pH in solution benefited better reduction of hardness, silica, barium, and iron. Flocs formed in EC were porous and lighter than flocs formed by conventional CC treatments. Zhao et al. experimented the use of EC as pretreatment for produced water obtained from an oil field in Saskatchewan, Canada [22]. They focused on the removal of hardness, oil and grease content in terms of chemical oxygen demand (COD), and turbidity. At the operating conditions of pH 7.36, a reaction time of 31 min, and a current density of 5.9 mA/cm^2 , the removal of hardness, COD, and turbidity reached 85.8%, 66.6%, and 93.8%, respectively [22].

EC technology utilized in full-scale applications, such as the CleanWave[®] water treatment mobile device (Halliburton, Houston, TX, USA), can treat up to 26,000 barrels (4100 m^3) of produced water per day with a low energy consumption. This equipment can reduce total suspended solids (TSS) by 99% while bringing turbidity to $<10 \text{ NTU}$. The TDS range in which the device is completely functional is 100–300,000 mg/L [23]. Some studies show the feasibility of combining EC and biological processes to treat produced water and specifically address organic contaminants such as total petroleum hydrocarbons (TPH) [24].

Table 1 summarizes the operating conditions and parameters selected for EC reactors in laboratory and pilot scale for produced water treatment. Although EC has been employed for produced water treatment, there is limited knowledge regarding the optimal design and operating parameters during treatment of highly saline produced water, so as to enable more economical full-scale applications [22,25].

Table 1. Electrocoagulation technologies applied in produced water treatment: design parameters.

Ref.	HRT (min)	Experimental Set up/Arrangement	Current Density (mA/cm ²)	Produced Water Characteristics
[26]	4	Continuous flow goes 4 times through the reactor (each time 1 min), Al and Fe electrodes	10 and 20	Conductivity 150–160 mS/cm, COD 27 mg/L, 68% COD removal
	45	Batch operation PW 400 mL, Al and Fe electrodes	13.9	Conductivity 160–167 mS/cm, COD 32 mg/L, 67% COD removal
[22]	30	Continuous flow, pilot scale PW 80 L Fe electrodes	5.56	COD 280 mg/L, Turbidity 135 NTU; Max. turbidity removal 93.8% and 67% COD removal
[21]	1	Continuous flow at 1.14 L/min Al electrodes Coal seam PW	0.8	Turbidity 8.5 NTU, DOC 6.4 mg/L; 54% DOC removal Significant removal in scale formation species
[27]	15–90	Batch operation PW 500 mL Aluminum electrodes	1.2–3.6	TDS 15 g/L, boron 10mg/L 15 min removes 60% boron; 90 min removes 98% boron
[28]	30–90	Batch operation, Volume of oil sands PW 1.5 L Al and Fe electrodes; AlCl ₃ added	6–30	TDS 1.7 g/L TOC 475–720 mg/L 39% TOC removal

COD—chemical oxygen demand; DOC—dissolved organic carbon; HRT—hydraulic retention time; NTU—nephelometric turbidity units; PW—produced water; TDS—total dissolved solids; TOC—total organic carbon.

A variety of media have been employed for produced water filtration to remove organic matter and suspended solids. Dastgheib et al. [15] employed sand, anthracite coal, and walnut shell to filter oilfield produced water. They found that the media with the greatest capacity to remove suspended particles was sand, while the best to remove oil droplets was anthracite coal. Although walnut shell showed the potential to remove particles and oil components, it had a lower adsorption capacity and reached turbidity breakthrough faster than anthracite and sand. For the removal of dissolved organic carbon (DOC), anthracite coal, walnut, and sand removed 70%, 60%, and 45% respectively after 15 h of operation. These experiments proved the effectiveness of filtration for saline produced water with a TDS concentration of 100,000 mg/L [15]. Zhang et al. also utilized walnut shell in a packed-bed arrangement to filter produced water as a pretreatment prior to membrane distillation [29]. This study showed ≥95% removal of organic compounds such as BTEX.

Adsorption is usually conducted using organoclay and granular activated carbon (GAC) as adsorbent materials. The use of GAC is recommended over organoclay, because GAC has a greater specific surface area which removes greater quantities of DOC from produced water [15,30]. Adsorption technologies, including the use of a chitosan polymer extracted from shrimp shell, also showed promising potential to remove oil from produced water [31].

The effective media such as GAC can be costly; developing innovative, low-cost filter media is important to reduce the treatment costs for produced water reuse. These media may include agricultural waste products, such as various woodchips, nut shells, biochar, and spent GAC from drinking water treatment plants of which the adsorption capacity may be exhausted but can still be used as a filter media for removal of suspended solids during produced water treatment.

1.2. Research Objective

It is critical to develop produced water treatment alternatives to reduce the amount of produced water for disposal and reuse it as a valuable water resource. Innovative approaches are needed to lower treatment costs and improve efficiency for produced water treatment. The objective of this study is to assess different technologies to remove suspended solids, organic matter, and other constituents in produced water, to generate a clean brine for the hydraulic fracturing operation of unconventional oil and gas reservoirs. EC and conventional CC methods using alum and ferric chloride as coagulants were compared in terms of removal efficiency and operating costs. EC has the advantages of working effectively for saline produced water and creating coagulant species in situ without the hassle of chemical transport, handling, and storage. Besides conventional GAC, innovative

low-cost filter media were evaluated, including agricultural waste products (pecan shell, walnut shell, and biochar), and spent GAC from a local drinking water treatment plant. This study aims to provide recommendations and optimization of operating and design parameters for treatment of highly saline produced water (~120–140 g/L salinity) in the Permian Basin for onsite reuse.

2. Materials and Methods

2.1. Produced Water

Produced water samples were collected from a salt water disposal facility in Jal, New Mexico. This site has basic treatment to remove suspended solids that may clog disposal wells. The chemical composition of the produced water collected from the Permian Basin is summarized in Table 2. The TDS concentration of the produced water varied between 120 and 140 g/L with electrical conductivity between 200 and 300 mS/cm. The major constituents in the produced water included Na⁺ (42,720 ± 2093 mg/L), Ca²⁺ (4247 ± 752 mg/L), Mg²⁺ (727 ± 54 mg/L), K⁺ (805 ± 230 mg/L), Sr²⁺ (257 ± 20 mg/L), Cl⁻ (65,800 ± 1600 mg/L), SO₄²⁻ (1010 ± 9 mg/L), Br⁻ (591 ± 16 mg/L), and SiO₂ (32 ± 2 mg/L). The pH was 7.30 ± 0.21 with alkalinity of 2345 ± 329 mg/L as CaCO₃. The total organic carbon (TOC) concentration varied in the range of 83.1 ± 30.8 mg/L. The produced water also contained high concentration of ammonia (655 ± 77 mg/L). The produced water tested in this study represents the typical produced water quality in the Permian Basin, in which the TDS concentration varies from 20 to 300 g/L with an average of 90 g/L [2,4,7].

Throughout the study, electrical conductivity and pH were measured using an OAKTON meter (Vernon Hills, IL, USA). Turbidity was measured using a HATCH 2100N Turbidimeter (Loveland, CO, USA). Alkalinity was measured employing a HATCH Digital Titrator model 16,900, Method 8203 (Loveland, CO, USA). The major ions were analyzed by a DIONEX ion chromatography system model ICS-2100 (Dionex, Sunnyvale, CA, USA). TOC was determined by the non-purgeable organic carbon (NPOC) analysis using a Shimadzu TOC analyzer model VCSH (Shimadzu TOC-L, Kyoto, Japan). The trace metals analysis was conducted employing inductively coupled plasma–optical emission spectrometry (ICP-OES, Perkin Elmer Optima 4300 DV, Norwalk, CT, USA).

Table 2. Chemical characteristics of the produced water from the Permian Basin, Jal, NM.

Parameter	Unit	Value
pH		7.30 ± 0.21
Alkalinity	mg/L as CaCO ₃	2345 ± 329
Electrical conductivity	mS/cm	201.2 ± 13.3
Total dissolved solids	g/L	129.3 ± 8.5
Total organic carbon	mg/L	83.1 ± 30.8
Total phosphorus	mg/L	<0.1
Turbidity	NTU	53.4 ± 5.0
Ammonium	mg/L	655 ± 77
Arsenic	mg/L	1.1 ± 0.0
Barium	mg/L	1.0 ± 0.0
Bromide	mg/L	591 ± 16
Calcium	mg/L	4247 ± 752
Chloride	mg/L	65,800 ± 1600
Iron	mg/L	11 ± 9
Lithium	mg/L	18.8 ± 0.3
Magnesium	mg/L	727 ± 54
Manganese	mg/L	0.66 ± 0.02
Nickel	mg/L	0.02 ± 0.004
Potassium	mg/L	805 ± 230
Silica	mg/L	32 ± 2
Sodium	mg/L	42,720 ± 2093
Strontium	mg/L	257 ± 20
Sulfate	mg/L	1010 ± 9

2.2. Produced Water Treatment

2.2.1. Chemical coagulation (CC)

Standard jar testing was conducted using ferric chloride and alum as coagulant agents; both were analytical grade and obtained from Fisher Scientific. Chemicals were added to produced water in different concentrations ranging from 250 to 1321 mg/L. For the operational parameters of jar testing, rapid mixing was performed 1 min at 100 rpm; the flocculation stage lasted 25 min at 40 rpm; then 40 min settling prior to taking water samples for analysis. The parameters monitored were pH and turbidity to determine and compare the removal capacity of each chemical.

2.2.2. Electrocoagulation (EC)

The EC unit included a set of eight aluminum plate electrodes ($10.2 \times 16 \times 1.3$ cm) assembled in parallel. Electricity was applied to the electrodes by a direct current power supply LH110-3 (Sorensen, San Diego, CA, USA). Electrodes were placed in a 2.5 L cylindrical reactor made of clear acrylic material. The surface area of electrodes in contact with produced water was 379 cm^2 , and the distance between each electrode was 2 cm (Figure 2).

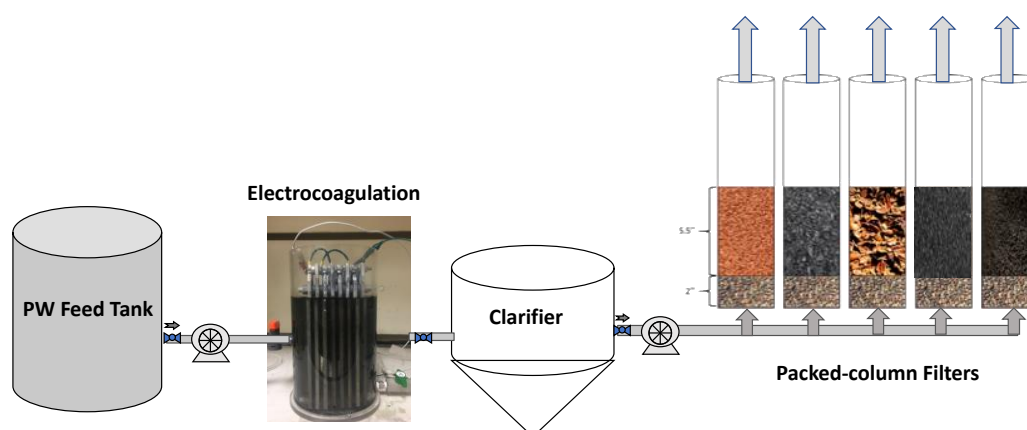


Figure 2. Schematic diagram of the continuous-flow experimental set up. The packed columns employed different media, from left to right: walnut shell, biochar, pecan shell, new GAC, and spent GAC.

Batch EC experiments were designed to study the effect of current density and electrocoagulation time (ECT) on turbidity removal from produced water. In this study, ECT was defined as the time (in minutes) that produced water was in direct contact with the aluminum electrodes during an EC batch experiment. Before every batch experiment, electrodes were gently polished using sandpaper to remove deposits and smooth out any sharp spots [28].

To study the effect of current density applied during EC on turbidity removal, an electric current ranged from 0.5 to 3.0 amperes (A) with 0.5 A intervals (equivalent to current density of $1.32\text{--}7.92 \text{ mA/cm}^2$) applied to the electrodes in individual experiments. For each experiment, ECT was set at 25 min with a sedimentation time of 40 min, and the volume of produced water treated was 2.5 L. The optimal current density value obtained after these experiments was employed to study the effect of ECT in further electrocoagulation batch experiments.

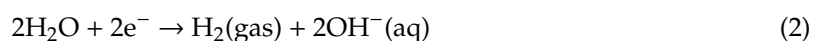
To determine an optimal ECT, six batch experiments were conducted at ECT of 3, 6, 9, 12, 15, and 20 min. For each experiment, sedimentation time was 40 min and the volume of produced water treated was 2.5 L. The optimal ECT was employed as hydraulic retention time (HRT) for the EC stage during continuous-flow experiments.

In the EC cell, the fundamental oxidation and reduction processes occurring can be represented as follows [27].

Anode, aluminum is oxidized from solid metal (s) to ionic species in aqueous solution (aq):



Cathode, water is reduced to hydrogen gas and hydroxyl ions:



After the oxidation of aluminum in the anode, different polymeric species form and eventually transform into $\text{Al}(\text{OH})_3(\text{s})$, as shown in Equation (3) [27]:



In produced water, $\text{Al}(\text{OH})_3(\text{s})$ flocs can capture particles and adsorb metals and organic contaminants. Flocs can be further removed by hydrogen gas flotation or by sedimentation after EC treatment.

The amount of aluminum generated during the EC operation can be calculated theoretically using Faraday's law. The mass of metal m is a function of the electrolysis time t and of the electric current I :

$$m = (M \times I \times t) / (z \times F) \quad (4)$$

where m is the mass in grams of aluminum generated at a specific current applied (I), amperes; M is the atomic weight of aluminum, 26.98 g/mol; t is the operating time, s; z is the number of electrons transferred per aluminum atom; and F is Faraday's constant, 96,486 C/mol.

2.2.3. Filtration

Packed-column filtration experiments were carried out using 2-inch I.D. (5.1 cm) by 15-inch length (38 cm) acrylic columns. Types of filter media used for experiments were walnut shells, pecan shells, biochar, new and spent GAC. Walnut shells and pecan shells were obtained as agricultural wastes from farmers in Las Cruces area, and biochar was obtained from Wakefield Agricultural Carbon LLC, which was produced through thermal treatment of wood chips. Biochar, walnut and pecan shells were sieved to obtain particle size of 1.68–2 mm. The specific surface area of biochar was measured 370 g/m² [32]. The new GAC was FILTRASORB 816 from Calgon Carbon Corporation (Moon Township, PA, USA). The GAC has an effective particle size of 1.2–1.3 mm, specific surface area of 900–1000 m²/g, and iodine number of 900 mg/g. The spent GAC was the same type but had been used for nine years in a conventional surface water treatment plant. The GAC was used for potable water production and is deemed non-hazardous. The spent GAC can be either disposed of to landfill or returned to the manufacturer for re-activation.

Prior to packing the columns, all the filter media (except spent GAC) were washed with distilled water and dried overnight at 105 °C. To pack each column, a 2-inch thick gravel layer was set in the base; then a 5.5-inch thick media layer was packed on top (Figure 2). For the operation of the columns in continuous-flow mode, a Masterflex peristaltic pump was used to pump produced water through the columns at a flow rate of 20 mL/min with an empty bed contact time (EBCT) of 19 min.

2.3. Continuous-Flow Experiments

Batch experiments were conducted for CC and EC to study and evaluate their performances. Once the optimal conditions were defined, continuous-flow experiments were conducted. The experimental set up was composed of EC stage as pretreatment for filtration. Produced water flowed through the EC reactor at 208 mL/min rate based on the optimal ECT determined during batch experiments.

3. Results

3.1. Chemical Coagulation (CC)

Alum was demonstrated to have a higher efficacy than ferric chloride to remove suspended solids from produced water (Figure 3a). While added in the same molar concentration, the turbidity removal by Al(III) could be up to 1.5 times higher than by Fe(III). Over 80% turbidity was removed at Al(III) dose of 2.6 mmol (71 mg/L), while 60% of turbidity was removed by Fe(III) at dose of 2.4 mmol (135 mg/L). The consumption of alkalinity in produced water to form $\text{Al}(\text{OH})_3$ and $\text{Fe}(\text{OH})_3$ flocs was the same, and the pH drop by using alum as coagulant exhibited the same trend as using ferric chloride (Figure 3b).

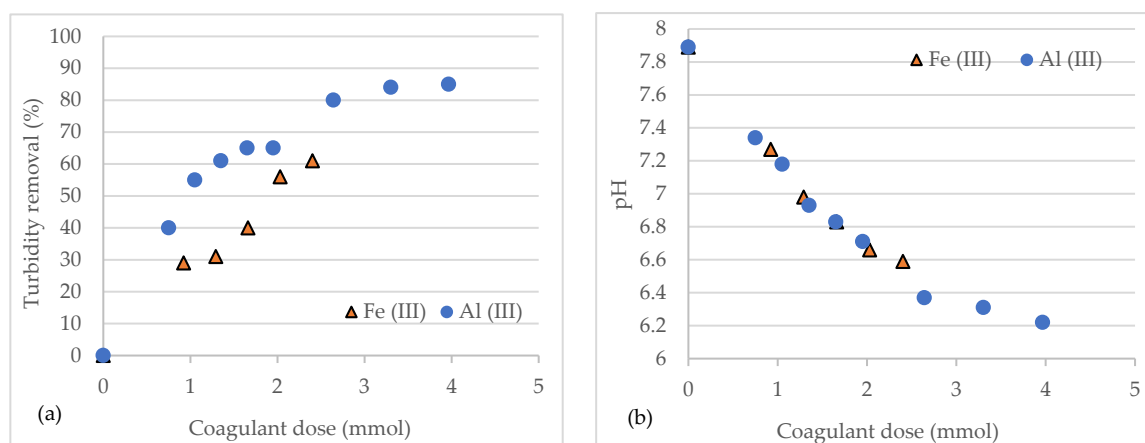


Figure 3. Turbidity removal (a) and pH change (b) during chemical coagulation of produced water.

Recently, Chang et al. [33] employed both alum and ferric chloride to coagulate flowback and produced water. At an optimal dose of 900 mg/L, ferric chloride showed a greater capacity to remove turbidity and organics. Alum exhibited a slightly inferior efficiency, which is different from the results obtained in the current study. The difference, however, resides in the fact that Chang et al. [33] compared the efficiency of the chemicals added in mg/L of the chemical molecules and not the molar concentration of the metal itself. If the coagulant dose is converted to molar concentrations, Chang et al.'s study reached the same conclusion as this study: that Al(III) coagulant outperformed Fe(III) for better removal of turbidity.

Nadella et al. reported that the zeta-potential of colloids present in the raw produced water collected in the Permian Basin was slightly negatively charged and near neutral owing to its high ionic strength and the presence of high concentrations of multivalent cations, such as Mg, Ca, and Fe [34]. During coagulation, the positively charged metal coagulant is attracted to the negatively charged colloids via electrostatic interaction. Flocs form during the charge neutralization process, and particle collisions occur. Adding excess coagulant beyond charge neutralization results in the formation of metal coagulant precipitates (e.g., $\text{Al}(\text{OH})_3$ or $\text{Fe}(\text{OH})_3$). Colloidal contaminants in produced water were entrained or swept down by the precipitates as they settled in the suspension. This study showed alum was more effective for charge neutralization and enmeshment/entrainment of colloidal particles in produced water than ferric chloride.

Considering the current market prices of coagulants (US \$500–\$590/metric ton for alum and US \$460–\$800/ton for ferric chloride), the use of alum as a coagulant for produced water represents an economic advantage. For example, to achieve 60% removal of turbidity from the produced water, it requires 36 mg/L Al(III) (444 mg/L $\text{Al}_2(\text{SO}_4)_3 \cdot 8\text{H}_2\text{O}$) and 134 mg/L Fe(III) (650 mg/L $\text{FeCl}_3 \cdot 6\text{H}_2\text{O}$) as coagulant. Assuming the price for both coagulants would be \$500/ton, the chemical cost of using Fe(III) as coagulant (\$0.325/m³ water) is 1.46 times higher than using Al(III) as coagulant (\$0.222/m³ water).

For a conventional CC, the energy consumption required for mixing in coagulation and flocculation processes was estimated to be 0.4 kWh/m^3 [35]. Assuming the electrical cost is $\$0.10 \text{ kWh}$, the electrical power cost of CC is estimated to be $\$0.04/\text{m}^3$. The total operating costs for Al and Fe coagulation are approximately $\$0.26/\text{m}^3$ and $\$0.37/\text{m}^3$, respectively.

3.2. Electrocoagulation (EC)

Aluminum electrodes were selected over iron electrodes for EC based on the CC test results and because hydraulic fracturing requires low concentration of iron. Figure 4 shows the experimental results to optimize Al(III) dose through changing current density and hydraulic retention time in EC process. The optimal Al(III) dose achieved $74 \pm 1.2\%$ turbidity removal at current density of 6.6 mA/cm^2 (1.8 volts). Further increase of current density levels did not have significant improvement in turbidity removal.

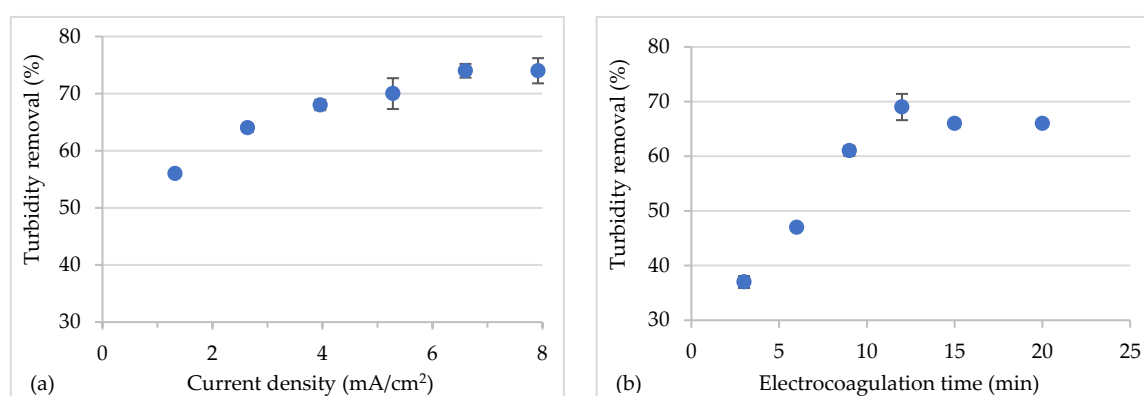


Figure 4. Effect of applied current density (a) and electrocoagulation time (b) during electrocoagulation on turbidity removal. The error bars represent the variability of duplicate experiments.

Once current density was optimized, the effect of ECT on turbidity removal was studied, as shown in Figure 4b. The optimal ECT was determined to be 12 min because turbidity removal reached the highest at 70%. ECT longer than 12 min did not improve turbidity removal. Therefore, for continuous-flow experiments, the design parameters were set at the current density 6.6 mA/cm^2 and an ECT of 12 min.

pH dropped from 7.47 to 6.41 after 20 min of operation due to the consumption of hydroxyl anions during the formation of aluminum hydroxide, which precipitates as flocs according to Equation (3). The organic carbon concentration in the EC effluent was considerably variable, with a value of $26.78 \pm 14.71 \text{ mg/L}$, representing a TOC removal of 53–78%. Due to relatively low pH during EC operation, the removal of hardness was marginal: $6.4\% \pm 2.8\%$ for calcium and $2.1\% \pm 0.5\%$ for magnesium.

Based on the Faraday's law, the theoretical amount of Al(III) generated from anode at optimal conditions (i.e., 6.6 mA/cm^2 and 12 min ECT) is estimated to be 67 mg/L of Al(III). The EC calculation result is comparable with the optimal alum dose obtained from CC, where at Al(III) dose of 80 mg/L , 80% of turbidity was removed; in EC, 74% of turbidity was removed at the theoretical Al(III) dose of 67 mg/L . Meanwhile, pH dropped to 6.4 in both coagulation processes. The actual consumption of aluminum electrodes is higher than the theoretical value, due to electrochemical corrosion of both the anode and cathode that contributes to the extra-faradaic aluminum dosing [36]. Picard et al. demonstrated cathodic dissolution in the EC process due to chemical attack by hydroxyl ions generated during water reduction [37]. The actual coagulant dose in Al-EC can be 1.2 to 2.2 times higher than the calculated faradaic aluminum amount [36,37].

The unit operating costs for EC can be estimated by adding the electrical costs and the costs for the sacrificial anodes. To achieve 70% turbidity recovery, the energy requirement was calculated to be 0.36 kWh/m^3 of water treated; this value is 2–10 times lower than other EC studies generating

the same amount of aluminum dose during treatment of synthetic water and wastewater [35–37], because higher salinity of produced water reduced the electrical resistance of the solution during EC. Given an electrical cost of \$0.10/kWh, the electrical power cost was estimated \$0.036/m³. The current market price for aluminum sheets (thickness 0.2 to 200 mm) varies in the range of \$1000–\$3000 per ton. Assuming aluminum electrode cost is ~\$3.00/kg, and the actual blade consumption is two times higher than the theoretical amount (i.e., $2 \times 67 = 134$ mg/L) due to electrode dissolution [35], the cost of aluminum electrode consumed is estimated \$0.40/m³ of treated water. Therefore, the total operating costs for EC were estimated \$0.44/m³ of treated water, which is 1.7 and 1.2 times higher than using alum and ferric chloride as chemical coagulants (\$0.26/m³ and \$0.37/m³), respectively. The EC operating costs can be reduced and comparable to CC by using low-cost aluminum electrodes. It should be noted that the costs for chemical handling and waste disposal were not included in this preliminary cost analysis.

3.3. Continuous-Flow Filtration

Filtration experiments were conducted for 60 h to evaluate the impacts of different filter media on the removal of suspended solids and adsorption of contaminants. Samples were taken after 0.5, 1, 2, 4, 8, 12, 18, 24, 30, 36, 48, 54, and 60 h filtration, for turbidity measurement. Since the EC stage removed about 70% of initial turbidity, the packed-columns had a turbidity of 14.1 ± 5.3 NTU. In addition to turbidity, TOC analysis was conducted for samples from 0 to 36 h of operation, since all filter media had reached turbidity breakthrough (defined as below 50% removal in this study) by around that point. Figure 5 illustrates the removal of turbidity and TOC over time in different media filters.

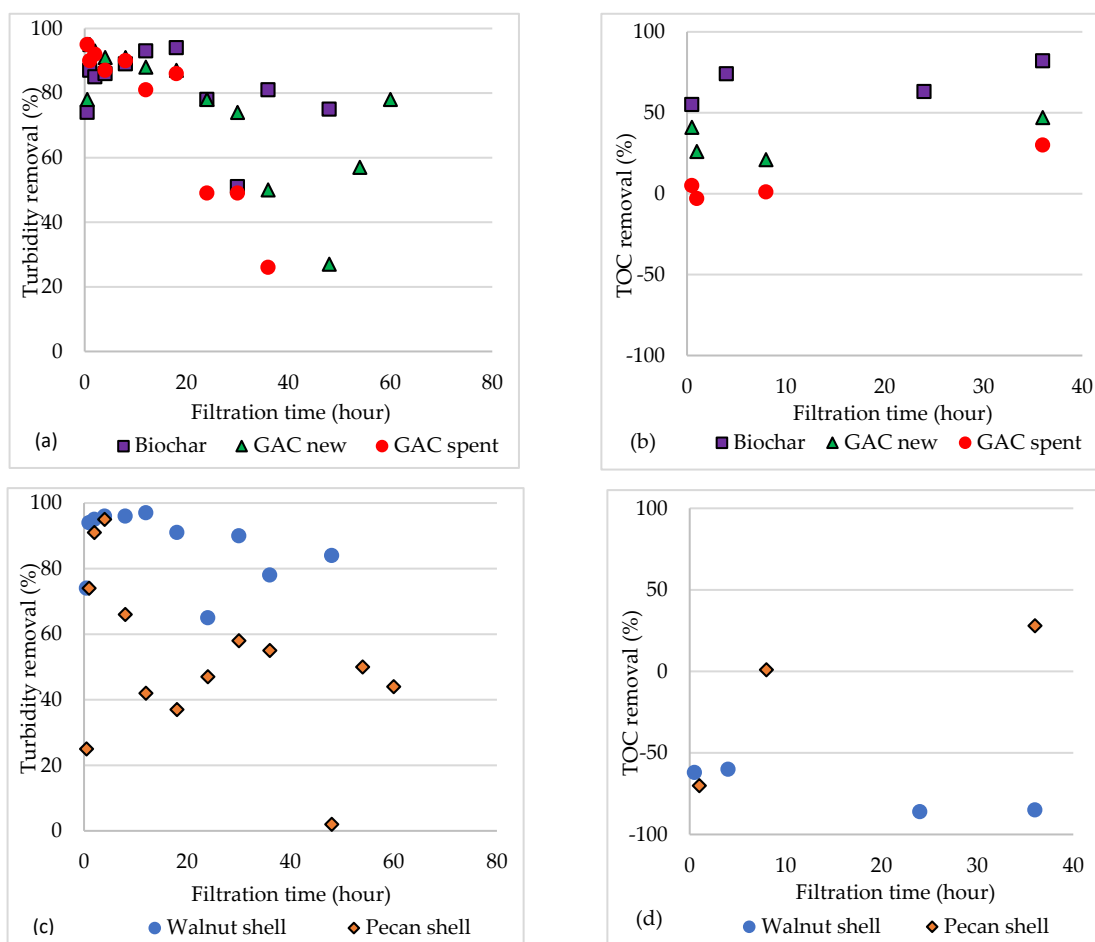


Figure 5. Removal of turbidity (a) and (c), and removal of TOC (b) and (d) in different media filters.

Removal of salts was negligible because the conductivity reduction was less than 4% in all media filters. None of the filter media had a significant impact on pH, as all the columns reduced it to a range where the lowest value was 6.92. This indicates that there was no significant consumption of alkalinity or generation of chemical species that affected pH during filtration.

3.3.1. New and Spent GAC

New GAC removed 80% turbidity during the first 24 h of filtration and the removal dropped to ~50% after 36 h (Figure 5a,b). Organic contaminants were reduced by 21% during the first 8 h of filtration, and the removal increased to 47% after 36 h. The results obtained in this study are similar to that Dastgheib et al. [15] reported; for GAC in a column experiment with EBCT of 6 min, the greatest removal of organics occurred at 24 h of operation, reaching ~55% removal. The EBCT of the GAC packed-column was designed and operated in this study for 19 min. When comparing these EBCT time to general standards, they all fit to commonly applied values because according to the U.S. Environmental Protection Agency (EPA), typical EBCT for water treatment applications of activated carbon ranges between 5 to 25 min [38].

In addition to the use of new GAC, this study explored an innovative use of spent GAC. One of the advantages of using this media is the low cost. When GAC is no longer useful for filtration in conventional water treatment plants, it becomes a waste; therefore, there is no cost related to acquiring spent GAC for filtration in this study.

According to the results obtained, the spent GAC demonstrated potential for produced water treatment; it reached half turbidity breakthrough after 24 h of operation compared to 36 h for the new GAC. Turbidity removal rates are acceptable at least in the first few hours of operation, since both new and spent GAC achieved over 90% during the first 8 h of operation and maintained greater than 80% after 18 h.

The main differences between new and spent GAC rely on their capacity to remove organics. Because the adsorption capacity of the spent GAC was exhausted during 9-year filtration of surface water, it barely adsorbed organic matter (5%) during the first 8 h of filtration. After 8 h it started showing a TOC removal of 30%.

Leaching test was conducted to investigate the release of adsorbed contaminants into deionized water from the spent GAC in comparison with new GAC. The conductivity of new GAC and spent GAC leachates was 16.4 $\mu\text{S}/\text{cm}$ and 57.6 $\mu\text{S}/\text{cm}$ after 24-h shaking, respectively. Release of organics from the GAC was 21-times of new GAC. The turbidity of new GAC and spent GAC leachates was 1.98 NTU and 6.72 NTU. The leaching experimental results imply that spent GAC was not as effective as new GAC to remove organic matter.

3.3.2. Walnut and Pecan Shell

Walnut media had great turbidity removal capacity during the first 18 h of operation reducing turbidity from 16.6 NTU to 0.49 NTU (Figure 5c,d). Turbidity breakthrough was reached after 24 h of operation. In terms of organics, TOC increased in the filter effluent right after starting the column operation due to the leaching of organic matter from the media. In contrast, literature reports that walnut shell filtration can decrease produced water turbidity from 33 to 0.02 NTU and remain stable for about 80 h of operation, with an average removal rate of organics of 60% [15]. This difference may be related to the media particle size and EBCT. In this study, the particle size of walnut shell was 1.68–2 mm and the EBCT was 19 min. Dastgheib et al. employed a particle size much smaller of 0.30–0.42 mm and a greater EBCT of 47 min, which may be attributable to the different removal results [15]. Smaller particle size and longer EBCT result in better removal but it increases the operating cost of filtration. Longer operation time for the columns can also represent a disadvantage in larger scale applications due to requirements of larger filters and footprint. Cost-benefit analysis should be conducted before selecting operating parameters for walnut shell.

There are limited studies reporting the use of pecan shell in produced water filtration. Although it reached good turbidity removal during the first 4 h (from 16.6 to <1 NTU), the removal was not maintained thereafter. In addition, pecan shell presented organic leaching during the first hour of operation, increasing TOC concentration in the effluent (Figure 5d). The leaching was visibly observed as the effluent from pecan shell had a light-yellow color during the first couple of hours of operation. Pretreatment procedures for pecan shell would need to be researched and tested to reduce the organic leaching and improve the TOC removal from produced water.

3.3.3. Biochar

Biochar was the filter media that took the longest to reach its best turbidity removal rate (Figure 5a,b). It took 8–12 h to get to 93%, while other filter media like new GAC and walnut shell removed the same percentage only after 1–2 h of operation. Biochar turbidity removal started to decrease after 24 h and reached half turbidity breakthrough.

The greatest advantage of filtering produced water with biochar is its outstanding capacity of removing organic matter. Biochar removed 74% TOC within the first 4 h of operation and maintained the removal rate for 36 h. It was the best filter media to remove organics, since new GAC was the closest to biochar and it only removed <50% of TOC. In this study, the adsorbent capacity of biochar turned out to be the greatest for organic matter removal.

It has been reported some biochars have stronger adsorption and binding affinities to organic contaminants than commercial GACs [39,40]. Our previous study investigated the factors affecting the use of biochar as an alternative adsorbent to treat pharmaceuticals from desalination concentrate in comparison with commercial GAC [32]. The adsorption capacity of biochar was comparable to GAC and achieved higher removal for some organic chemicals. High salinity and electrolyte ions in feedwater improved adsorption process due to neutralization of the negative charge of biochar with cations and compression of electrical double layer near the surface. Also, divalent cations (Ca^{2+} and Mg^{2+}) in produced water can form complex compound with organics via O-, N-, S- donors—such as carboxyl, hydroxyl, and phenolic functional groups, which benefits the interaction with a negatively charged biochar (coordinates with carboxyl groups on the biochar surface). Although biochar has a less-specific surface area than GAC, biochar achieved comparable turbidity removal and better TOC removal. Further studies are needed to elucidate the mechanisms of contaminants removal from highly saline produced water.

Moreover, biochar could be a low-cost alternative. The biochar used in this study is $\$287/\text{m}^3$, which could be 5 or 6 times less expensive than GACs, and thus could significantly reduce water treatment costs.

3.3.4. Removal of metals

The removal of metals was monitored in biochar and walnut column filters, given they showed the best performance in TOC and turbidity removal, respectively (Table 3). Both biochar and walnut filter media showed great potential of removing iron from produced water to the level below the instrumental detection limit. These media also removed SiO_2 to higher than 50% during filtration. There was no removal of other metals in filters.

3.4. Potential for Onsite Produced Water Reuse

Hydraulic fracturing is a highly water intensive process that requires cross-linked gel fluids for vertical wells and slick-water fluids for horizontally drilled wells. The cross-linked gel fluid usually has a high viscosity to transport sand, ceramics, and other proppant materials to induce fractures in the formation. The slick-water has lower viscosity but contains other friction reducers and chemical additives. Despite their differences in composition and purposes within the fracking process, both fluids can use brackish water [13] instead of freshwater for its operation, such as clean brine. In this study, after EC and filtration, the turbidity of the treated produced water reached less

than 1 NTU, and iron was not detected. With the advances in hydraulic fracturing, the high salinity in produced water may not be a limiting factor for reuse. For example, Schlumberger tested the fluid in a variety of mix waters with salinity levels ranging from 43,000 to 350,000 mg/L of TDS from formations in the Marcellus Shale and the Permian Basin. Identical formulations showed improved performance as the salinity increased [41].

Table 3. Metal concentrations in filtrate from biochar and walnut column filters.

Water Sample	Time (Hours)	As (mg/L)	Ba (mg/L)	Fe (mg/L)	Ca (mg/L)	Mg (mg/L)	SiO ₂ (mg/L)	Na (mg/L)
Filter influent	0	1.12	1.03	13.4	3799	529	34.7	33,190
	0.25	0.98	2.18	ND	2943	448	14.3	26,840
Biochar	0.5	1.04	1.25	ND	3682	527	13.2	33,840
	36	1.04	0.95	ND	3907	539	18.4	34,840
	0.25	1.03	1.29	ND	3807	555	16.9	33,990
Walnut	0.5	1.15	1.01	ND	3837	550	13.7	34,310
	36	1.01	0.94	0.3	3933	553	17.9	35,140
MDL		0.1	0.001	0.0287	0.016	0.24	0.015	0.0483

ND: non-detectable; MDL: minimum detectable level.

4. Conclusions

This study aims to generate a clean brine with low suspended solids, iron, and organic matter, which can be reused onsite for hydraulic fracturing process. Reuse of produced water can significantly reduce the current freshwater consumption during unconventional oil and gas exploration, and decrease the volume of produced water for deep well disposal. This study evaluated different alternatives for produced water treatment, including through a comparison between chemical and electro-coagulation, and different low-cost filter media.

During chemical coagulation, alum exhibited higher removal of turbidity than ferric chloride at the same molar concentration, resulting in lower chemical demand and cost. To achieve 60% removal of turbidity from the produced water, it requires 36 mg/L Al(III) (444 mg/L Al₂(SO₄)₃·18H₂O) and 134 mg/L Fe(III) (650 mg/L FeCl₃·6H₂O) as the coagulant. The total operating costs, including the electrical power cost and chemical cost for Al and Fe coagulation, were estimated approximately \$0.26/m³ and \$0.37/m³, respectively.

EC removed 70% of turbidity and an average of 63% of TOC from the produced water under optimal Al dose (current density of 6.60 mA/cm² and EC treatment time of 12 min). The energy requirement was calculated 0.36 kWh/m³ of water treated, which is much lower than EC treatment of lower salinity water and wastewater. EC has the advantage of shorter retention time, no need for additional chemicals, lesser sludge generation, and high mobility for onsite produced water treatment. Assuming the aluminum electrodisolution yield of 200% due to faradaic reaction and electrode corrosion, the total operating cost of EC was estimated \$0.44/m³ of treated water, which is 1.7 or 1.2 times higher than CC using alum or ferric chloride as the coagulant.

After EC, media filtration contributed to further turbidity removal: up to 97% for walnut shell, 95% for new GAC, and 94% for biochar. In terms of organic removal, only biochar and new GAC were considered effective. Spent GAC had very low organic matter removal rates, and walnut and pecan shell leached out organics which caused an increase rather than a removal. All of these occur with reasonable pH changes (reducing from 7.44 to 6.92). Regarding metals in filtrate from walnut shell and biochar, iron was reduced to an undetectable level; SiO₂ was reduced by 50%; and other elements, such as calcium, sodium, and magnesium, were not significantly removed.

The use of agricultural waste products (e.g., pecan, walnut shell, and biochar) for packed-column filtration represents a promising economic advantage. Although walnut shell had a greater contaminant removal capacity compared to pecan shell, both can contribute to treating produced water into a clean brine. The economic investment of applying these filter media would be minimal, as the costs related

are energy (pumping water) and materials. Spent shells after useful lifetime could be landfilled or used as fuels to generate energy.

Author Contributions: A.Z.R. conducted experiments; A.Z.R., P.X., and H.W. wrote the original draft; A.Z.R., P.X., H.W., L.H., and Y.Z. reviewed and edited the manuscript. P.X. managed the research project. All authors have read and agreed to the published version of the manuscript.

Funding: The authors thank the Mexican Energy Department and the National Council for Science and Technology for providing the funds to conduct this study through the scholarship CONACYT–SENER Sustentabilidad Energética, Quinto Periodo.

Conflicts of Interest: The authors declare no conflict of interest. The funders had no role in the design of the study; in the collection, analyses, or interpretation of data; in the writing of the manuscript, or in the decision to publish the results.

References

1. Veil, J.U.S. *Produced Water Volumes and Management Practices in 2012*; Veil Environmental, LLC: Annapolis, MD, USA, 2015.
2. Arthur, J.D.; Dillon, L.W.; Frazan, D.J.; Hochheiser, W.H. *Management of Produced Water from Oil and Gas Wells*; National Petroleum Council: Washington, DC, USA, 2011.
3. Jiménez, S.; Micó, M.M.; Arnaldos, M.; Medina, F.; Contreras, S. State of the art of produced water treatment. *Chemosphere* **2018**, *192*, 186–208. [[CrossRef](#)] [[PubMed](#)]
4. Khan, N.A.; Engle, M.; Dungan, B.; Holguin, F.O.; Xu, P.; Carroll, K.C. Volatile-organic molecular characterization of shale-oil produced water from the Permian Basin. *Chemosphere* **2016**, *148*, 126–136. [[CrossRef](#)] [[PubMed](#)]
5. Dahm, K.G.; Guerra, K.L.; Xu, P.; Drewes, J.E. Composite geochemical database for coalbed methane produced water quality in the Rocky Mountain region. *Environ. Sci. Technol.* **2011**, *45*, 7655–7663. [[CrossRef](#)] [[PubMed](#)]
6. Xu, P.; Drewes, J.E.; Heil, D. Beneficial use of co-produced water through membrane treatment: Technical-economic assessment. *Desalination* **2008**, *225*, 139–155. [[CrossRef](#)]
7. Chaudhary, B.K.; Sabie, R.; Engle, M.A.; Xu, P.; Willman, S.; Carroll, K.C. Produced Water Quality Spatial Variability and Alternative-Source Water Analysis Applied to the Permian Basin, USA. *Hydrogeol. J.* **2020**, *27*, 2889–2905. [[CrossRef](#)]
8. USEPA. U.S. Environmental Protection Agency. Study of Oil and Gas Extraction Wastewater Management Under the Clean Water Act. EPA-821-R19-001. Available online: https://www.epa.gov/sites/production/files/2019-05/documents/oil-and-gas-study_draft_05-2019.pdf (accessed on 29 January 2019).
9. Hu, L.; Yu, J.; Luo, H.; Wang, H.; Xu, P.; Zhang, Y. Simultaneous recovery of ammonium, potassium and magnesium from produced water by struvite precipitation. *Chem. Eng. J.* **2020**, *382*, 123001. [[CrossRef](#)]
10. Liden, T.; Santos, I.C.; Hildenbrand, Z.L.; Schug, K.A. Treatment modalities for the reuse of produced waste from oil and gas development. *Sci. Total Environ.* **2018**, *643*, 107–118. [[CrossRef](#)]
11. Guglielmi, Y.; Cappa, F.; Avouac, J.P.; Henry, P.; Elsworth, D. Induced seismicity. Seismicity triggered by fluid injection-induced aseismic slip. *Science* **2015**, *348*, 1224–1226. [[CrossRef](#)]
12. Scanlon, B.R.; Reedy, R.C.; Xu, P.; Engle, M.; Nicot, J.P.; Yoxtheimer, D.; Yang, Q.; Ikonnikova, S. Can we beneficially reuse produced water from oil and gas extraction in the U.S.? *Sci. Total Environ.* **2020**, *717*, 137085. [[CrossRef](#)]
13. Reyes, F.R.; Engle, M.; Lixin, J.; Jacobs, M.A.; Konter, J.G. Hydrogeochemical controls on brackish groundwater and its suitability for use in hydraulic fracturing: The Dockum Aquifer, Midland Basin, Texas. *Environ. Geosci.* **2018**, *25*, 37–63. [[CrossRef](#)]
14. Wang, M.; Wang, M.; Chen, D.; Gong, Q.; Yao, S.; Jiang, W.; Chen, Y. Evaluation of pre-treatment techniques for shale gas produced water to facilitate subsequent treatment stages. *J. Environ. Chem. Eng.* **2019**, *7*, 102878. [[CrossRef](#)]
15. Dastgheib, S.A.; Knutson, C.; Yang, Y.; Salih, H.H. Treatment of produced water from an oilfield and selected coal mines in the Illinois Basin. *Int. J. Greenh. Gas Control* **2016**, *54*, 513–523. [[CrossRef](#)]
16. Younker, J.M.; Walsh, M.E. Bench-scale investigation of an integrated adsorption–coagulation–dissolved air flotation process for produced water treatment. *J. Environ. Chem. Eng.* **2014**, *2*, 692–697. [[CrossRef](#)]

17. Hakizimana, J.N.; Gourich, B.; Chafi, M.; Stiriba, Y.; Vial, C.; Drogui, P.; Naja, J. Electrocoagulation process in water treatment: A review of electrocoagulation modeling approaches. *Desalination* **2017**, *404*, 1–21. [[CrossRef](#)]
18. Kuokkanen, V.; Kuokkanen, T.; Rämö, J.; Lassi, U. Recent Applications of Electrocoagulation in Treatment of Water and Wastewater—A Review. *Green Sustain. Chem.* **2013**, *3*, 89–121. [[CrossRef](#)]
19. Valero, D.; Ortiz, J.M.; Expósito, E.; Montiel, V.; Aldaz, A. Electrocoagulation of a synthetic textile effluent powered by photovoltaic energy without batteries: Direct connection behaviour. *Sol. Energy Mater. Sol. Cells* **2008**, *92*, 291–297. [[CrossRef](#)]
20. Jain, P.; Sharma, M.; Dureja, P.; Sarma, P.M.; Lal, B. Bioelectrochemical approaches for removal of sulfate, hydrocarbon and salinity from produced water. *Chemosphere* **2017**, *166*, 96–108. [[CrossRef](#)]
21. Millar, G.J.; Lin, J.; Arshad, A.; Couperthwaite, S.J. Evaluation of electrocoagulation for the pre-treatment of coal seam water. *J. Water Process Eng.* **2014**, *4*, 166–178. [[CrossRef](#)]
22. Zhao, S.; Huang, G.; Cheng, G.; Wang, Y.; Fu, H. Hardness, COD and turbidity removals from produced water by electrocoagulation pretreatment prior to Reverse Osmosis membranes. *Desalination* **2014**, *344*, 454–462. [[CrossRef](#)]
23. CleanWave-FactSheet. CleanWaveSM Water Treatment Service. In *Mobile Service for Produced and Flow Water*; Halliburton: Houston, TX, USA, 2017.
24. Mousa, I.E. Total petroleum hydrocarbon degradation by hybrid electrobiochemical reactor in oilfield produced water. *Mar. Pollut. Bull.* **2016**, *109*, 356–360. [[CrossRef](#)]
25. Camarillo, M.K.; Domen, J.K.; Stringfellow, W.T. Physical-chemical evaluation of hydraulic fracturing chemicals in the context of produced water treatment. *J. Environ. Manag.* **2016**, *183*, 164–174. [[CrossRef](#)] [[PubMed](#)]
26. Gomes, J.; Cocke, D.; Das, K.; Guttula, M.; Tran, D.; Beckman, J. Treatment of produced water by electrocoagulation. In Proceedings of the PD Congress 2009: Proceedings of sessions and symposia held during TMS 2009 Annual Meeting & Exhibition, San Francisco, CA, USA, 15–19 February 2009; pp. 459–466.
27. Ezechi, E.H.; Isa, M.H.; Kutty, S.R.M.; Yaqub, A. Boron removal from produced water using electrocoagulation. *Process Saf. Environ. Prot.* **2014**, *92*, 509–514. [[CrossRef](#)]
28. Shamaei, L.; Khorshidi, B.; Perdicakis, B.; Sadrzadeh, M. Treatment of oil sands produced water using combined electrocoagulation and chemical coagulation techniques. *Sci. Total Environ.* **2018**, *645*, 560–572. [[CrossRef](#)] [[PubMed](#)]
29. Zhang, Z.; Du, X.; Carlson, K.H.; Robbins, C.A.; Tong, T. Effective treatment of shale oil and gas produced water by membrane distillation coupled with precipitative softening and walnut shell filtration. *Desalination* **2019**, *454*, 82–90. [[CrossRef](#)]
30. Kusworo, T.D.; Aryanti, N.; Qudratun; Utomo, D.P. Oilfield produced water treatment to clean water using integrated activated carbon-bentonite adsorbent and double stages membrane process. *Chem. Eng. J.* **2018**, *347*, 462–471. [[CrossRef](#)]
31. Hosny, R.; Fathy, M.; Ramzi, M.; Abdel Moghny, T.; Desouky, S.E.M.; Shama, S.A. Treatment of the oily produced water (OPW) using coagulant mixtures. *Egypt. J. Pet.* **2016**, *25*, 391–396. [[CrossRef](#)]
32. Lin, L.; Jiang, W.; Xu, P. Comparative study on pharmaceuticals adsorption in reclaimed water desalination concentrate using biochar: Impact of salts and organic matter. *Sci. Total Environ.* **2017**, *601*, 857–864. [[CrossRef](#)]
33. Chang, H.; Liu, B.; Yang, B.; Yang, X.; Guo, C.; He, Q.; Liang, S.; Chen, S.; Yang, P. An integrated coagulation-ultrafiltration-nanofiltration process for internal reuse of shale gas flowback and produced water. *Sep. Purif. Technol.* **2019**, *211*, 310–321. [[CrossRef](#)]
34. Nadella, M.; Sharma, R.; Chellam, S. Fit-for-purpose treatment of produced water with iron and polymeric coagulant for reuse in hydraulic fracturing: Temperature effects on aggregation and high-rate sedimentation. *Water Res.* **2020**, *170*, 115330. [[CrossRef](#)]
35. Cañizares, P.; Martínez, F.; Jiménez, C.; Sáez, C.; Rodrigo, M.A. Technical and economic comparison of conventional and electrochemical coagulation processes. *J. Chem. Technol. Biotechnol.* **2009**, *84*, 702–710. [[CrossRef](#)]

36. Gu, Z.; Liao, Z.; Schulz, M.; Davis, J.R.; Baygents, J.C.; Farrell, J. Estimating Dosing Rates and Energy Consumption for Electrocoagulation Using Iron and Aluminum Electrodes. *Ind. Eng. Chem. Res.* **2009**, *48*, 3112–3117. [[CrossRef](#)]
37. Picard, T.; Cathalifaud-Feuillade, G.; Mazet, M.; Vandensteendam, C. Cathodic dissolution in the electrocoagulation process using aluminium electrodes. *J. Environ. Monit.* **2000**, *2*, 77–80. [[CrossRef](#)] [[PubMed](#)]
38. EPA, U.S. Granular Activated Carbon. Available online: <https://iaspub.epa.gov/tdb/pages/treatment/treatmentOverview.do?processId=2074826383#content> (accessed on 29 January 2019).
39. Ahmad, M.; Lee, S.S.; Dou, X.; Mohan, D.; Sung, J.-K.; Yang, J.E.; Ok, Y.S. Effects of pyrolysis temperature on soybean stover-and peanut shell-derived biochar properties and TCE adsorption in water. *Bioresour. Technol.* **2012**, *118*, 536–544. [[CrossRef](#)] [[PubMed](#)]
40. Tong, X.J.; Li, J.Y.; Yuan, J.H.; Xu, R.K. Adsorption of Cu(II) by biochars generated from three crop straws. *Chem. Eng. J.* **2011**, *172*, 828–834. [[CrossRef](#)]
41. Whitfield, S. Permian, Bakken Operators Face Produced Water Challenges. *J. Pet. Technol.* **2017**, *69*, 48–51. [[CrossRef](#)]



© 2020 by the authors. Licensee MDPI, Basel, Switzerland. This article is an open access article distributed under the terms and conditions of the Creative Commons Attribution (CC BY) license (<http://creativecommons.org/licenses/by/4.0/>).